# Proteome analysis, biochemical and structural characterization of the outer membrane and secretory proteins from pathogenic Leptospira

#### **A Thesis**

Submitted for the Degree of

# **Doctor of Philosophy**

By

**Umate Nachiket Shankar** 

(Regd. No. 16LBPH06)





Department of Biochemistry
School of Life Sciences, University of Hyderabad
Hyderabad-500046
Telangana, India
March 2024



# Certificate

This is to certify that this thesis entitled "Proteome analysis, biochemical and structural characterization of the outer membrane and secretory proteins from pathogenic Leptospira" submitted by Mr. Umate Nachiket Shankar bearing registration number 16LBPH06 in partial fulfilment of the requirement for the award of Doctor of Philosophy in the Department of Biochemistry, School of Life Sciences, is a bonafide work carried out by her under my supervision and guidance. This thesis is free from plagiarism and has not been submitted previously in part or in full to this University or any other University or Institution for the award of any degree or diploma.

Part of this thesis has been published in the following journal,

- Shankar UN, Mohit, Padhi SK, Akif M. (2023) Biochemical characterization, substrate and stereoselectivity
  of an outer surface putative α/β hydrolase from the pathogenic Leptospira. *Int J Biol Macromol*. 28;229:803813. (Chapter 3 and 4)
- Kumar P., Lata S., Shankar U.N., and Akif M., (2021) Immunoinformatics Based Designing of a Multi-Epitope Chimeric Vaccine From Multi-Domain Outer Surface Antigens of Leptospira. Frontiers in Immunology. 12:735373.
- Shiraz M, Lata S, Kumar P., Shankar UN, Akif M. (2021) Immunoinformatics analysis of antigenic epitopes and designing of a multi-epitope peptide vaccine from putative nitro-reductases of Mycobacterium tuberculosis DosR. *Infect Genet Evol.* Oct; 94:105017.
- Shankar UN, Shiraz M, Kumar P, Akif M. (2024) A comprehensive *In-silico* analysis of putative outer membrane and secretory hydrolases from pathogenic *Leptospira*: Possible Implications in pathogenesis. *Biotechnology and applied biochemistry* (Under Revision) Chapter 2.
- Shankar UN, Akif M. (2024) Refolding and Biophysical characterization of leptospiral complement Regulator acquiring protein A (LcpA) (Under Preparation) Chapter 5.

Part of this thesis has been presented in the following conferences,

- Umate Nachiket Shankar, Mohd. Akif, Identification and characterization of the outer membrane and secretory putative hydrolases from pathogenic Leptospira, participated in oral presentation at International conference on Frontiers in Basic Biology, Biotechnology and Bioinformatics, 15-18<sup>th</sup> February 2024, University of Hyderabad, Hyderabad.
- Umate Nachiket Shankar, Mohd. Akif, Crystallographic studies of Complement Evasion Proteins from pathogen *Leptospira*, participated in oral presentation at International conference on Recent trends in Biotechnology, ICRTB-2022, 22-23 June 2022, Centurion University of technology and management, Bhubaneswar, Odisha.
- Umate Nachiket Shankar, Mohd. Akif, Refolding and Biophysical characterization of leptospiral complement regulator- acquiring protin A (LcpA), presented poster at International conference on frontier areas of science and technology, ICFAST-2022", 09-10 September 2022, University of Hyderabad.
- Umate Nachiket Shankar and Mohd. Akif, Refolding and Biophysical characterization of leptospiral complement regulator- acquiring protin A (LcpA), Presented poster at Bioquest, 12-13 Oct, 2017, UoH.

Further, the student has passed the following courses towards fulfilment of the coursework requirement for Ph.D.

Course code	Name	Credits	Pass/Fail
BC 801	Analytical Techniques	4	Passed
BC 802	Research ethics, Data analysis and Biostatistics	3	Passed
BC 803	Lab seminar and Records	5	Passed

Mohd. Akif, Supervisor अतिकृष, पीएवर्ड Associate Professor / एसोसिए अधिकृष्ट Department of Biochemistry / जैव रसायन विभाग School of Life Sciences / जीव विज्ञान विद्यालय University of Hyderabad / हैदराबाद विश्वविद्यालय

Prof. CR Rao Road / प्रो सी आर राव रोड Gachibowli / गाचीवावली , Hydarabad / हैदराबाद-48 Head, Dept. of Biochemistry

प्रशाह / Head जीवरसायनविभाग / Department of Biochemistry जीवितज्ञान स्थाप / School of Life Sciences जीवितज्ञान स्थाप / School of Life Sciences इंद्रसंघाद विशो उद्योग / (University of Hyderabad) Dean, School of Life Sciences संकाय अध्यक्ष / Dean

जीव विज्ञान संकाय / School of Life Science: हैदराबाद विश्वविद्यालय / University of Hyderabod हैदराबाद / Hyderabad-500 046.



University of Hyderabad

Hyderabad -500046, India

# Declaration

I, Umate Nachiket Shankar, hereby declare that this thesis entitled "Proteome analysis, biochemical and structural characterization of the outer membrane and secretory proteins from pathogenic *Leptospira*" submitted by me under the guidance and supervision of **Dr. Mohd.** Akif, is original and independent research work. I also declare that it has not been submitted previously in part or in full to this University or any other University or Institution for the award of any degree or diploma.

Date: 04/03/2024 Signature of the Student

Himste.

Signature of the Supervisor 4/3 /24

Mohd. Akif, Ph.D. / मुहम्मद आकिफ, पीएवडी Associate Professor / एसोसिएट प्रोफेसर Department of Biochemistry / जैव रसायन विभाग School of Life Sciences / जीव विज्ञान विद्यालय University of Hyderabad / हैदराबाद विश्वविद्यालय Prof. CR Rao Road / प्रो सी आर राव रोड Gachibowli / गांचीबावली, Hyderabad / हैदराबाद-46.

#### **ACKNOWLEDGEMENT**

This thesis would not have been possible without the support of many people. I'd especially like to express my sincere thanks to each and every one of them.

At the very beginning, I express my deepest sense of gratitude towards my Supervisor *Dr. Mohd. Akif*, for giving me an opportunity to pursue my PhD under his constant guidance. He is honest, generous, inspiring person and good mentor. I appreciate his unwavering support, critical discussions and fruitful suggestions throughout my doctoral journey. His upbeat attitude and constant faith in my research motivated and encouraged me. I consider myself grateful to be among those who received his constant support and valuable suggestions in academic and personal life as well.

I extend my sincere gratitude to my doctoral committee members *Prof. Ravi Kumar Gutti* and *Dr. Insaf Ahmed Qureshi* for their critical remarks and insightful suggestions on my PhD work and presentations.

I am extremely thankful to the present Head of Biochemistry department *Prof. Naresh Babu V Sepuri* and former Heads *Prof. Krishnaveni Mishra, Prof. Mrinal Kanti Bhattacharyya and Prof. N. Siva Kumar* for maintaining the Departmental facilities. I am obliged to the present Dean, School of Life Sciences, *Prof. Anand K. Kondapi*, and former Deans *Prof. N. Siva Kumar, Prof. S. Dayananda, Prof. Kolluru V A Ramaiah, and Prof. P. Reddanna* for allowing me to use the school facilities.

I truly appreciate the administrative assistance and cooperation from *Mr. Chary*, *Mr. Prabhu* and also the other non-teaching staff members of the Department of Biochemistry and School of Life Sciences as well.

I owe *Dr. Santosh Kumar Padhi* an immense debt of gratitude for his support, guidance, and extending the lab facility in studying the enantioselectivity of one of my proteins. I also thank *Mohit* for helping me in performing this experiment.

I greatly acknowledge *Prof. Noorudin Khan* and his student *Suman* for helping me in studying the immunomodulatory effect of one of my proteins. Mohit and Suman have been incredibly polite and helpful.

I am grateful to *Dr. N. Prakash Prabhu* for allowing me to use the Fluorescence spectroscopy facility of Department of Biotechnology and Bioinformatics and *Prof. Rajagopal Subramanyam* for CD spectroscopy facility of Department of Plant sciences.

I heartily appreciate *Dr. S M Faisal* (NIAB, Hyderabad) for providing the *Leptospira* genome and *Dr. R Sankaranarayanan* (CCMB, Hyderabad) for allowing me to use the X-Ray diffraction facilities.

I am thankful to *BBL* for the financial support in initial time of my PhD and also to *ICMR* for awarding me the ICMR-SRF fellowship. I acknowledge the funding agencies *DST-SERB*, *IoE-Grant*, and *DBT* for providing the funds to the Lab and *DST-FIST* and *UGC-SAP* for funding the department.

During my PhD, I had the great opportunity to have the amazing and fantastic lab members who extended generous assistance whenever needed. I am grateful to my present and former lab members *Pankaj*, *Shiraz*, *Faisal*, *Surabhi*, *Kousamvita*, *Dipanwita*, *Venkat*, and MSc project students *Hitakshi*, *Pooja*, *Pranita*, *Pranati*, *Haneesh*, *Ruchira*, *Aayushi*, *Nikita*, *Anjali*, *Kritika*, and *Nikhil*.

I am fortunate to have the amazing lab mates cum friends *Pankaj*, *Shiraz* and *Faisal* who supported and generously helped me during my entire PhD journey. Pankaj has been my guiding light whenever I stumbled into technical issues, particularly those pertaining to bioinformatics. I am also thankful to Shiraz and Faisal for taking the great efforts during the preparation for my pre-PhD seminar.

I am extremely thankful to *Rahat ma'am* for treating us with the delicious homemade food. Ma'am, your enthusiasm and hospitality during our visits are truly appreciated.

I am incredibly grateful to my best friends, *Anant, Gopal, Akash, Umesh, Vikas, Pranay, Janish, Raj Kishor, Ashish, Dushyant, Rajat, Ashraf,* and *Ravi*. I am so thankful to all of them for maintaining the good environment around me. I would like to thank all the members of cricket stars and natural selection cricket team.

I am grateful for having the caring and supportive seniors *Dr. Rohith Anna, Tirumal Anna, Niranjan anna, Gopal Anna* and *Ramji Anna* during my PhD.

I really feel very fortunate to have my dear friends *Parmeshwar*, *Dnyaneshwar*, *Dr. Bhausaheb*, *Sangmeshwar*, *Ravi* and *Sachin*. We have several beautiful moments in college time.

Gratitude fills my heart as I reflect on the journey that brought me to this moment. I eternally thankful to my parents *Aai* and *Baba* who have been the pillars of support. Their constant support, patience and understanding have been the bedrock upon which I have built this achievement. Their relentless inspiration helps me to bring the best out of me throughout my research journey. I would like to thank my dear younger sister *Swati*, brother *Rushikesh* and uncle *Nagesh* for bringing the incredible presence into my life.

This acknowledgment would not be complete without mentioning the efforts and patience of my wife *Ruchi*. I am profoundly grateful to her love and sacrifices. Thank you for being my partner, my best friend and my great supporter. Finally, I am forever grateful to my son *Vedant* and nephew *Devansh* who are my biggest source of motivation.

**Nachiket** 

# **TABLE OF CONTENTS**

Contents	Page No.
List of figures	I
List of tables	Ш
Abbreviations	${f v}$
Unit of measurements	VII
Preface	VIII
Chapter-1	1-26
Introduction and Review of literature	
1.1. INTRODUCTION	
1.2. Leptospira, the disease-causing spirochete	
1.2.1. Size and morphology	2
1.2.2. Classification and taxonomy	3
1.2.3. Cell biology	5
1.2.4. In-vitro cultivation	6
1.3. Leptospirosis, the disease	6
1.3.1. Phases of Leptospirosis	7
1.3.2. Mode of transmission	7
1.4. Diagnosis of the disease	8
1.4.1. Laboratory approaches	8
1.4.2. Challenges in diagnosis	9
1.5. Global burden	10
1.6. Pathogenesis and virulence	11
1.6.1. Lipopolysaccharides	13
1.6.2. Microbial surface components recognizing adhe	
1.6.3. Lipoproteins	
1.6.4. Hemolysins	
1.6.5. Adhesins	
1.7. Host-immune response	
1.7.1. Factor H (FH)	
1.7.2. C4b binding protein (C4BP)	
1.8. Leptospiral immune evasion	

1.9. Leptospiral complement regulator acquiring protein A (LcpA)	23
1.10. Hydrolytic functions of bacterial proteins in immune evasion	23
1.11. The α/β hydrolase superfamily	24
1.12. Major challenges and aim of the thesis	25
1.13. Objectives of the Study	26
Chapter-2	27-51
Prediction of outer membrane and secretory putative hydrolases from pathogenic Lepto.	spiral
species	-
2.1. INTRODUCTION	
2.2. METHODOLOGY	
2.2.1 Prediction of outer membrane and secretory proteins	30
2.2.2. Identification of proteins with enzymatic functions	
2.2.3. Physicochemical properties	
2.2.4. Annotations of virulence factors	33
2.2.5. Three-dimensional structural model of α/β hydrolases	33
2.2.6. Conservation analysis among different Leptospiral species	34
2.3. RESULTS	34
2.3.1. Exported proteins contain signal peptides	34
2.3.2. Potent outer membrane and secretory proteins are devoid of Lipo-box	35
2.3.3. Outer membrane and secretory proteins belong to many enzymatic classes	36
2.3.4. Characterization of putative α/β hydrolases	37
2.3.5. Three dimensional Model and Structural Comparison	46
2.3.6. Conservation analysis among different Leptospiral species	49
2.4. CONCLUSIONS	51
Chapter-3	52-67
Cloning, expression, and purification of the putative hydrolases	52
3.1. INTRODUCTION	53
3.2. MATERIALS	54
3.2.1. Chemical reagents	54
3.2.2. Chemical compositions	55
3.3. METHODOLOGY	56
3.3.1. Preparation of transformation competent E. coli	56
3.3.2. Molecular cloning	57
3.3.3. Bacterial transformation	58
3.3.4. Site-directed mutagenesis	59

3.3.5. Expression and purification	60
3.3.6. Size-exclusion chromatography	61
3.4. RESULTS	61
3.4.1. Cloning in expression vector under the influence of T7 promoter	61
3.4.2. Recombinant purification of LABH-1	62
3.4.3. LABH-1 exists as monomer in solution	63
3.4.4. Purification of active site mutant of LABH-1	64
3.4.5. Recombinant purification of LABH-2	65
3.4.6. Oligomeric state of LABH-2	66
3.5. CONCLUSIONS	67
Chapter-4	68-104
Biochemical characterization, substrate, and stereo-selectivity of the outer membrane p	utative
α/β hydrolases from Leptospira	
4.1. INTRODUCTION	
4.2. MATERIALS	
4.3. METHODOLOGY	
4.3.1. Circular Dichroism measurements	
4.3.2. Enzymatic activity assay	72
4.3.3. Effect of pH and temperature on the enzymatic activity	
4.3.4. Determination of steady-state kinetics parameters	
4.3.5 Inhibition assay	
4.3.6. Crystallization screening	74
4.3.7. X-ray diffraction	74
4.3.8. Protein modelling and structural alignment	74
4.3.9. Molecular Docking	75
4.3.10. Phylogenetic analysis	75
4.3.11. Biocatalytic kinetic resolution	75
4.3.12. Cell viability assay	76
4.3.13. Quantitative real time polymerase chain reaction (qRT-PCR)	77
4.4. RESULTS	78
4.4.1. Leptospiral α/β hydrolase-1 (LABH-1)	78
4.4.1.1. LABH-1 contains mostly helical content and displays moderate stability	78
4.4.1.2. Kinetics parameters and substrate specificity of LABH-1	80
4.4.1.3. Inhibition kinetics of LABH-1	85
4.4.1.4. Crystallization and data collection	86

4.4.1.5. Structural features and comparison with other $\alpha/\beta$ hydrolases	89
4.4.1.6. Inhibitor binds to the allosteric site of LABH-1	91
4.4.1.7. Conservation analysis among different organisms	93
4.4.1.8. Biocatalytic application of LABH-1 in the production of enantiopure 1-phenylethanol	95
4.4.1.9. LABH-1 shows immunomodulatory functions in mice macrophage cell line	98
4.4.2. Leptospiral α/β hydrolase-1 (LABH-2)	100
4.5. CONCLUSIONS	103
Chapter-5	.105-131
Biophysical characterization of an outer membrane Leptospiral complement Regulator-ac	quiring
protein A (LcpA)	
5.1. INTRODUCTION	106
5.2. MATERIALS	107
5.3. METHODOLOGY	107
5.3.1. Cloning of <i>lcpA</i> gene into expression vector	107
5.3.2. Heterologous Expression and Solubility	107
5.3.3. Purification of recombinant protein	108
5.3.4. Circular Dichroism measurements	110
5.3.5. Prediction of metal ion binding	110
5.3.6. Intrinsic Fluorescence Spectroscopy	110
5.3.7. Secondary structure prediction and homology modelling	111
5.3.8. Crystallization Screening	111
5.3.9. X-ray diffraction	111
5.3.10. Molecular Docking	112
5.3.11. Molecular Dynamic Simulation	112
5.3.12. Phylogenetic analysis	113
5.4. RESULTS	113
5.4.1. LcpA overexpressed as inclusion body	113
5.4.2. Refolded LcpA exits as a monomer in solution	
5.4.3. LcpA exhibits moderate structural stability	
5.4.4. LcpA has ability to bind zinc	119
5.4.5. Zinc binding brings structural modifications	119
5.4.6. Crystallization and Diffraction	
5.4.7. 3-D Structural model of LcpA	
5.4.8. C4BP and FH bind to mid to N-terminus of the LcpA	124

5.4.9. Molecular Dynamic Simulation	126
5.4.10. Conservation analysis among pathogenic, saprop Leptospira	-
5.5. CONCLUSIONS	130
Chapter-6	132-142
Discussion	132
BIBLIOGRAPHY	143-170
APPENDIX	171-176
PUBLICATIONS	177-180
ANTI-PLAGIARISM REPORT	181-196

# LIST OF FIGURES

Pag	e No.
Figure 1.1. Architecture of Leptospira species	3
Figure 1.2. Taxonomy classification system	4
Figure 1.3. Phylogenetic study of <i>Leptospira</i> based on 16S rRNA analysis	5
Figure 1.4. Transmission cycle of Leptospira	8
Figure 1.5. Laboratory tests for the diagnosis of <i>Leptospira</i> .	9
Figure 1.6. Worldwide basis distribution of leptospirosis cases in terms of DALY index	x 11
Figure 1.7. Outer membrane architecture of Leptospira	12
Figure 1.8. Interaction of Leptospira MSCRAMM with the host ECMs	14
Figure 1.9. Schematic representation of factor H.	19
Figure 1.10. Schematic representation of C4BP	20
Figure 1.11. Complement evasion strategies of pathogenic Leptospira.	22
Figure 2.1. Methodology and tools used in the prediction of potent outer membran	ne and
secretory proteins	30
Figure 2.2. Prediction and sub-cellular localization of leptospiral proteins	35
Figure 2.3. Representation of potent outer membrane and secretory proteins with enzy	ymatic
functions	36
<b>Figure 2.4.</b> Sequence analysis of putative $\alpha/\beta$ hydrolases	40
Figure 2.5. Sequence alignment of putative proteases of $\alpha/\beta$ hydrolases family proteins	41
Figure 2.6. Three-dimensional structures and domain architecture	47
Figure 2.7. Structure alignment of 3-D models with Staphylococcus aureus lipase	49
Figure 2.8. Evolutionary analysis by maximum likelihood method among Leptospiral s	pecies
	50
Figure 3.1. 1% agarose gel showing PCR amplification and separation of inserts from	m the
vector backbone	62
Figure 3.2. Purification of LABH-1	63
Figure 3.3. Determination of the oligomeric state of LABH-1	64
Figure 3.4. 12% SDS-PAGE showing purification of mutant LABH-1	65
Figure 3.5. Purification of LABH-2	66
Figure 3.6. Determination of the oligomeric state of LABH-2	<b>67</b>
Figure 4.1. CD-spectra measurements of LABH-1	<b>79</b>
<b>Figure 4.2.</b> Enzymatic activity of LABH-1 at room temperature against <i>p</i> -nitrophenyl be	utyrate

	80
Figure 4.3. Effect of pH and temperature on the hydrolytic activity	81
Figure 4.4. Effect of metals on the hydrolytic activity	82
Figure 4.5. The hydrolytic activity of the LABH-1 against different esters of fatty acids	83
Figure 4.6. Enzymatic specific activity of the wild-type and mutant LABH-1 at the	room
temperature against p-nitrophenyl butyrate	85
Figure 4.7. Inhibition of the hydrolytic activity of LABH-1	86
Figure 4.8. Crystallization conditions obtained for LABH-1	87
Figure 4.9. Crystal optimization of LABH-1	88
Figure 4.10. X-ray diffraction pattern of LABH-1 protein	88
Figure 4.11. 3-D structural representation and structure-based sequence alignment of LA	ABH-
1.	90
Figure 4.12. Molecular docking of LABH-1 with substrate and inhibitor	92
Figure 4.13. Phylogenetic analysis of LABH-1 and related sequences	94
Figure 4.14. Chiral Resolution	96
Figure 4.15. HPLC chiral analysis of biocatalytic kinetic resolution of racemic 1-phenyl	ethyl
acetate, 8 h sample	97
Figure 4.16. Cytokine profile in Mice macrophage Raw 264.7 cells stimulated with LAB	3H-1.
	99
Figure 4.17. Enzymatic activity of LABH-2 at room temperature against p-nitroph	nenyl
butyrate	100
Figure 4.18. Effect of pH and temperature on the hydrolytic activity	101
Figure 4.19. The hydrolytic activity of the LABH-2 against different esters of fatty acids	102
Figure 5.1. 12% SDS-PAGE showing overexpression and solubility of recombinant I	_cpA
	114
Figure 5.2. Refolding and purification of recombinant LcpA	116
<b>Figure 5.3.</b> Structural stability analysis of LcpA using circular dichroism spectroscopy	118
Figure 5.4. Metal binding analysis	120
Figure 5.5. Crystallization conditions obtained for LcpA	121
Figure 5.6. Three-dimensional structural model	123
Figure 5.7. Electrostatic surface charge	124
Figure 5.8. Complex structure model	125
Figure 5.9. MDS plots of LcpA and LcpA-CCP6-8 complex	128
<b>Figure 5.10.</b> Phylogenetic analysis of LcpA and related sequences	129

# LIST OF TABLES

J	Page No.
Table 1.1. Features of adhesin proteins of Leptospira interrogans	16
Table 2.1. List of the potent outer membrane proteins and functional motifs identified	by Pfam
and NCBI-CDD databases	37
Table 2.2. List of the potent secretory proteins and functional motifs identified by F	fam and
NCBI-CDD databases	39
Table 2.3. Prediction of molecular functions and biological processes of puta	tive α/β
hydrolases	42
<b>Table 2.4.</b> List of predicted putative $\alpha/\beta$ hydrolases and their physical and chemical pa	rameters
	44
<b>Table 2.5.</b> Virulence and toxin prediction of putative $\alpha/\beta$ hydrolases	45
<b>Table 2.6.</b> Structure validation of putative $\alpha/\beta$ hydrolases	47
Table 2.7. Secondary structure contents of modelled three-dimensional structures of	putative
$\alpha/\beta$ hydrolases	48
Table 3.1. List of chemical reagents and their sources	54
Table 3.2. Composition of 1 litre Luria Bertani Broth (LB) medium	55
Table 3.3. Composition of antibiotic stocks	55
Table 3.4. Composition of agarose gel electrophoresis solutions	55
<b>Table 3.5.</b> Composition of protein purification solutions	56
Table 3.6. Composition of SDS-PAGE solutions	56
Table 3.7. List of primers used in PCR amplification and mutation	57
Table 3.8. PCR reaction compositions	58
Table 3.9. PCR programme used in gene amplifications	58
Table 3.10. Bacteria Strains/plasmids used in this study	59
Table 4.1. List of chemical reagents and their sources	71
<b>Table 4.2</b> List of primers for qRT-PCR	77
<b>Table 4.3.</b> Kinetic parameters of the purified LABH-1	84
Table 4.4. LABH-1 catalyzed kinetic resolution in the enantioselective production	of (R)-1-
phenylethanol	98
<b>Table 4.5.</b> Kinetic parameters of the purified LABH-2	103
<b>Table 5.1.</b> Amino acid residues involved in interactions	126
Table 5.2. Identity of LonA among different Lentospiral species	130

1	7	1
		,

**Appendix Table 1.** List of Uniport IDs potent outer membrane and secretory proteins 172

#### **ABBREVIATIONS**

ANN Artificial neural network

bp Base pair

BLAST Basic local alignment search tool

BSA Bovine Serum Albumin

C4BP C4b binding protein

CCMB Centre for Cellular and Molecular Biology

CD Circular Dichroism

DALY Disability Adjusted Life Years DNA Deoxyribose Nucleic Acid

ECM Extracellular matrix

EDTA Ethylene diamine tetraacetic acid

EMJH Ellinghausen – McCullough-Johnson – Harris

FH Factor H

GRAVY Grand average hydropathicity

HCl Hydrochloric acid

IPTG Isopropyl thio-β-D-galactoside

LABH Leptospiral  $\alpha/\beta$  hydrolase

LcpA Leptospiral complement regulator-acquiring protein A

LB Luria Bertani broth
LPS Lipopolysaccharide

MAT Microscopic Agglutination Test

MSCRAMMs Microbial surface components recognizing adhesive matrixmolecules

MPD 2-Methyl-2, 4-pentanediol

MQ Milli-Q

NCBI National Center for Biotechnology Information

NTA Nitrilotriacetic acid

PAGE Poly acrylamide gel electrophoresis

PAMP Pathogen-associated molecular patterns

PBS Phosphate Buffer Saline

PCR Polymerase Chain Reaction

PDB Protein data bank

PEG Polyethylene glycol

PMSF Phenylmethylsulfonyl fluoride

Rg Radius of gyration

RMSD Root Mean Square Deviation

RMSF Root Mean Square fluctuation

RNA Ribonucleic Acid

SDS Sodium Dodecyl Sulfate

SUMO Small Ubiquitin-like Modifier
TAE Tris base, acetic acid and EDTA

TE Tris EDTA

TEMED Tetramethylethylenediamin

# **UNITS AND MEASUREMENT**

# **Unit of Length**

nm nanometre

μm micrometre

Å Angstrom

#### **Unit of Concentration**

mg/ml milligram/millilitre

M Molar

mM millimolar

μM micromolar

# Unit of weight

gm grams

mg milligram

kDa Kilo Dalton

μg microgram

#### **Unit of Volume**

l litre

ml millilitre

μl microliter

# **Unit of Temperature**

°C Degree Celsius

K Kelvin

# Preface

Ever since Adolph Weil identified *Leptospira interrogans* as the causal agent of leptospirosis in 1886, it remained one of the most common widespread zoonosis globally. It has emerged as an important public health problem worldwide (Palaniappan et al. 2007). Leptospira colonizes a wide range of hosts, including humans and domestic and wild animal species. A severe form of the disease is characterized by Jaundice, multi-organ failure (Weil Syndrome), or pulmonary hemorrhage syndrome (Ko et al. 2009a). There is no effective vaccine, and the current vaccine (inactivated whole cell) doesn't induce long-term protection and does not provide crossprotective immunity against leptospiral serovars (Palaniappan et al. 2007). Though antibiotics are effective in treating only the early stage of leptospirosis, few are associated with a severe reaction, such as Jarisch-Herxheimer's reaction (Guerrier and D'Ortenzio 2013). Hence, emphasis is being given to identifying novel virulent factors by exploring outer membrane proteins. Virulent factors of leptospires are poorly characterized (Picardeau 2017). A few virulent factors from pathogenic *Leptospira* include outer membrane/ surface proteins crucial for evading the immune response and successful colonization in the host (Fraga et al. 2016). The Chapter 1 discusses about leptospirosis, pathogen leptospira and involvement of outer membrane/surface and secretory proteins in pathogenesis. Like other pathogens, Leptospira also uses a range of strategies to avoid or successfully evade the complement system, an important arm of the host's innate immunity. Pathogenic Leptospira binds soluble host complement regulators via surface proteins such as Leptospiral endostatin-like proteins A and B (LenA and LenB) (Verma et al. 2006; Stevenson et al. 2007), Leptospira immunoglobulinlike proteins (LigA and LigB) (Castiblanco-Valencia et al. 2012) and Leptospiral complement regulator-acquiring protein A (LcpA) (Barbosa et al. 2010). These proteins have been shown to bind more than one complement regulator and seem to be involved in immune evasion, adhesion, and invasion by interacting with ECM and plasma proteins such as plasminogen (PLG) (Choy 2012). Stunningly, a single LcpA protein binds to the C4b binding protein (C4BP), Factor H (FH), and complement component of the terminal pathway, C9, and hence plays a critical role in hijacking the host complement system (Breda et al. 2015).

Apart from adhesion and acquiring the complement regulators, LigA from Leptospira has recently been demonstrated in hydrolyzing activity, which may involve hydrolyzing the DNA of neutrophil extracellular traps (Kumar et al. 2022a). In addition, one of the secretory proteases, thermolysin, reportedly engages in complement evasion by degrading a complement factor, C3 (Chura-Chambi et al. 2018). These reports suggest that *Leptospira* possess a diverse function in their OMPs and secretory protein components, which may involve modulating the host proteins for establishing successful infection. Only a few from this set of proteins possess hydrolytic functions that have been reported to date.

Several proteins with hydrolytic functions usually possess an  $\alpha/\beta$  hydrolase superfamily fold. The  $\alpha/\beta$  hydrolase fold generally consists of a core of five to eight  $\beta$ -strands connected by  $\alpha$ -helices (Hotelier et al. 2004). These proteins catalyze the hydrolysis of a wide range of ester, amide, and thioester bonds and are involved in many biological processes. The members of the  $\alpha/\beta$  hydrolase superfamily include lipases, esterases, serine proteases, epoxide hydrolases, and acetylcholinesterase (Nardini and Dijkstra 1999). Very recently, it has been shown that a secretory lipase of *S. aureus* hydrolyzes TLR ligands and is involved in immune evasion (Chen and Alonzo 2019). Therefore, we addressed three queries: first, do the outer membrane and secretory hydrolytic enzymes remain unidentified? Second, what are the biochemical and structural characteristics features of those enzymes? Third, what are the structural basis of interactions of one of the outer membrane proteins, a Leptospiral complement regulator-acquiring protein  $\underline{A}$  (LcpA) with host complement regulators?

**Chapter 2** addresses the first question. It explains the prediction of potent outer and secretory proteins from the whole proteome (total number of proteins: 3654) of *Leptospira interrogans*. Then, the proteins with probable enzymatic activity were identified using different

bioinformatics tools. The proteins with enzymatic activity include proteases,  $\alpha/\beta$  hydrolases, nucleases, kinases, oxidases, reductases, glycosyl hydrolases, etc. LIC\_12988 and LIC\_10995 were *in-silico* characterized as putative  $\alpha/\beta$  hydrolases. The blast of LIC\_10995, LIC\_11183, LIC\_11103, LIC\_11463, and LIC\_12988 against the UniProtKB Swissprot database revealed their sequence identity of approximately 20-37% with the previously reported lipases or esterases from different organisms. These proteins possessed a conserved consensus lipase motif G/AXSXG. The sequence alignment of all five putative  $\alpha/\beta$  hydrolases with two known lipases that also belong to an  $\alpha/\beta$  hydrolase superfamily revealed the conservation of catalytic triad residues (serine nucleophile, histidine, and aspartic acid residue) in the LIC\_11463, LIC\_11463, and LIC\_12988 proteins.

Protein structure and folding study of LIC\_12988, LIC\_11463, LIC\_11183, LIC\_11103, and LIC\_10995 proteins are not available yet. Therefore, these proteins were modelled using an artificial intelligence-based homology modelling system using AlphaFold. Structures were modelled with considerable Ramachandran plot statistics and ProsA Z-scores values. These modelled structures possessed ideal bond lengths and angles. On-an-average structural models comprised sixteen α-helices and seven β-strands. The average secondary structure composition of the structure models had 42.40 % and 12.15 % α-helices and β-strands, respectively. Significant structural alignment was not observed among the five structure models. Interestingly, the canonical lipase motif (G/AXSXG) was conserved and observed to be structurally superimposed among the five. The nucleophilic serine of the catalytic triad is present in the lipase motif.

Chapter 3 reports the cloning, expression, and recombinant purification of Leptospiral  $\alpha/\beta$  hydrolases (LABHs) such as LABH-1 (LIC\_11463) and LABH-2 (LIC\_11103). Part of the chapter also reports on the oligomeric state of these recombinant proteins in solution. The size

exclusion chromatography results showed that LABH-1 and LABH-2 exist as the monomers in the solution.

Chapter 4 contains results on biochemical characterization and substrate selectivity of LABHs. Since the LABH-1 contains an  $\alpha/\beta$  hydrolase fold, conserved catalytic triad (Ser-Asp-His), and possesses a conserved lipase motif (Ala-X-Ser-X-Gly), it may have esterase or lipase activity. Moreover, LABH-2 also contains an  $\alpha/\beta$  hydrolase fold, a conserved lipase motif (Ala-X-Ser-X-Gly), but lacks the histidine in the catalytic triad. Therefore, we have biochemically and biophysically characterized the LABH-1 and LABH-2 to understand such proteins fully. At room temperature, its hydrolytic activity was assayed with a non-natural substrate, p-nitrophenyl butyrate. Protein-catalyzed hydrolysis of *p*-nitrophenyl butyrate to p-nitrophenolate has confirmed that the purified proteins are enzymatically active.

Usually, esterases and lipases display enzymatic activity over the broader range of temperature and pH. Hence, the impact of pH and temperature on the LABH's hydrolytic activity was also assayed using the same substrate. The LABH-1 displayed the optimum activity at pH 8, while LABH-2 showed optimum activity at pH 8.5. This observation suggests that the purified LABHs preferred alkaline pH for its activity. Temperature is an essential parameter for the catalytic activity of an enzyme. Various α/β hydrolases exhibit different thermostability due to structural diversity and secondary structure contents. Lipases display a range of optimum temperatures. For example, an extracellular lipase from *A. niger* GZUF36 showed maximum activity at 40 °C (Xing et al. 2021). An esterase from *T. tengcongensis*, thermophilic lipases from *Burkholderia ubonensis* and *Janibacter* spp R02 exhibit optimum temperatures of 65 and 80 °C, respectively (Rao et al. 2011; Yang et al. 2016; Castilla et al. 2017). The activity of LABH-1 and LABH-2 was investigated under different reaction temperatures (25-80 °C), and LABH-1 displayed the highest activity in the range of 50- 65 °C while LABH-2 was at room temperature (25 °C).

To identify the substrate specificity, the hydrolytic activity was examined against the pnitrophenyl acetate, p-nitrophenyl butyrate, p-nitrophenyl laurate, and p-nitrophenyl palmitate at pH 8 for LABH-1 and pH 8.5 for LABH-2. Both LABH-1 and 2 showed highest activity  $(V_{\text{max}})$  with the substrate p-nitrophenyl acetate followed by p-nitrophenyl butyrate. The Vmax, Kcat, Kcat/Km of LABH-1 was 1795.55±79.51 μmol·min<sup>-1</sup>mg<sup>-1</sup>, 29.93± 1.33 (s<sup>-1</sup>) and  $82.17\pm12.1$  (s<sup>-1</sup>mM<sup>-1</sup>), while of LABH-2 was  $12.65\pm1.86$ ,  $0.21\pm0.03$  and  $0.16\pm0.006$ . This study shows that LABH-1 outperformed LABH-2 in the kinetic study. Further, the active site mutant (S151A) LABH-1 protein did not display any activity, suggesting the catalytic role of Ser151 in the native LABH-1. The inhibitory effect of Lipase inhibitor or listat on LABH-1 was investigated. Interestingly, a decrease in LABH-1 activity was observed with an increasing concentration of orlistat. However, the  $K_{\rm M}$  remained the same. The Lineweaver-Burk plot of LABH-1 inhibition by increased concentration of orlistat using p-nitrophenyl butyrate as the substrate suggests it could be non-competitive. Moreover, the IC50 value of the orlistat was ~1.8 µM. In addition, LABH-1 catalyzed kinetic resolution of racemic 1-phenylethyl acetate revealed excellent enantioselectivity in producing (R)-1-phenylethanol, a valuable chiral synthon in several industries. To determine the three-dimensional structure of LABH-1, the purified LABH-1 was subjected to crystallization screening. Few crystallization conditions were obtained. Those conditions were improved to get diffraction-quality crystals. Despite successful crystallization, the crystals could not diffract with good resolutions. Hence, the 3Dstructure could not be solved experimentally. The 3D model was generated with the alpha fold, and the same was utilized for molecular docking with substrate and inhibitor to identify preferred binding sites. Docking results show the binding site of the substrate is near the catalytic site, different from that of the inhibitor, which supports our inhibition assay results. Moreover, LABH-1 showed some immunomodulatory effects when treated with the mouse macrophage cell line RAW264.7. This study demonstrates the biochemical and structural

characterization of two (LABH-1 and LABH-2) from the predicted Leptospiral  $\alpha/\beta$  hydrolases. Moreover, LABH-1 can be a potentially pathogenic component for the host.

Chapter 5 discusses the study on biophysical characterization and interaction study of Leptospiral complement regulator-acquiring protein A (LcpA) with the complement regulators C4BP and FH. The outer membrane protein LcpA was cloned into a pET23a vector, heterologously expressed into BL21 (DE3) expression cells, and purified using a refolding protocol with the outstanding yield of 25mg from 1 L of bacterial culture. Since LcpA is an outer membrane protein of *Leptospira*, which was isolated using a refolding procedure, it is important to examine its secondary structure composition and the effects of varying pH and temperature. In our investigation, secondary structure contents were determined from the data derived from CD spectroscopy using the Dichroweb analysis tool. It showed  $\alpha$ -helical content of 18% and β-strands of 34% in the purified protein at pH 7. Interestingly, the theoretical estimation of secondary structure contents yielded 23% and 41% α-helix and β-strands, respectively, which are similar to the experimental values. However, the non-covalent interactions in any molecule are disturbed when it is subjected to physical changes, such as a change in temperature or pH. In proteins, variation in pH and temperature causes the globules to unfold and the helical structure to uncoil. As a result, the biological activity of proteins gets disturbed. As expected, the structure composition was changed when it shifted from neutral to acidic pH and even at an alkaline pH of 10. However, there were no significant structural changes with the pH range of 7.5 to 9. Moreover, thermal stability analysis using CD spectroscopy where different spectra were recorded at varying temperature points starting from 20°C to 85°C. The plot of the fraction of unfolded protein Vs. Temperature displayed a Tm value of 55°C, indicating the protein's moderate thermostability.

The zinc-acquiring outer membrane proteins bind to FH, which leads to complement evasion (Moulin et al. 2019; Sharma et al. 2020). We found the Zinc finger motif in LcpA

using bioinformatic analysis. In addition, the fluorescence spectroscopy results revealed an increase in fluorescence intensity and a considerable shift in wavelength with increasing Zn<sup>2+</sup> concentrations. This demonstrates unequivocally that zinc binding introduces conformational changes in LcpA. The CD spectroscopy findings demonstrated the modifications in secondary structure compositions with protein-to-zinc ratios of 1:1 and 1:2. The percentage of  $\alpha$ -helices increased and decreased in  $\beta$ -strands when LcpA was incubated with increasing moles of ZnCl<sub>2</sub> in the ratio of 1:1 and 1:2. This depicts Zn<sup>2+</sup> ions binding to LcpA. Furthermore, the purified LcpA was subjected to crystallization screening, and we successfully found some crystallization conditions. Despite successfully crystallizing LcpA, its structure remained unsolved due to poor resolution. Therefore, the LcpA three-dimensional protein structure was generated using AlphaFold, followed by structure validation using Ramachandran plot statistics and ProsA Z-scores values. Additionally, the complement regulators C4BP and FH binding regions on LcpA were identified using molecular docking followed by molecular dynamics simulation. C4BP and FH bind to N-terminus to mid-region residues of LcpA where few residues such as His13, Arg55, Arg92, Glu94, and Glu115 are common.

Chapter 6 discusses all results obtained in our study in the context of *Leptospira*. Overall, this study improves the fundamental understanding of outer membrane and secretory hydrolases and their substrate preferences in vitro. In addition, the study on the complement regulators acquiring proteins, LcpA, from *Leptospira* provides basic information about the interacting residues of LcpA where human complement regulators C4BP and FH bind. This information may be utilized to develop preventive strategies to interfere with C4BP and FH binding.

# Chapter-1

Introduction and Review of literature

#### 1.1. INTRODUCTION

Ever since Adolph Weil identified *Leptospira interrogans* as the causal agent of leptospirosis in 1886, it remained one of the most common widespread zoonosis in the globe. Several cases are reported in tropical regions where environmental moisture favours the survival of the pathogen. Leptospirosis is one of the 17 neglected tropical diseases and is reported to be highly endemic in South Asian regions, Oceania, Caribbean, regions of sub-Saharan Africa, and regions of Latin America. In South Asia, countries such as India (19.7 cases per 100,000 population), Indonesia (39.2 per 100,000 population) are reported to be highly endemic for the disease (WHO Report, 2011 and Costa et al. 2015). Leptospirosis primarily affects farmers, veterinarians, dairy workers, military personnel and all those who come into close contact with animals or with contaminated urine, water, food, soil, mud etc. Portals of entry into the host body include skin cuts, abrasions or mucosal membranes like oral, eye and genital surface membranes. Leptospira colonizes in the host and successfully establishes infection mainly through the outer membrane and secretory proteins, which are mostly structural or enzymatic in functions. The symptoms of leptospirosis overlap with other diseases such as malaria, dengue, influenza, murine typhus, spotted fevers, etc. Leptospirosis imposes serious human and veterinary health problems. Leptospira has the ability to establish infection in a broad range of hosts that include rodents, livestock, domestic animals like dogs and cats, while humans are considered incidental host (Karpagam and Ganesh 2020; Dirar 2021).

#### 1.2. Leptospira, the disease-causing spirochete

#### 1.2.1. Size and morphology

*Leptospira* is a thin, motile, spiral-shaped, slow-growing aerobic bacteria comprising of pathogenic, saprophytic and non-pathogenic species. Due to its slim, slender shape and high motility, it cannot be visualised under normal light microscopy. However, dark field and scanning electron microscopy are suitable techniques for visualizing *Leptospira*. Under dark-

field microscopy, the size of *Leptospira* is about 0.15 μm in diameter, 10–20 μm in length and possesses an unusual hook shaped-end which gives an unique identity from other spirochetes (**Figure 1.1A**) (Ko et al. 2009b; Abe et al. 2020). The movement of cells in a single direction is driven by an irregular arrangements of cell morphology at the anterior and posterior ends (**Figure 1B**).

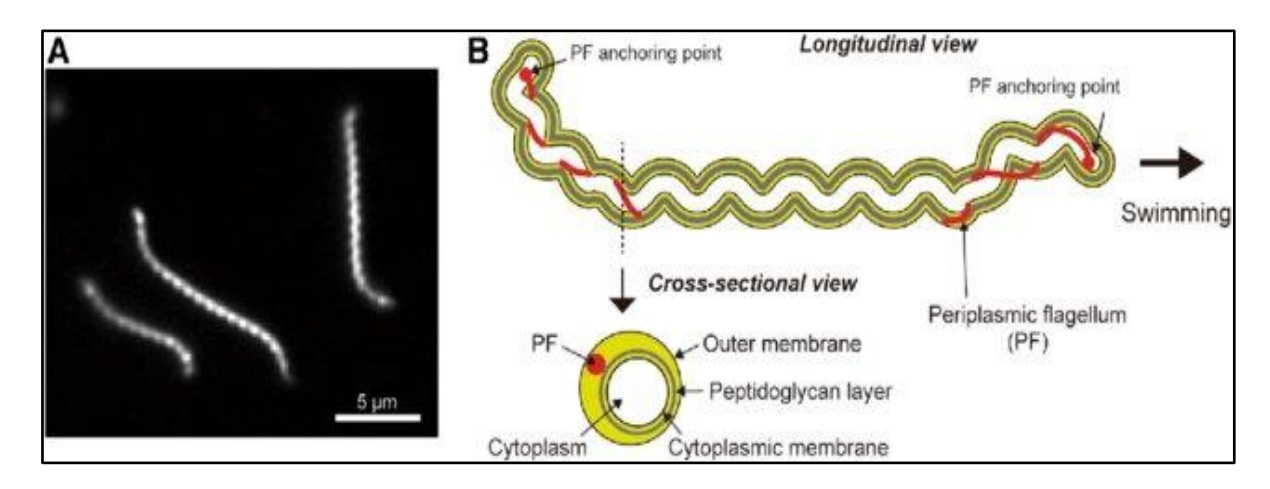


**Figure 1.1. Architecture of** *Leptospira species*. **(A)** Dark-field microscopy image of thin, helical, *Leptospira*, **(B)** Morphology of *Leptospira*; cell depicts spiral shaped anterior part (Right end) and the hook shaped posterior part (left end) (Adapted from Abe K et al, *Scientific reports*, 2020).

Unlike other spirochetes, the cell envelope of *Leptospira* possesses a unique characteristics feature. Its outer cell envelope usually consists of a characteristic LPS layer which makes the basis to classify it into 24 serogroups and more than 250 serovars (Evangelista and Coburn 2010; Picardeau 2017).

#### 1.2.2. Classification and taxonomy

The membrane of *Leptospira* shares the characteristic features of Gram-positive as well as Gram-negative bacteria. A double membrane and LPS are the features of Gram-negative bacteria, while the relationship between the peptidoglycan layer and inner cytoplasmic membrane depicts the Gram-positive envelope architecture (Evangelista and Coburn 2010).

The Leptospires belong to the order Spirochaetales and family Leptospiraceae. The detailed taxonomic classification is described in **Figure 1.2A**. The order Spirochaetal consists of two families, Spirochaetaceae and Leptospiraceae. The genus Treponema, Serpulina and Borrelia belong to Spirochaetaceae. A causal factor of leptospirosis, the genus *Leptospira* corresponds to Leptospiraceae family (**Figure 1.2B**) (Ko et al. 2009a; Mohammed et al. 2011; Chiriboga et al. 2015).

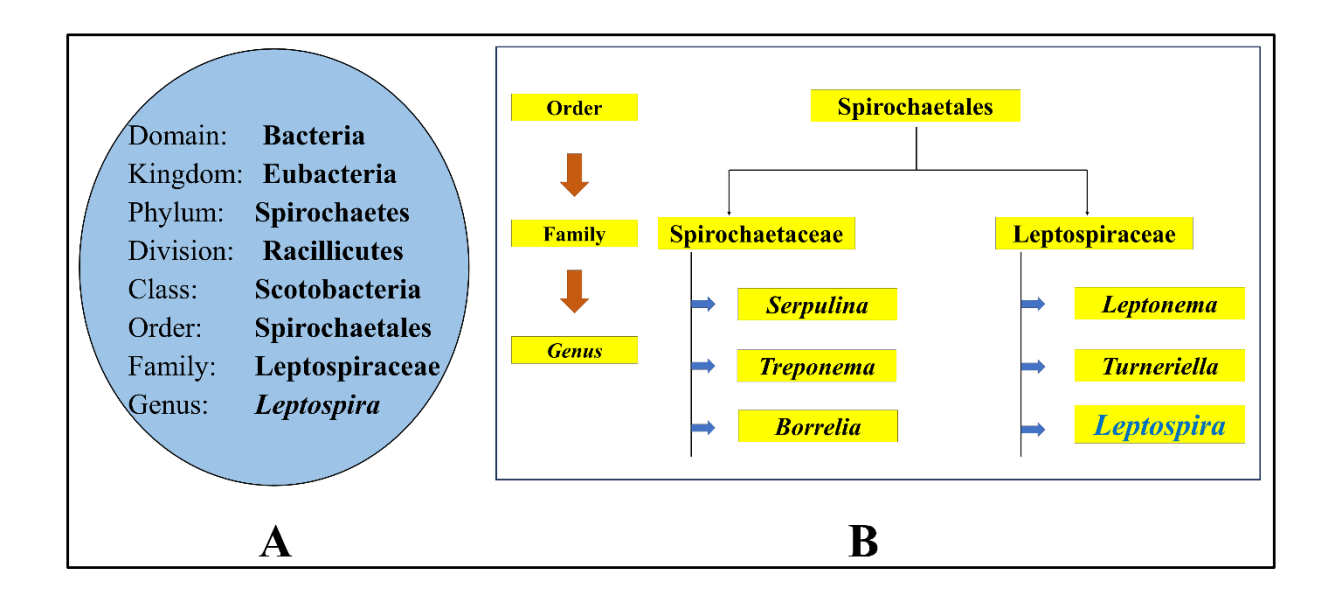


**Figure 1.2. Taxonomy classification system. (A)** Taxonomical classification of *Leptospira* (B) Detailed categorization of Spirochaetes of order Spirochaetales.

As per the 16S rRNA-based phylogram, the genus *Leptospira* is further categorized into the pathogenic, non-pathogenic, and intermediates types (Lehmann et al. 2014). **Figure 1.3** depicts the genetic diversity of the genus *Leptospira*. The pathogenic, intermediates and non-pathogenic *Leptospira* consist of ten, seven and five species, respectively. Furthermore, *Leptospira species* are sub-divided into approximately 300 serovars based on their diversity in carbohydrate contents of lipopolysaccharides (LPS) of the outer membrane and are assigned to >24 serogroups (Picardeau 2017).

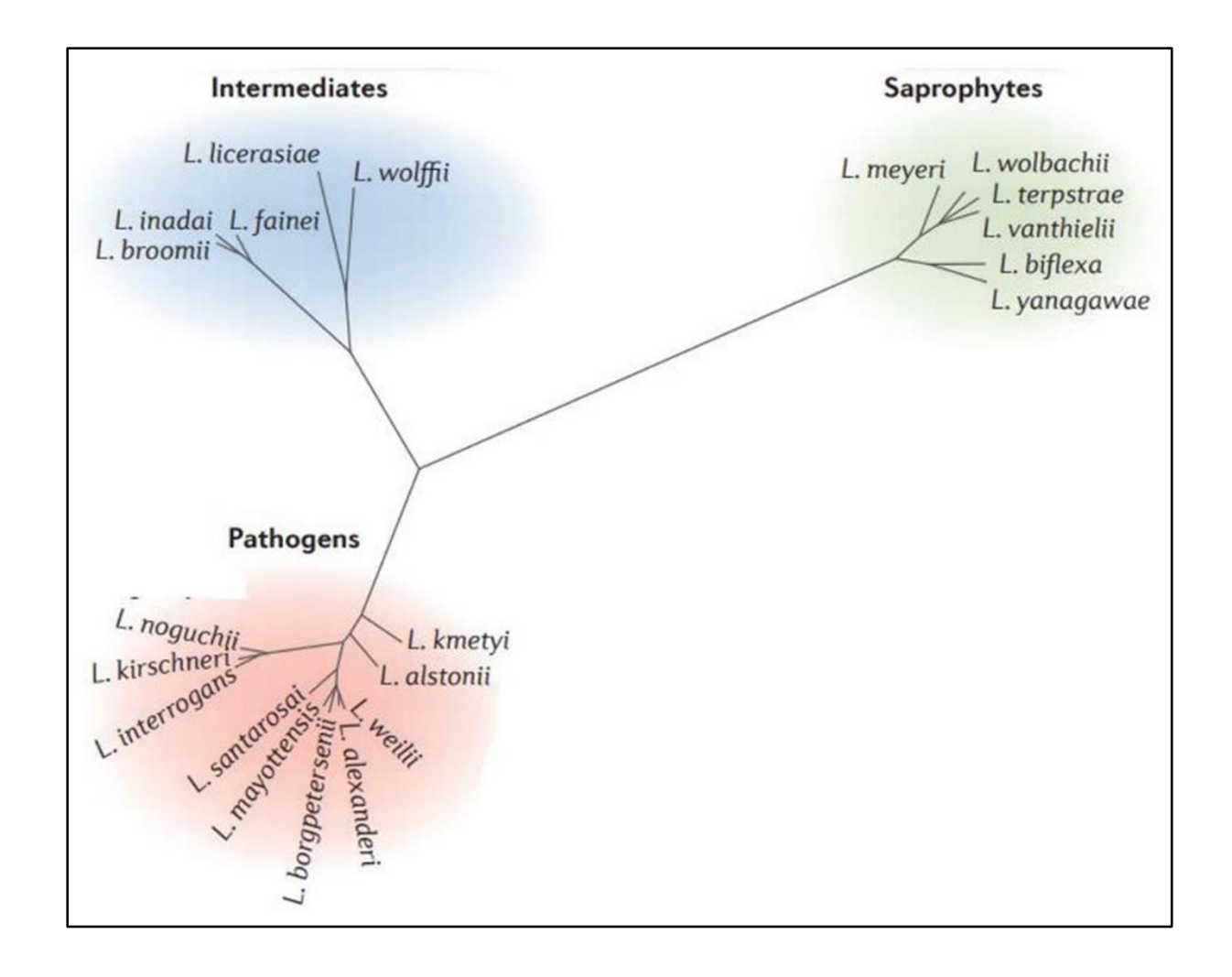


**Figure 1.3. Phylogenetic study of** *Leptospira* **based on 16S rRNA analysis** (Adapted from Picardeau, 2017, *Nat Rev Microbiol*).

#### 1.2.3. Cell biology

Leptospires are obligate aerobic bacteria, and the survival time of *Leptospira* reduces in environment other than its hosts. Survival of *Leptospira* depends on several environmental components such as pH, temperature, presence of disinfectants, etc. They are able to survive in particular circumstances, such as alkaline soil, mud, river water, and different organs of host animals. *Leptospira* prefers 28 to 30 °C temperature, pH of 7.2 to 8 and high humidity for its growth (Mohammed et al. 2011; Casanovas-Massana 2018). The motility of the cell is a function of two flagella emerging from both ends of the *Leptospira*. The genes encoding a flagella and motility of the bacterium are *flab*, and *fliY*. The pigs injected with *Leptospira* 

*Interrogans* mutated with *fliY* gene shows higher survival rate compare to that of wild type *Leptospira interrogans*, displayed the functional role of flagella and the movement of *Leptospira* into the pathogenesis (Evangelista and Coburn 2010).

#### 1.2.4. In-vitro cultivation

The average generation time of *Leptospira* is 6 to 16 hours in the Ellinghausen McCullough Johnson Harris (EMJH) medium, and few pathogenic strains grow even slower. The EMJH medium is commercial medium used to culture leptospires which is supplied with high carbon chain fatty acids, chlorides, sulphides, vitamins, tween 80 and 1% BSA. (Hornsby et al. 2020; Guedes et al. 2022). The fatty acids are the sole carbon source of leptospires, which are metabolized by  $\beta$ -oxidation. The contaminations in the media are restricted by sterilizing water and base medium and using the 5-fluorouracil and antibiotics like, nalidixic acid or rifampicin. The microscopic investigations displayed the ability of leptospires to cluster together and produce biofilm, which is helpful to its survival from physical and chemical stress factors (Meganathan et al. 2022).

#### 1.3. Leptospirosis, the disease

Leptospirosis is a systemic, zoonotic, and widespread infectious disease (Bharti 2003; Adler and de la Pena Moctezuma 2010). The disease is becoming more common due to increased urbanization, intensive farming, and climatic changes and their ability to transmit from animals to humans through a direct contact or indirectly with contaminated food, water, and environment (Mcarthur 2019; Suminda et al. 2022). Symptoms are non-specific and it resembles to other medical conditions such as high fever, vomiting, jaundice, headache, chills, malaise, and muscle aches. Due to similar symptoms with other diseases, diagnosis of many human leptospirosis cases are quite challenging (Bharti 2003; Haake 2015). The icteric phase of the disease, known as Weil's disease, is linked to multi-organ failure including kidney, heart, CNS, and muscles which may lead to death (Nguyen and Chimunda 2023).

#### 1.3.1. Phases of Leptospirosis

It includes mainly two phases: Leptospiremic and Immune phase.

#### 1.3.1.1. Leptospiremic phase

Leptospiremic phase is also known as acute phase or septicemic phase. It usually starts within 2-14 days post infection and persists for three to 10 days. The sudden onset of flu-like symptoms and presence of bacterium in blood are the typical feature of leptospiremic phase. The hosts in Leptospiremic phase show mild or no symptoms.

#### 1.3.1.2. Immune phase

Immune phase is also known as the delayed phase where *Leptospira* bacteria is disseminated in various organs of the host. In immune phase, Leptospira is mostly concentrated in kidney also found in liver and lung. Severe symptoms are observed in immune phase which may lead to Weil's syndrome where the fever, jaundice, pulmonary haemorrhages, kidney dysfunction are the common symptoms.

#### 1.3.2. Mode of transmission

From the source of infection, such as contaminated urine, water, food, soil, mud, aborted fetuses, *Leptospira* enters into the body of the host by engulfing the contaminated water, food or through eyes, nose, vagina, or via abraded skin of the host. The main carriers of the pathogen are rodents like mice, rat where the *Leptospira* persists without affecting the host. Rodents carry the pathogen throughout their lives and are, therefore, known as permanent carrier. Other reservoirs, such as domestic animals like cattle, dogs, sheep, pigs, etc, carry the pathogen for months, and are called temporary carrier (**Figure 1.4**). However, humans are known as incidental hosts for *Leptospira species*.

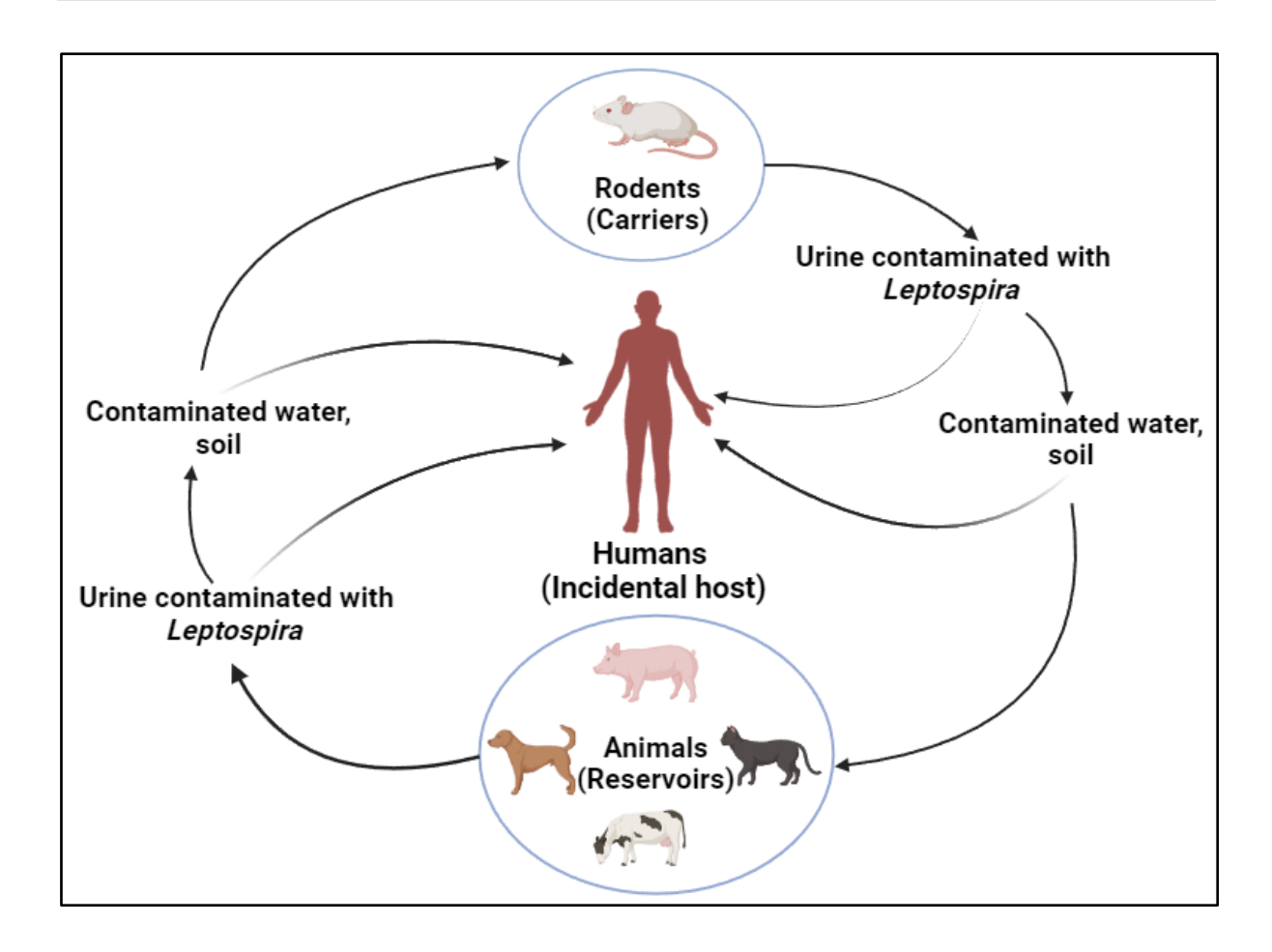


Figure 1.4. Transmission cycle of Leptospira

#### 1.4. Diagnosis of the disease

Leptospirosis is suspected in the patients depending primarily on clinical symptoms such as high fever, vomiting, jaundice, headache, chills, malaise, and muscle aches. According to the regional epidemiology of infection, if patients have experienced an outbreak of the disease due to flood situations, need a laboratory test for the infection.

#### 1.4.1. Laboratory approaches

Several laboratory tests have been developed to diagnose the disease based on molecular, microscopic, and immunological techniques. The blood sample is collected during the first ten days of illness, and if it is more than ten days, then urine sample is preferred for detection. The various laboratory tests have been developed and are listed in **Figure 1.5. A** dark field microscope is used to identify the *Leptospira* from the blood or urine sample. A polymerase

chain reaction is one of the important tools to detect pathogens in the early phase of infection. In addition, the microscopic agglutination test (MAT) is the gold standard method for serological diagnosis of *Leptospira*. The traditional ELISA method is also used to detect anti-*Leptospira* IgM and IgG antibodies in serum.

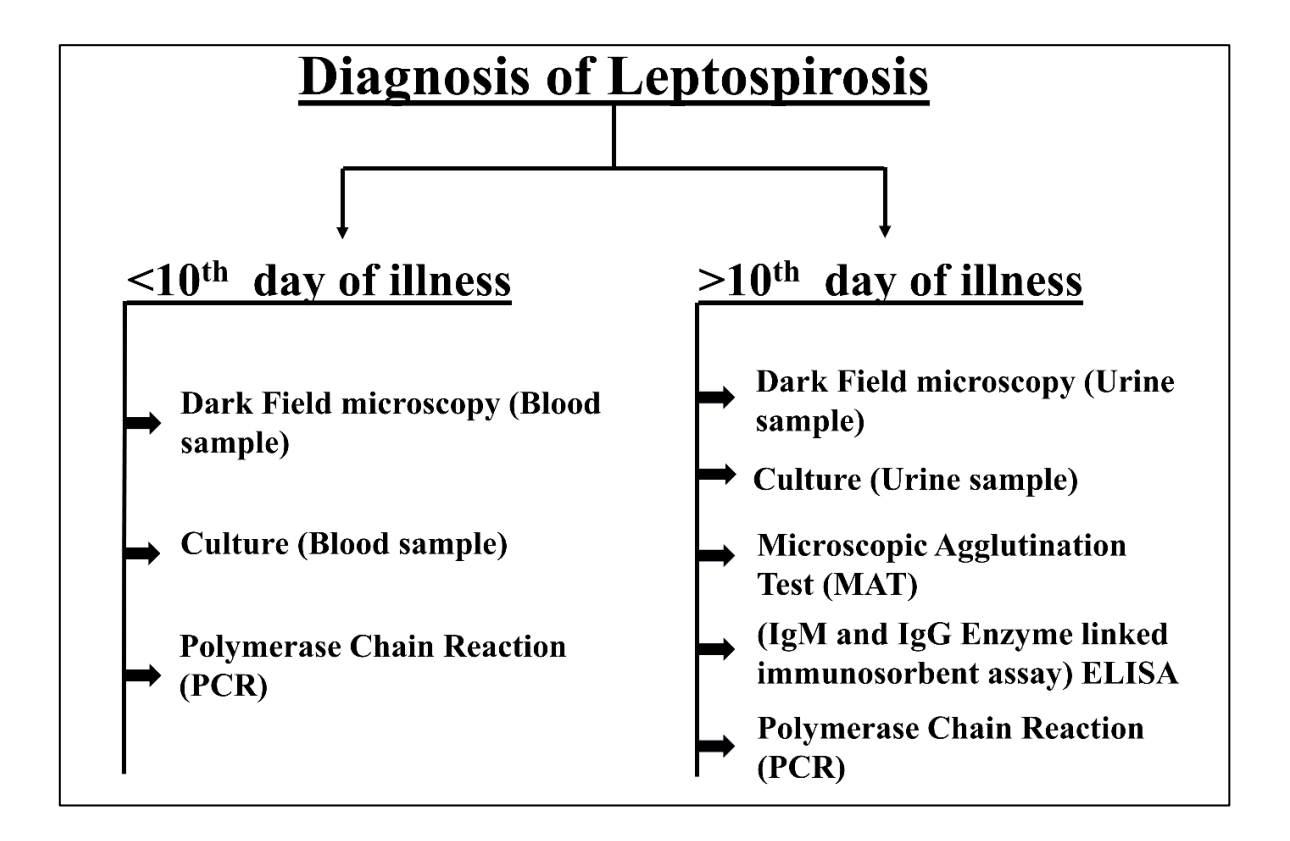


Figure 1.5. Laboratory tests for the diagnosis of *Leptospira*.

#### 1.4.2. Challenges in diagnosis

Since the symptoms of Leptospirosis are not specific, the accurate diagnosis is a challenging task. The disease is always confused with other diseases, like malaria, dengue, influenza, murine typhus, spotted fevers, etc. The widely used diagnostic methods for Leptospirosis are serological tests comprising of the Microscopic Agglutination Test (MAT) and ELISA.

The MAT is a sensitive technique and detects IgM and IgG classes of agglutinating antibodies. In the early phase of infection, it also gives false negative results as IgM detectable to MAT is produced after eight days of infection. Moreover, it also needs both technical expertise as well as maintenance of various live *Leptospira* standard cultures. Therefore, it becomes tough for routine laboratory use. ELISA is most widely used diagnostic method for detecting IgM and IgG antibodies in a patient's serum sample. The limitation of this technique is the possibility of false positive results, as IgM and IgG cannot be detected in the early stage of infection (Budihal and Perwez 2014).

#### 1.5. Global burden

Leptospirosis carries huge geographical distributions, is predominantly found in tropical regions, and causes larger epidemics during rainy season and also due to floods (Costa et al. 2015; Haake 2015). With approximately 1 million cases reported annually and 60,000 deaths, it is perceived as a public health concern globally (Costa et al. 2015; Dunay et al. 2016; Putz and Nally 2020). Leptospirosis occurs predominantly in tropical and subtropical climates. A metric known as DALY (Disability Adjusted Life Years) displays the overall burden of the disease (Figure 1.6). The literature study suggests that worldwide, nearly 2.90 million DALYs are lost annually from the reported 1 million cases. However, this data is highly underestimated due to insufficient knowledge of the disease, vague clinical presentations, and scarcity of diagnostic facilities. Surprisingly, males are largely affected with 2.33 million DALYs which is nearly 80% of the total burden (Torgerson et al. 2015). Tropical regions of Asia, America, and Africa had the highest estimated leptospirosis disease burden (Garba Bashiru & Abdul Rani Bahaman 2018). Prevalence of human leptospirosis was 5 cases per 100,000 people on average worldwide, excluding cases brought on by outbreaks, although it might reach 975 cases per 100,000 people in some places. According to the few studies that have been reported, the African region has the highest median annual incidence (95.5 per 100 000 people), thereafter

the Western Pacific (66.4), the Americas (12.5), South-East Asia (4.8), and Europe (0.5). As many as 975 cases per 100,000 people are reported in some regions (**WHO report, 2011 and** (Costa et al. 2015).

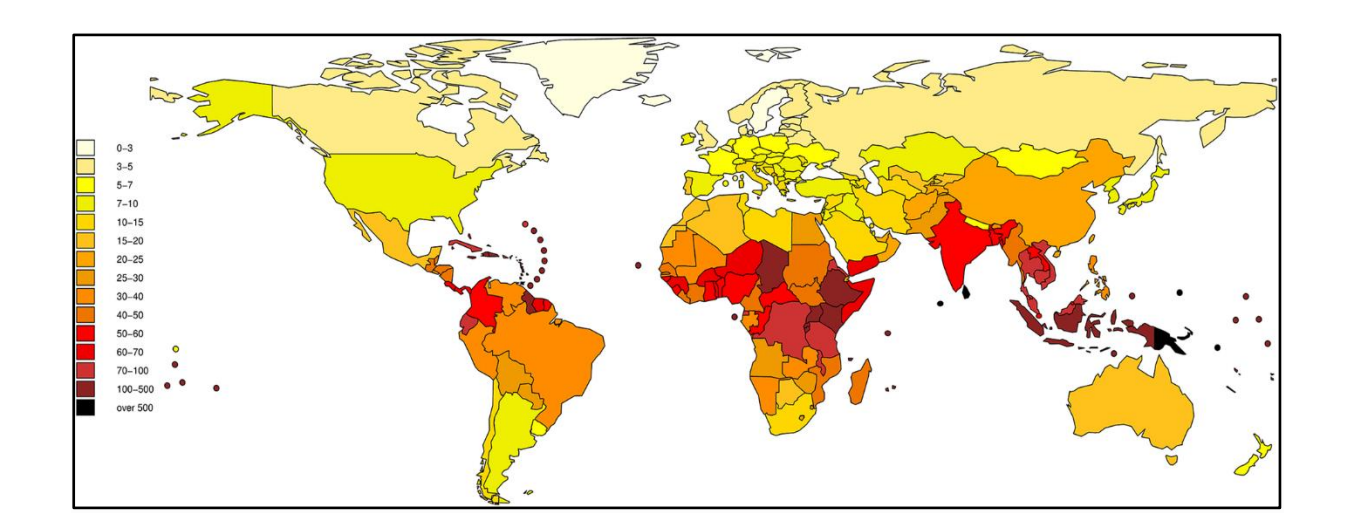


Figure 1.6. Worldwide basis distribution of leptospirosis cases in terms of DALY index (Adapted from Torgerson PR, *PLoS Negl Trop Dis*, 2015).

The bulk of leptospirosis infections in India were discovered in states with high rainfall rates and coastal areas, including Gujarat, Maharashtra, Tamil Nadu, Kerala, and the Andaman & Nicobar Islands (Sambasiva 2003; Izurieta et al. 2008; Sethi et al. 2010).

#### 1.6. Pathogenesis and virulence

Leptospira possesses adhesins on its outer membrane, which help them to attach to the host tissues, especially endothelial cells of blood vessels. These adhesins usually enable Leptospira to establish an infection. The outer membrane is the first point of contact between Leptospira and its surroundings including the mammalian hosts. It is responsible for mediating various interactions, such as nutrient uptake, waste elimination, and interaction with the host targets. The outer membrane architecture of Leptospira and its important biomolecules are shown in Figure 1.7.

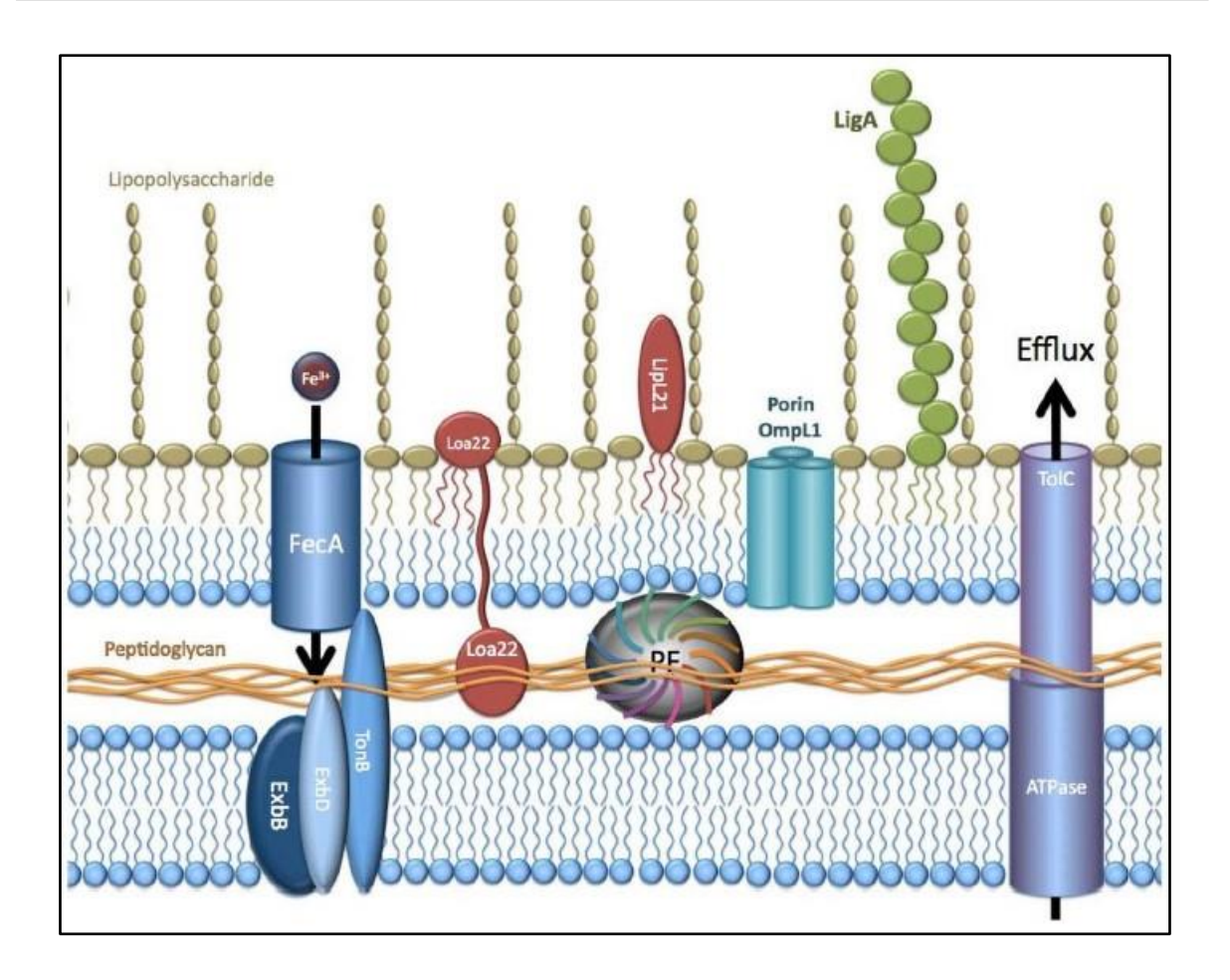


Figure 1.7. Outer membrane architecture of *Leptospira*. (Adapted from Haake DA, *Curr Top Microbiol Immunol*, 2015).

Once the pathogenic *Leptospira* enters into the body of host, very commonly it exists in host bloodstream, hence, widely considered as extracellular pathogen (Samrot et al. 2021). Few reports also suggest the occurrence of *Leptospira* into the peritoneal macrophages, kupffer cells, microglial cells and non-phagocytic cells (Li et al. 2010; Toma et al. 2011; Samrot et al. 2021).

However, the complete mechanism of pathogenesis is enigmatic. *Leptospira* successfully establishes an infection with the help of potential virulent factors such as Lipopolysaccharides (LPS), microbial surface components recognizing adhesive matrix molecules (MSCRAMMs), Lipoproteins, hemolysins, adhesins, and other outer membrane proteins such as LcpA, LigA & B, and secretory proteins such as thermolysins.

# 1.6.1. Lipopolysaccharides

Most Gram-negative bacteria consist of LPS in the outermost leaflet of the outer membrane which are popularly known as Pathogens Associated Molecular Patterns (PAMPS). Such LPS is recognized by host receptors, CD14 and TLR4, which lead to activation of several signalling pathways, including NF-κB and IRF3, and synthesis of proinflammatory cytokines (Park and Lee 2013).

However, leptospiral LPS is unconventional in its binding by host receptors, TLR4. Leptospiral LPS is unable to activate human TLR4 and shows a week stimulation of mouse TLR4 (Nahori et al. 2005; Bonhomme et al. 2020). This characteristic features of Leptospiral LPS triggers the immune evasion phenomenon in *Leptospira* and hence helps in pathogenesis.

# 1.6.2. Microbial surface components recognizing adhesive matrix molecules (MSCRAMMs)

Several pathogens establish infection with the help of a group of outer membrane proteins called microbial surface components recognizing adhesive matrix molecules (MSCRAMMs). The MSCRAMMs play crucial roles in interaction with the host extracellular matrix (ECM), such as fibronectin, collagen, laminin and fibrinogen. MSCRAMMs are important bacterial virulence factors and potential for drugs vaccines targets. Several MSCRAMMs have been found in *Leptospira* as well, and a few of the MSCRAMMs, such as LipL32, LigA, LigB, LenA, Loa22, are found to be involved in the interactions with the host ECM, shown in Figure 1.8 (Syed M. Faisal, Sean P. McDonough 2012).

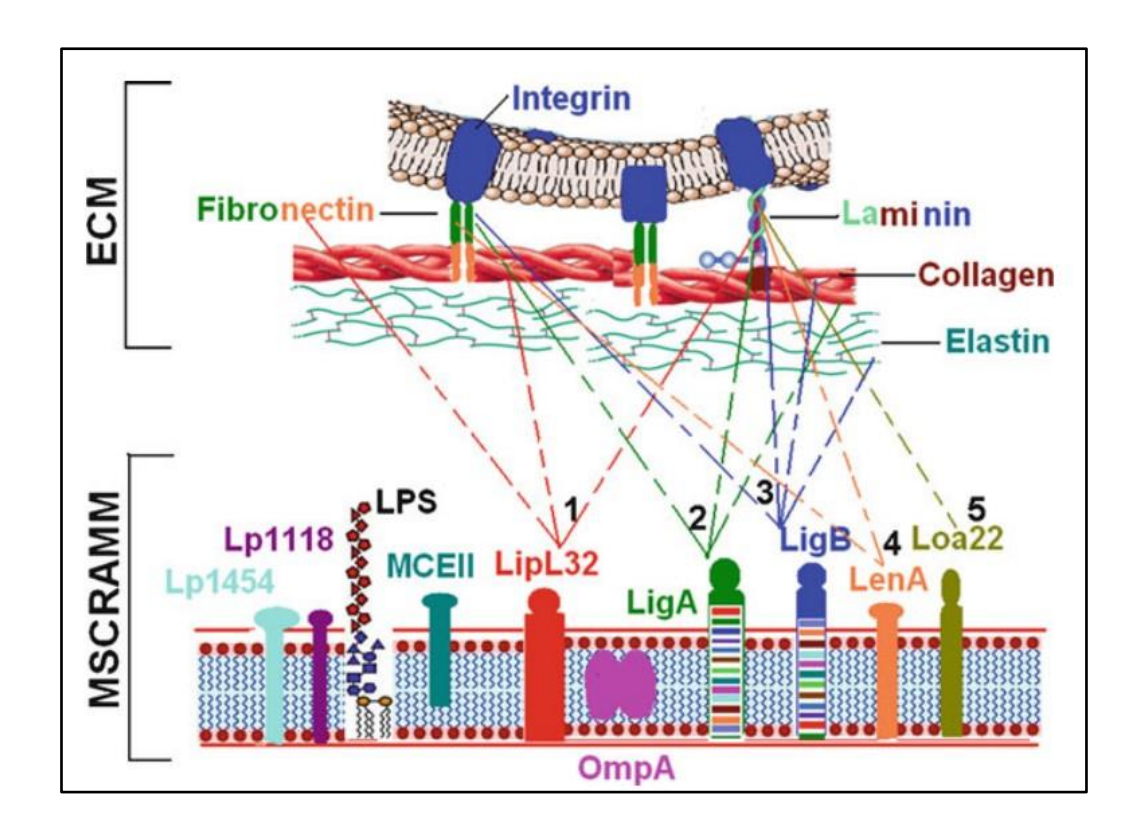


Figure 1.8. Interaction of *Leptospira* MSCRAMM with the host ECMs. (Adapted from Faisal SM et al., *The Pathogenic Spirochetes: strategies for evasion of host immunity and persistence*, 2012).

# 1.6.3. Lipoproteins

Lipoproteins are connected with bacterial membranes through hydrophobic interactions between N-terminal acyl moieties and the phospholipids of the lipid bilayer. Leptospiral lipoproteins are the most abundant membrane proteins comprised of LipL32, LipL53, LipL41, Loa22, HbpA, LipL36, LipL21, and LipL46. The LipL21 and LipL41 are predominantly expressed on the outer membrane interacting with the host ECM components such as collagen IV, laminin, E-cadherin, and elastin. LipL21 and LipL41 are conserved in pathogenic *Leptospira species* and hence are used as diagnostic markers and vaccine candidates (MB et al. 2021). Moreover, the surface-exposed lipoprotein OmpL1 is well known recombinant vaccine that provides an immune protecting role (Garba Bashiru & Abdul Rani Bahaman 2018).

# 1.6.4. Hemolysins

Hemolysins are phospholipases that cleave phospholipids of the host cell membranes. *Leptospira* secrete five hemolysins, Sph1, Sph2, Sph3, HlpA and TlyA and these are well characterized for possessing hemolytic activity. Moreover, these hemolysins are responsible for the higher expression of IL-1b, IL-6 and TNF-a in human and mouse, and considered as potent inducers of proinflammatory cytokines (Wang et al. 2012). *Leptospira* hemolysin SphH is responsible for pore formation on mammalian cell membranes and disrupts the host cells, including erythrocytes (Lee et al. 2002).

# **1.6.5. Adhesins**

*Leptospira* adhere to mammalian cells using different adhesins. The cells were correlated with virulence of pathogens (Thomas and Higbie 1990). The multiple adhesion molecules have a significant role in the adherence of *Leptospira* to ECM components. The ECM components are composed of laminin, collagen type I, collagen type IV, and fibronectin (Barbosa et al. 2006). The leptospiral protein Lsa24 (leptospiral surface adhesin; encoded by LIC\_12906), that binds strongly to laminin (Barbosa et al. 2006).

The Leptospiral adhesins LenB (LIC\_10997), LenC (LIC\_13006), LenD (LIC\_12315), LenE (LIC\_13467), LenF (LIC\_13248) are reported to interact with fibronectin and laminin (Stevenson et al. 2007). Other adhesins such as Lig's, LipL's, Lsa's, OmpL's and their host targets for attachment have been described in Table 1.1. The Lig proteins are identified as markers in the diagnosis of the disease due to their expression in the initial stage of infection. Lig proteins, LigA, B and C are mainly encoded by *Lig A*, *Lig B*, and *Lig C* genes of pathogenic species of *Leptospira*. Several studies have been investigated to establish the role of Lig A and Lig B proteins in adherence with the host ECM components including fibronectin, elastin, tropoelastin, collagen, and laminin (Choy et al. 2007; Figueira et al. 2011; Haake and Matsunaga 2021). The expression level of Lig A and Lig B upregulates in mammalian host

physiological environment such as temperature and osmolarity factors, depicts the role of Lig's in pathogenesis. The knockdown of *ligA* and *ligB* genes, suggests essentiality of at least one lig genes in *Leptospira* infection (Matsunaga et al. 2005, 2013; Haake and Matsunaga 2021). In addition, Lig proteins have the ability to control the host complement pathways by binding with complement regulators such as FH, FHL-1, FHR-1, and C4BP (**Figure 1.11**) (Barbosa and Isaac 2020).

Table 1.1. Features of adhesin proteins of Leptospira interrogans.

Proteins	Gene ID	ECM ligand	Method of detection
Lsa24/ LenA	LIC12906	Laminin	ELISA Western blot
LipL32	LIC11352	Laminin, Collagen I, Collagen V, Collagen IV, Collagen XX, fibronectin	ELISA Phage display¶
LigA	LIC10465	Collagen I, Collagen IV, Laminin, Fibronectin, Tropoelastin	ELISA, SSFS** ITC**
LigB	LIC10464	Collagen I, Collagen IV, Laminin, Fibronectin, Collagen III, Elastin, Tropoelastin, Heparin	ELISA, SSFS**, ITC**, Phage display††
Lsa66	LIC10258	Laminin, Fibronectin	ELISA Protein microarray
Lsa27	LIC12895	Laminin	ELISA
Lsa20	LIC11469	Laminin	ELISA, SPR
Lsa25	LIC12253	Laminin	ELISA
Lsa33	LIC11834	Laminin	ELISA
rLIC12976	LIC12976	Laminin	Phage display, ELISA
Lp95	LIC12690	Laminin, Fibronectin	Western blot

LipL53	LIC12099	Laminin, Collagen IV, Fibronectin	ELISA
Lsa21	LIC10368	Laminin, Collagen IV, Fibronectin	ELISA
Lsa63	LIC10314	Laminin, Collagen IV	ELISA
Lsa30	LIC11087	Laminin, Fibronectin	ELISA
OmpL1	LIC10973	Laminin, Fibronectin	ELISA
OmpL37	LIC12263	Laminin, Fibronectin, Elastin	ELISA
OmpL47	LIC13050	Laminin, Collagen III, Fibronectin, Elastin	ELISA
MFn1	LIC11612	Fibronectin	Protein microarray, Western blot
TlyC	LIC13143	Laminin, Collagen IV, Fibronectin	ELISA

SSFS, steady-state fluorescence spectroscopy; ITC, isothermal titration calorimetry; SPR, surface plasmon resonance. ¶ For laminin and collagen type XX. \*\* For elastin and tropoelastin. †† For heparin. (The review article (Vieira et al. 2014) has been used as the source for the tabular contents).

# 1.7. Host-immune response

The host innate and adaptive immune responses are two arms against *Leptospira* infection. The T-cell mediated immune response in cattle and hamsters involves the production of IFN- $\gamma$  and the proliferation of CD4<sup>+</sup> T-cells after the administration of the killed *L. borgpetersenii* serovar Hardo and *L. interrogans* serovar Pomona. Moreover, the alternative and classical pathways of the complement activation play the important roles in detection and killing of leptospires in the early phase of infection (Meri et al. 2005; Barbosa et al. 2009). However, considering the destructive action of complement pathways, there is a continuous need for regulators that could

negatively regulate the complement activation. At present, Factor H and C4BP are well-studied negative regulators of the complement pathways.

# 1.7.1. Factor H (FH)

Several proteins possessing inhibitory action on the complement system are encoded by the regulators of complement activation (RCA) gene clusters on human chromosome 1q32. Factor H is negative complement regulator, encoded by factor H gene *HF1*, located in the RCA gene cluster. A soluble glycoprotein with a single polypeptide chain of 155 kDa, called factor H, was first reported by Nilsson and Mueller Eberhard in 1965. It contains 20 repetitive domains of approximately 60 amino acids, named complement control protein modules (CCP) or short consensus repeats (SCR) (Ripoche et al. 1988; Rodriguez De Cordoba et al. 2004).

Factor H binds to C3b and promotes the break-down of the C3-convertase. It acts as a cofactor for the serine protease factor I in proteolysis of C3b (Weiler 1976, Santiago 2004). Factor H controls complement activation by 1) participating in C3b binding which results in the unavailability of C3b for factor B binding and hence inhibits the assembling of C3 and C5 convertase enzymes, 2) dislodging the factor Bb from convertases, 3) serving as a cofactor for the factor I during the proteolytic breakdown of C3b (Anne 2012, Weiler 1976, Whaley 1976). These regulatory mechanisms are performed by N-terminal SCR1-4 domains and the target identification is achieved by SCR 19-20 (**Figure 1.9**) (Kopp et al. 2012; Cserhalmi et al. 2019).

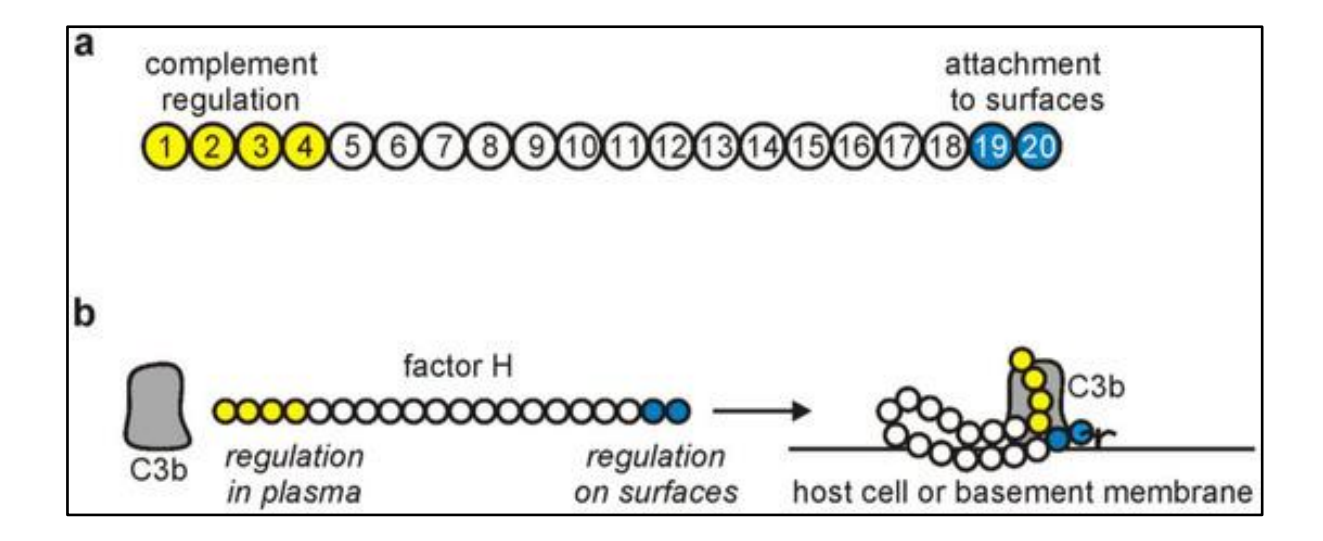


**Figure 1.9. Schematic representation of factor H. a**) FH consists of 20 complement control protein modules with complement binding through CCP1-4 and CCP19-20 shows engagement in attachment to cell surfaces, **b**) CCP19-20 allows binding to host cell surfaces for inhibiting the complement activation. (Figure adapted from (Kopp et al. 2012).

# 1.7.2. C4b binding protein (C4BP)

C4BP is a 570 kDa multimeric glycoprotein made up of seven  $\alpha$ -chains and one  $\beta$ -chain linked by their c-terminal ends in the central core. The open reading frame, encodes  $\alpha$  and  $\beta$ -chains, are located in the RCA gene clusters on chromosome 1q32. The approximate molecular weight of each  $\alpha$ -chain is 70kDa while  $\beta$ -chain is of 45 kDa. Each  $\alpha$ - and  $\beta$ -chain consists of eight and three CCP domains, respectively (**Figure 1.10**) (Andersson et al. 1990; Hofmeyer et al. 2013; Breda et al. 2015).

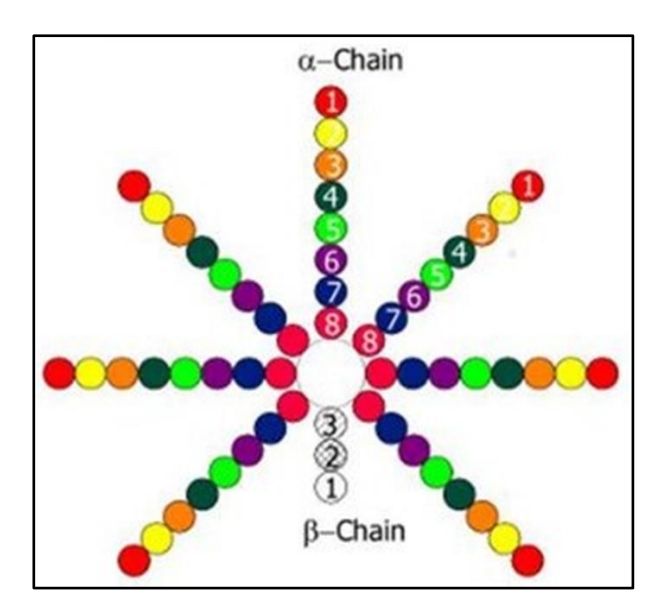


Figure 1.10. Schematic representation of C4BP (Adapted from Breda et al. 2015).

C4BP regulates the classical and lectin pathways by binding to the nascent C4b molecules via the α-chain of C4BP, thus preventing assembly of the classical C3 convertase and inhibiting the membrane attack complex (MAC) (Potempa et al. 2008). Moreover, C4BP also serves as a cofactor of Factor I in the proteolytic cleavage of C4b as well as C3b. The C4b and C3b function as opsonin to phagocytic cells and the unavailability of these components leads to the inhibition of phagocytosis of pathogens (Blom et al. 2003, 2004; Varghese et al. 2021).

# 1.8. Leptospiral immune evasion

Immune evasion is the phenomenon by which pathogens employ strategies to override host immune activation and continue their growth and transmission into new hosts. The immune system comprises components such as, a complement system, cytokines, lymphoid organs, lymphocytes, antigen-presenting cells, antibodies, natural killer cells, phagocytes etc. A complement system is the first line of the immune system where a group of proteins act together to stimulate the host immune response, which leads to eradicate pathogens. To counter the immune surveillances, pathogens employ different strategies to evade. These are, 1) Acquisition of complement regulators of the host, 2) By binding to C7, C8 C9, and/or VN, 3)

By secreting the metallopeptidases that inactivate complement components (Barbosa and Isaac 2020). Pathogenic *Leptospira* acquires the negative complement regulators like C4BP, FH, FH-like protein 1 (FHL-1) and sequesters on the outer membrane surface with the help of outer membrane proteins. The acquisition of FH and FHL-1 by Leptospiral protein such as LigA, LigB, LenA, lenB, LcpA, enolase, EF-Tu and Lsa23 lead to conversion of C3b into iC3b. This causes prevention of C3 convertase C3bBb, which is an essential component of alternative pathway. Moreover, LcpA, LigA, LigB, enolase, Lsa30 bind to the C4BP and downregulate the classical and lectin pathways (**Figure 1.11**). *Leptospira*, sequesters the host plasminogen through surface proteins such as LigA/B, EF-Tu, and Lsa23 and cleaves C3b, C4b and C5.

Additionally, *Leptospira* also secretes proteases that cleaves components of the complement pathways and facilitate bacterial survival in the host. The complement components C3, factor B, C4b, C2, C6, C7, C8 and C9 are also cleaved by metalloproteases, thermolysins (Amamura et al. 2017).

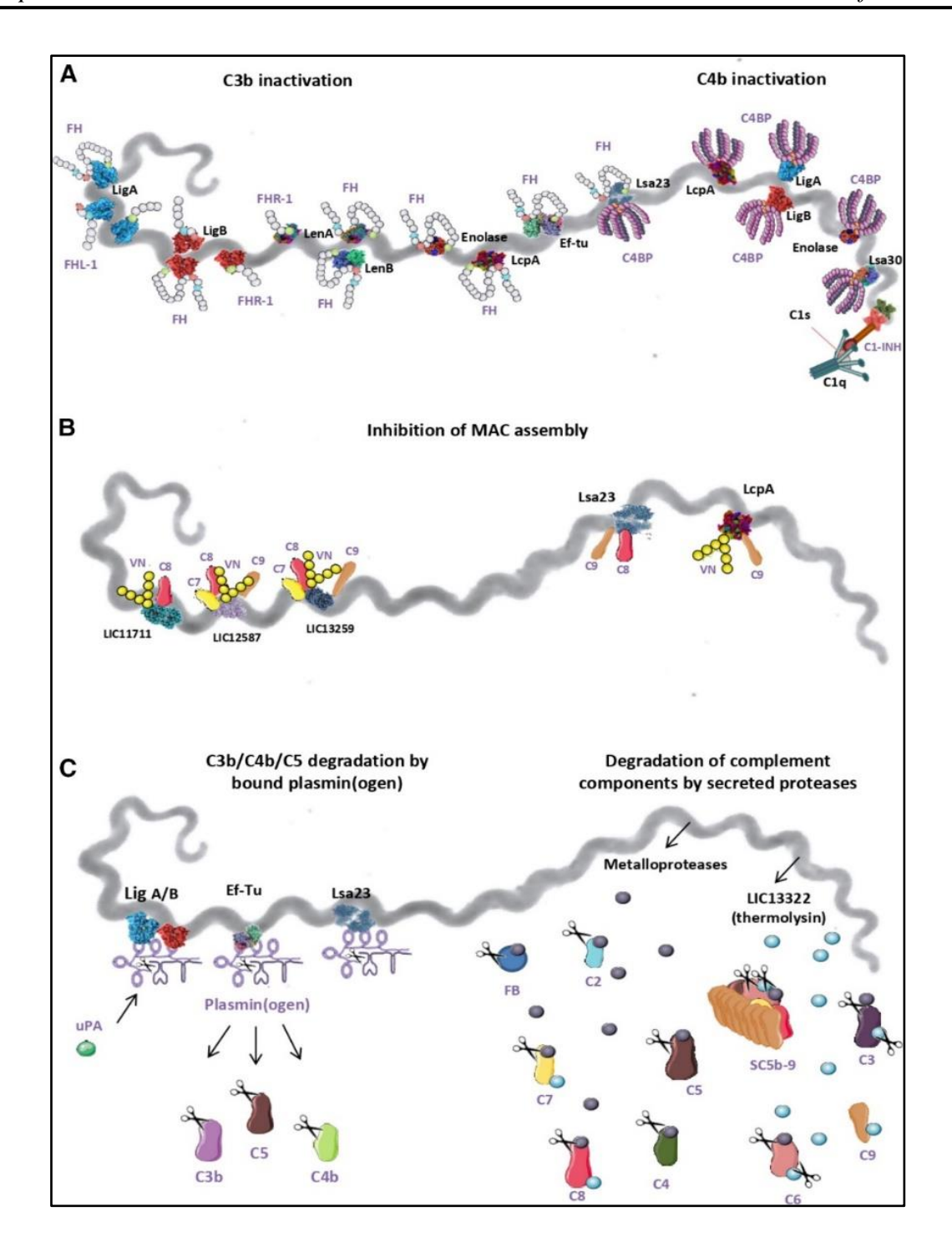


**Figure 1.11. Complement evasion strategies of pathogenic** *Leptospira*. **(A)** Alternate pathway and Classical pathway inhibition by binding of complement regulators to *Leptospiral* proteins. **(B)** Hijacking the Terminal pathway by binding of C7, C8 C9, and/or VN to *Leptospiral* proteins. **(C)** Proteolytic cleavage of complement components via plasmin (left), and Proteolytic cleavage of complement components by secretory proteases (right). (Adapted from Barbosa AS, *FEBS Letters*, 2020).

# 1.9. Leptospiral complement regulator acquiring protein A (LcpA)

The Leptospiral complement regulator acquiring protein A (LcpA) is encoded by the LIC\_11947 gene of *Leptospira interrogans* serovar copenhageni and has been discovered to be conserved among pathogenic species of *Leptospira*. The localization study using different techniques such as immunoelectron microscopy, cell surface proteolysis and triton X fractionation, indicates LcpA as an outer membrane protein. The LcpA is a 20 kDa protein and has been reported to bind a complement regulator protein, C4BP (Barbosa et al. 2010). The role of C4BP bound to immobilized rLIC\_11947 was reported by showing Factor I mediated proteolysis of C4b (Barbosa et al. 2010). Moreover, LcpA was also reported to bind with the host Factor H (FH) and vitronectin. Studies have shown that the LcpA is a multi-ligand interacting protein. Acquisition of FH and C4BP results in hijacking the alternative, classical, and lectin pathways of the complement system. Additionally, it also interacts with vitronectin and C9 and binding downregulates the terminal pathway and arrest the membrane attack complex formation on bacterial membranes (Barbosa et al. 2010; da Silva et al. 2015).

# 1.10. Hydrolytic functions of bacterial proteins in immune evasion

Several pathogens express outer membrane and secreted proteins with hydrolytic functions that disrupt the host defence mechanism. Reports from other pathogens highlighted the involvement of the hydrolytic proteins towards immune evasion. Elastase from *Pseudomonas aeruginosa*, an immunoglobulin degrading enzyme from *Entamoeba histolytica* have been reported to cleave the IgA antibodies (Heck et al. 1990; Garcia-Nieto et al. 2008). Moreover, deS, a protease from *Streptococcus pyogenes* cleaves IgG (Johansson et al. 2008). Furthermore, pathogens also target the first line of host innate defence, a complement system. The aureolysin, staphylokinase and extracellular fibrinogen-binding proteins from *Staphylococcus aureus*, has displayed proteolytic activity against C3 complement component, Streptococcal C5a peptidase (ScpA) from *Streptococcal pyogenes* cleaves C5a (Cleary et al. 1992; Laarman et al. 2011;

Pietrocola et al. 2017). Moreover, enterohemorrhagic *Escherichia coli* strain produces Shiga toxins that can cleave complement component C3b leading to Hemolytic Uremic Syndrome (HUS). The recent report also showed that, a *staphylococcus aureus* lipase belongs to the α/β hydrolase superfamily modifies the membrane composition and pathogen associated molecular patterns (PAMPS). These modifications lead pathogens to be recognized by the host immune system. Many pathogens produce thermolysin-like proteases to degrade the host tissues and modulate the host defences causing a successful establishment of the infection (Chung et al. 2006; Miyoshi 2013). The leptospires also release a zinc-dependent metalloprotease of M4 family, known as thermolysins. The thermolysin encoded by the LIC\_13322 gene displayed the huge affinity towards the complement factors C6, C7, C8 and C9 and prevented the MAC mediated lysis of erythrocytes (Barbosa and Isaac 2020). The previous reports showed proteolytic activity of the LIC\_13322 towards C3, C6 complement components (Fraga et al. 2014; Amamura et al. 2017; Chura-Chambi et al. 2018).

# 1.11. The $\alpha/\beta$ hydrolase superfamily

Several proteins with hydrolytic functions possess an  $\alpha/\beta$  hydrolase superfamily fold. The  $\alpha/\beta$  hydrolase fold contains a core made up of five to eight  $\beta$ -strands connected by  $\alpha$ -helices (Hotelier et al. 2004). These proteins catalyze a wide range of ester, amide, and thioester bonds and are involved in many biological processes. The various studies suggest that  $\alpha/\beta$  hydrolases are primarily involved in metabolic and cellular processes (Holmquist 2005). Some bacteria display their role in the immune evasion also. The important role of  $\alpha/\beta$  hydrolases in the immune evasion include host lipid metabolism, cell membrane modification, host immune cell signalling modification, biofilm formation, etc (Mei et al. 2010; Lu et al. 2021). Very recently, it has been shown that a secretory lipase belongs to the  $\alpha/\beta$  hydrolase superfamily of *S. aureus* hydrolyzes the TLR ligands and is involved in the immune evasion (Chen and Alonzo 2019). The members of the  $\alpha/\beta$  hydrolase superfamily include several lipases, esterases, serine

proteases, epoxide hydrolases, and acetylcholinesterase (Nardini and Dijkstra 1999). In *Leptospira*, the Lsa45 protein belong to the  $\alpha/\beta$  hydrolase superfamily exhibits an esterase activity and binds to penicillin antibiotic leading to minimize the bactericidal effect (Santos et al. 2023). However, very few information is available about the leptospiral  $\alpha/\beta$  hydrolases and their functional roles in establishing the infection in *Leptospira*.

# 1.12. Major challenges and aim of the thesis

The challenges for the disease leptospirosis begin immediately with its diagnosis itself, as the symptoms are very non-specific and always suspicious with other febrile illnesses. Although the disease Leptospirosis had been reported long back in 1886 by Adolph Weil, the *Leptospira* specific and effective treatment has not been developed yet. Patients are treated with different antibiotics such as amoxicillin (or penicillin), tetracycline, or ceftriaxone and the choice of antibiotics is more commonly based on their efficiency over broad range of bacterial infections, rather than tailored to *Leptospira* bacteria (Goarant 2016; Hornsby et al. 2020). Moreover, vaccine development is also remained as a challenging task due to availability of several serogroups. The currently available vaccines are less effective, lack of cross-protection, have terrible side effects, and call for numerous shots (Garba Bashiru & Abdul Rani Bahaman 2018; Maia et al. 2022; de Oliveira et al. 2023). Recent studies on the involvement of outer membrane and secreted proteins in evading the immune system, chemotaxis, adherence, hydrolytic activity against host targets, and virulence ability have generated a lot of interest, supporting the idea that these are the most potential targets in molecular therapeutics as well as in vaccine development. However, there are incredibly very few leptospiral outer membrane or secreted hydrolytic enzymes showing proteolytic or lipolytic activities are reported such as, Lsa45 protein which belong to  $\alpha/\beta$  hydrolase superfamily exhibits the esterase activity and binds to penicillin antibiotic lead to minimize the bactericidal effect (Santos et al. 2023). Other report which showed proteolytic activity of thermolysin against C3 and C6 lead to inhibition of MAC

formation and hence help in immune evasion (Fraga et al. 2014; Amamura et al. 2017; Chura-Chambi et al. 2018).

The available limited information makes it necessary to address the questions such as; Are there any unidentified secreted or outer membrane  $\alpha/\beta$  hydrolases? If so, what is their structure, substrate preference, and function in immune evasion?

Additionally, to hydrolases, there is one of the outer membrane proteins, LcpA which is known to interact with complement regulators C4BP, FH and complement component C9. Moreover, it is also found that LcpA interact with human vitronectin that play crucial role in cell adhesion, blood coagulation and the regulation of the immune response. Interestingly, Silva et al., reported the binding of C4BP, FH and vitronectin to LcpA molecule using competitive binding assay and concluded their binding at distinct sites of LcpA (da Silva et al. 2015). However, the 3-dimensional structure and interacting regions of LcpA have not been explored yet. Therefore, the in detail biophysical characterization, 3-dimensional structure and interaction of distinct host targets with LcpA protein is indeed warranted.

# 1.13. Objectives of the Study

- I. In-silico identification of outer membrane and secretory  $\alpha/\beta$  hydrolases and their analysis across different Leptospira species
- II. Biochemical and biophysical characterization of outer membrane putative  $\alpha/\beta$  hydrolases from the pathogenic *Leptospira*
- III. Structural and interaction studies of Leptospiral complement regulator-acquiring protein A (LcpA)

# Chapter-2

Prediction of outer membrane and secretory putative hydrolases from pathogenic Leptospiral species

#### PART OF THIS CHAPTER IS IN REVISION:

**Shankar UN,** Shiraz M, Kumar P, Akif M. (2024) A comprehensive *In-silico* analysis of putative outer membrane and secretory hydrolases from pathogenic *Leptospira*: Possible Implications in pathogenesis. *Biotechnology and applied biochemistry*.

# 2.1. INTRODUCTION

Many of the outer membrane and secretory proteins of bacteria interact with surroundings, communicate with other microbes, and are also involved in host-pathogen interactions, and in nutrition uptake (Koebnik et al. 2000). The outer membrane proteins from E. coli, including type 1 fimbriae, P fimbriae, and S. fimbriae, are involved in cell adhesion and colonization (Melican et al. 2011). Moreover, OmpA of E. coli has been shown to interact with host immune cells and modulate host immunity (M. Kim 2004). The secreted α-hemolysin from E. coli is the pore-forming toxin that disrupts the host cell membrane and causes cell lysis. The outer membrane vesicles (OMVs) formed by gram-negative bacteria such as P. aeruginosa and A. baumannii contain a variety of secreted proteins, including hydrolases such as phospholipases and proteases which cause host cell lysis and immune evasion (Jan 2017). Outer membrane protein, OprF of P. aeruginosa, binds to the host molecules, such as complement and antibodies, thereby inhibiting their ability to be recognized by the host. This helps pathogens to evade phagocytosis and other immune responses (Mishra et al. 2015). Pathogenic Leptospiral species also express a variety of outer membrane proteins (OMP) and secretory proteins. Like other gram-negative bacteria, Leptospiral outer membrane and secretory proteins are reported to play a crucial role in pathogenesis. Proteins such as leptospiral lipoprotein 32 (LipL32), LipL41, and Leptospira immunoglobulin-like proteins A & B (LigA & LigB) are abundant outer membrane/surface proteins. These have been shown to play a role in adhesion, invasion, and immune evasion (Hoke et al. 2008; Witchell et al. 2014). Leptospiral lipoprotein, LipL21, and LipL41 proteins adhere to the ECM components, exhibit a wide range of ECM binding, and contribute significantly during the initial steps of leptospiral infection (MB et al. 2021). Moreover, LipL21 and LipL45 inhibit the myeloperoxidase activity of host neutrophils and inactivate the neutrophil-mediated immune response (Vieira et al. 2018). LigA and LigB are well-studied for their multifunctional roles

in adhesion, invasion, and immune evasion (Faisal et al. 2008; Yan et al. 2009; Castiblanco-Valencia et al. 2016; Evangelista et al. 2017). Recently, LigA has been demonstrated to have hydrolyzing activity, which may involve hydrolyzing the DNA of neutrophil extracellular traps (Kumar et al. 2022b). In addition, one of the secretory proteases, thermolysin, is reportedly involved in complement evasion by degrading a complement factor, C3 (Chura-Chambi et al. 2018). These reports suggest that *Leptospira* possess a diverse function in their OMPs and secretory protein components, which may involve modulating the host proteins for establishing successful infection. Only a few from this set of proteins possess hydrolytic functions that have been reported to date.

Proteins with hydrolytic functions usually possess an  $\alpha/\beta$  hydrolase superfamily fold. The  $\alpha/\beta$  hydrolase fold generally consists of a core of five to eight  $\beta$ -strands connected by  $\alpha$ -helices (Hotelier et al. 2004). These proteins catalyze the hydrolysis of a wide range of ester, amide, and thioester bonds and are involved in many biological processes. The members of the  $\alpha/\beta$  hydrolase superfamily include lipases, esterases, serine proteases, epoxide hydrolases, and acetylcholinesterase (Nardini and Dijkstra 1999). Very recently, it has been shown that a secretory lipase of *S. aureus* hydrolyzes TLR ligands and is involved in immune evasion (Chen and Alonzo 2019).

This chapter reports, prediction of outer and secretory proteins from the proteome of *Leptospira* followed by identification of proteins comprising of enzymatic activity. The proteins with enzymatic activity include different classes of enzymes such as proteases,  $\alpha/\beta$  hydrolases, nucleases, kinases, oxidases, reductases, glycosyl hydrolases, etc. Furthermore, the sequence and structural similarity studies of potential  $\alpha/\beta$  hydrolases, LIC\_12988, LIC\_11463, LIC\_11103, LIC\_11183, and LIC\_10995 have been performed which resemble the class of lipases.

#### 2.2. METHODOLOGY

# 2.2.1 Prediction of outer membrane and secretory proteins

Methodology and the tools applied for prediction of potent outer membrane and secretory proteins from the whole proteome of *Leptospira* is described in a flow chart shown in **Figure 2.1**.

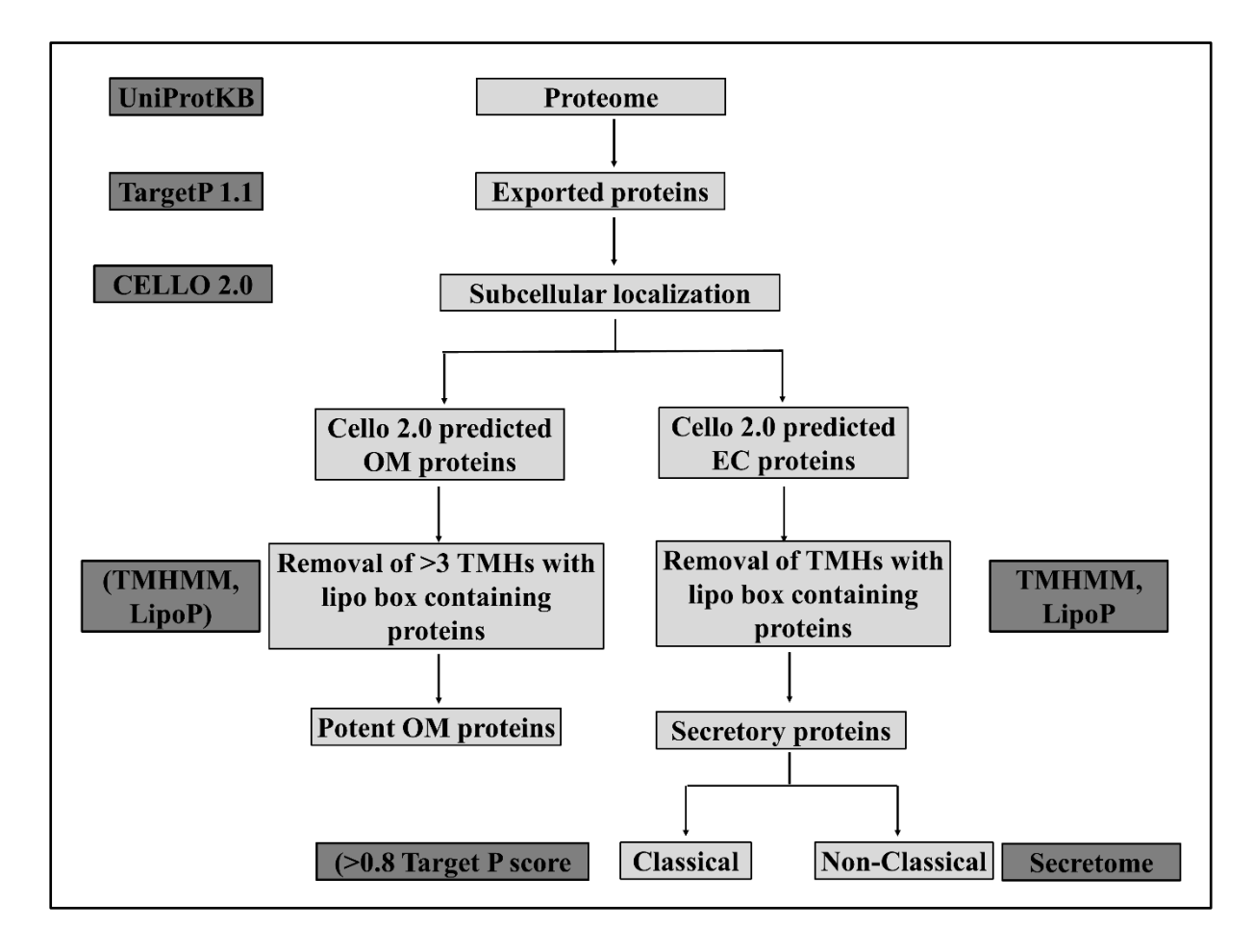


Figure 2.1. Methodology and tools used in the prediction of potent outer membrane and secretory proteins.

# 2.2.1.1 Retrieval of proteome

Pathogenic species *Leptospira interrogans* serogroup Icterohaemorrhagiae serovar Copenhageni strain Fiocruz L1–130 was selected, and the proteome sequence of the same was retrieved from the UniProt consortium. UniProt consortium is the comprehensive resource for protein sequence and annotation data.

# 2.2.1.2. Prediction of exported proteins

A total number of 3654 protein sequences from the proteome was subjected to Target P 1.1 web server (<a href="http://www.cbs.dtu.dk/services/TargetP/">http://www.cbs.dtu.dk/services/TargetP/</a>) for exported protein prediction. The non-plant version of Target P 1.1 web was applied. It predicts signal peptides and signal peptidase cleavage site into the protein sequences (Emanuelsson et al. 2000). Classical exported proteins were predicted based on the presence of signal sequences. The cut-off for the signal sequence was set to 0.532 (Nielsen and Engelbrecht 1997; Emanuelsson et al. 2000). The signal peptides containing proteins were considered potential exported proteins. The signal peptides were removed manually and were assessed for more in-depth investigation.

# 2.2.1.3. Subcellular localization of proteins

The predicted exported proteins may localize in the inner or outer membrane, periplasmic space, or extracellular milieu. Hence, subcellular localization prediction was performed using the CELLO 2.0 server (<a href="http://cello.life.nctu.edu.tw/">http://cello.life.nctu.edu.tw/</a>). It uses the support vector machines trained by multiple feature vectors based on amino acid compositions, dipeptide compositions, partitioned compositions etc. It predicts probable subcellular localization of the query protein in cytoplasm, periplasm, inner membrane, outer membrane or extra-cellular depending on various parameters such as amino acid composition. This method has the prediction accuracy of 89% which is 14 % higher than that of the recently developed PSORT-B prediction tool (Yu et al. 2004).

The proteins predicted as the outer membrane or extracellular were considered for further *insilico* characterization.

# 2.2.1.4. Prediction of the potent outer membrane and secretory proteins

The anticipated outer membrane proteins discovered by CELLO 2.0 might contain lipoproteins, which are known to bind to membranes via an acyl chain to the periplasmic surface of the outer

or inner membrane. These lipoproteins have been identified by the LipoP 1.0 server (http://www.cbs.dtu.dk/services/LipoP/) (Juncker et al. 2003). Generally, three and more than three transmembrane α-helices (TM helices) are the characteristic signature of integral inner membrane proteins. Hence, using the TMHMM 2.0 (http://www.cbs.dtu.dk/services/TMHMM/) server, proteins containing >3 TM helices were predicted. The predicted lipoproteins, inner membrane proteins, and transmembrane proteins were removed from further study. Only three or less than three TM helices containing proteins were considered potent outer membrane proteins, and the zero TM helices containing proteins were believed to be secretory proteins (Moller et al. 2001).

# 2.2.1.5. Analysis of secretory proteins

The predicted secretory proteins could be destined to extra-cellular space by classical secretory pathway (Signal peptide dependent) or non-classical secretory pathway (Signal peptide independent). The proteins from classical secretory pathways were confirmed by the TargetP 1.1, with signal peptide cut-off value > 0.8 (Emanuelsson et al. 2007). Proteins secreted through non-classical pathways were predicted using the secretomeP 2.0, and proteins with more than 0.5 scores were expected to be secretory (Bendtsen et al. 2005).

# 2.2.2. Identification of proteins with enzymatic functions

A set of the potent outer membrane and secretory proteins were subjected to identify motifs through the motif finder (https://www.genome.jp/tools/motif/) (Punta et al. 2012). The motif finder searches the probable domains or motifs among Pfam and NCBI-CDD databases. Additionally, pBLAST was employed with default parameters to compare sequences containing the lipase motif to the UniProtKB SwissProt database to characterize the  $\alpha/\beta$  hydrolases. The multiple sequence alignments of 35 amino acids with a lipase motif in the middle were performed using Clustal omega, and the figures were generated using ESpript 3.

# 2.2.3. Physicochemical properties

The physicochemical properties of predicted  $\alpha/\beta$  hydrolases were analysed using the Expasy ProtParam server (www.web.expasy.org/protparam). The ProtParam server gives the basic information of proteins such as MW, theoretical pI, extinction coefficients. It also predicts the instability, and hydropathicity (GRAVY) values using the protein sequence. The instability index study provides the stability of proteins in a test tube. The aliphatic index is the relative volume occupied by the proteins' aliphatic side chain amino acids. The GRAVY score is the sum of the amino acids' hydropathy values divided by the number of residues in the query sequence.

# 2.2.4. Annotations of virulence factors

The set of predicted α/β hydrolases was tested for their virulence ability using the VirulentPred server (Garg and Gupta 2008). With an accuracy of 81.8%, the VirulentPred server uses Support Vector Machine (SVM) based techniques to estimate the potential virulence ability in the proteins. The BTXpred server was also employed to predict bacterial toxins (Saha and Raghava 2006, 2007). The DBETH tool was employed to predict their possibility of being exotoxins to hosts (Chakraborty et al. 2012). The virulence factor database, VFDB, is used to identify virulence factor-related proteins. The VFDB tool performs BLAST analysis against the VFDB core dataset by keeping the E-value of 0.1 (Chen et al. 2005). The probable molecular functions and biological processes were predicted using distantly related sequences by PFP (Protein Function Prediction) (Hawkins et al. 2006).

# 2.2.5. Three-dimensional structural model of $\alpha/\beta$ hydrolases

The 3-D structure models of the putative α/β hydrolases were generated using the AlphaFold (<a href="https://alphafold.ebi.ac.uk/">https://alphafold.ebi.ac.uk/</a>) (Jumper et al. 2021). All the modelled structures were refined through the GalaxyWEB server (<a href="http://galaxy.seoklab.org/cgi-bin/submit.cgi?type=REFINE2">http://galaxy.seoklab.org/cgi-bin/submit.cgi?type=REFINE2</a>) (Shin et al. 2014). Further, modelled structures were validated

through Ramachandran plot by using pro-check (<a href="https://servicesn.mbi.ucla.edu/PROCHECK/">https://servicesn.mbi.ucla.edu/PROCHECK/</a>) and Prosa tools (<a href="https://prosa.services.came.sbg.ac.at/prosa.php">https://prosa.services.came.sbg.ac.at/prosa.php</a>) (Laskowski et al. 1993; Wiederstein and Sippl 2007). The proteins were visualized using the PyMOL program (<a href="https://pymol.org/2/">https://pymol.org/2/</a>).

# 2.2.6. Conservation analysis among different Leptospiral species

Each protein was selected from the genome of *L. interrogans* serovar Copenhageni based on *in-silico* analysis. The evolutionary history for LIC\_12988, LIC\_11463, LIC\_11103, LIC\_11183, and LIC\_10995 proteins was deduced using the maximum likelihood method (Tamura et al. 2021)(Tamura et al. 2021)(Tamura et al. 2021). The phylogenetic trees were generated by Neighbor-Join and BioNJ algorithms using Jones-Taylor-Thornton model. Percentage of repetitive trees where the associated taxa grouped in the phylogenetic test (1000 repetitions) has been indicated next to the branches. The percentage values of more than 60 were taken into consideration. For each gene, this investigation used the amino acid sequences from 20 species of *Leptospira*, including pathogenic, intermediate, and saprophytes. MEGA 11 was used to undertake evolutionary research (Tamura et al. 2021).

# **2.3. RESULTS**

# 2.3.1. Exported proteins contain signal peptides

Leptospira proteome consists of a total of 3654 proteins. Proteins are destined to different locations based on their signal peptides. The outer membrane and secretory proteins were sorted out based on the features of having signal peptides and their cleavage site. A total of 1114 proteins were predicted to be exported proteins, representing 30.48% of the whole proteome (Figure 2.2A). Target P uses a minimum value of signal peptide scores of 0.532. The same value was set as a cut-off for predicting exported proteins. The signal peptides identified of all the exported proteins were removed manually, followed by the prediction of sub-cellular localizations. The probable sub-cellular localizations of exported proteins are shown in Figure

**2.2B**. The sub-cellular localization program predicted 228 proteins as outer membrane proteins and 125 as extra-cellular proteins, approximately 20% and 11 % of total exported proteins from our study, respectively.

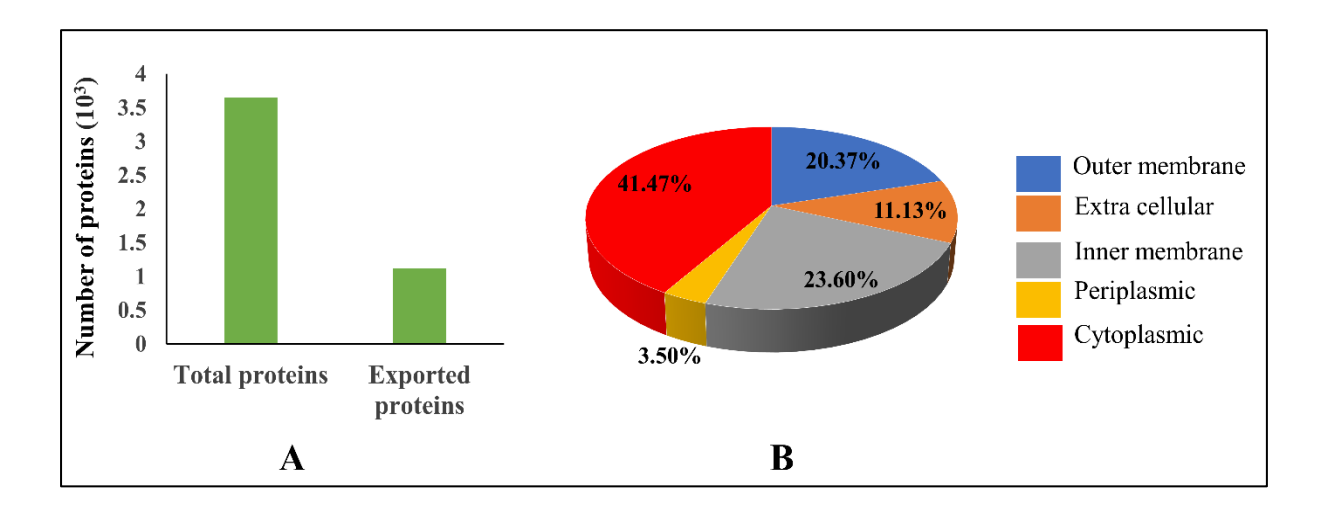


**Figure 2.2. Prediction and sub-cellular localization of leptospiral proteins**. (**A**) Number of total and exported proteins from the whole Leptospiral proteome. (**B**) Pi diagram showing the percentage localization of these proteins in different cellular fractions.

# 2.3.2. Potent outer membrane and secretory proteins are devoid of Lipo-box

The proteins predicted as outer membrane may have transmembrane helices and lipo-box. These sorts of proteins are categorized as either integral transmembrane proteins or lipoproteins. Moreover, a few proteins may belong to the inner membrane and anchored with a lipo-box. There were 13 proteins containing more than three transmembrane  $\alpha$ -helices and 16 proteins possessing lipo-box removed from the dataset. Applying these criteria, 199 proteins were considered potent outer membrane proteins (**Figure 2.3A and Appendix table 1**).

The extra-cellular proteins without transmembrane  $\alpha$ -helices and lipo-box were considered secretory proteins. Proteins generally secrete out either by the classical or non-classical

secretory pathways. Proteins with signal peptide (SP) cutoff of > 0.8 scores were considered secretory through classical pathways. A total of 13 proteins with  $\le 0.8$  scores were removed from the potent classical secretory proteins set. Proteins secreted through non-classical pathways were sorted out using the Secretome 2 server. The final proteins secreted by the classical and non-classical secretory pathways were 117 (Figure 2.3B and Appendix table 1).

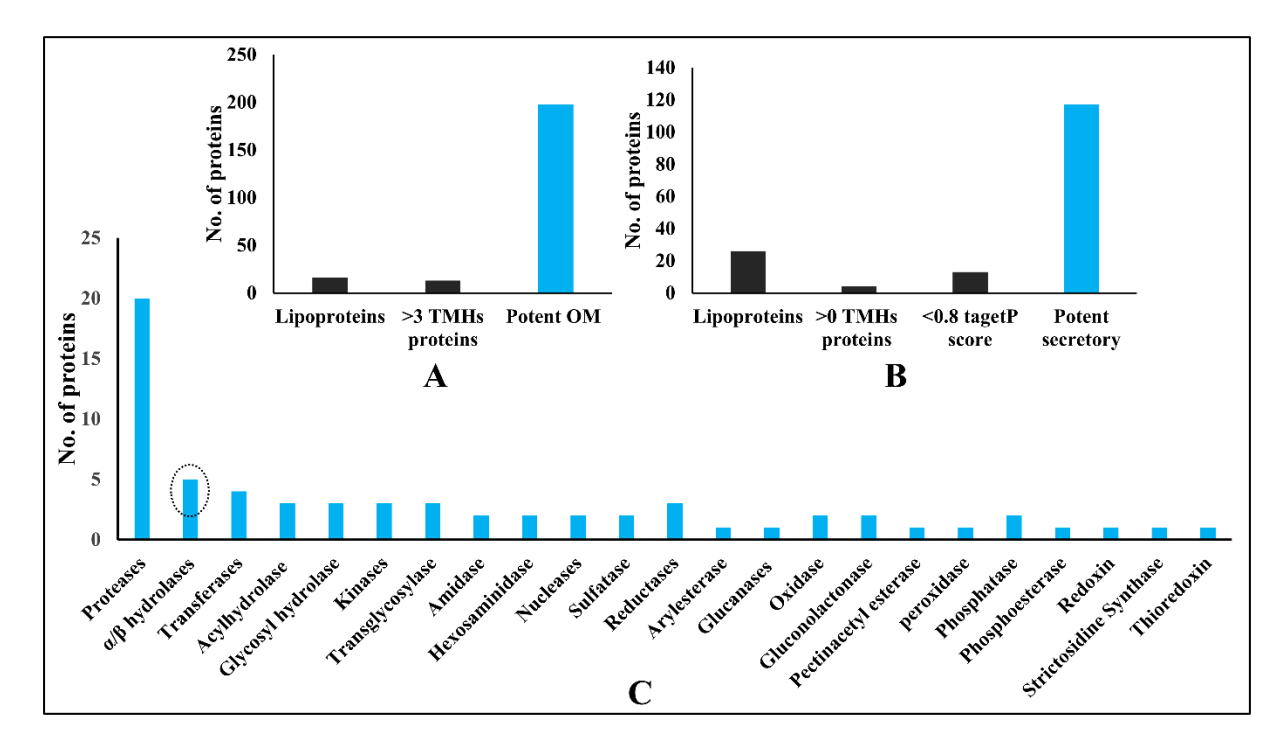


**Figure 2.3. Representation of potent outer membrane and secretory proteins with enzymatic functions.** (**A**) Histogram showing a number of lipoproteins, proteins containing >3TMH, and potent outer membrane. (**B**) Histogram showing a number of lipoproteins, proteins with >0 TMH and 0.8 Targets P scores, respectively, and secretory proteins. (**C**) A number of potent outer membrane and secreted proteins showing probable enzymatic functions.

# 2.3.3. Outer membrane and secretory proteins belong to many enzymatic classes

Potent outer membrane and secretory proteins usually have a wide range of functions. Most of these proteins are involved in adhesin functions and are responsible for pathogenesis. In addition, these exported proteins may have enzymatic functional motifs. The Motif finder and Conserved Domain (CD) search suggested probable enzymatic functions among the potent outer membrane and secretory proteins list. Several outer membrane and secretory proteins belong to the different classes of enzymes, including proteases,  $\alpha/\beta$  hydrolases, nucleases, kinases, oxidases, reductases, glycosyl hydrolases, etc. (**Figure 2.3C**). Their number varies, but the protease class of proteins was observed to be the highest among all. Protease and hydrolase classes of proteins may involve cleaving the host components to establish the infection.

# 2.3.4. Characterization of putative α/β hydrolases

Outer membrane and secretory proteins have been shown to encompass the functional motifs that describe the  $\alpha/\beta$  hydrolase superfamily's distinguishing characteristics. (**Tables 2.1 and 2.2**). The proteins LIC\_10995, LIC\_11183, LIC\_11103, LIC\_11463, LIC\_20201, and LIC\_12988 were predicted to contain  $\alpha/\beta$  hydrolase motifs. However, the protein LIC\_20201 showed neither lipase motif nor sequence homology with any known  $\alpha/\beta$  hydrolases.

Table 2.1. List of the potent outer membrane proteins and functional motifs identified by Pfam and NCBI-CDD databases.

Sr. No.	Gene ID	Pfam		NCBI-CDD		
		Position (Independent E-value)	Description	Position (Score and E-value)	Description	
1	LIC_11463	63188 (0.00022)	α/β hydrolase family	45313 (48.1, 3e-06)	COG0596, MhpC, Predicted hydrolases or acyltransferases (α/β hydrolase superfamily)	
		140183 (0.013)	α/β hydrolase fold	144187 (37.1, 0.012)	COG1075, LipA, Predicted acetyltransferases and hydrolases with	

		129180	PF06259,	116180	the $\alpha/\beta$ hydrolase fold pfam00561, $\alpha/\beta$
		(0.056)	α/β hydrolase	(36.3, 0.017)	hydrolase fold
		131164	PF05990,	63215	pfam12697, $\alpha/\beta$
		(0.15)	α/β hydrolase of	(34.8, 0.057)	hydrolase family.
2	LIC_20201	30106 (0.077)	PF12695, α/β	19208 (38.8, 0.002)	COG0596, MhpC, Predicted hydrolases
		(0.077)	hydrolase	(36.6, 0.002)	or acyltransferases
			family		(α/β hydrolase
					superfamily)
		47107	PF00561,	19108	pfam00561, $\alpha/\beta$
		(0.079)	α/β hydrolase	(34.8, 0.036)	hydrolase fold.
			fold		
3	LIC_11183	88195	PF00561,	88269	COG0596, MhpC,
		(3.7e-14)	α/β hydrolase	(75.8, 1e-15)	Predicted hydrolases or acyltransferases
			fold		$(\alpha/\beta \text{ hydrolase})$
		89279	PF12697,	89269	pfam00561, $\alpha/\beta$
		(1.2e-10)	$\alpha/\beta$	(67.9, 5e-13)	hydrolase fold
			hydrolase family		
		155196	PF07859,	78189	PLN02894,
		(0.035)	$\alpha/\beta$	(39.9, 0.002)	hydrolase, $\alpha/\beta$ fold
			hydrolase fold		family protein
4	LIC_11103	46265	AB	46161	PRK14875
	_	(1.3e-13)	hydrolase	(61.5, 2e-10)	superfamily
		46137(1.6e-	AB	44335	(acetyltransferase) MhpC (alpha/beta
		07)	hydrolase	(59.6, 5e-10)	hydrolase
		,	11) 01 01000	(37.0, 30 10)	superfamily)

Table 2.2. List of the potent secretory proteins and functional motifs identified by Pfam and NCBI-CDD databases.

S.	Gene ID	Pfa	am	NCB	I-CDD
No		Position (Independent E-value)	Description	Position (Score and E-value)	Description
1	LIC_1099 5	48277 (2.4e-14)	PF12697, α/β hydrolase family	29341 (65.4, 6e-12)	COG0596, MhpC, Predicted hydrolases or acyltransferases (α/β hydrolase superfamily)
		47140 (1.8e-08)	PF00561, α/β hydrolase fold	48140 (54.0, 3e-08)	pfam00561, $\alpha/\beta$ hydrolase fold.
		48171 (0.015)	PF05990, α/β hydrolase of unknown function (DUF900)	48142 (51.7, 1e-07)	pfam12697, $\alpha/\beta$ hydrolase family.
2	LIC_1298 8	13134 (1.8e-05)	PF00561, α/β hydrolase fold	12234 (78.3, 1e-16)	COG1075, LipA, Predicted acetyltransferases and hydrolases with the α/β hydrolase fold
		14115 (0.00047)	PF12697, α/β hydrolase family	12232 (51.7, 1e-07)	pfam00561, $\alpha/\beta$ hydrolase fold.
		57119 (0.073)	PF06028, α/β hydrolase of unknown function (DUF915)	9233 (36.5, 0.012)	COG0596, MhpC, Predicted hydrolases or acyltransferases (α/β hydrolase superfamily)
		60107 (0.19)	PF05990, α/β hydrolase of unknown function (DUF900)	1494 (31.7, 0.34)	pfam12697, α/β hydrolase family.

The pBLAST of LIC\_10995, LIC\_11183, LIC\_11103, LIC\_11463, and LIC\_12988 against the UniProtKB Swissprot database revealed their sequence identity of approximately 20-37% with the previously reported lipases or esterases from different organisms and also possessed a

conserved consensus lipase motif G/AXSXG (**Figure 2.4**). The proteins with the conserved consensus lipase motifs are categorized as carboxylesterases (EC 3.1.1.1) or lipases (EC 3.1.1.3).

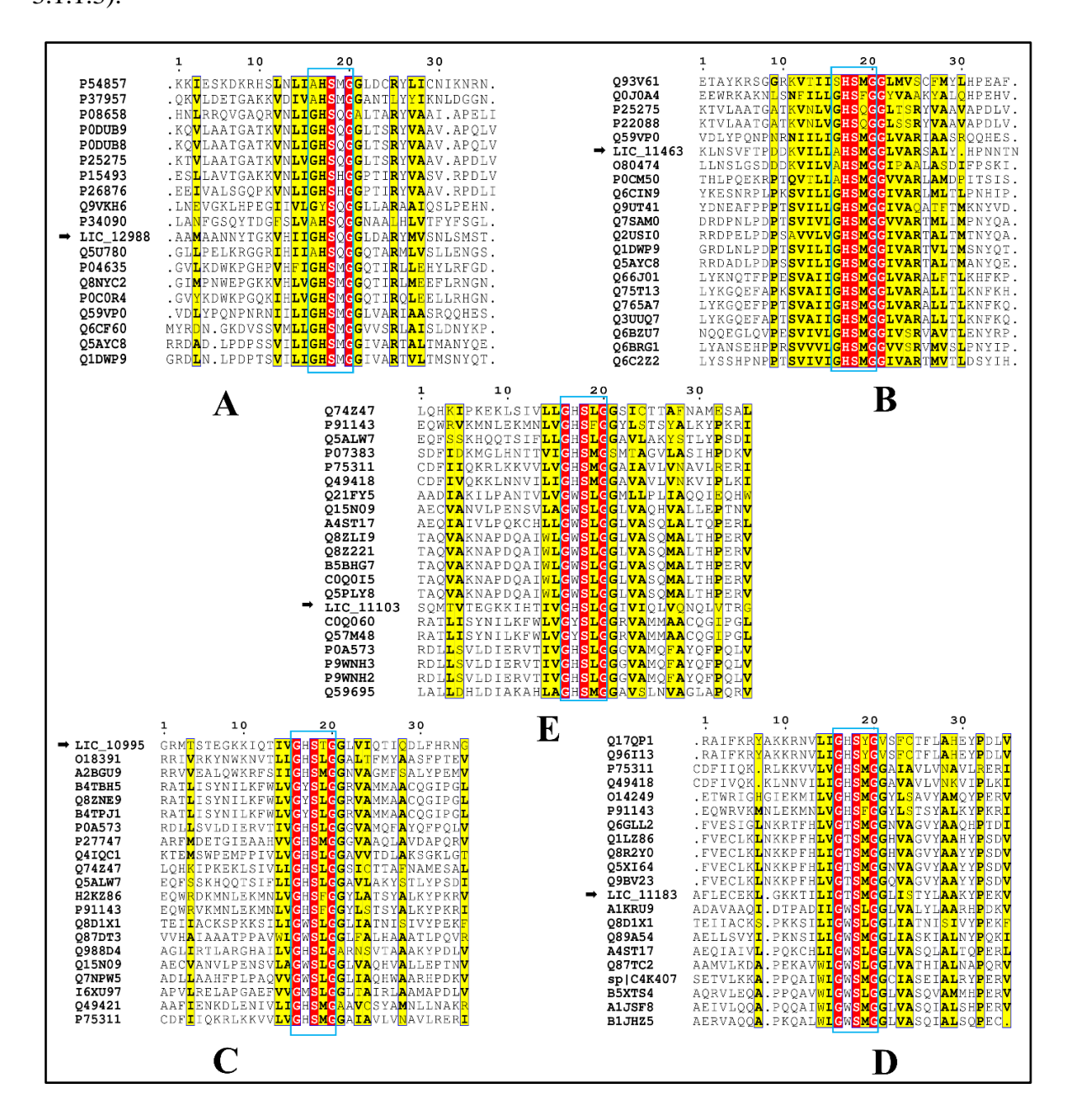


Figure 2.4. Sequence analysis of putative α/β hydrolases. Multiple sequence alignment of a stretch of 35 residues including consensus lipase motif, "G/AXSXG" of (A) LIC\_12988, (B) LIC\_11463, (C) LIC\_10995, (D) LIC\_11183, and (E) LIC\_11103 proteins with the respective top hits found from different organisms in pBLAST against UniProtKB Swissprot database. The green box represents the conserved consensus sequence of lipase motif, G/AXSXG.

The sequence alignment of all five putative  $\alpha/\beta$  hydrolases with two known lipases (PDS IDs: 6KSI and 2HIH) that also belong to an  $\alpha/\beta$  hydrolase superfamily revealed the conservation of catalytic triad residues (serine nucleophile, histidine, and aspartic acid residue) in the LIC\_11463 and LIC\_12988 proteins. The catalytic site of LIC\_11463 possesses S174, D315, and H341, while LIC\_12988 has S112, D247, and H275 (residues numbered before signal peptide removal). However, the catalytic triads of the LIC\_10995 and LIC\_11183 were devoid of histidine residue (**Figure 2.5**). Moreover, all five LIC\_10995, LIC\_11183, LIC\_11103, LIC\_11463, and LIC\_12988 proteins were predicted as ester hydrolases in their molecular function predictions.

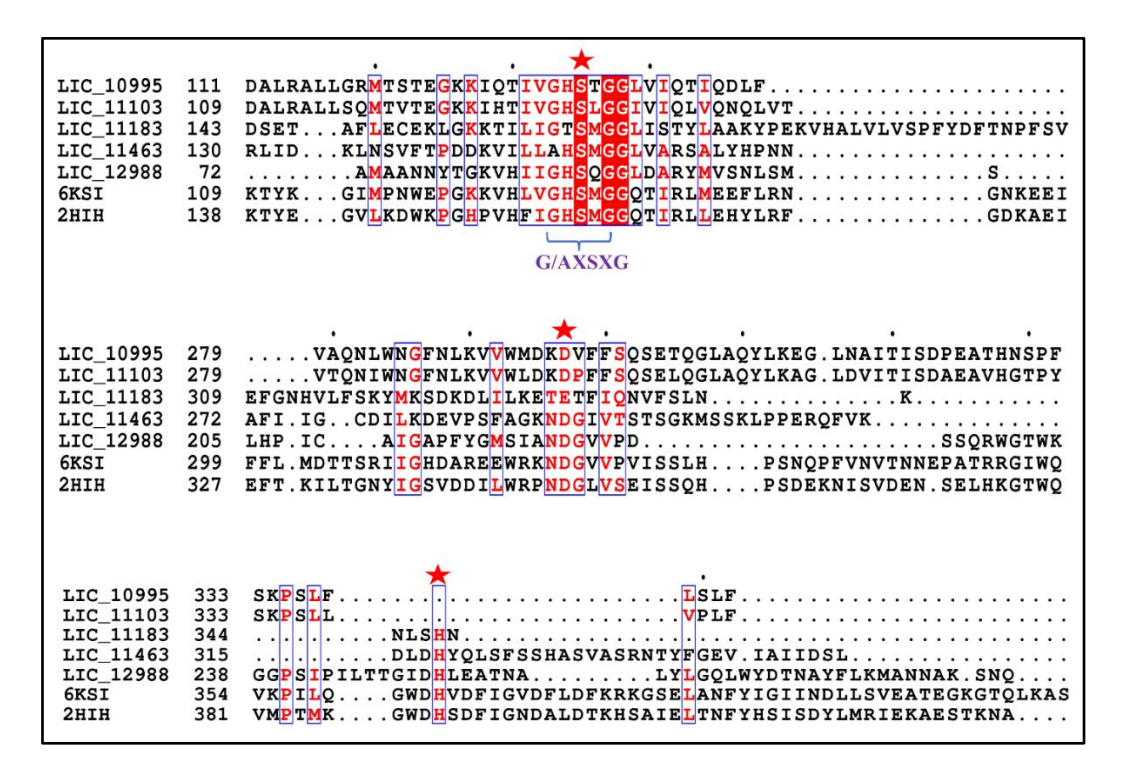


Figure 2.5. Sequence alignment of putative proteases of  $\alpha/\beta$  hydrolases family proteins. 6KSI and 2HIH are the PDB IDs of the reported lipases from *Staphylococcus aureus* and *Staphylococcus hyicus* respectively. Lipase motif is shown in blue box.

The probable biological function prediction suggests the role of LIC\_11463 and LIC\_12988 proteins in lipids and Biotin metabolism. The remaining LIC\_10995 and LIC\_11183 proteins were predicted to be involved in vitamin K metabolism/synthesis (menaquinone) (**Table 2.3**).

Several variables, including isoelectric point, molecular mass, instability and aliphatic indices, and GRAVY index, play an important role in protein isolation, separation, purification, and crystallization (Tokmakov et al. 2021).

Table 2.3. Prediction of molecular functions and biological processes of putative  $\alpha/\beta$  hydrolases.

Sr. No.	Gene ID	Molecular functions (MF)	Biological Processes (BP)
1	LIC_10995	2-succinyl-6-hydroxy-2,4- cyclohexadiene-1-carboxylate synthase activity, carboxylic ester hydrolase activity	Menaquinone metabolic process, cellular ketone metabolic process
2	LIC_11183	Carboxylic ester hydrolase activity, 2-succinyl-6-hydroxy-2,4-cyclohexadiene-1-carboxylate synthase activity	Lipid catabolic process, biotin metabolic process, menaquinone metabolic process.
3	LIC_11463	Phosphatidylinositol deacylase activity, hydrolase activity, acting on ester bonds.	GPI anchor metabolic process, protein-lipid complex remodeling, lipid catabolic process, biotin metabolic process
4	LIC_12988	Carboxylic ester hydrolase activity, triglyceride lipase activity, metal/Cation ion binding,	Biotin metabolic process, lipid catabolic process, 3-phenylpropionate catabolic process, xenobiotic catabolic process, phosphatidylinositol deacylase activity
5	LIC_11103	Carboxylic ester hydrolase, hydrolase activity	Biotin metabolic process, lipid catabolic process

The physicochemical parameters of LIC\_11463, LIC\_11183, LIC\_11103, LIC\_12988, and LIC\_10995 are mentioned in **Table 2.4**, except LIC\_12988, the length of all three proteins contained around 360 amino acid residues. The LIC\_12988 was shorter in all five proteins and possessed 282 amino acids. Accordingly, molecular weight was observed to be around 30 kDa for LIC\_12988, and the other three were approximately 40 kDa. The LIC\_12988 and LIC\_11183 displayed an alkaline range pI of 9 and 8.9, respectively. LIC\_10995 showed a

neutral pI, and LIC\_11463 carried a slightly acidic pI of 5.88. Moreover, the instability index of LIC\_10995, LIC\_11463, and LIC\_12988 was less than 40, which means they are stable. However, LIC\_11183 carries a slightly higher instability index of 40.38, indicating its instability (**Table 2.4**). All five putative α/β hydrolases, LIC\_11463, LIC\_12988, LIC\_11183, LIC\_11103, and LIC\_10995, were predicted to be bacterial toxins and virulent in our analysis. Moreover, the LIC\_11463 and LIC\_12988 proteins showed close sequence similarity with the recently reported *Staphylococcus aureus* derived virulent factor (known as Glycerol ester hydrolase, geh or *Staphylococcus aureus* lipase, SAL) (**Table 2.5**).

Table 2.4. List of predicted putative  $\alpha/\beta$  hydrolases and their physical and chemical parameters.

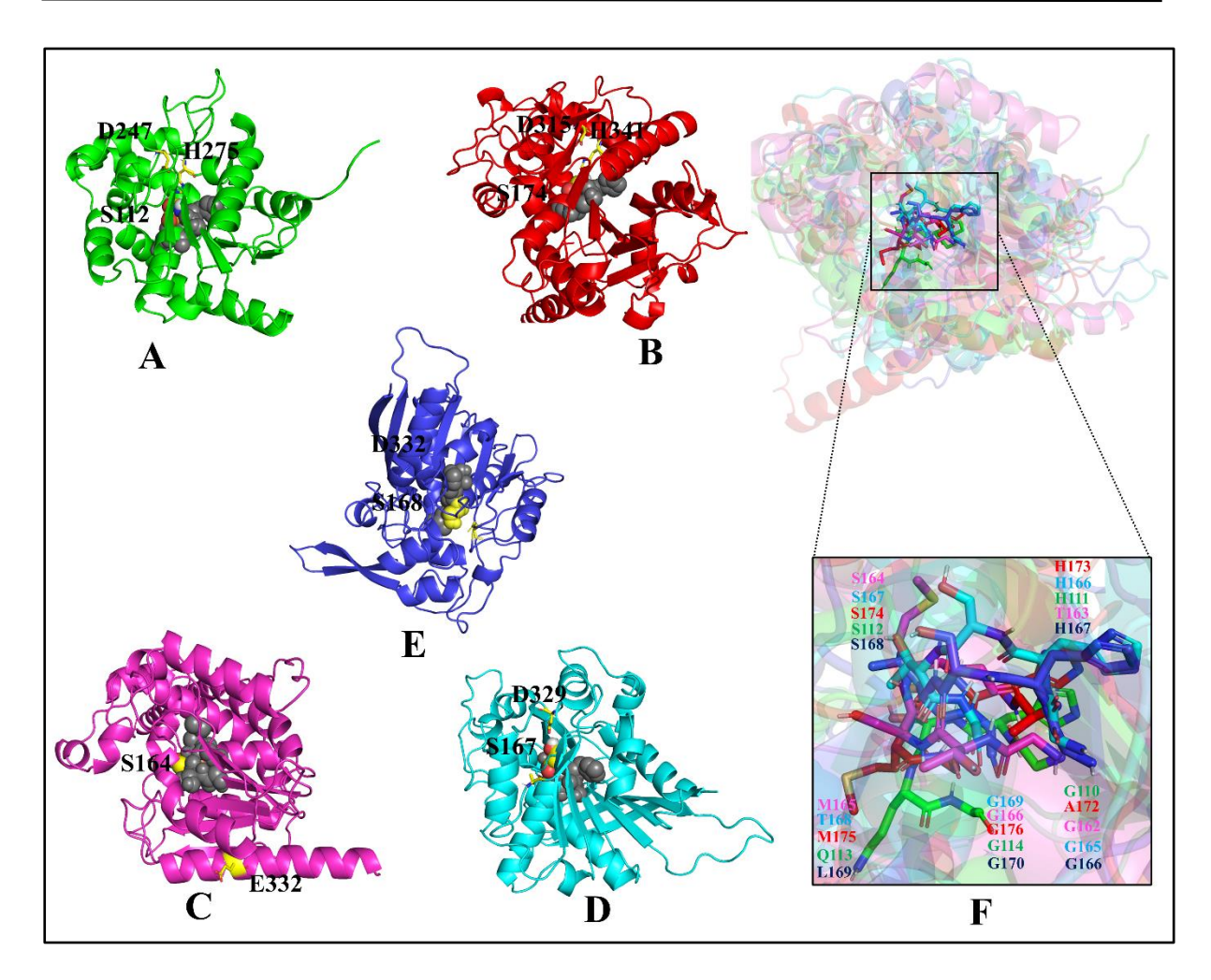
Sr.	Gene ID	Accession No.	No. amino acids	Mol. Wt (Da)	Theoretical pI	Extinction coefficients	Instability index Score (Stable/	Aliphatic index	GRAVY
110.						(M <sup>-1</sup> cm <sup>-1</sup> )	<b>Unstable</b> )		
1	LIC_11463	Q72SC1	369	41374.11	5.88	38975	28.60 (Stable)	82.57	-0.262
2	LIC_11183	Q72T38	348	40028.75	8.90	47915	40.38 (Unstable)	81.81	-0.378
3	LIC_10995	Q72TM2	374	41319.28	7.02	54320	38.37 (Stable)	87.25	-0.106
4	LIC_12988	Q72N50	282	29766.77	9.05	55350	28.87 (Stable)	91.35	0.095
5	LIC_11103	Q72TB8	377	41538.45	7.02	58330	31.34 (Stable)	97.43	-0.049

Table 2.5. Virulence and toxin prediction of putative  $\alpha/\beta$  hydrolases

Sr. No.	Gene ID	Virulence prediction (Virulent-Pred)	Toxin protein (DBETH server)	Prediction of Bacterial Toxins (BTXpred server)	Virulence prediction (VFDB server)
1	LIC_11463	+ (0.9981)	+	+	+ (Putative lipase/glycerol ester hydrolase)
2	LIC_11183	+ (0.1567)	+	+	-
3	LIC_10995	+ (1.0904)	-	+	-
4	LIC_12988	+ (1.0125)	+	+	+ (glycerol ester hydrolase/triacylglycerol lipase)
5	LIC_11103	+ (1.5314)	-	+	+ (non-ribosomal peptide synthetase)

# 2.3.5. Three dimensional Model and Structural Comparison

The three-dimensional structures of LIC\_12988, LIC\_11463, LIC\_11183, LIC\_11103, and LIC\_10995 proteins were modelled with considerable Ramachandran plot statistics and ProsA Z-scores values (**Table 2.6**). These modelled structures possessed ideal bond lengths and angles. On-an-average structural models comprised sixteen  $\alpha$ -helices and seven  $\beta$ -strands (**Figure 2.6A-D and Table S6**). The average secondary structure composition of the structure models had 42.40 % and 12.15 %  $\alpha$ -helices and  $\beta$ -strands, respectively (**Table 2.7**). The LIC\_12988 protein possesses the conserved catalytic triad residues S112, D247, and H275 in the loop region of  $\beta$ 3- $\alpha$ 3,  $\alpha$ 10- $\alpha$ 11, and  $\beta$ 6- $\alpha$ 12 while in LIC\_11463, catalytic triad residues S174, D315, and H341 were found in the loops connecting  $\beta$ 5- $\alpha$ 10,  $\alpha$ -19- $\alpha$ 20 and  $\beta$ 8- $\alpha$ 22, respectively. The LIC\_11183, LIC\_10995, and LIC\_11103 have serine nucleophiles, and S164, S167, and S168 were situated in the loops connecting  $\beta$ 4- $\alpha$ 8,  $\beta$ 6- $\alpha$ 5, and  $\beta$ 6- $\alpha$ 4 respectively. Significant structural alignment was not observed among the five structure models. Interestingly, the canonical lipase motif (G/AXSXG) was conserved and observed to be structurally superimposed among the five (**Figure 2.6E**). The nucleophilic serine of the catalytic triad was present in the lipase motif.



**Figure 2.6. Three-dimensional structures and domain architecture**. (A) LIC\_12988, (B) LIC\_11463, (C) LIC\_11183, (D) LIC\_10995 proteins, (E) LIC\_11103 and (F) depicts the structure superimposition of all five proteins while emphasizing the alignment of lipase motifs.

Table 2.6. Structure validation of putative  $\alpha/\beta$  hydrolases.

Sr.	Gene ID Ramachandran plot statistics			statistics	ProsA
No.		Most Favoured region (%)	Allowed region (%)	Disallowed Region (%)	Score
1	LIC_12988	94.5	5.5	0	-5.54
2	LIC_11463	94.1	5.6	0.3	-7.49
3	LIC_11183	94.7	5.0	0.3	-7.36
4	LIC_10995	96.2	3.4	0.3	-7.53
5	LIC_11103	98.3	1.4	0.3	-7.32

Table 2.7. Secondary structure contents of modelled three-dimensional structures of putative  $\alpha/\beta$  hydrolases.

Sr.	Gene ID	Structure composition (PDBsum)		
No.		Number of α-helices	Number of β-strands	
		(% of residues)	(% of residues)	
1	LIC_10995	14 (30.41)	14 (13.74)	
2	LIC_11183	16 (52.30)	9 (13.50)	
3	LIC_12988	14 (41.49)	6 (9.22)	
4	LIC_11463	23 (45.37)	8 (12.13)	
5	LIC_11103	15 (29.24)	14 (25.15)	

As importantly, analyzing the structure alignment of modelled putative  $\alpha/\beta$  hydrolases with one of the well-structured and biochemically characterized  $\alpha/\beta$  hydrolases provides valuable insights into the structure-function relationship of enzymes. The structural models of LIC\_12988, and LIC\_11463 were not well structurally aligned with the *Staphylococcus aureus* lipase (6KSI) and displayed RMSD of 11.761, and 14.036 respectively. Despite overall high RMSD, the catalytic sites of LIC\_12988 and LIC\_11463 were observed structurally superimposed with the *Staphylococcus aureus* lipase (6KSI) (**Figure 2.7**). The catalytic residues, S112, D247, and H275 of LIC\_12988 and S174, D315, and H341 of LIC\_11463 are structurally aligned with the catalytic triad residues, S116, D307, and H349 of *Staphylococcus aureus* lipase (SAL).

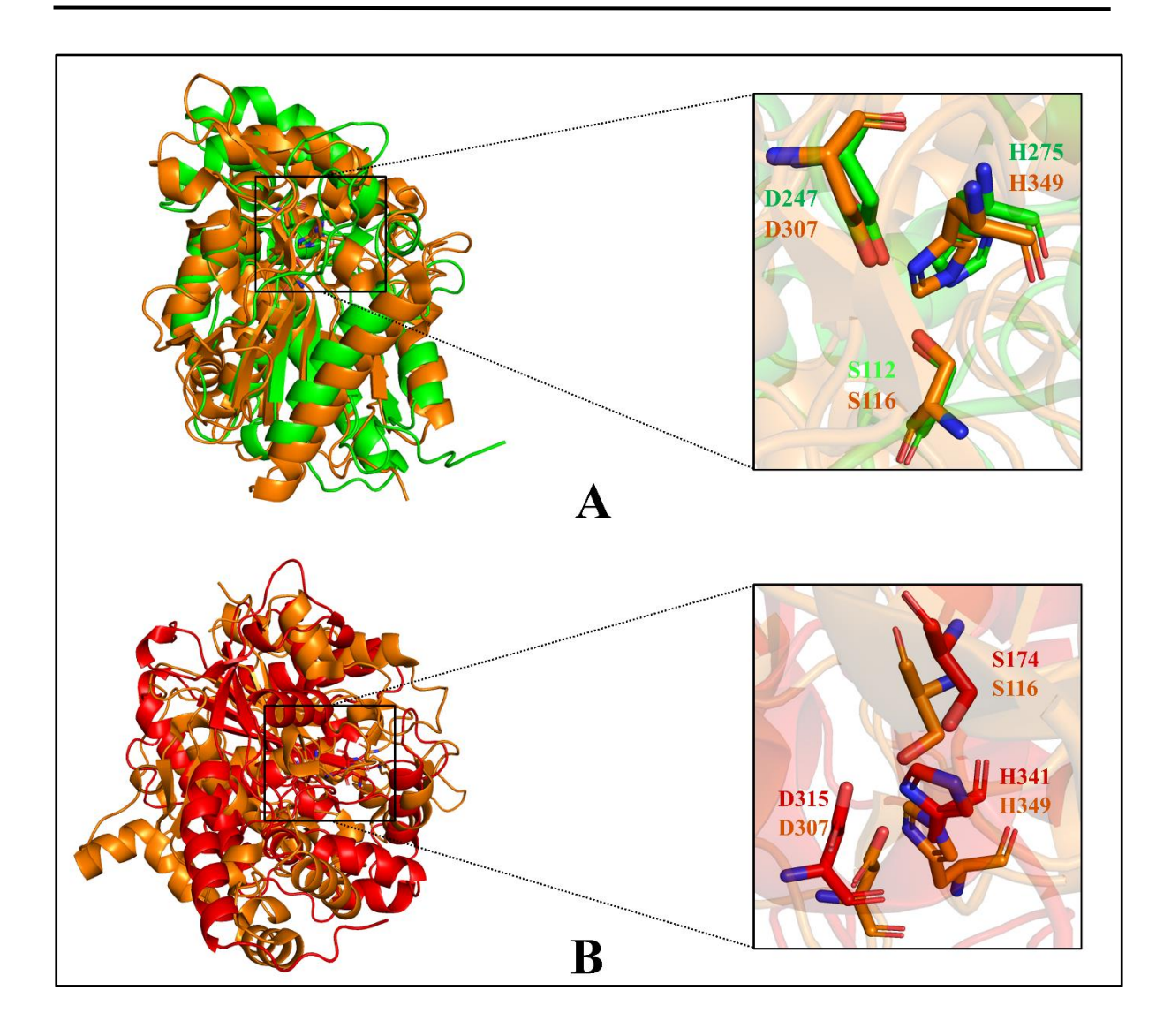
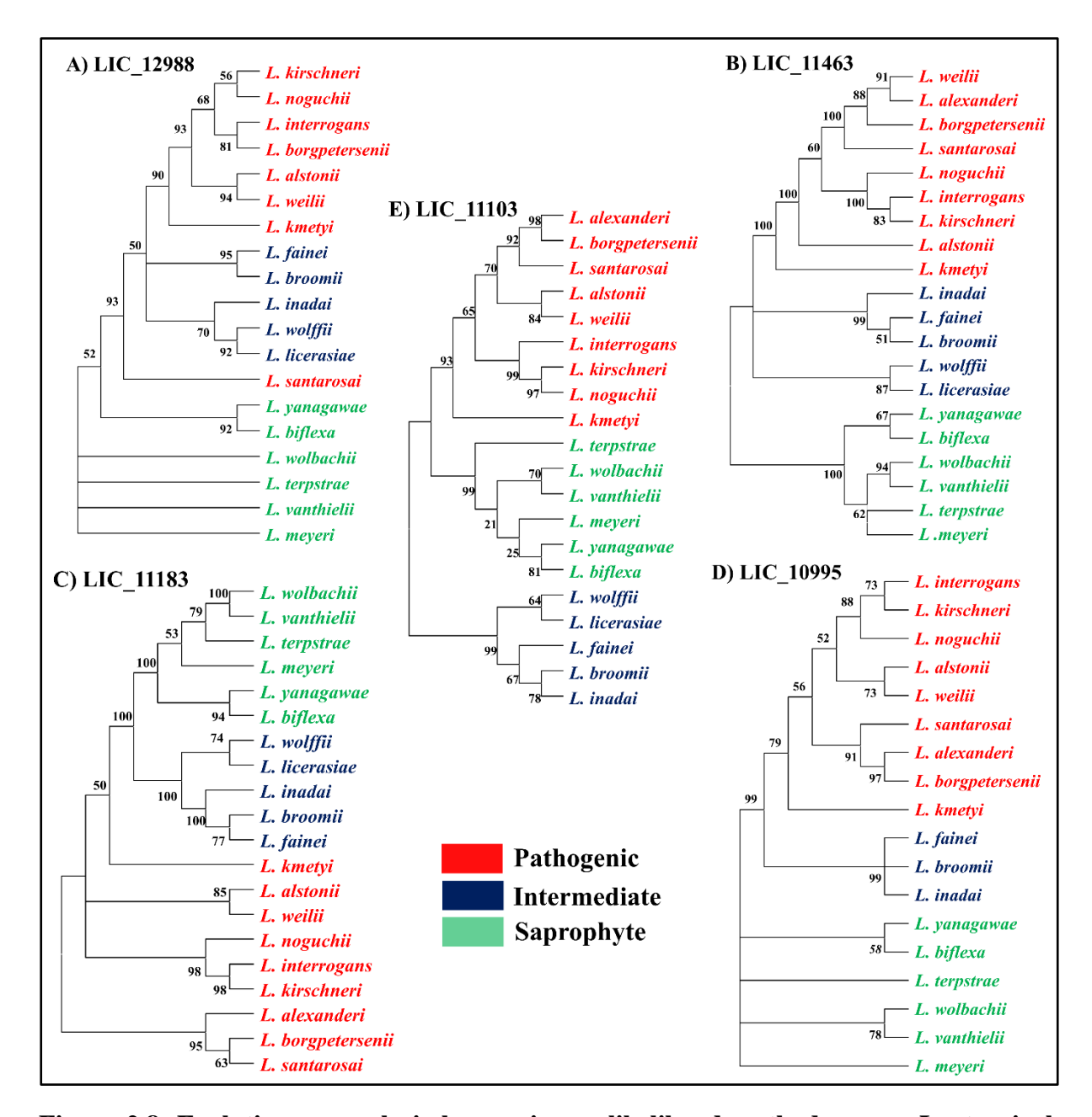


Figure 2.7. Structure alignment of 3-D models with *Staphylococcus aureus* lipase. (A) LIC\_12988 and (B) LIC\_11463 yield the closest fit between catalytic triad residues in three dimensions.

# 2.3.6. Conservation analysis among different Leptospiral species

Pathogenic categories of all five proteins (indicated in red) comprise a high bootstrap percentage, which characterizes their common evolutionary origin. The bootstrap percentage in the phylogram suggests the frequency of the taxa found in a cluster reliant on identity among proteins. Here, the phylograms demonstrated that the pathogenic species exhibited a significant level of identity, whereas the saprophytic species displayed a lesser conservation of the protein sequences (**Figure 2.8**).



**Figure 2.8. Evolutionary analysis by maximum likelihood method among Leptospiral species**. The phylogenetic tree of (A) LIC\_12988, (B) LIC\_11463, (C) LIC\_11183, (D) LIC\_10995, (E) LIC\_11103 with the set of respective similar proteins from pathogenic (red), intermediate (blue) and saprophytic (green) species of *Leptospira*. The *L. interrogans* in the trees designate the clustering of LIC\_12988, LIC\_11463, LIC\_11183, LIC\_10995, LIC\_11103 proteins in their respective phylogram. The branches are displayed with the bootstrap scores (1000 replicates). Mega 11 was employed to generate the trees.

#### 2.4. CONCLUSIONS

This chapter reports the prediction of potent outer membrane and secretory proteins from the whole proteome of *Leptospira interrogans*. Among them, five putative  $\alpha/\beta$  hydrolases, LIC\_11463, LIC\_12988, LIC\_11183, LIC\_11103, and LIC\_10995, were identified and characterized. These proteins possessed a conserved consensus lipase motif, G/A-X-S-X-G. A nucleophile Ser in the protein's canonical lipase motif is typically part of the catalytic triad. Our pBLAST and multiple sequence alignment study suggests that the putative  $\alpha/\beta$  hydrolases may function as lipases or esterases. In phylogenetic analysis, all five proteins were clustered in pathogenic *Leptospira species*, which indicates their essentiality in pathogenesis. Moreover, the putative  $\alpha/\beta$  hydrolases, LIC\_11463 and LIC\_12988, were predicted as virulent factors and showed homology with *Staphylococcus aureus* lipase (SAL), which was reported as a potent virulent factor. Hence, this study suggests the probable role of putative  $\alpha/\beta$  hydrolases in *Leptospira* pathogenesis.

# Chapter-3

# Cloning, expression, and purification of the putative hydrolases

# PART OF THIS CHAPTER IS PUBLISHED IN:

**Shankar UN**, Mohit, Padhi SK, Akif M. (2023) Biochemical characterization, substrate and stereoselectivity of an outer surface putative  $\alpha/\beta$  hydrolase from the pathogenic Leptospira. *Int J Biol Macromol*. 28;229:803-813.

#### 3.1. INTRODUCTION

An  $\alpha/\beta$  hydrolase superfamily is a vast and diverse group of enzymes with widely differing phylogenetic origins. Despite having a diverse group and different phylogenetic origins, it consists of similar structural motifs. The group of enzymes includes carboxyl esterases, lipases, proteases, serine proteases, epoxide hydrolases, acetylcholinesterase, etc. The  $\alpha/\beta$  hydrolase superfamily proteins possess diverse functions with similar structural features. All enzymes are evolved to effectively act on their substrates with different chemical compositions or physicochemical properties and in various biological contexts. Members of  $\alpha/\beta$  hydrolase superfamily contain hydrogen bonds at their catalytic site comprising a triad of serine, aspartate/glutamate, and histidine residues. Additionally, lipases and carboxylesterases of the  $\alpha/\beta$  hydrolase superfamily consist of a canonical consensus lipase motif, Gly-X-Ser-X-Gly. Carboxylesterases (EC 3.1.1.1) hydrolyze the ester bonds in small-chain fatty acids, while lipases (EC 3.1.1.3) cleave the ester bonds of long-chain fatty acids. Significant variability is seen in molecular features of lipases, including the molecular mass, 19-96 kDa. The optimal temperature and pH range from 15 to 70 °C and 5 to 11, respectively (Javed et al. 2018). Our previous bioinformatics analysis of the  $\alpha/\beta$  hydrolase superfamily from the potent outer membrane and secretory proteins from Leptospira mentioned in Chapter 2 revealed that LIC\_11463, LIC\_11103, LIC\_10995, LIC\_11183, and LIC\_12988 proteins belong to α/β hydrolase superfamily, hence named as Leptospiral  $\alpha/\beta$  hydrolases (LABHs). The conserved Gly of the first position from the motif is replaced with Ala in LIC\_11463. Similar to the LIC 11463 sequence, lipases from *Bacillus spp.*, LipB esterase from *Bacillus subtilis*, TaLipA from T. asahii, and ThaL from T. harzianum also possess Ala-His-Ser-Met-Gly sequence motif (Eggert et al. 2002; Kanjanavas et al. 2010; Kumari and Gupta 2015). Although the cloning and protein purifications of all in-silico characterized LABHs were attempted, we could successfully purify two LABHs, LIC 11463 (LABH-1) and LIC 11103 (LABH-2). This chapter describes the molecular cloning, protein purification, and determination of oligomeric states of LABH-1 and LABH-2.

# 3.2. MATERIALS

# 3.2.1. Chemical reagents

Chemical reagents used to design the construct, over-expression, and protein purification were purchased from many commercial resources. The list of chemical reagents and their suppliers are listed in Table 3.1.

Table 3.1. List of chemical reagents and their sources

Purpose	Chemical Reagents/ kits	Suppliers
Molecular	Plasmid isolation	Qiagen
Cloning	DNA gel-extraction	Qiagen
	Quick-site-directed mutagenesis kit	Invitrogen
	DNA polymerases, dNTPs, T4 DNA	New England Bio Labs (NEB)
	Ligase, Restriction Endonucleases	
	Oligonucleotides	Integrated DNA Technology, Inc
	Agarose	Himedia, India
	Ethidium bromide	Himedia, India
	DNA molecular weight marker	Magspin, Thermofisher
Protein	Isopropyl $\beta - D - 1$ -	Sigma, Himedia
Purification	thiogalactopyranoside (IPTG)	
	Tris HCl	Himedia, India
	NaCl	Himedia, India
	Lysozyme	Himedia
	PMSF	Himedia
	Imidazole	Omnipur
	Ni-NTA agarose beads	Sigma Aldrich,
	Acrylamide	Sigma Aldrich,
	Coomassie Brilliant blue R - 250	Himedia, India
	Protein molecular weight marker	Biorad, Puregene
	Protein molecular weight marker	

# 3.2.2. Chemical compositions

All media, buffers, and stock solutions were prepared in Milli-Q or double-distilled water with standard procedures mentioned in Sambrook *et al.* 1989. The chemical compositions of the stock solutions have been described in the Tables below.

Table 3.2. Composition of 1 litre Luria Bertani Broth (LB) medium

Ingredients	Weight (gm)
Tryptone	10
Yeast extract	5
Sodium chloride	10
pH	$7.5 \pm 0.2$

Table 3.3. Composition of antibiotic stocks

Antibiotic	Stock solution	Working concentration
Ampicillin	100mg/ml in Milli-Q	100μg/ml
Kanamycin	50mg/ml in Milli-Q	$50\mu g/ml$
Chloramphenicol	34mg/ml in ethanol	$34\mu g/ml$

The antibiotics were sterilized using 0.22µm filter.

Table 3.4. Composition of agarose gel electrophoresis solutions

Reagents	Compositions		
50X TAE	242g Tris base +57.1ml of glacial acetic acid + 100ml of 0.5M		
	EDTA per litre		
6X sample loading dye	0.25% Xylene, 0.25% Bromophenol Blue, 30% Glycerol		
Ethidium bromide	Stock of 10mg/ml		

Table 3.5. Composition of protein purification solutions

Buffer	Composition
1X Tris HCl buffer	Tris HCl 20mM, NaCl 250mM, pH 7.5
Lysis Buffer	1X Tris HCl buffer with 1mg/ml lysozyme, 0.1mM PMSF
Washing Buffer	1X Tris HCl buffer and 50mM Imidazole
Elution Buffer	1X Tris HCl buffer and 250mM Imidazole

Table 3.6. Composition of SDS-PAGE solutions.

Reagents	Compositions
30% acrylamide	29.2% acrylamide +0.8% Bis-acrylamide
Stacking Buffer	1.5M Tris-HCl, pH8.8 + 0.4% SDS
Resolving buffer	1M Tris-HCl, pH 6.8 + 0.4% SDS
1X Running buffer	3g Tris-HCl +14.4g glycine +1g SDS per liter
De-staining solution	Water: Acetic acid: Methanol:: 5:1:4
Staining solution	2g/L of coomassie brilliant blue R250 in de-staining solution
1X Laemmli sample buffer	10% glycerol +1% $\beta$ -mercaptoethanol + 2% SDS + 0.1%
	bromophenol blue in 1X separating buffer

#### 3.3. METHODOLOGY

# 3.3.1. Preparation of transformation competent E. coli

The DH5α and XL blue *E. coli* competent cells were used for the cloning and propagation of genes. BL21 (DE3) and Rosetta (DE3) were used to express genes. Competent cells were prepared using the CaCl<sub>2</sub> chemical method. Briefly, the inoculum of 1% from overnight grown culture was added to 100ml of Luria Broth medium with or without antibiotics. The cells were allowed to grow at 37 °C on a shaker incubator till the absorbance at 600nm reached 0.4-6. The culture was further allowed to incubate on ice for 30 minutes. Cells were harvested by centrifugation at 7,105 g (4000 rpm) for 30min at 4 °C. The cells were suspended in a sterile

100mM CaCl<sub>2</sub> solution and incubated on ice for 3 hrs. The cells were then harvested by centrifugation and dissolved in 100 mM CaCl<sub>2</sub> containing 10% glycerol. The aliquots of final cell suspension were snap-frozen using liquid nitrogen and preserved at -80°C. The contamination test and transformation efficiency were analyzed before the use.

#### 3.3.2. Molecular cloning

The open reading frame of LABH-1 and LABH-2 (excluding signal sequences; size ~1 Kb) from the genome of *Leptospira interrogans* was PCR amplified by utilizing the gene specific forward primers (FP) and reverse primers (RP) described in **Table 3.7.** The PCR reaction mixture and PCR programme used to amplify the genes, *labh1* and *labh2* are mentioned in **Tables 3.8 and 3.9,** respectively. The PCR product of LABH-1 gene was restriction double digested with BamHI and HindIII while, LABH-2 gene was double digested with NdeI and XhoI restriction enzymes. The digested gene LABH-1 was cloned into the pET28a(+) expression vector under restriction sites BamHI and HindIII and LABH-2 was cloned with pET28a(+) expression vector under restriction sites NdeI and XhoI restriction enzymes. The integration of the gene was confirmed by double digestion and DNA sequencing.

Table 3.7. List of primers used in PCR amplification and mutation

Sr. No.	Genes	Primers (5'-3')
1	labh-1	FP: GAGGATCCAAACCAAAAGCAGAAAATACAAATAC
		RP: CGCAAGCTTCTACAATGAGTCAATGATAGCTATAAC
2	labh-2	FP: GACATATGGCTTATGAAAGAACGGTTTTGACCTAT
		RP: CGCTCGAGCTAAAATAAAGGAACTAACAAACTAGG
3	∆labh-1	FP: AGACCACCCATAGCATGAGCTAACAAA
		RP: TTTGTTAGCTCATGCTATGGGTGGTCT

**Table 3.8. PCR reaction compositions** 

Component	Concentration	
Template	25 ng	
Forward Primers	0.5 μΜ	
Reverse Primers	0.5 μΜ	
dNTPs	$100  \mu M$	
DNA Polymerase	1 unit	

Table 3.9. PCR programme used in gene amplifications.

Gene	Initial	Denaturation	Annealing	Extension	Final
	Denaturation				Extension
LABH-1	98°C	98°C	55°C	72°C	72°C
	(2 min)	(30 sec)	(30 sec)	(60 sec)	(10 min)
LABH-2	98°C	98°C	56 °C	72°C	72°C
	(2 min)	(30 sec)	(30 sec)	(60 sec)	(10 min)

# 3.3.3. Bacterial transformation

*E. coli* competent cells were taken out from the -80°C refrigerator and thawed for 10 min on ice. The plasmid constructs of 20 ng were incubated with *E. coli* competent cells and put on ice for more than 30 minutes. Heat shock treatment was provided at 42°C for 90 seconds and immediately placed on ice for 5 minutes. LB broth of 900μL was added into the mixture and allowed to incubate in a shaking incubator of 1hr at 180rpm. Further, the cells were harvested by centrifuging at 4000rpm for 5 min and was spread on an LB agar plate containing appropriate antibiotics. The agar plate was kept in an incubator at 37°C overnight.

Table 3.10. Bacteria Strains/plasmids used in this study

Bacterial	Description	Source/	
Strains/plasmids		reference	
DH5α	$λ$ $^ φ80dlacZΔM15$ $Δ(lacZYA-argF)U169$ $recA1$	(Taylor et al.	
	$endA\ hsdR17\ (rk^-\ mk^-)\ supE44\ thi-1\ gyrA\ relA1$	1993)	
BL21(DE3)	$F^-$ omp $T$ hsd $S_B$ ( $r_B^ m_B^-$ ) gal dcm (DE3)	(Jeong et al.	
		2009)	
Rosetta (DE3)	$F^-$ ompT hsdS <sub>B</sub> ( $r_B^ m_B^-$ ) gal dcm (DE3) pRARE	Novagen	
	(Cam <sup>R</sup> )		
XL-1 Blue	recA1 endA1 gyrA96 thi-1 hsdR17 supE44 relA1	Invitogen	
	lac [F' proAB lacIq ZΔM15 Tn10 (Tetr )]		
TOP10	F- mcrA $\Delta$ (mrr-hsdRMS-mcrBC) $\phi$ 80lacZ $\Delta$ M15	Invitrogen	
	ΔlacX74 nupG recA1 araD139 Δ(ara-leu)7697		
	galE15 galK16 rpsL(Str <sup>R</sup> ) endA1 $\lambda$ <sup>-</sup>		
	Plasmids/Clones/mutant plasmids	·	
pET28a-His-	P <sub>T7</sub> -based expression vector, with SUMO tag	ThermoFisher	
SUMO			
pET28a	P <sub>T7</sub> -based expression vector	ThermoFisher	
pET28a-labh-1	pET28a- bearing labh-1 within BamHI/HindIII	This study	
	restriction sites		
pET28a-labh-2	pET28a- bearing labh-2 within NdeI/XhoI	This study	
	restriction sites		
Mutant plasmids/clones			
pET28a/Δ <i>labh-1</i>	pET28a-bearing Labh-1 S151A mutation	This study	

# 3.3.4. Site-directed mutagenesis

Codon of active site residue, Ser151 of LABH-1, was replaced with codon of Ala by sitedirected mutagenesis using primers mentioned in Table 3.7. The active site residue mutant of the LABH-1 clone in pET28a is named pET28a\_labh\_S151A. The required mutation was confirmed by sequencing. The recombinant active site mutant LABH-1 was purified with the same protocol as the wild-type.

# 3.3.5. Expression and purification

The resulting pET28a-labh-1 and pET28a-labh-2 constructs encoding full-length LABH-1 and LABH-2 proteins with an N-terminal 6X-histidine tag were transformed separately into Rosetta (DE3) and BL21 (DE3) competent cells, respectively. A single transformant of pET28a-labh-1 was grown in 1 litre Luria Bertani Broth (LB) containing 50 μg/mL kanamycin and 35 µg/mL chloramphenicol at 37 °C while pET28a-labh-2 transformant needed only kanamycin. Protein expression was induced with 0.5 mM isopropyl-D-thiogalactopyranoside (IPTG) at 18 °C, and the post-induction culture was incubated for 16 hours. Cells expressing LABHs were harvested by centrifugation at 8000 rpm for 10 min, followed by pellet resuspension using the lysis buffer [20 mM Tris-HCl, pH 7.5, 250 mM NaCl, and one mM phenylmethylsulfonyl fluoride (PMSF)]. The suspension mixture was treated with a 1 mg/mL lysozyme, incubated on ice for one hour, and then sonicated to break the cells. The cell lysate was centrifuged at 13,000 rpm for 45 min at 4 °C, and the supernatant was loaded on the Ni-NTA column pre-equilibrated with buffer containing 20 mM Tris-HCl (pH 7.5), 250 mM NaCl. The wash buffers of varying imidazole concentrations were used to eliminate impurities. The bound protein was eluted with the elution buffer [20 mM Tris-HCl, pH 7.5, 250 mM NaCl, and 250 mM imidazole]. The eluted fractions were concentrated using an Amicon concentrator with 10,000-Da-cutoff membranes. The protein was further purified through size-exclusion chromatography using the Hiload 16/600 200pg Superdex column (provided by GE Healthcare), which was pre-equilibrated with a buffer containing 20 mM Tris HCl pH 7.5 and 250 mM NaCl. The elution fractions were examined on 12% SDS-PAGE. The pure protein fractions were pooled together, and concentration was measured using a Nano drop.

#### 3.3.6. Size-exclusion chromatography

The oligomeric states of the purified protein were analyzed by size-exclusion chromatography. The experiments were performed with Hiload 16/600 Superdex 200 pg column on AKTA-FPLC (GE Healthcare) using 20 mM Tris HCl pH 7.5 and 250 mM NaCl as a running buffer. The elution time/volume of the recombinant protein was recorded, and the molecular weights were calculated by estimating the elution volumes of standards of known molecular weights.

#### 3.4. RESULTS

Our previous bioinformatics analysis (mentioned in chapter 2) revealed that the LABH-1 and LABH-2 belong to  $\alpha/\beta$  hydrolase superfamily that can hydrolyze small esters or long-chain acylglycerols. The outcomes of molecular cloning and protein purification are presented in this part.

#### 3.4.1. Cloning in expression vector under the influence of T7 promoter

After removing the nucleotide sequence encoding the signal peptide, the molecular size of *labh-1* and *labh-2* genes was found to be 1041bps and 1029bps, respectively. The ORFs of *labh-1* and *labh-2* genes were amplified using appropriate primers by polymerase chain reaction (PCR) method. The right size of PCR amplified product was observed for both genes (**Figure 3.1.A**). Cloning fidelity is confirmed using restriction-double digestion. The electrophoretic separation of inserts from the plasmid construct pET28a-*labh-1* and pET28a-*labh-2* were observed at approximately 1kb, which suggests the size of gene interests (**Figure 3.1.B and C**). The correct insertion of the genes was further confirmed by DNA sequencing.

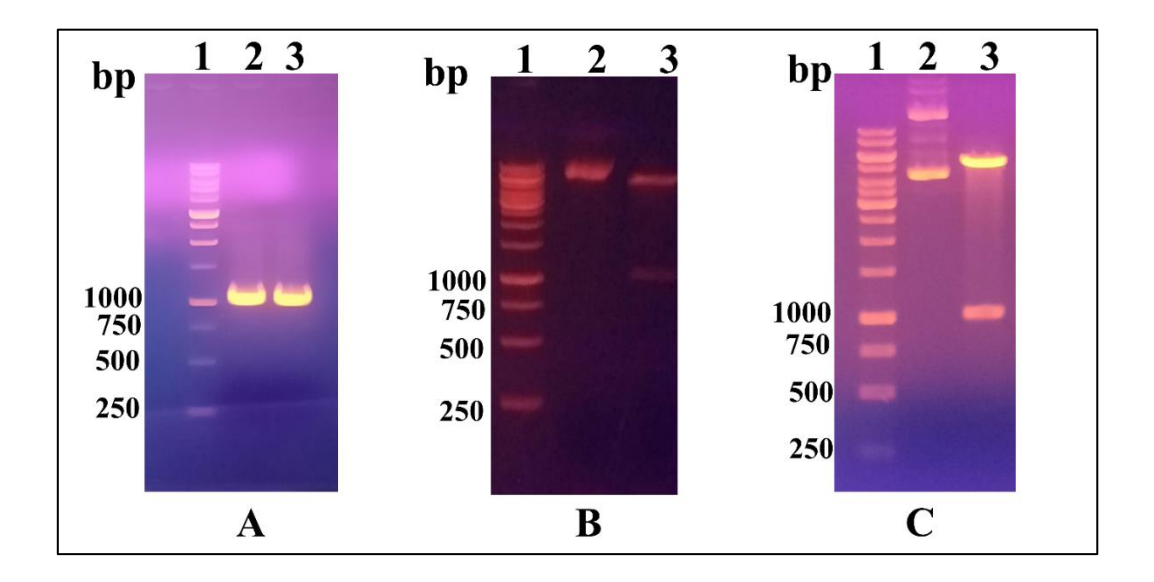


**Figure 3.1. 1% agarose gel showing PCR amplification and separation of inserts from the vector backbone.** (A). PCR amplification of *labh-1* and labh-2 gene products. The lane 1, 2 and 3 indicates DNA ladder, PCR products of *labh-1* and *labh-2* genes, respectively, (B) restriction double digestion of pET28a-*labh-1* plasmid construct using BamHI/HindIII, and (C) restriction double digestion pET28a-*labh-2* construct using NdeI/XhoI. In both B and C figures, Lane 1 depicts DNA ladder whereas lane 2 and 3 contain undigested and digested DNA samples.

# 3.4.2. Recombinant purification of LABH-1

The plasmid construct of pET28a-labh-1 encoding LABH-1 protein was transformed into recombinant *E. coli* BL21 (DE3) expression cells. The cells harbouring corresponding ORF were overexpressed in the soluble fraction. Soluble fraction obtained after sonication of cell lysate was utilised to purify LABH-1 using Ni-NTA affinity chromatography followed by size exclusion chromatography (**Figure 3.2**).

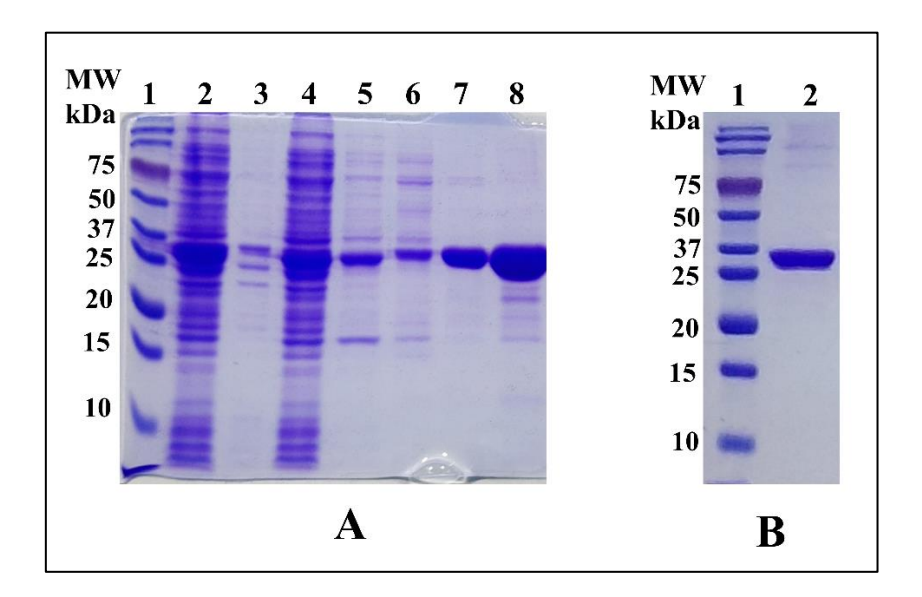
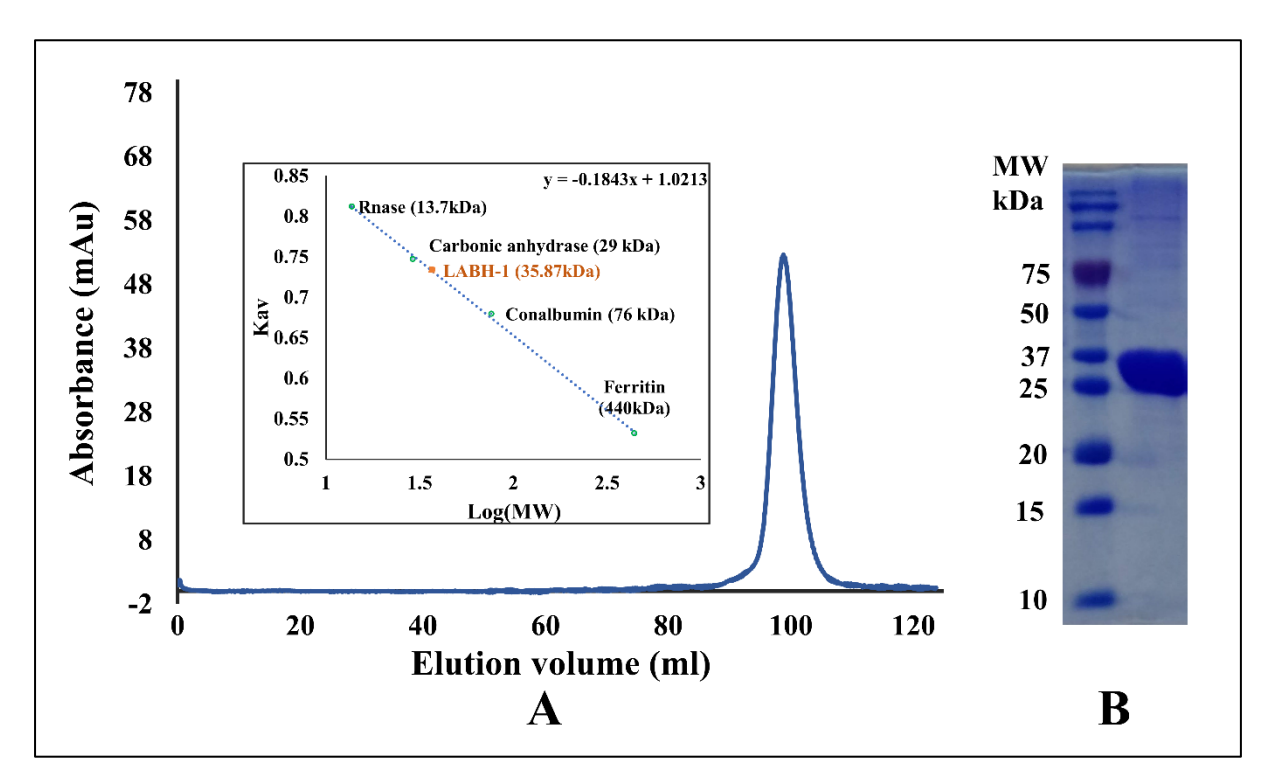


**Figure 3.2. Purification of LABH-1. (A)** 12% SDS-PAGE represents supernatant, pellet, flow through, wash through 1-3 (20mM, 50mM and 150mM imidazole), and elution with 250mM imidazole from Ni-NTA affinity coloum, **(B)** LABH-1 elution fraction after size exclusion chromatography

The recombinant protein LABH-1 was purified with 99% homogeneity with an adequate yield of 25mg from one litre of bacterial culture.

# 3.4.3. LABH-1 exists as monomer in solution

The oligomeric state of LABH-1 was determined using the size-exclusion chromatography experiment. The protein markers of different molecular weights, such as Rnases A (13.7kDa), Carbonic anhydrase (29kDa), Conalbumin (76kDa), and Ferritin (440kDa), were passed through the Superdex 200 column. The elution volume of each protein marker was determined. When the LABH-1 was passed through the column, it was eluted at the volume corresponding to a protomer mass of 36 kDa, suggesting that the purified LABH-1 exists as a monomer in the solution (**Figure 3.3 A**). When the electrophoretic mobility of the fraction collected at approximately 98ml was assayed using 12% SDS-PAGE, we found the molecular weight at



around 36kDa, which is the corresponding protomer mass of LABH-1 (Figure 3.3 B).

**Figure 3.3. Determination of the oligomeric state of LABH-1.** (**A**) The chromatogram obtained from the from the size-exclusion chromatography. The plot indicates Log (MW) and Kav (normalized elution volumes) of the standards. The normalized elution volume of the protein corresponds to a protomer size of 36 kDa, and (**B**) 12% SDS-PAGE depicts homogeneity in the recombinant protein purification after size-exclusion chromatography.

#### 3.4.4. Purification of active site mutant of LABH-1

The Codon of active site residue, Ser151 of LABH-1, was replaced with the codon of Ala by site-directed mutagenesis using forward and reverse primers (**Table 3.7**). The required mutation was confirmed by sequencing. Similar to LABH-1, the mutant of LABH-1 (S151A) was also purified using the Ni-NTA affinity chromatography (**Figure 3.4.4**). The mutant LABH-1 was purified with a sufficient yield of 14mg from 1 litre of bacterial culture.

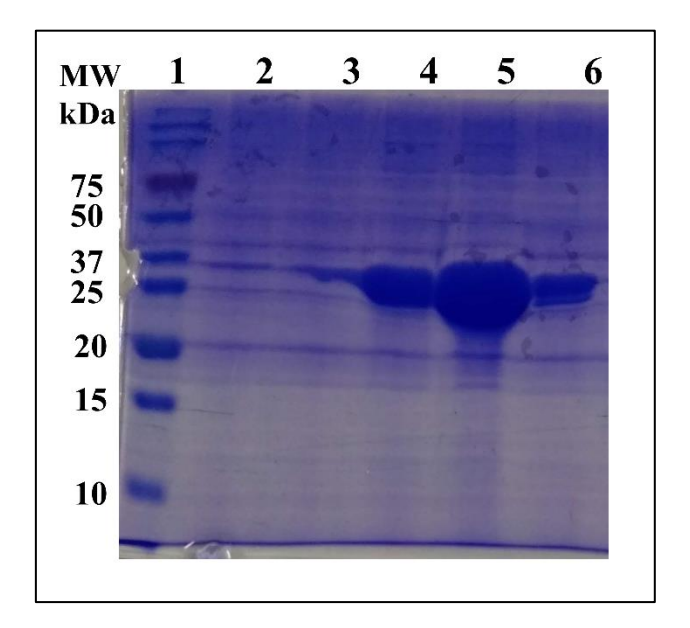


**Figure 3.4. 12% SDS-PAGE showing purification of mutant LABH-1.** Lanes 1, 2, and 3, depict protein markers, flow through, and wash through. Lanes 4, 5, and 6 show elution with 250mM imidazole from the Ni-NTA affinity column.

# 3.4.5. Recombinant purification of LABH-2

The plasmid construct of pET28a-labh-2 encoding LABH-2 protein was transformed into recombinant *E. coli* BL21 (DE3) expression cells. The cells harbouring corresponding ORF of LABH-2 were overexpressed in the soluble fraction. Soluble fraction obtained after sonication of cell lysate was allowed to purify using Ni-NTA affinity chromatography. In Ni-NTA affinity chromatography, the protein of interest was appeared at LABH-2 protomer size of 38kDa (**Figure 3.5**).

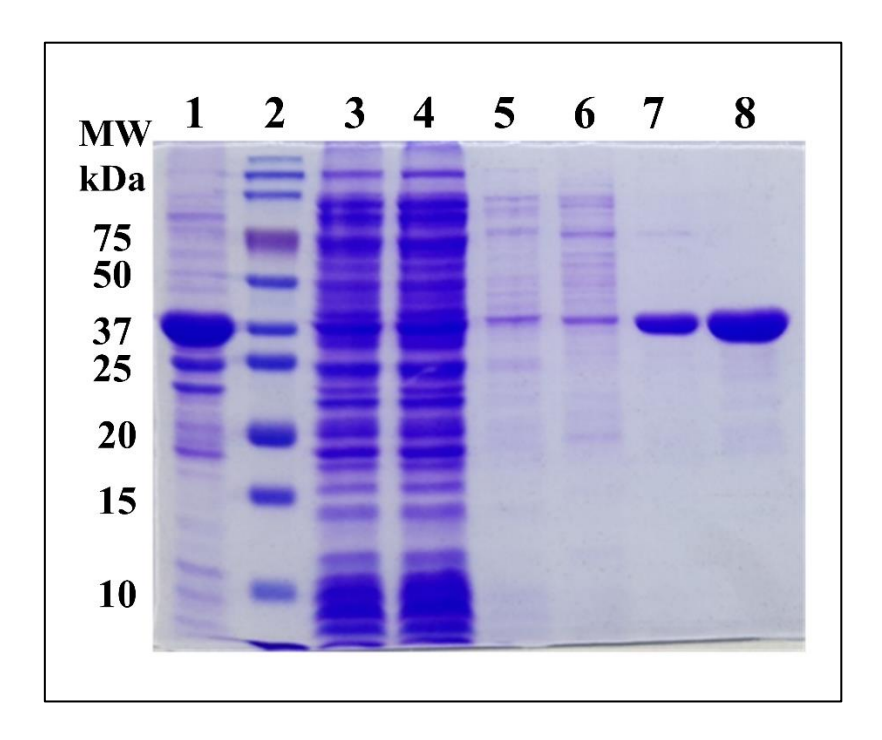


**Figure 3.5. Purification of LABH-2.** 12% SDS-PAGE represents supernatant, protein marker, pellet, flowthrough, wash 1-3 (20mM, 50mM and 100mM imidazole), and elution with 250mM imidazole in lane 1-8 respectively during purification using Ni-NTA affinity chromatography.

# 3.4.6. Oligomeric state of LABH-2

The size exclusion chromatography of purified recombinant LABH-2 was performed to identify the oligomeric state. Surprisingly, the LABH-2 was eluted at the volume corresponding molecular mass of approximately 6 kDa (**Figure 3.6 A**). The same fraction was examined on the 12% SDS polyacrylamide gel with a size corresponding to the 38kDa protein band (**Figure 3.6 B**). Suggesting the correct molecular size of a protomer of LABH-2. Unfortunately, this observation was contradictory with the size-exclusion chromatography. Such observation in the size exclusion chromatography could be the outcome of non-specific interactions of LABH-2 with the resin, leading to the late elution of the protein. At this point, we might conclude that LABH-2 is present in a monomeric solution. The purification yield was 9 mg from one litre of bacterial culture.

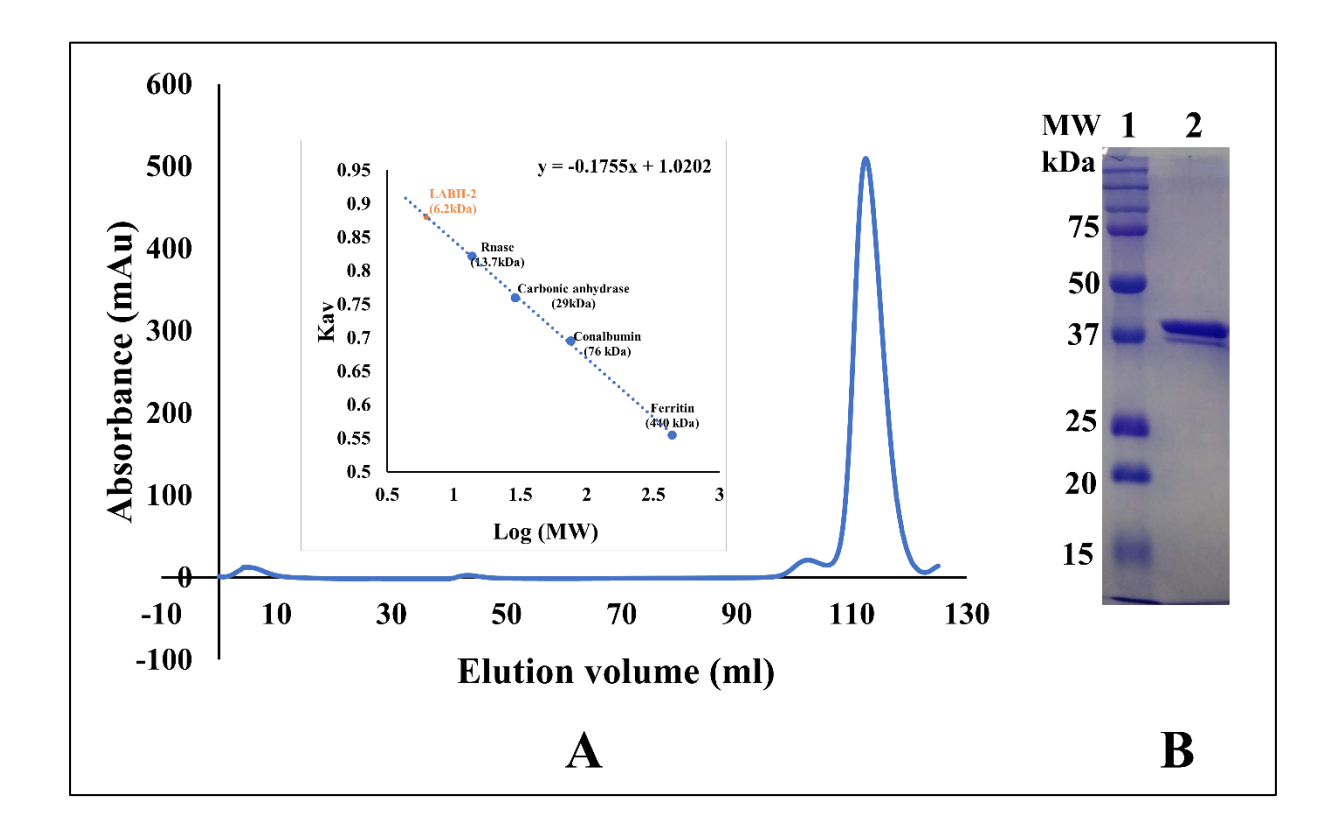


Figure 3.6. Determination of the oligomeric state of LABH-2. (A) Size-exclusion chromatogram. The plot indicates the Log (MW) and Kav (normalized elution volumes) of the standards. The normalized elution volume of the protein corresponds to a size of 6 kDa, (B) 12% SDS-PAGE depicts the recombinant protein in elution fractions of size exclusion chromatography at approximately 38kDa, which is the protomer size of LABH-2.

# 3.5. CONCLUSIONS

Genes encoding Leptospiral  $\alpha/\beta$  hydrolases, LABH-1 and LABH-2 were successfully cloned into the expression vector pET28a. LABH-1, mutant of LABH-1, and LABH-2 showed the good level of expression in *E. coli* cells. All the proteins were purified using Ni-NTA affinity chromatography followed by size exclusion chromatography with a sufficient yield from one litre of bacterial culture. Chromatogram and the fraction on 12% SDS-PAGE clearly show the monomeric nature of LABHs in solution and were purified with more than 95% of purity. The purified proteins described in this chapter are further used in biophysical, biochemical characterizations and virulence study mentioned in chapter 4 of thesis.

# Chapter-4

Biochemical characterization, substrate, and stereo-selectivity of the outer membrane putative α/β hydrolases from Leptospira

#### PART OF THIS CHAPTER IS PUBLISHED IN:

**Shankar UN**, Mohit, Padhi SK, Akif M. (2023) Biochemical characterization, substrate and stereoselectivity of an outer surface putative  $\alpha/\beta$  hydrolase from the pathogenic Leptospira. *Int J Biol Macromol*. 28;229:803-813.

#### 4.1. INTRODUCTION

Pathogenic *Leptospira* express a plethora of proteins targeted on the outer membrane and as secretory proteins. Functional roles of many of these proteins are not yet investigated in details. Surface proteins such as Leptospiral Immunoglobulin-like protein (Lig), *Leptospira* surface antigens (Lsa), Leptospiral complement acquiring protein A (LcpA), and a few leptospiral lipoproteins (LipL) are well characterized as their roles in virulence and pathogenesis (da Silva et al. 2015; Raja and Natarajaseenivasan 2015; Faisal et al. 2016; Haake and Matsunaga 2021). Lig is a well-known vaccine candidate whose antigenic region is well-described (Kumar et al. 2021). Many of these membrane proteins bind to the host extracellular matrix components laminin and fibronectin and facilitate the infection (Choy et al. 2007; Palaniappan et al. 2007). Few are reported to play a crucial role in evading the host complement system (Haake and Matsunaga 2021). A recent report suggests that Ig-domains of Lig proteins possess a novel nuclease activity, which may be required to cleave host NET (Kumar et al. 2022c). However, the role of many other outer membrane and secretory proteins needs to be investigated.

Our *in-silico* study identified many outer membrane and secretory proteins with probable hydrolyzing functions (mentioned in Chapter 2). Proteins with the  $\alpha/\beta$  hydrolase domains that possess hydrolyzing functions are classified into an  $\alpha/\beta$  hydrolase superfamily. This class of proteins hydrolyzes small esters or ester bonds found in acylglycerols. Carboxylesterases, lipases, and some proteases mainly possess this fold and contain serine residue in a canonical Gly-X-Ser-X-Gly lipase consensus motif. Serine as a nucleophile, histidine as a base, and an acidic residue (either aspartic or glutamic acid) constitute a highly conserved catalytic triad (Kourist et al. 2010). In addition, hydrolases mostly share common structural features and biochemical characteristics. Elastase and alkaline proteases from *Pseudomonas aeruginosa*, gelatinase from *Enterococcus faecalis*, and aureolysin from *Staphylococcus aureus* cleave the complement C3 have already been well characterized (Hong and

Ghebrehiwet 1992; Park et al. 2008; Laarman et al. 2011). Moreover, *streptococcal* secreted esterase is a crucial virulent factor and protects against subcutaneous GAS infection (Zhu et al. 2009). In a recent study, the extracellular lipases from *Staphylococcus aureus* are reported to have lipolysis of immune-activating ligands and promote evasion from innate host immunity (Chen and Alonzo 2019). An  $\alpha/\beta$ -hydrolase domain protein from *Haemonchus contortus* possesses lipolytic activity. It also modulates the host cytokines, mainly by enhancing IL-10 production and suppressing the production of IL-4, IFN- $\gamma$ , and TGF- $\beta$  (Lu et al. 2021).

However, biochemical and structural features and the substrate selectivity of many outer membrane or secretory leptospiral  $\alpha/\beta$  hydrolases (LABHs) are not yet investigated. Our bioinformatic analysis yielded five outer/secretory putative  $\alpha/\beta$  hydrolases displaying similarity with the esterase/lipase family of proteins (described in Chapter 2). In Chapter 3, we reported the cloning, expression, and recombinant purification of LABHs. This chapter reports biochemical characterization, substrate selectivity, and kinetic parameters of LABHs (LABH-1 and LABH-2). Moreover, this chapter also reports the crystallization trials and optimization of LABH-1 crystals. LABH-1 catalyzed kinetic resolution of racemic 1-phenylethyl acetate reveals excellent enantioselectivity in producing (R)-1-phenylethanol, a valuable chiral synthon in several industries. Moreover, LABH-1 also showed immunomodulatory effects on mice macrophages.

#### 4.2. MATERIALS

Reagents or chemicals used for enzyme assays, crystallization and study of potential virulence were procured from multiple resources. All solutions were prepared in double-distilled water. Different *p*-nitrophenyl esters and inhibitor orlistat were prepared in acetonitrile and DMSO solvents respectively. Briefly, the list of chemical reagents and their sources are listed in table 4.1.

Table 4.1. List of chemical reagents and their sources

Purpose	Chemicals	Made
Buffer	Tris HCl	Himedia
	Potassium phosphate buffer	Himedia
	Acetate buffer	Himedia
	MES	Himedia
	CAPS	Himedia
Substrate	<i>p</i> -nitrophenyl acetate	Sigma Aldrich
	<i>p</i> -nitrophenyl butyrate	Sigma Aldrich
	<i>p</i> -nitrophenyl laurate	Sigma Aldrich
	<i>p</i> -nitrophenyl palmitate	Sigma Aldrich
	racemic 1-phenylethyl acetate	Sigma
Inhibitor	Orlistat Sigma Aldrich	
Organic Solvent	Acetonitrile	Merck
	Diethyl ether	Sigma
	Hexane	Sigma
	Isopropanol	Sigma
	DMSO	Sigma
Crystallization	Wizard 1&2, JGSG++, and Wizard 3 & 4	Jena biosciences
	crystal screen 1&2), Qiagen (JCSG++	Hampton
	Morpheus, structure screen 1 &2, PACT	Molecular dimensions
	Premier and JGSC Plus	
	Siliconized glass coverslips	Hampton
	crystallization screening sitting drop	Hampton
	plates (96 wells, two drops)	
	24 well plates	Hampton and Thermo
		scientific
Analysis of	mice macrophage cell line Raw 264.7	(American Type Culture
potential virulence		Collection, Rockville, Md.
		USA
	DMEM	Gibco, Life Technologies,
	FBS	(Invitrogen, UK)
	1% penicillin streptomycin	(Invitrogen, UK)
	Polymyxin B	Sigma
	Lipopolysacharides (LPS) (E. coli	Sigma Aldrich, Merk
	0111:B4)	Germany
	Proteinase K	(G.Biosciences, USA
	MTT [3-(4,5-dimethylthiazol-2-yl)-2,5-	Hi media
	diphenyltetrazolium bromide]	
	trizol reagent	Takara
	Phenol, chloroform	Honeywell
	cDNA synthesis kit	Takara

# **4.3. METHODOLOGY**

#### 4.3.1. Circular Dichroism measurements

Secondary structure composition and thermal denaturation of LABHs were analyzed by circular dichroism (CD) spectra on a JASCO-J1500 CD spectrometer equipped with a Peltier temperature controller system. Far-UV CD spectra were recorded from 190 to 250 nm in 10 mM Tris-HCl (pH 7.5) at 25 °C in a quartz cuvette with a path length of 0.2 cm. The protein concentration used for the experiments was 5μM. Three scans were accumulated at a scan speed of 50 nm min<sup>-1</sup> to generate the final spectra. Consequently, secondary structure contents were analyzed with the Dichroweb using K2D programme (Andrade et al. 1993; Whitmore and Wallace 2008). Further, the thermal denaturation of protein was performed by monitoring the change of ellipticity at 222 nm at different temperatures ranging from 20-90 °C. Fractions that unfolded in varying temperatures were determined as per the procedure mentioned by Greenfield N.J. (Norma J. Greenfield 2009).

#### 4.3.2. Enzymatic activity assay

The enzymatic activity assay was performed on a 96-well plate. The reaction volume of 200 μL contained 50 mM Tris HCl buffer (pH 7.5), and various concentrations (0- 1.2 mM) of *p*-nitrophenyl butyrate. One μM purified LABHs was added to each reaction mixture and incubated at 25° C. The control reaction sample had all the reaction components except the protein, which is replaced with the buffer. All measurements were performed in triplicates. The release of yellow-colored *para*-nitrophenolate ion due to the hydrolysis of *p*-nitrophenyl butyrate at 25 °C was monitored on a UV- visible spectrometer at 405 nm (Tanaka et al. 2018). Under assay conditions, one international lipase unit is the amount of enzyme required to release 1 μmol of *p*-nitrophenol per minute.

# 4.3.3. Effect of pH and temperature on the enzymatic activity

To determine the pH optima of LABHs, the activity was measured at 25 °C in 50 mM acetate buffer (for pH 4 and 5), 50 mM MES (for pH 6 and 6.5), 50 mM Tris HCl (pH 7-9), and 100 mM CAPS buffer (pH 9.5-11). Similarly, to find the optimum temperature of the enzymatic activity, the reaction mixture containing 50 mM Tris HCl buffer (pH 8), 1 μM purified protein, and *p*-nitrophenyl butyrate was incubated with no shaking for 5 min at varied temperatures (25-80 °C) and release of *para*-nitrophenolate ion was monitored on a UV- visible spectrometer at the wavelength of 405 nm.

#### 4.3.4. Determination of steady-state kinetics parameters

Kinetic parameters were determined for four different substrates, i.e., *p*-nitrophenyl acetate (C2), *p*-nitrophenyl butyrate (C4), *p*-nitrophenyl laurate (C12), and *p*-nitrophenyl palmitate (C16). A typical experiment contained (0- 5 mM) of respective substrate, 50 mM Tris HCl buffer (pH 8), and 0.5% Triton X-100, in 200 μL of reaction volume. One micro molar purified LABHs was added in the reaction mixture and conversion of *para*-nitro phenol substrates to yellow color *para*-nitro phenolate was measured spectrophotometrically. The intensity of the yellow color of *p*-nitrophenol was used to quantify the hydrolase activity of LABHs with different substrates.

#### 4.3.5 Inhibition assay

To analyze the inhibition of LABH-1 activity, a lipase inhibitor, or listat, was employed. A 100  $\mu$ M stock of or listat dissolved in DMSO was prepared and used. Inhibition kinetics was performed with various concentrations of or listat (0-20  $\mu$ M). A decrease in the release of *para*-nitrophenolate ions was monitored at 25 °C on a UV-visible spectrometer at the wavelength of 405 nm. Further, the IC50 of the or listat was determined with the inhibition assay. A Lineweaver-Burk plot of 1/[S] versus 1/V was plotted in the presence of different inhibitor concentrations to know the inhibition mode. All reactions were performed in triplicate.

## 4.3.6. Crystallization screening

The crystallization screening of homogeneously purified LABH-1 was set up with various commercial screens provided by Jena Biosciences, Hampton, Qiagen, and Molecular Dimensions. A 9mg/ml purified protein was allowed to combine with crystallization screens using the crystallization robot. The sitting drop vapor diffusion method was used to screen the crystallization conditions. The incubation temperatures were 22°C and 4°C, respectively. Crystallization plates were observed using a stereo microscope until the drops were at different time points. Crystallization hits were recorded and optimized to improve the crystal size using the hanging drop method into 24 well plates. Moreover, seeding techniques were also used to improve the quality of crystals.

# 4.3.7. X-ray diffraction

The crystals were obtained from LABH-1 protein in different crystallization conditions. A single crystal was fished from the drop and exposed to an X-ray beam at the in-house XRD facility at CCMB, Hyderabad. Cryoprotectants, such as polyethylene glycol, glycerol, and sucrose, were used to stabilize the protein crystals.

#### 4.3.8. Protein modelling and structural alignment

The three-dimensional structure of the LABH-1 was modelled using the alphafold online server (Jumper et al. 2021). A model with the lowest  $\Delta G$  was chosen out of five generated structures and further energy minimization was done using a Swiss PDB viewer (SPDV) (Guex and Peitsch 1997). The stereo-chemical quality of the model was analyzed with Procheck and ProSA online programs (Laskowski et al. 1993; Wiederstein and Sippl 2007). Structural homologs were identified using the Dali search tool (Holm 2022). The multiple sequence alignment of the Top 5 structurally similar proteins with the LABH-1 was performed using the CLUSTAL omega and the figure was generated using ESpript3 (Sievers et al. 2011; Robert and Gouet 2014).

## 4.3.9. Molecular Docking

Molecular docking studies were performed using AutoDock Vina 1.1.2 (Trott and Olson 2009; Eberhardt et al. 2021). The structural coordinate of the substrate, *p*-nitrophenyl butyrate (pNPB), and an inhibitor, orlistat, were retrieved from the Ligand PubChem database. The protein and ligand were prepared and pdbqt files were generated in AutoDock tools. A grid box size of  $10 \times 10 \times 14$  dimension with spacing of 1 Å, and the center as 0.640, -5.779, and -6.121 for x, y, and z coordinates respectively was set for the pNPB. Similarly, the grid box size of 24  $\times$  24  $\times$  22 dimensions with spacing 1 Å and the centre were -12.950, 0.947, and 15.096 for x, y, and z, respectively, was set for orlistat. The pdbqt files were executed using AutoDock Vina to get the docked complex. PyMOL was used to visualize and analyze structures (http://www.pymol.org). The inhibitor binding site for the protein model was predicted by the 3D DogSite scorer (Volkamer et al. 2012). Interacting residues in the docked structures were identified using PDBsum online server (Laskowski et al. 2018).

# 4.3.10. Phylogenetic analysis

All protein sequences were retrieved from NCBI and Uniprot databases. Multiple sequence alignment was performed using CLUSTAL omega and the phylogenetic analysis was inferred using the Maximum Likelihood method based on the Jones-Taylor-Thornton (JTT) model. The bootstrap consensus tree inferred from 500 replicates was considered to represent evolutionary history. The percentage of trees (>50 %) in which the associated taxa clustered together is shown next to the branches. Phylogenetic analysis was conducted in MEGA11 (Jones et al. 1992; Tamura et al. 2021).

# 4.3.11. Biocatalytic kinetic resolution

To evaluate the enantioselectivity of LABHs, we aimed to carry out kinetic resolution-based hydrolysis of racemic 1-phenylethyl acetate. The reaction mixture consisted of 33  $\mu$ L of 50 mM potassium phosphate buffer (KPB), pH 7.0, 571  $\mu$ L of distilled water, 61  $\mu$ L of purified

LABH-1 (16.3  $\mu$ g/ $\mu$ L × 61  $\mu$ L= ~1 mg), and 313  $\mu$ L of diethyl ether. To this reaction mixture, 20  $\mu$ L of 5 mM racemic 1-phenylethyl acetate was added and incubated in a ThermoMixer at 300 rpm, 40°C. A control experiment was carried out in an identical manner, except the enzyme was replaced by its corresponding buffer, i.e., 20 mM Tris HCl, 250 mM NaCl, pH 7.5. The reaction was monitored by taking aliquots at three different time points, 4, 6, and 8 h. Each aliquot of 100  $\mu$ L was mixed with 100  $\mu$ L of hexane (90): isopropanol (10), dried over a pinch of Na<sub>2</sub>SO<sub>4</sub>, followed by centrifugation at 15000g for 5 mins, and the upper organic layer was taken for HPLC analysis. Prior to the analysis of the biocatalysis reaction mixture, chiral resolution of racemic 1-phenylethyl acetate was performed. The chiral resolution was carried out in a HPLC using Chiralcel® OD-H column with a solvent system consisting of hexane: isopropanol (98:02), flow rate of 0.4 mL/min, at 254 nm. The retention time of (R)-1-phenylethyl acetate, (S)-1-phenylethyl acetate, (S)-1-phenylethy

#### 4.3.12. Cell viability assay

Mice macrophage cell line Raw 264.7 was cultured in DMEM medium supplemented with 10% Fetal Bovine Serum (FBS) and 1X penicillin streptomycin at 37 °C, 5% CO<sub>2</sub>. Purified LABH-1 was treated with Polymyxin B for 2hrs at 4 °C to remove the endotoxin. Polymyxin B-treated LABH-1 was used to test the toxicity of the protein and for cytokine assays. Cells were seeded into a 96-well plate, 5×10<sup>4</sup> cells/well, followed by incubation with LABH-1 protein with 10ng, 100ng, 1μg, 10μg, and 100μg for 24 hrs and 48 hrs. After incubation, 0.5mg/ml of MTT reagent was added to the cells followed by the colorimetric measurement at 570nm using a microplate reader (Infinite 200 PRO).

#### 4.3.13. Quantitative real time polymerase chain reaction (qRT-PCR)

Raw cells were treated with the optimized quantity of LABH-1 (1 μg and 10 μg) for 6hrs. Further, cells were washed with ice-cold 1x PBS to isolate the RNA. RNA was isolated from the LABH-1 treated and untreated cells using the triazole-chloroform extraction method (Afroz et al. 2016). In brief, cell pellets were resuspended in 1 ml of trizol reagent and incubated on ice for 10 min. After incubation, the tubes were filled with 200 μl chloroform and shaken vigorously for 15 sec, and incubated on ice for 15 min. Subsequently, after the centrifugation at 12000 rpm for 15 min at 4°C, and the aqueous layer was collected in a fresh tube. An isopropanol of 500 μl was gradually mixed with the aqueous phase followed by its incubation on ice for 30 minutes. Further, the samples were centrifuged at 12000rpm for 30 min at 4°C. The supernatant was removed after centrifugation, and the RNA pellet was dissolved in the TE buffer. A total of 1 μg of RNA was used to synthesize cDNA using the standard protocol of cDNA synthesis kit (Takara, USA). 50ng of cDNA was utilized for qRT PCR using gene-specific primers for IL6, IL12, TNFα, and IL10 in the concentration of 0.3 pmol/μL. The primer details are mentioned in **Table 4.2**. The relative mRNA expression was determined relative to the housekeeping gene GAPDH.

Table 4.2 List of primers for qRT-PCR

S.No.	Gene from Mouse	Primers (5'- 3')
1	IL-6	FP: CTGCAAGAGACTTCCATCCAG
		RP: AGTGGTATAGACAGGTCTGTTGG
2	IL-10	FP: GCTCTTACTGACTGGCATGAG
		RP: CGCAGCTCTAGGAGCATGTG
3	IL-12	FP: TGGTTTGCCATCGTTTTGCTG
		RP: ACAGGTGAGGTTCACTGTTTCT
4	TNF-α	FP: CCTGTAGCCCACGTCGTAG
		RP: GGGAGTAGACAAGGTACAACCC
5	GAPDH	FP: AGGTCGGTGTGAACGGATTTG
		RP: TGTAGACCATGTAGTTGAGGTCA

#### 4.4. RESULTS

The recombinant *E. coli* BL21 (DE3) cells harboring corresponding ORFs were overexpressed in the soluble fraction. The homogeneous, monomeric form of LABH-1 and LABH-2 was purified using Ni-NTA affinity chromatography followed by Size exclusion chromatography (**described in Chapter 3**). The outcomes of biophysical, biochemical, and structural studies of potential virulence are presented in this chapter.

#### 4.4.1. Leptospiral α/β hydrolase-1 (LABH-1)

#### 4.4.1.1. LABH-1 contains mostly helical content and displays moderate stability

The proteins belong to  $\alpha/\beta$  hydrolase superfamily mostly share a common fold but vary greatly in terms of sequences and their biological roles. This fold usually consists of eight parallel βstrands and six α-helices grouped in a half-barrel like structure (Dimitriou et al. 2017). The overall content of secondary structures varies among lipases, esterases, and proteases. In order to estimate secondary structure content in LABH-1, CD spectra were analyzed. The far-UV CD spectrum of the protein displayed two negative peaks at 222 and 208 nm and one positive peak at 193 nm, indicating the predominance of α-helical content. Furthermore, analysis of secondary structure composition using Dichroweb analysis tool showed α-helical content of 56% and a  $\beta$ -strands of 9% at pH 7.5 (**Figure 4.1 A**). The theoretical estimation of secondary structure contents of the same yielded 45% and 12% α-helix and β-strands, respectively. These values are almost similar to our experimental analysis. The stability of the LABH-1 at different temperatures and pH was also investigated. The thermal denaturation of LABH-1 displayed a melting temperature (Tm) of approximately 60 °C, suggesting moderate stability in the protein (Figure 4.1 B). Protein secondary structure was significantly lost at the acidic pH of 5 and 6. The effect of neutral as well as alkaline pH was not very significant. Minor changes in the ellipticity were observed at pH 11. This suggests that the protein is moderately stable at pH 7 to 11 (**Figure 4.1 C**).

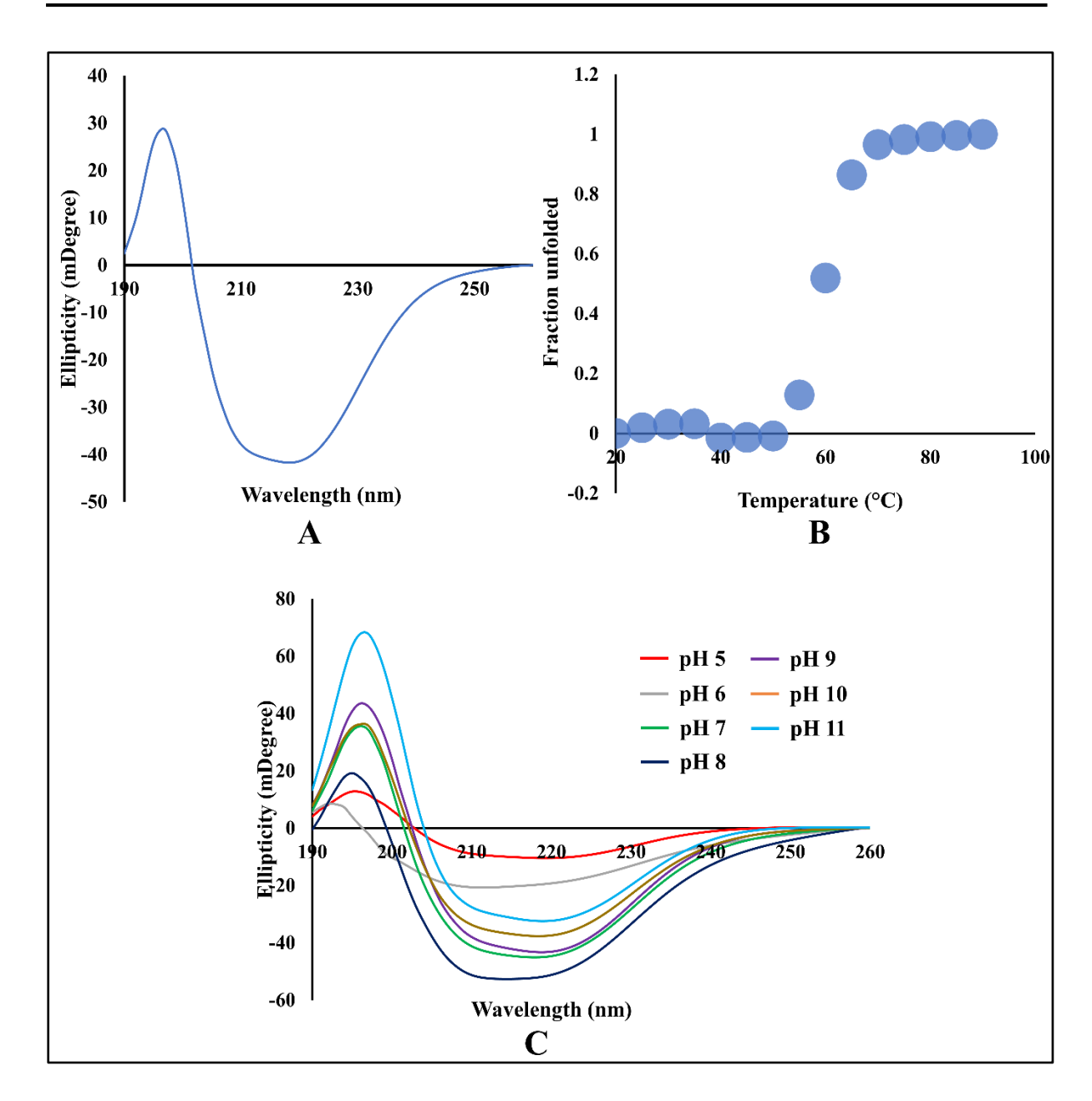


**Figure 4.1. CD-spectra measurements of LABH-1.** (A) Far UV-CD spectra from 250 to 195 nm using 5  $\mu$ M of protein. (B) Thermal denaturation curve plotted in terms of the fraction of unfolding at different temperature points. (C) Far UV-spectra at different pH conditions, where pH 5, 6, 7, 8, 9, 10, and 11 are represented with red, gray, green, blue, purple, orange, and cyan, respectively.

#### 4.4.1.2. Kinetics parameters and substrate specificity of LABH-1

Since the LABH-1 contains an  $\alpha/\beta$  hydrolase fold and possesses a conserved lipase motif (Ala-X-Ser-X-Gly), it may have esterase or lipase activity. Its activity was assayed with a non-natural substrate, p-nitrophenyl butyrate, at room temperature. Protein-catalyzed hydrolysis of p-nitrophenyl butyrate to p-nitrophenolate has confirmed that the purified protein is enzymatically active (**Figure 4.2**).

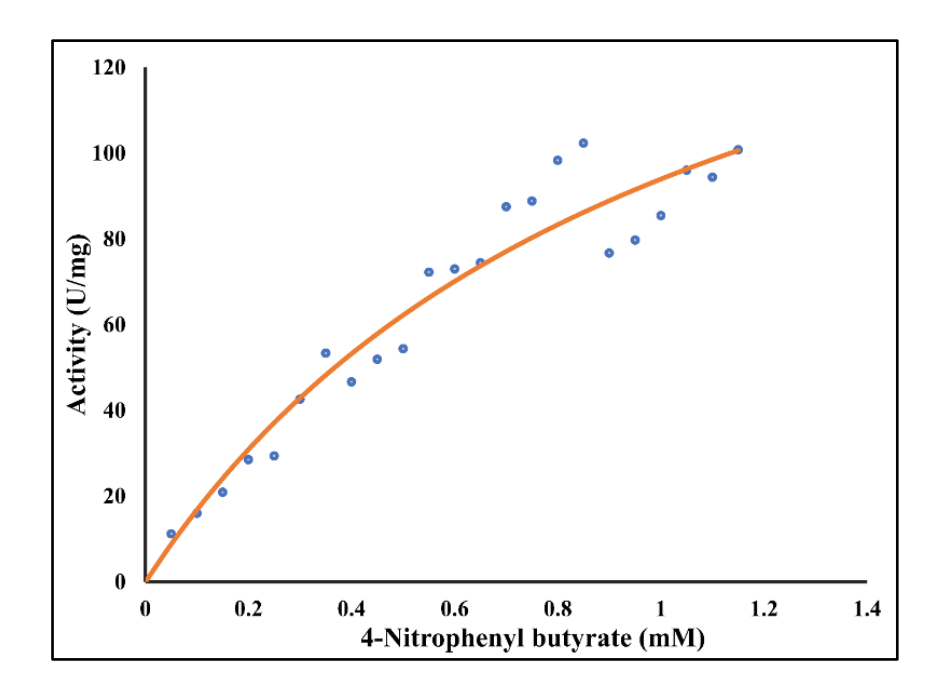
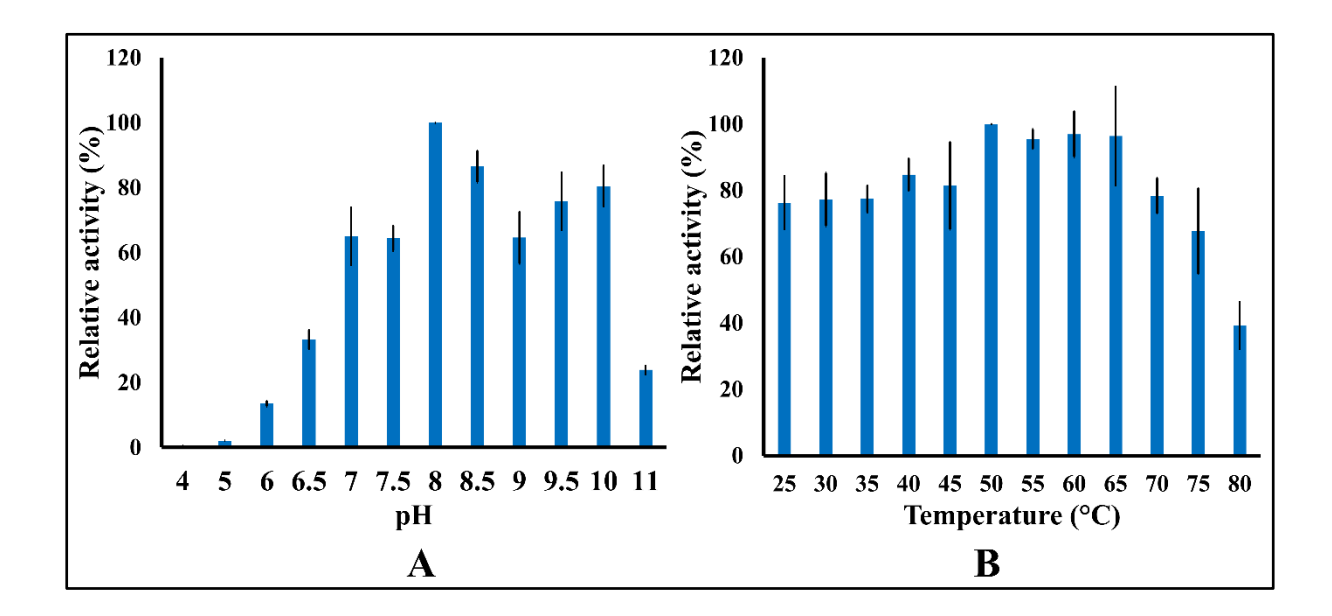


Figure 4.2. Enzymatic activity of LABH-1 at room temperature against p-nitrophenyl butyrate.

Usually, esterases and lipases display enzymatic activity over the broader range of temperature and pH. A lipase from *C. viswanathii* exhibits its maximum activity at a pH 4 (Yao et al. 2021). Hence, the impact of pH and temperature on the LABH's hydrolytic activity was also assayed using the same substrate. The LABH-1 displayed the optimum activity at pH 8. The activity at pH 8.5 to pH 10 was almost similar but slightly lower than pH 8 (**Figure 4.3 A**). This observation suggests that the LABH-1 preferred alkaline pH for its activity. Temperature is an essential parameter for catalytic activity of an enzyme. Various  $\alpha/\beta$  hydrolases exhibit different thermostability due to structural diversity and secondary structure contents. Lipases display a

range of optimum temperatures. For example, an extracellular lipase from *A. niger* GZUF36 displayed maximum activity at 40 °C (Xing et al. 2021). An esterase from *T. tengcongensis*, thermophilic lipases from *Burkholderia ubonensis* and *Janibacter* spp R02 exhibit optimum temperatures of 65 and 80 °C, respectively (Rao et al. 2011; Yang et al. 2016; Castilla et al. 2017). The activity of LABH-1 was investigated under different reaction temperatures (25-80 °C), and it displayed highest activity in the range of 50- 65 °C (**Figure 4.3 B**).



**Figure 4.3. Effect of pH and temperature on the hydrolytic activity.** (**A**) The hydrolytic activity of LABH-1 was examined in varying pH 4-11 conditions using a substrate, *p*-nitrophenyl butyrate. (**B**) The hydrolytic activity at different temperatures (25-80 °C).

Temperature is an essential parameter for catalytic activity of an enzyme. Various  $\alpha/\beta$  hydrolases exhibit different thermostability due to structural diversity and secondary structure contents. Lipases display a range of optimum temperatures. For example, an extracellular lipase from *A. niger* GZUF36 displayed maximum activity at 40 °C (Xing et al. 2021). An esterase from *T. tengcongensis*, thermophilic lipases from *Burkholderia ubonensis* and *Janibacter* spp R02 exhibit optimum temperatures of 65 and 80 °C, respectively

(Rao et al. 2011; Yang et al. 2016; Castilla et al. 2017). The activity of LABH-1 was investigated under different reaction temperatures (25-80 °C), and it displayed highest activity in the range of 50-65 °C (**Figure 4.3 B**).

Many bacterial esterase/lipases activity is modulated by several divalent ions such as Ca<sup>2+</sup>, Zn<sup>2+</sup> etc. (Yang et al. 2009, 2010; Zarafeta et al. 2016; Xing et al. 2021). Therefore, Ca<sup>2+</sup> and Zn<sup>2+</sup> effects on hydrolytic activity of LABH-1 were examined, however, no significant change in LABH-1 activity was observed (**Figure 4.4**).

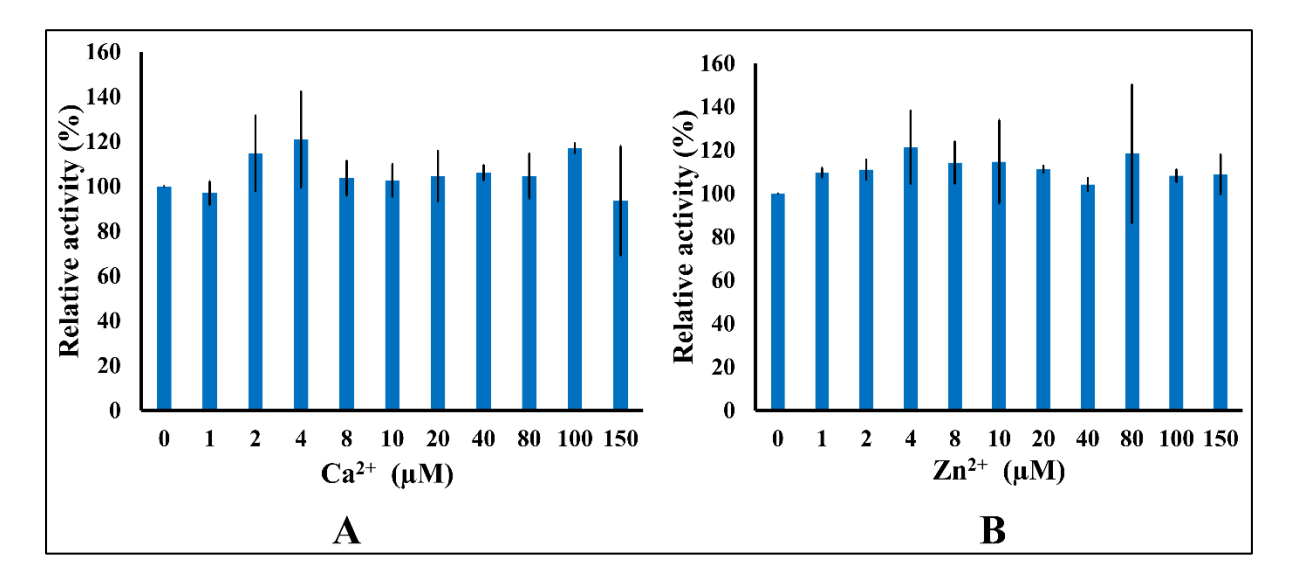


**Figure 4.4. Effect of metals on the hydrolytic activity.** The hydrolytic activity of LABH-1 was tested in varying metal concentrations (0-150μM) (**A**) Ca<sup>2+</sup>, and (**B**) Zn<sup>2+</sup>.

To identify the substrate specificity, the hydrolytic activity was examined against the p-nitrophenyl acetate, p-nitrophenyl butyrate, p-nitrophenyl laurate, and p-nitrophenyl palmitate at pH 8. The highest activity ( $V_{\text{max}}$ ) was observed with the substrate p-nitrophenyl acetate followed by p-nitrophenyl butyrate (**Figure 4.5**).

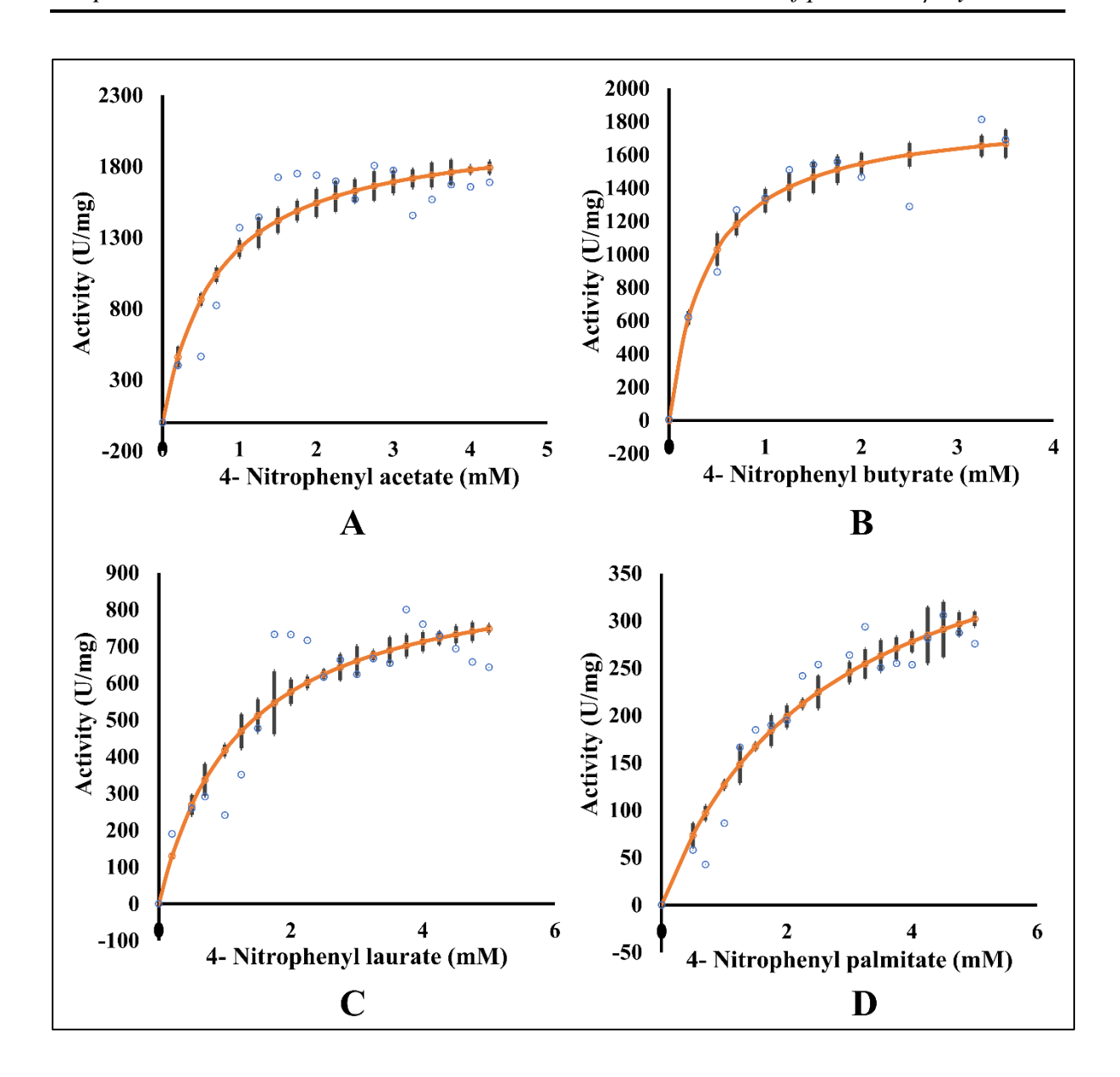


Figure 4.5. The hydrolytic activity of the LABH-1 against different esters of fatty acids.

The hydrolytic activity was assayed using a spectrophotometric method where the changes in absorbance after hydrolysis of (A) *p*-nitrophenyl acetate (B) *p*-nitrophenyl butyrate (C) *p*-nitrophenyl laurate and (D) *p*-nitrophenyl palmitate was measured at 405 nm.

The kinetic study of LABH-1 has revealed  $K_{\rm M}$  values of 0.71±0.05, 0.37±0.07, 1.25±0.23, and 2.66±0.49 mM for the substrates p-nitrophenyl acetate, p-nitrophenyl butyrate, p-nitrophenyl laurate, and p-nitrophenyl palmitate, respectively. The lowest  $K_{\rm M}$  value was observed for the substrate p-nitrophenyl butyrate, suggesting a better affinity of this substrate with the enzyme.

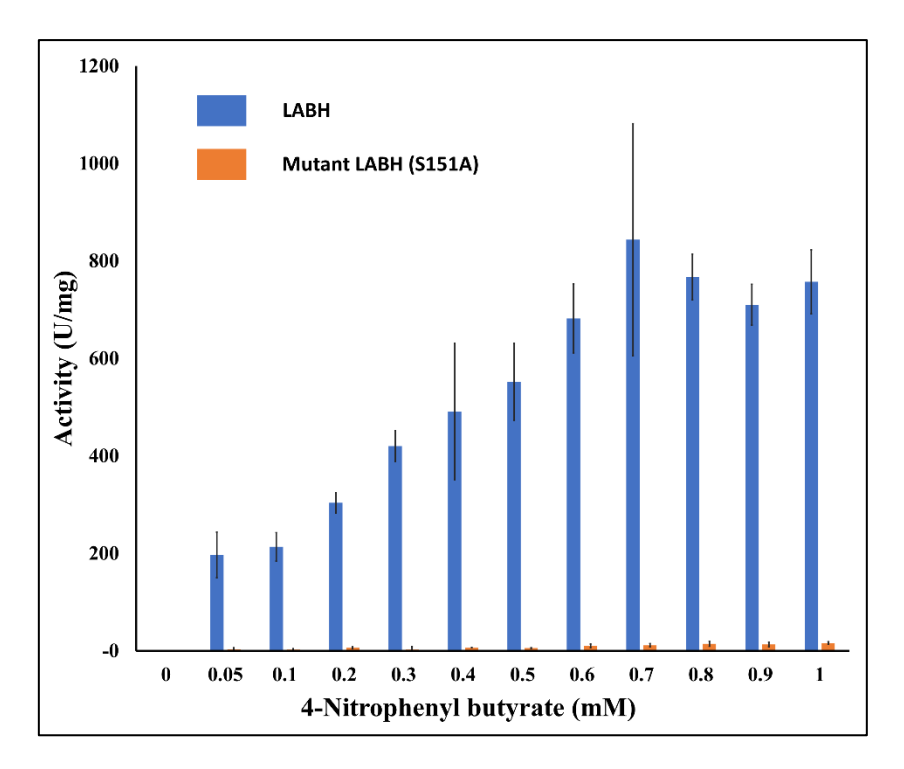
Comparable  $k_{\text{cat}}$  values were observed for the substrates p-nitrophenyl acetate and p-nitrophenyl butyrate. They were found to be  $34.86\pm0.33$  and  $29.93\pm1.33$  s<sup>-1</sup>, respectively. In addition to the relatively high affinity of LABH-1 towards p-nitrophenyl butyrate, the protein also showed the highest catalytic efficiency of  $82.17\pm12.1$  s<sup>-1</sup>mM<sup>-1</sup> with it compared to the other substrates. The kinetic parameters with all substrates are summarized in **Table 4.3**. These observations suggest that the purified LABH-1 hydrolyzes the esters of short-chain fatty acids more efficiently than that of long-chain fatty acids.

Table 4.3. Kinetic parameters of the purified LABH-1

S.No.	Protein	Substrate	K <sub>M</sub> (mM)	$V_{ m max}$	$k_{\rm cat}$ (s <sup>-1</sup> )	k <sub>cat</sub> /K <sub>M</sub>
				$(\mu mol{\cdot}min^{-1}mg^-$		$(s^{-1}mM^{-1})$
				1)		
1	N:	<i>p</i> -nitrophenyl	0.71±	$2091.42 \pm 19.59$	34.86±0.3	49.26±
		acetate	0.05		3	3.88
		<i>p</i> -nitrophenyl	$0.37\pm$	1795.55±79.51	$29.93 \pm$	82.17±12.
		butyrate	0.07		1.33	1
	Native					
	LABH-1	<i>p</i> -nitrophenyl	1.25±	935.76± 53.19	$15.60\pm$	12.69±
		laurate	0.23		0.89	1.66
		<i>p</i> -nitrophenyl	2.66±	$463.68 \pm 49.40$	$7.73 \pm 0.82$	$2.93 \pm 0.24$
		palmitate	0.49			
2	Mutant	<i>p</i> -nitrophenyl		ND*		
	LABH-1	butyrate				

<sup>\*</sup> ND- Not determined

In brief, the purified LABH-1 was observed to act more efficiently on the short-chain fatty alkyl esters in the alkaline pH (8-10). The active site mutant (S151A) protein did not display any activity suggesting the catalytic role of Ser151 in the native protein (**Figure 4.6**).



**Figure 4.6:** Enzymatic specific activity of the wild-type and mutant LABH-1 at the room temperature against p-nitrophenyl butyrate.

## 4.4.1.3. Inhibition kinetics of LABH-1

An anti-obesity drug, orlistat, is a potent inhibitor of human gastric and pancreatic lipases and has been reported to inhibit  $Staphylococcus \ aureus$  lipase (Kitadokoro et al. 2020). The LABH-1 was observed to have sequence similarity (38%) and structural homology with the lipases from  $Staphylococcus \ spp$ . Hence, the inhibitory effect of orlistat on LABH-1 was investigated. Interestingly, a decrease in LABH-1 activity was observed with an increasing concentration of orlistat, however, the  $K_{\rm M}$  remained the same. **Figure 4.7 B** demonstrates the Lineweaver-Burk plot of LABH-1 inhibition by increased concentration of orlistat using p-nitrophenyl butyrate

as the substrate, which suggests that it could be of non-competitive nature. Moreover, the IC50 value of the orlistat was found to be  $\sim$ 1.8  $\mu$ M (**Figure 4.7 A**).

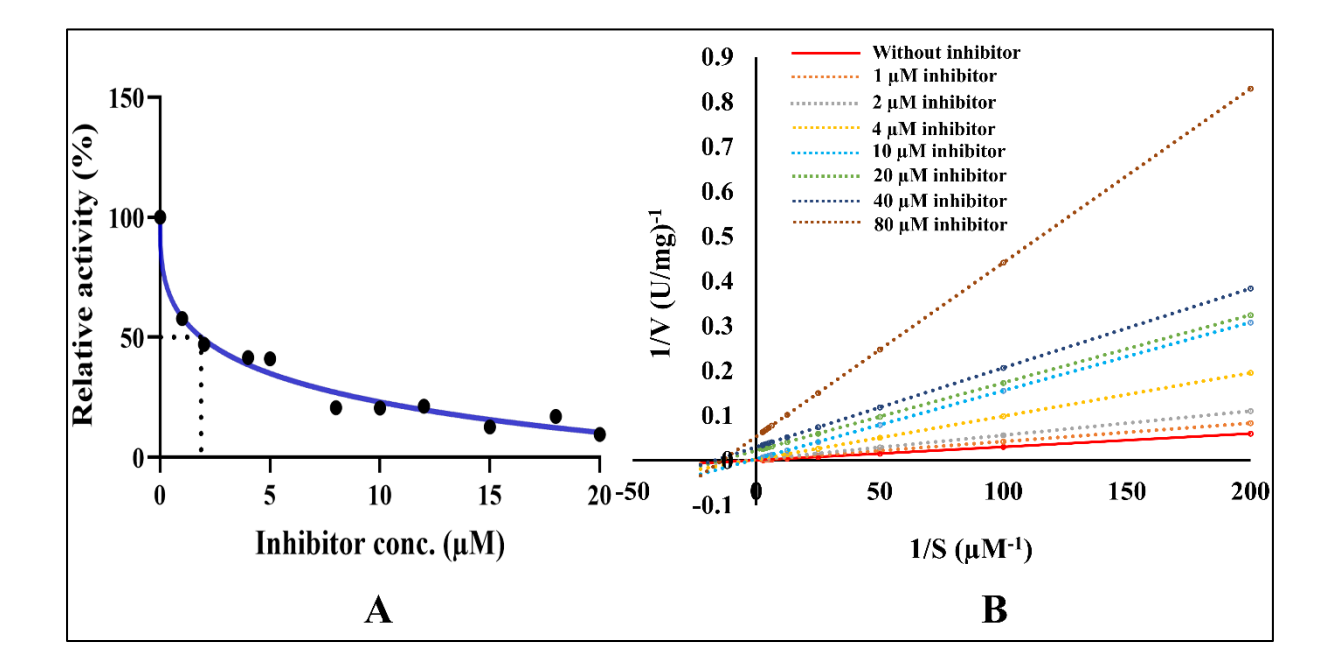


**Figure 4.7. Inhibition of the hydrolytic activity of LABH-1.** (**A**) Determination of IC50 value of inhibition with an inhibitor, orlistat. Representation of decrease of the relative activity of LABH-1 on *p*-nitrophenyl butyrate at 25 °C and pH 8 in presence of different concentrations of orlistat (193.1 U/ mg = 100% relative activity). (**B**) Lineweaver-Burk plot of 1/[S] versus 1/V using different orlistat concentrations. Red line depicts enzymatic activity in presence of no inhibitor, however, an orange, gray, yellow, cyan, green, blue and brown dotted lines represent 1, 2, 4, 10, 20, 40, and 80 μM concentrations of orlistat respectively.

## 4.4.1.4. Crystallization and data collection

LABH-1 protein was allowed for crystallization screening using commercially available screens. Few crystallization conditions gave crystal hits. These were (1) 0.2M MgCl<sub>2</sub>.6H<sub>2</sub>O, 0.1M HEPES sod. pH 7.5, 30% v/v polyethylene glycol 400), (2) 0.1M HEPES sod. pH 7.5, 10% v/v 2-propanol, 20% w/v polyethylene glycol 4000, (3) 0.1M HEPES sod. pH 7.5, 20%

v/v Jeffamine M600, and (4) 0.2M ammonium phosphate monobasic, 0.1M Tris pH 8.5, 50% (v/v)2-Methyl-2,4-pentanediol (**Figure 4.8**).

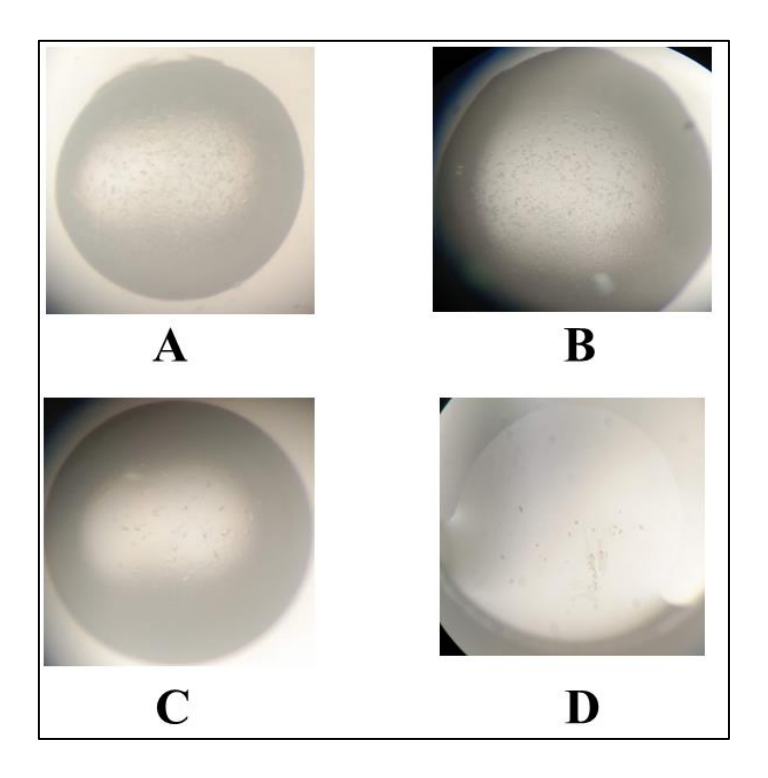


**Figure 4.8. Crystallization conditions obtained for LABH-1.** Four crystallization hits were observed from the commercially available Crystal Screen.

Furthermore, crystallization conditions were further optimized manually in 24-well plates by the vapor diffusion hanging drop method. One of the conditions yielded improved crystal under varying protein concentrations, PEG percentage, and pH of the reservoir buffer. The optimized conditions were 25mg/ml protein, 0.1M HEPES sod. pH 7, 20% PEG 4000, 8% 2-propanol (**Figure 4.9 A**), 30mg/ml protein, 0.1M HEPES sod. pH 6.8, 20% PEG 4000, 8% 2-propanol (**Figure 4.9 B**), 30mg/ml protein, 0.1M HEPES sod. pH 6.8, 24% PEG 4000, 8% 2-propanol (**Figure 4.9 B**).

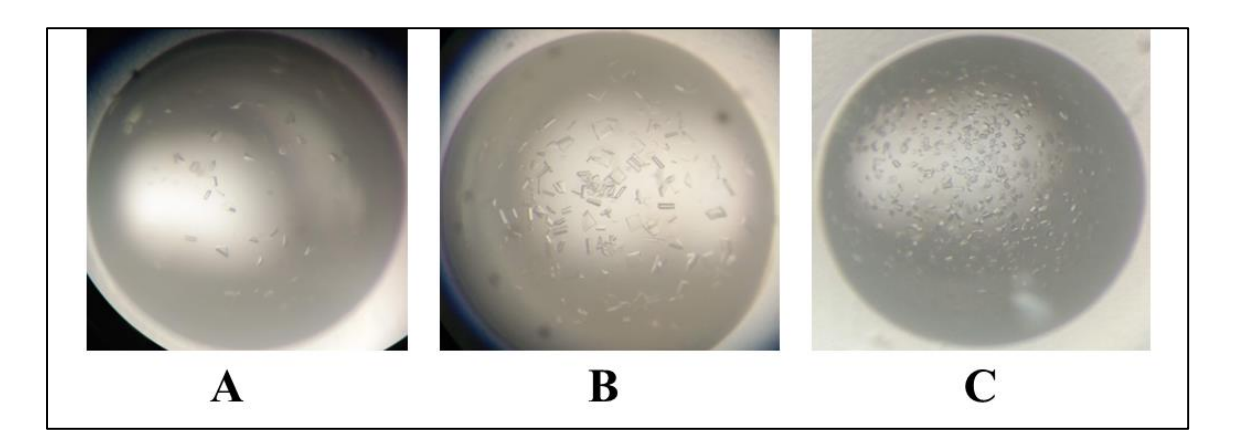


**Figure 4.9. Crystal optimization of LABH-1 (A)** 25mg/ml protein concentration, HEPES sodium pH 7, 20% PEG 4000, 8% 2-propanol, **(B)** 30mg/ml protein concentration, HEPES sodium pH 6.8, 20% PEG 4000, 8% 2-propanol, and **(C)** 30mg/ml protein concentration, HEPES sod. pH 6.8, 24% PEG 4000, 8% 2-propanol.

Single crystals of LABH-1 were mounted in the beam and adjusted carefully to allow it for X-ray diffraction. Unfortunately, some crystals were diffracted with at very low resolution (**Figure 4.10**). The poor diffraction may be due to the issues with crystal packing. Many attempts were made to improve the quality of crystals. Our efforts to improve the crystal size and packing were futile.

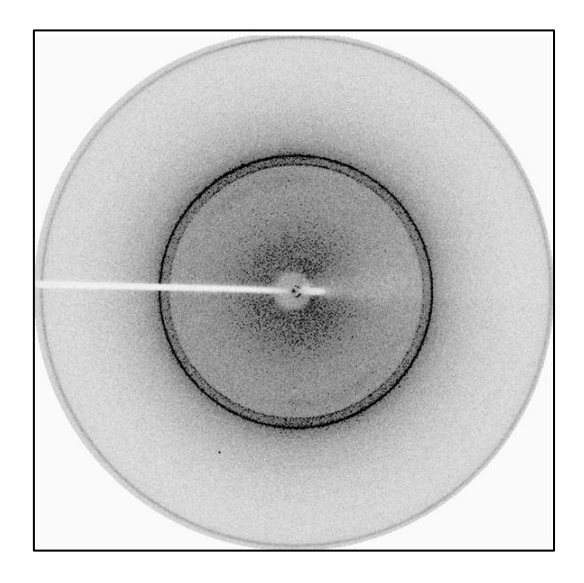


Figure 4.10. X-ray diffraction pattern of LABH-1 protein.

## 4.4.1.5. Structural features and comparison with other $\alpha/\beta$ hydrolases

The AlphaFold generated 3-dimensional structure of LABH-1 showed considerable Ramachandran plot statistics. Validation by Ramachandran plot showed approximately 98.6% residues in favored and allowed region while 1% of residues in generously allowed region (Figure 4.11 B). The model structure also possesses a ProSA Z-score of -7.55, which validates the quality of the model structure (Figure 4.11 C). These statistics indicated that the modelled structure posed ideal bond lengths and angles. The three-dimensional structure revealed that the LABH-1 contained eighteen  $\alpha$ -helices and eight  $\beta$ -strands (**Figure 4.11 A**). The catalytic triad Ser-Asp-His is situated in the active site cavity. Ser151 of the catalytic triad is present in the loop region connecting  $\alpha$ 7 helix and  $\beta$ 5. The connecting loop of  $\alpha$ -15 and  $\alpha$ -16 helices possesses Asp292 whereas His318 is present at the beginning of the α17 helix. The total secondary structure content in the 3D-structure model had 44% and 12% α-helices and βstrands, respectively. These contents were similar to the secondary structure composition (56%  $\alpha$ -helices and 9%  $\beta$ -strands) determined by the circular dichroism spectroscopy. The structural similarity search with the DALI server yielded the top 20 structural homologs with overall identity and root mean square deviation (RMSD) of 20% and 2.7 Å, respectively. These were from lipases, esterases, palmitoyl protein thioesterase-2, cholesterol acyltransferase, and lysosomal phospholipase A2 from different organisms. The multiple sequence alignment of the top 3 structural homologs, lipase from Staphylococcus hyicus (SHL; PDB ID: 2HIH), esterase from Clostridium botulinum (PDB ID: 5AH1), and lipase from Geobacillus stearothermophilus (PDB ID: 4X6U) with LABH-1 showed alignment of the conserved lipase motif (Gly/Ala-X-Ser-X-Gly) and catalytic triad (Ser-Asp-His) (**Figure 4.11 D**). Remarkably, Staphylococcus hyicus lipase and esterase from Clostridium botulinum belong to an α/β hydrolase superfamily (Tiesinga et al. 2007; Perz et al. 2016).

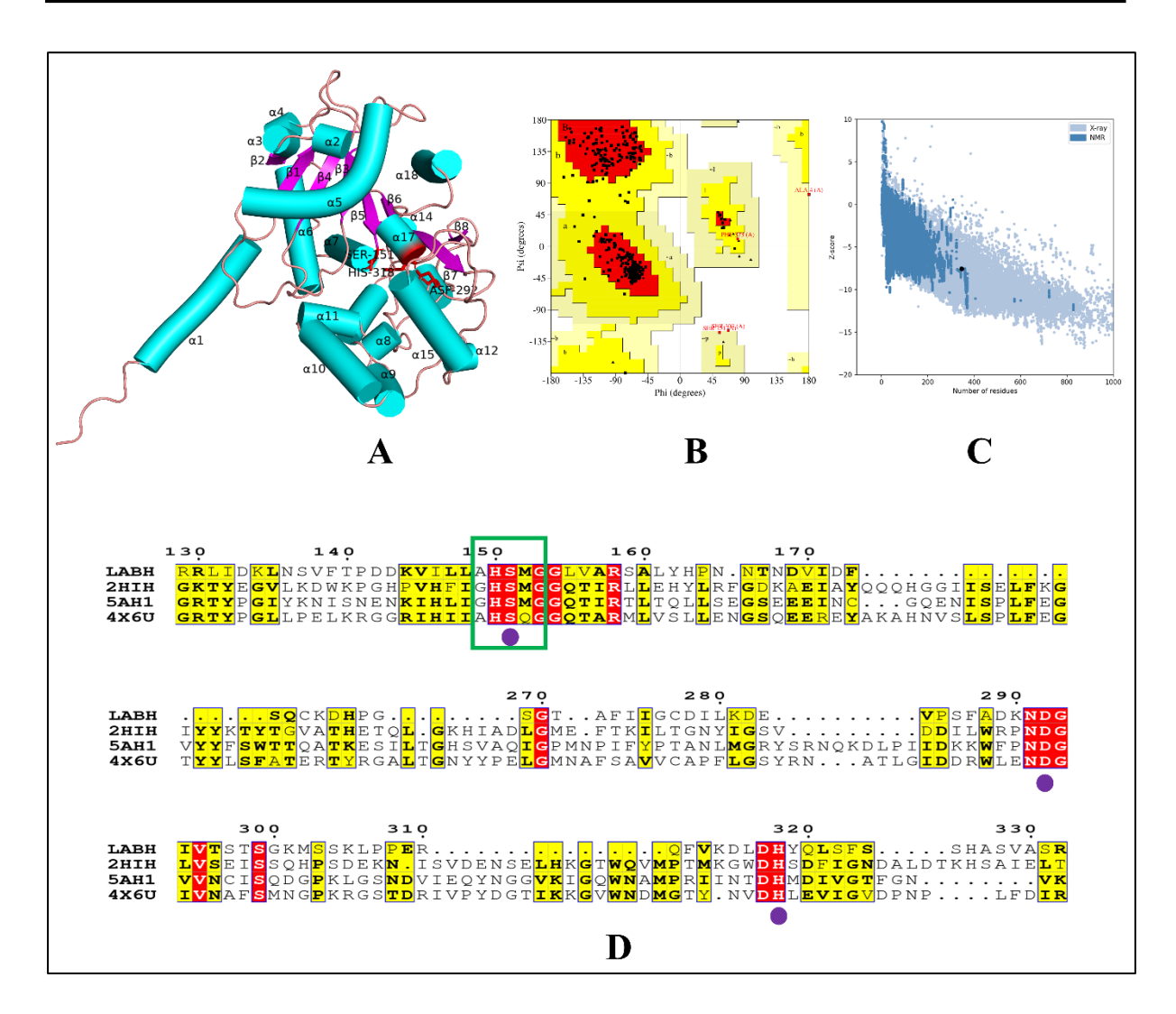
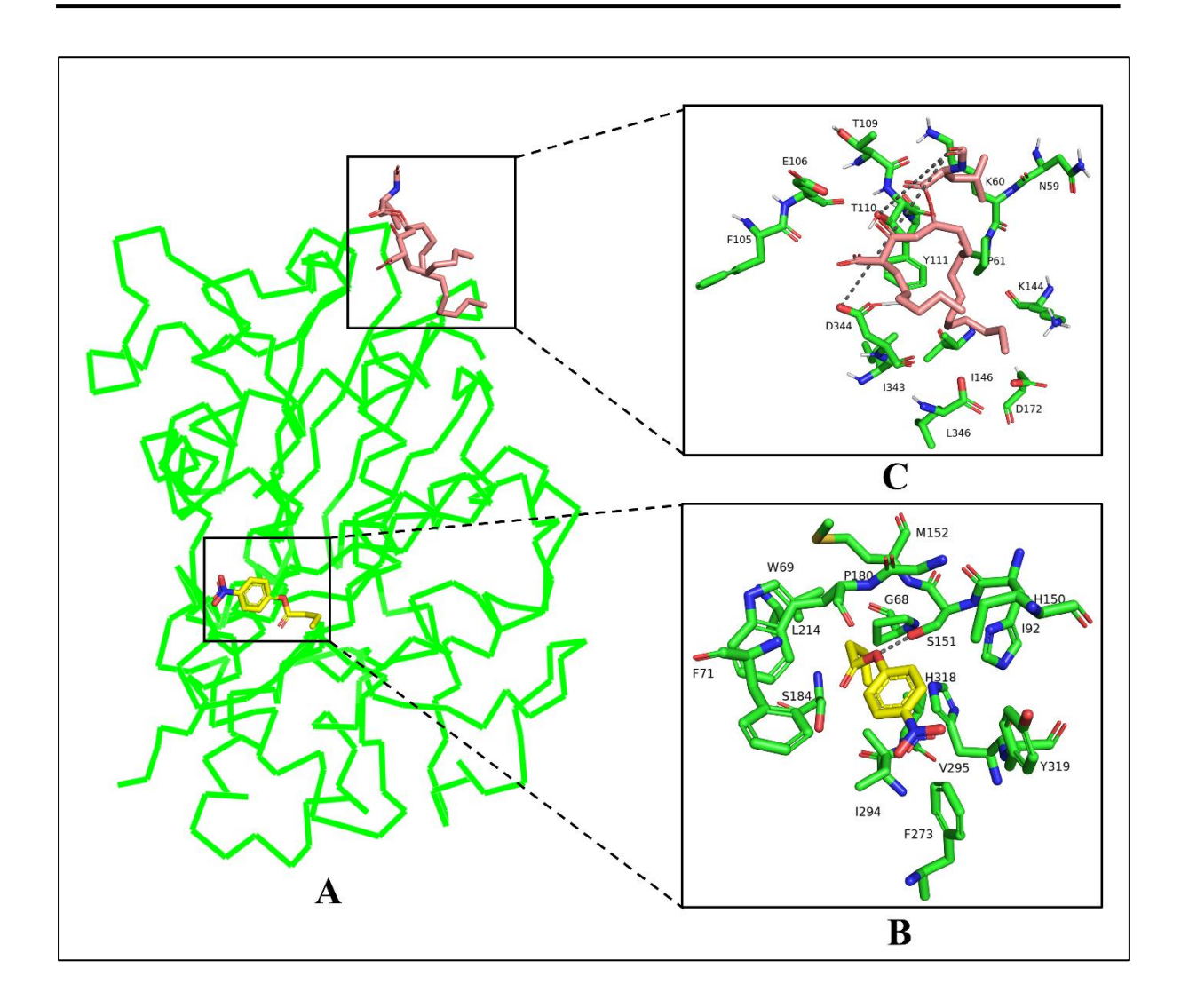


Figure 4.11. 3-D structural representation and structure-based sequence alignment of LABH-1. (A) Three-dimensional model showing the secondary structure elements. Eight  $\beta$  strands (magenta) are labeled  $\beta$ 1 to  $\beta$ 8 sequentially. Eighteen  $\alpha$  helices (cyan) are labeled sequentially from  $\alpha$ 1 to  $\alpha$ 18. The catalytic residues (Ser151, Asp292 and His318) are shown in red sticks. (B) Plot showing validation of the 3D model using Ramachandran plot and (C) ProSA server. (D) Multiple sequence alignment of LABH-1 with top 3 structural homologs recognized by DALI server. The three-dimensional structure was visualized in PyMOL and sequence alignment was generated with ESPript3.

## 4.4.1.6. Inhibitor binds to the allosteric site of LABH-1

The LABH-1 structural model was docked with the substrate, *p*-nitrophenyl butyrate, and inhibitor, orlistat, to check the protein-ligand interactions (**Figure 4.12 A**). The best-docked substrate was observed to bind at the active site cavity with docking energy of –6.7 kcal mol<sup>-1</sup>. The substrate was surrounded by protein residues W69, S151, P180, L214, F273, I294, V295, and H318 (within 5Å distance). The oxygen of the sessile ester bond of the substrate was near the active site residue, Ser151, and observed to form a hydrogen bond with the Ser151 residue (**Figure 4.12 B**). The inhibitor was observed to bind at the suggested binding pocket in the LABH-1 with a binding energy of –7.7 kcal mol<sup>-1</sup>. The binding was stabilized through the four hydrogen bonds with T110 and D344 residues and 56 non-bonded contacts with N59, K60, P61, E106, T109, T110, and Y111, K144, I343, D344, and L346 protein residues (**Figure 4.12 C**). Since the nature of orlistat inhibition was non-competitive with the LABH, it is assumed that the binding of orlistat may bring a structural change that may have an inhibitory effect on the activity. However, an X-ray crystallographic study of the LABH-1 in complex with orlistat is warranted to understand the molecular detail of inhibition, which we are currently investigating.



**Figure 4.12. Molecular docking of LABH-1 with substrate and inhibitor. (A)** Docking of LABH-1 was performed with ligands (*p*-nitrophenyl butyrate and orlistat) using the Autodock Vina. The LABH-1 and ligands were shown as green ribbon and stick view, respectively. A substrate, *p*-nitrophenyl butyrate and an inhibitor, orlistat are shown with a yellow and light orange sticks, respectively. **(B)** The residues showing the interaction between the protein and *p*-nitrophenyl butyrate **(C)** The residues showing the interaction between protein and orlistat. Residues are labeled and displayed as a stick model in element colors (carbon, nitrogen, oxygen, and phosphorus colored green, blue, and red, respectively).

## 4.4.1.7. Conservation analysis among different organisms

In order to perform a phylogenetic analysis of LABH-1, protein sequence similarity was searched against a non-redundant database through the pblast server of NCBI. No significant similarity was found. However, a similarity search against the target database UniProtKB-Swissprot yielded the proteins with the maximum sequence identity of 35.2% and similarity of 45.8% with only 24.4% of query coverage to LABH-1. This search yielded the top >17 hits corresponding to non-redundant protein sequences to perform a phylogenetic study with the LABH-1 (Figure 4.13 A). Moreover, the 3D-structure similarity search with DALI online tool yielded the top 20 structural homologs with overall identity and root mean square deviation (RMSD) of 20% and 2.7 Å respectively. The sequences of proteins that showed structural similarity in the DALI server with the LABH-1 also were selected for the phylogenetic analysis (Figure 4.13 B). This analysis revealed that LABH-1 did not cluster with any of the proteins. Many selected protein sequences were either putative lipases or esterases. Despite having a similar lipase box and conserved catalytic triad in LABH-1 compared to other proteins, the sequence of LABH-1 was not observed to cluster with any of the sequences. This analysis suggested its independent evolution among the set of proteins we used for phylogeny generation.

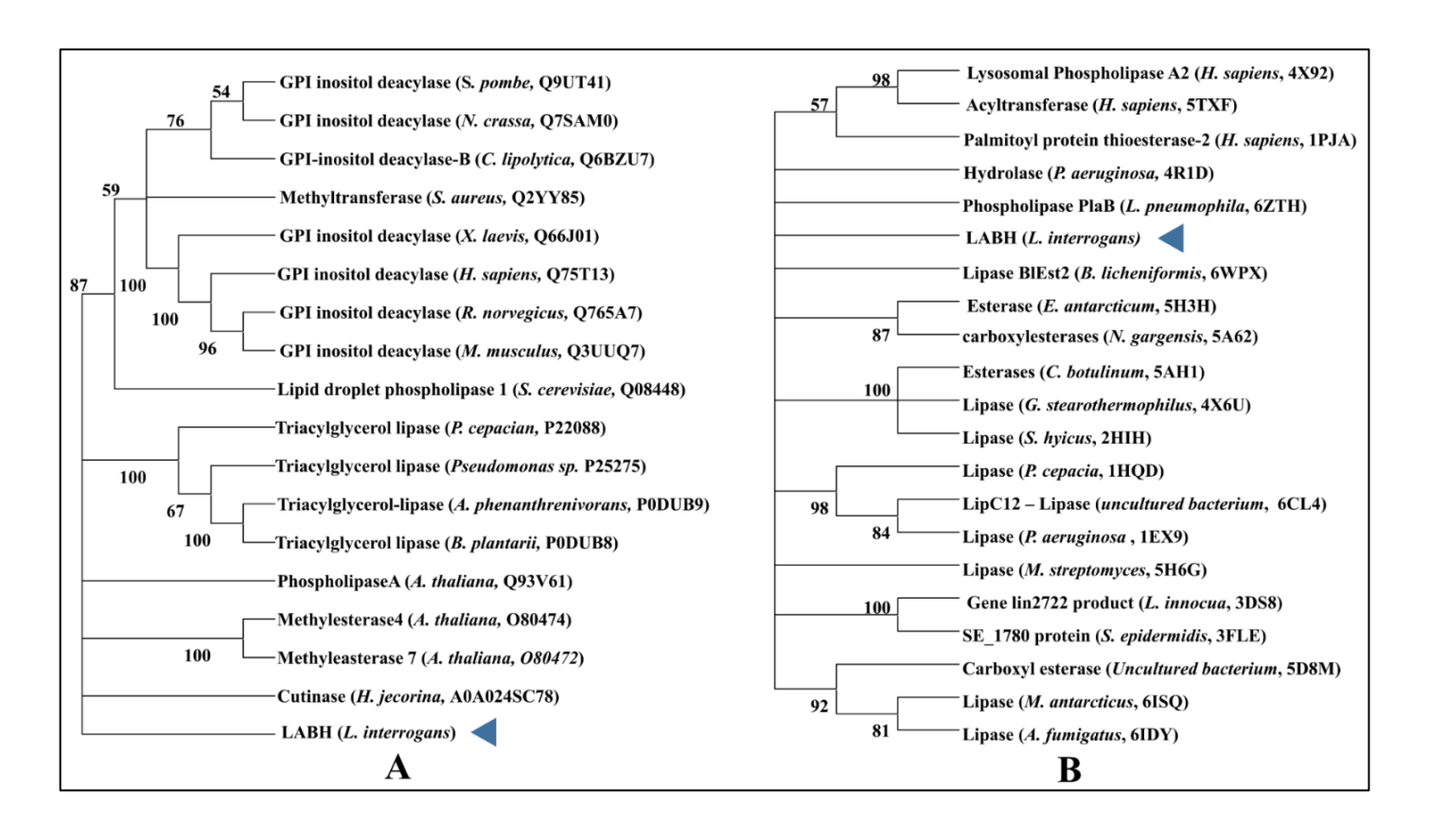


**Figure 4.13. Phylogenetic analysis of LABH-1 and related sequences.** (**A**) Phylogenetic tree with the set of proteins identified after pBLAT against swissprot database. (**B**) Phylogenetic tree with the top 20 structurally similar proteins identified by Dali server. The tree with the highest log likelihood is shown. The clustering of LABH-1 is indicated with a filled triangle. The bootstrap values (100 replicates) are shown next to the branches. The tree is drawn to scale, with branch lengths measured in the number of substitutions per site. The tree was generated using MEGA11.

## 4.4.1.8. Biocatalytic application of LABH-1 in the production of enantiopure 1phenylethanol

To explore the enantioselectivity and subsequent biocatalytic application of LABH-1 in the synthesis of chiral intermediates, we have evaluated the enzyme in the kinetic resolution of racemic 1-phenylethyl acetate (**Scheme 1**).

Scheme 1: LABH-1 catalyzed kinetic resolution of racemic 1-phenylethyl acetate

This enzymatic transformation involved lipase catalysed enantioselective hydrolysis and resulted in the production of (R)-1-phenylethanol or (R)-2 and (S)-1-phenylethyl acetate or (S)-1. (R)-1-Phenylethanol is an important chiral intermediate that finds application in Solvatochromic dye, an inhibitor of cholesterol intestinal adsorption, as an ophthalmic preservative and used in the pharmaceutical, fine chemical, and perfume industry (Suan and Sarmidi 2004). Prior to analyse the biocatalysis reaction mixture, HPLC based chiral resolution of racemic 1-phenylethyl acetate and racemic 1-phenylethanol was carried out (**Figure 4.14**).

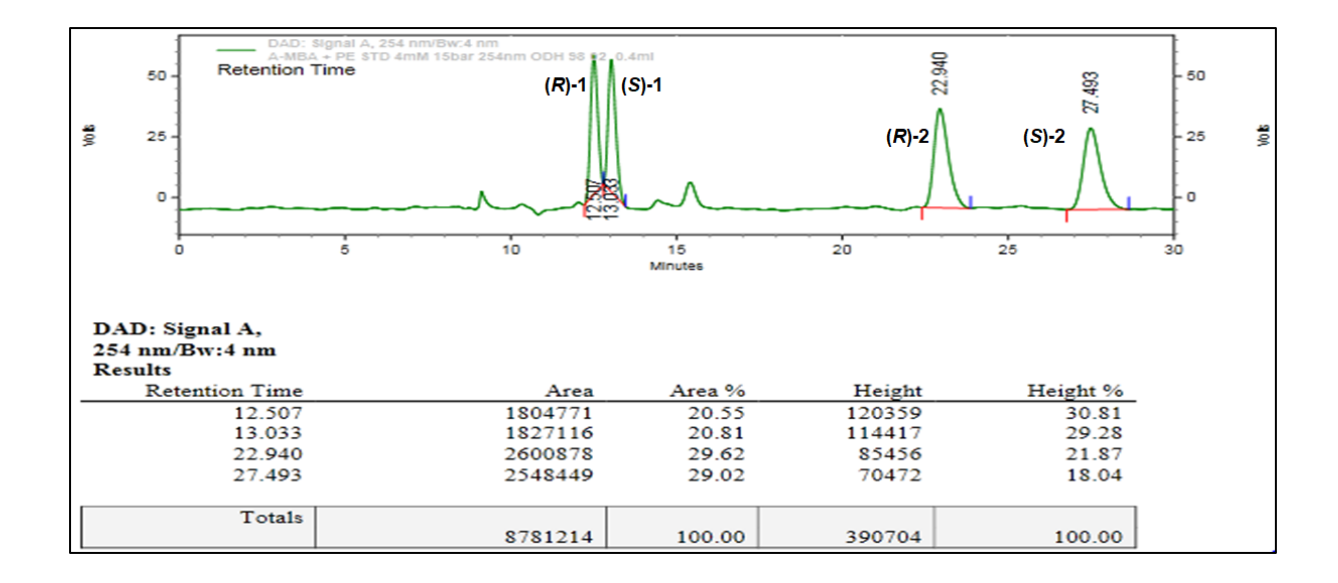


**Figure 4.14: Chiral Resolution.** Chiral resolution of mixture of racemic 1-phenylethyl acetate and 1-phenylethanol in chiral HPLC using Chiralcel® OD-H column. Retention time of (R)-1-phenylethyl acetate, i.e., (R)-1, (S)-1-phenylethyl acetate, i.e., (S)-1, (R)-1-phenylethanol, i.e., (R)-2 and (S)-1-phenylethanol, i.e., (S)-2 are found to be 12.5, 13.03, 22.94, and 27.49 min respectively.

Kinetic resolution of racemic 1-phenylethyl acetate by the LABH-1 has displayed excellent enantioselectivity, E>500 with 100% ee<sub>p</sub> in just four hours, however, with poor conversion of 17% and 21% ee<sub>s</sub> (**Scheme 1, Table 2**). A gradual increase in the conversion and ee<sub>s</sub> was observed with an increase in reaction time. At 8 h, LABH-1 has shown 49% conversion, 100% ee<sub>p</sub> and 96.1% ee<sub>s</sub> with maximum enantioselectivity of E>500 (**Figure 4.15**).

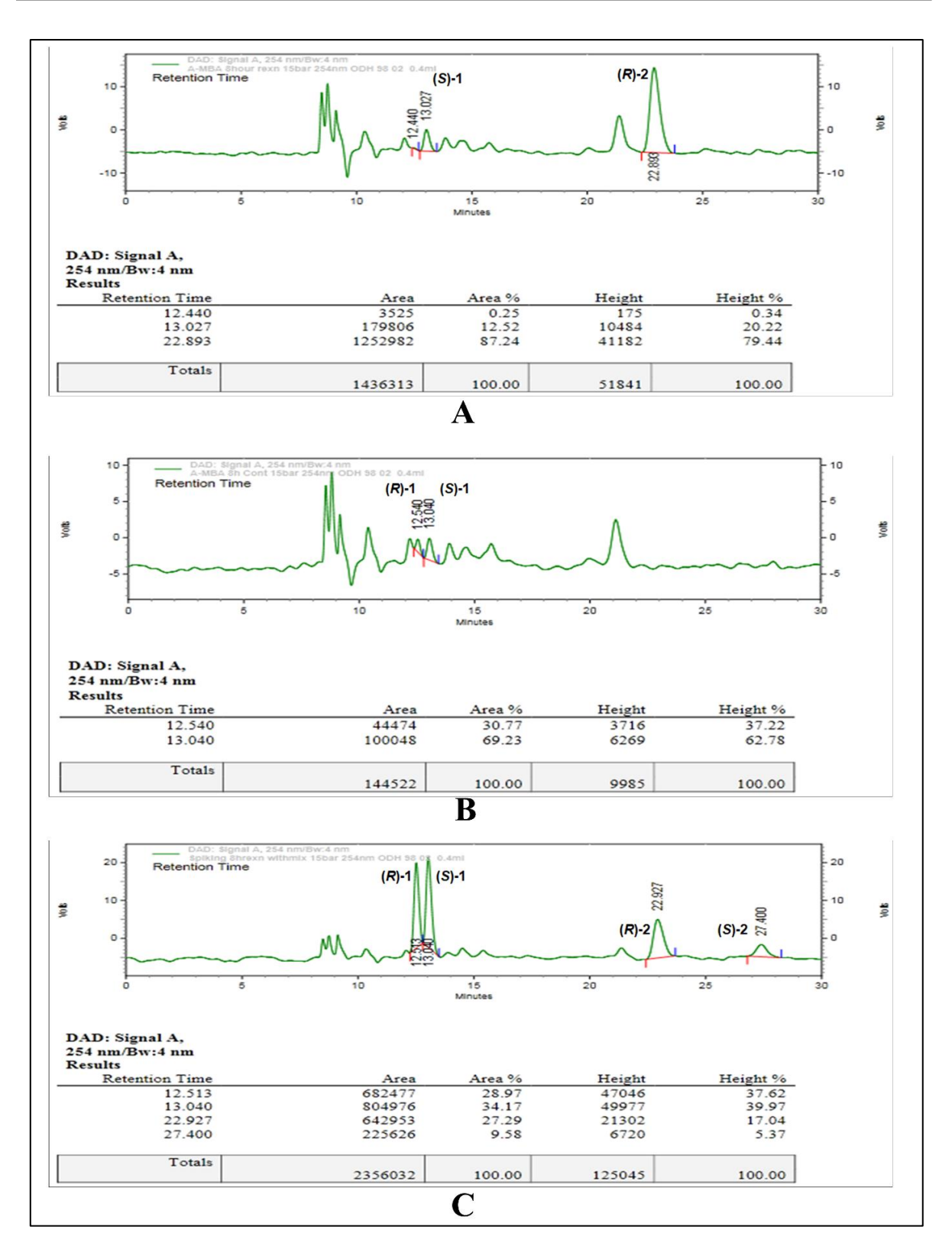


**Figure 4.15: HPLC chiral analysis of biocatalytic kinetic resolution of racemic 1- phenylethyl acetate, 8 h sample**. The figure (A) represents the analysis of the reaction mixture, (B) represents the control, while (C) represents spike which consists of reaction mixture + racemic mixture of 1-phenylethyl acetate and 1-phenylethanol.

Table 4.4: LABH-1 catalyzed kinetic resolution in the enantioselective production of (R)-1-phenylethanol. The reaction mixture (1 mL) containing ~1 mg of purified LABH-1, 33 μL of 50 mM KPB pH 7.0, 571 µL of double distilled water, 20 µL of 5 mM racemic 1-phenylethyl acetate (prepared in diethyl ether) and 313 µL of diethyl ether was incubated in a thermoshaker, at 40 °C 300 rpm. The reaction was monitored by taking aliquots at three different time points, 4, 6, and 8 h. The percentage enantiomeric excess (% ee), percentage conversion (% C) and calculated using formulas: selectivity (E) was (a) of product  $ee_{p}$ (Rp - Sp)/(Rp + Sp) \* 100 (b) %  $ee_s$  of substrate = (Rs - Ss)/(Rs + Ss) \* 100 (c)  $= (ee_s)/(ee_p + ee_s)$ Conversion Selectivity (*C*) (d) (*E*) = $\ln [(1-C)(1-ee_s)]/\ln [(1-C)(1+ee_s)]$ . Rp: percentage area of (R)-1-phenylethanol. Sp: percentage area of (S)-1-phenylethanol. Rs: percentage area of (R)-1-phenylethyl acetate. Ss: percentage area of (S)-1-phenylethyl acetate.

S. No.	Reaction time (h)	C (%)	ees %	eep %	$\boldsymbol{E}$
1	4	17.4	20.99	100	>500
2	6	30.8	44.55	100	>500
3	8	49	96.08	100	>500

## 4.4.1.9. LABH-1 shows immunomodulatory functions in mice macrophage cell line

The balance between pro- and anti-inflammatory cytokines is crucial in the immune responses directed against *Leptospira*. The cytokines such as IL-1b, IL-2, IL-4, IL-6, IL-8, IL-10 and TNF-α levels are found to be considerably greater in severe leptospirosis. Several reports suggest the equivocal findings on the relationship between IL-10/TNF-α ratio and disease severity. Low IL-10/TNF-α ratio associates with leptospirosis (Kyriakidis et al. 2011; Mikulski et al. 2015; Volz et al. 2015). However, other reports found the high IL-10/TNF-α ratio was associated with leptospirosis and fatal outcomes (Reis et al. 2013; Rizvi et al. 2014).

Importantly, IL-10/TNF-α ratio does not depend on sex or age (Kyriakidis et al. 2011). When we investigated the immunomodulatory effect of LABH-1 on macrophage cell line, interestingly we found increased mRNA expression of TNF- α and IL-10 (**Figure 4.16 C and D**). However, there is no significant effect on IL-6 and IL-12 (**Figure 4.16 B and E**). In preliminary qRT-PCR analysis, we found low IL-10/TNF-α ratio which is associated with leptospirosis (Kyriakidis et al. 2011; Mikulski et al. 2015; Volz et al. 2015).

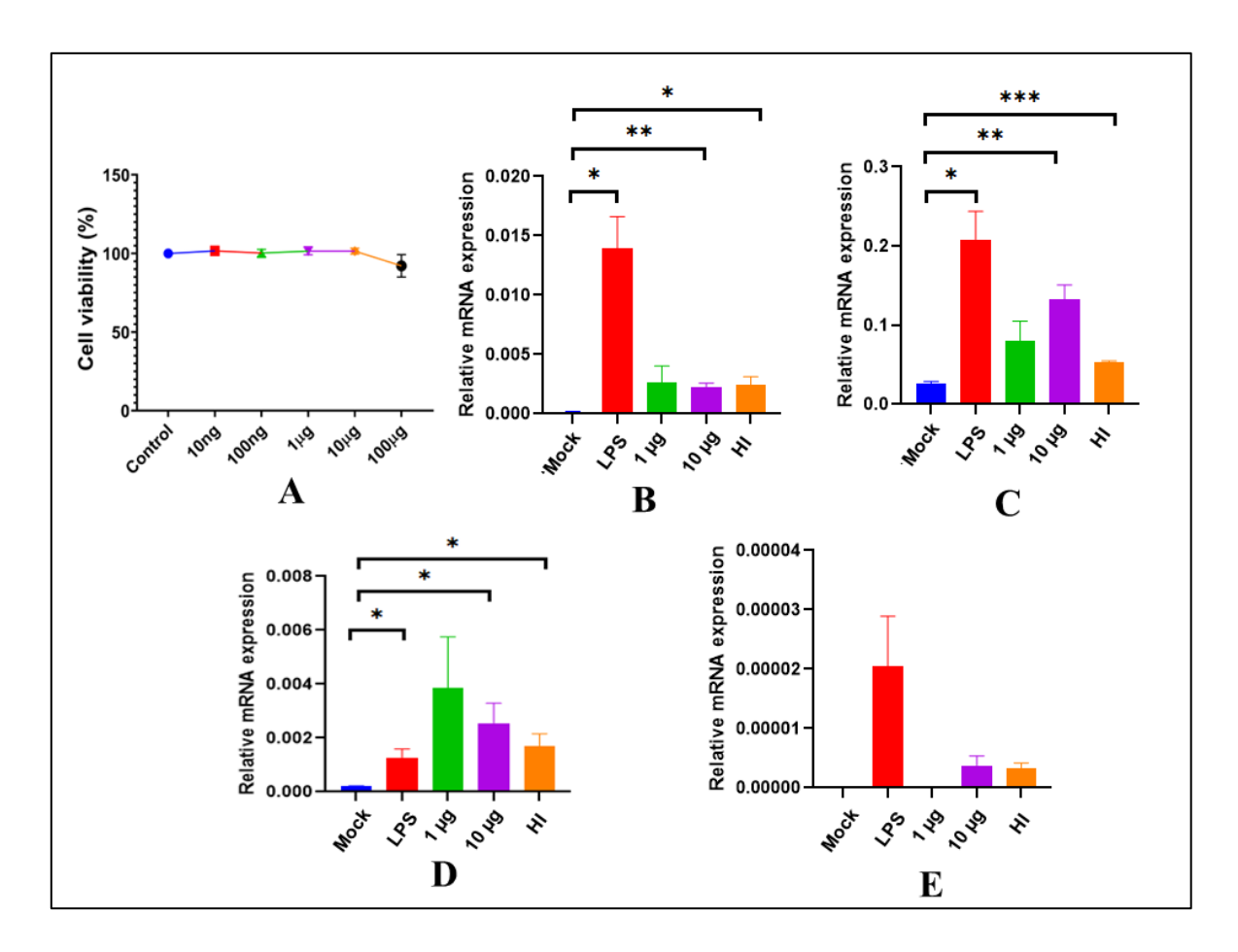


Figure 4.16. Cytokine profile in Mice macrophage Raw 264.7 cells stimulated with LABH-1. (A) MTT assay to determine the cytotoxicity in Macrophage cells after the incubation with LABH-1 for 48 hrs. (B-E) qRT-PCR analysis to study the mRNA expression of IL-6, TNF-α, IL-10 and IL-12 respectively in macrophages treated with LABH-1 and LPS. Statistical significance is determined by Student t-test. \* $P \le 0.05$ , \*\* $P \le 0.005$ , were taken into account as the statistically significant. Error bars represent mean ± SEM. Data is the average of triplicates.

## 4.4.2. Leptospiral α/β hydrolase-1 (LABH-2)

## 4.4.2.1. Kinetics parameters and substrate specificity of LABH-2

Similar to LABH-1, LABH-2 also possess conserved lipase motif (Gly-X-Ser-X-Gly) and the serine nucleophile of the catalytic triad, therefore, it may also have esterase or lipase activity. The purified LABH-2 catalyzed hydrolysis of *p*-nitrophenyl butyrate to *p*-nitrophenolate showed that the LABH-2 is enzymatically active (**Figure 4.17**). However, the activity is very less in compare of LABH-1.

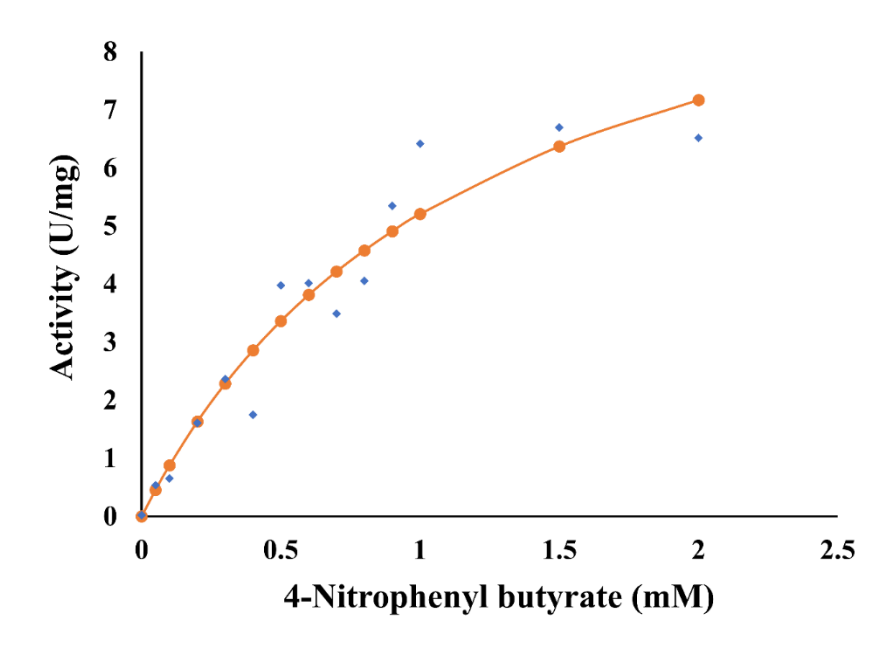
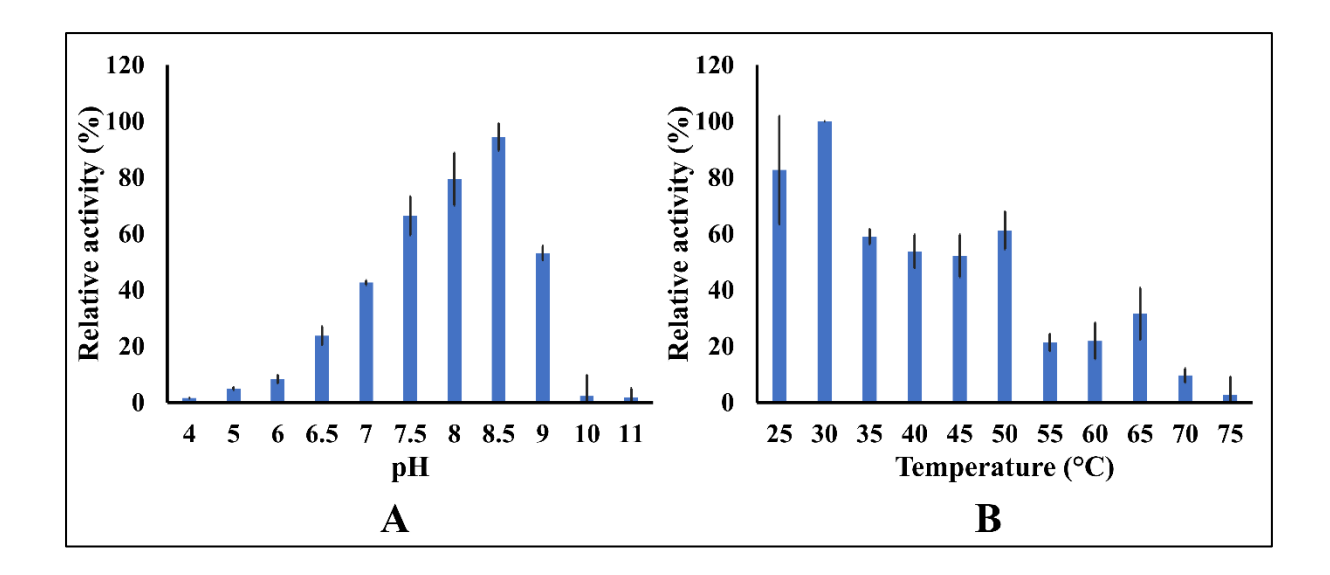


Figure 4.17. Enzymatic activity of LABH-2 at room temperature against p-nitrophenyl butyrate.

To determine the optimum pH and temperature for the hydrolytic activity of LABH-2, it was assayed with a non-natural substrate, *p*-nitrophenyl butyrate, at varying pH and temperature. LABH-2 also showed the pH preference in the range of alkaline pH where the maximum activity was showed at 8.5 pH. However, moving towards extreme acidic and alkaline pH, LABH-2 lost its activity (**Figure 4.18 A**). When the LABH-2 activity was assayed at varying pH, we found the optimum temperature of LABH-2 was in the range of room temperature (25 to 30 °C (**Figure 4.18 B**).



**Figure 4.18. Effect of pH and temperature on the hydrolytic activity.** (**A**) The hydrolytic activity of LABH-2 was studied in varying pH 4-11 conditions using a substrate, *p*-nitrophenyl butyrate. (**B**) The hydrolytic activity at different temperatures (25-75 °C).

To identify the substrate specificity, the hydrolytic activity was examined against the p-nitrophenyl acetate, p-nitrophenyl butyrate, p-nitrophenyl octanoate, p-nitrophenyl laurate, and p-nitrophenyl palmitate at pH 8. The highest activity ( $V_{\text{max}}$ ) was observed with the substrate p-nitrophenyl acetate followed by p-nitrophenyl butyrate (**Figure 4.19 A and B**). However, there was no activity against the substrates of long chain fatty acyls such as p-nitrophenyl laurate and p-nitrophenyl palmitate.

The kinetic study of LABH-2 showed the  $K_{\rm M}$  values of 0.97±0.39, 1.3±0.21, and 0.17±0.02 mM for the substrates p-nitrophenyl acetate, p-nitrophenyl butyrate, p-nitrophenyl octanoate, and p-nitrophenyl palmitate, respectively. The lowest  $K_{\rm M}$  value was observed for the substrate p-nitrophenyl octanoate, suggesting a better affinity of this substrate with the enzyme. Comparable  $k_{\rm cat}$  values were observed for the substrates p-nitrophenyl acetate and p-nitrophenyl butyrate. They were found to be 0.26±0.03 and 0.21±0.03 s<sup>-1</sup>, respectively. Although, the relatively high affinity of LABH-2 towards p-nitrophenyl octanoate, the protein

showed the highest catalytic efficiency of  $0.29\pm0.1~\text{s}^{-1}\text{mM}^{-1}$  against the *p*-nitrophenyl acetate. The kinetic parameters with all substrates are summarized in **Table 4.5**. Briefly, these observations suggest that the purified LABH-2 hydrolyzes the esters of short-chain fatty acids but the efficiency is very less compared to LABH-1.

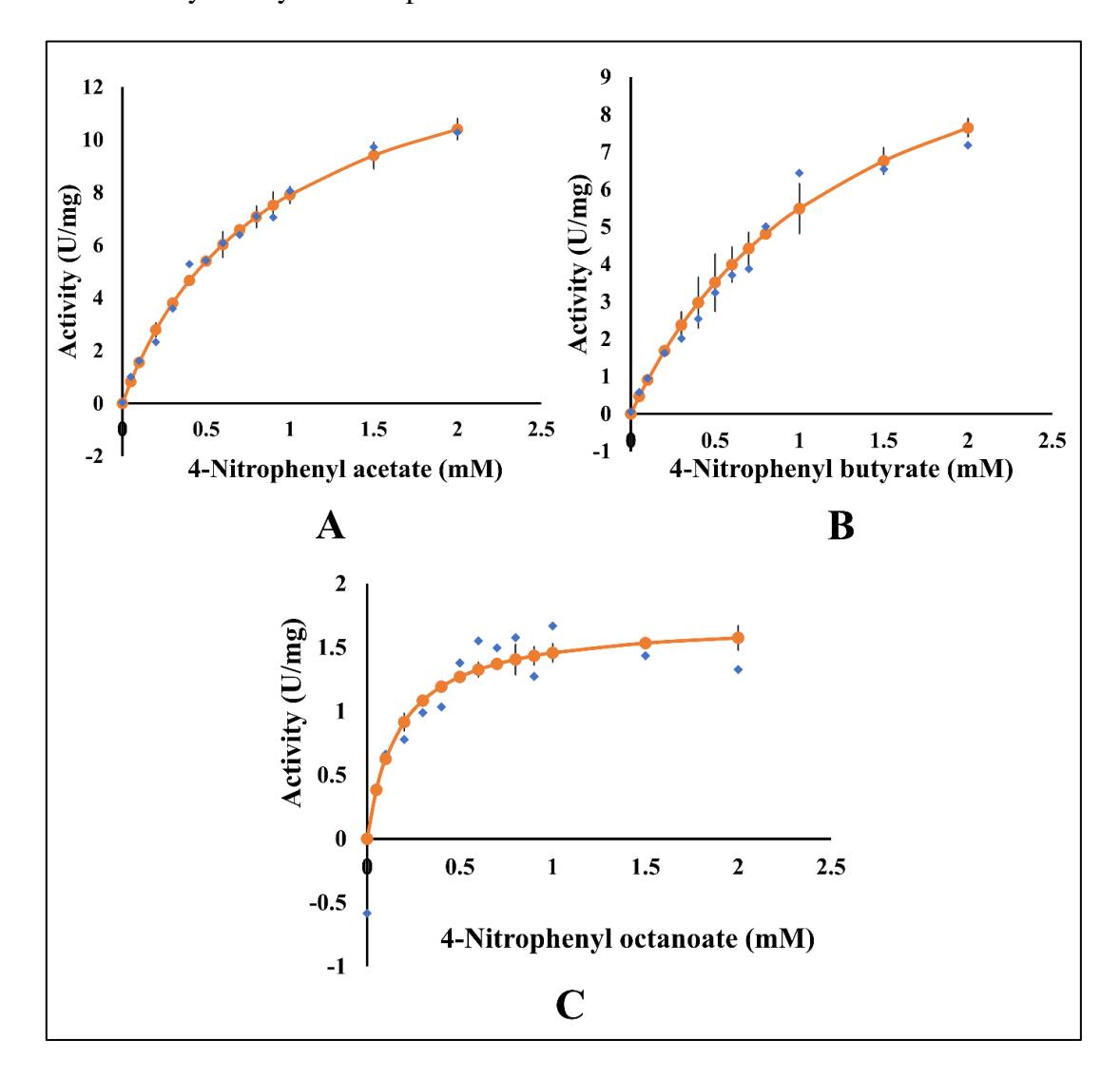


Figure 4.19. The hydrolytic activity of the LABH-2 against different esters of fatty acids.

The hydrolytic activity was assayed using a spectrophotometric method where the changes in absorbance after hydrolysis of (A) *p*-nitrophenyl acetate (B) *p*-nitrophenyl butyrate, and (C) *p*-nitrophenyl octanoate was measured at 405 nm.

Table 4.5. Kinetic parameters of the purified LABH-2

S.	Protein	Substrate	K <sub>M</sub> (mM)	$V_{ m max}$	$k_{\text{cat}}$ (s <sup>-1</sup> )	k <sub>cat</sub> /K <sub>M</sub>
No.				$(\mu mol \cdot min^{-1}mg^{-1})$		$(s^{-1}mM^{-1})$
		<i>p</i> -nitrophenyl acetate	0.97± 0.39	15.48± 2.19	0.26±0.03	0.29± 0.1
		<i>p</i> -nitrophenyl butyrate	$1.3 \pm 0.21$	12.65±1.86	$0.21 \pm 0.03$	0.16±0.006
1	LABH-2	<i>p</i> -nitrophenyl octanoate	$0.17 \pm 0.02$	$1.71\pm0.04$	$0.02\pm 0.0007$	$0.16 \pm 0.03$
		<i>p</i> -nitrophenyl laurate	ND	ND	ND	ND
		<i>p</i> -nitrophenyl palmitate	ND	ND	ND	ND

<sup>\*</sup> ND- Not determined

#### 4.5. CONCLUSIONS

The recombinant LABH-1 and LABH-2 displayed hydrolytic activity in alkaline pH; the optimum temperature for the activity was 50- 65 °C and 20- 25 °C, respectively. Moreover, both LABH-1 and 2 showed the typical hydrolytic activities towards the varying lengths of fatty acyl esters. The highest activity with the lowest K<sub>M</sub> was displayed towards the esters of small-chain fatty acids. However, LABH-1 outperformed LABH-2 in displaying the hydrolytic activity. Though the substrate preference was similar to the bacterial esterase family, LABH-1 does not cluster with other characterized bacterial esterases or lipases, suggesting its independent evolution. Structurally, LABH-1 shared some common features with Staphylococcus hycus lipase (SHL) and found the virulent factor per our preliminary study against mice macrophages. Similar to SHL, LABH-1 was observed to be inhibited by a lipase inhibitor, orlistat. Though LABH-1 showed similarity with Lipase, it was observed to prefer the substrate of esterases. A structural study was sought through the X-crystallography to get a structural insight into substrate preference. Many attempts were made to get good-quality crystals, but improving the crystal size and packing was futile. Moreover, LABH-1 was also found to be an efficient enzyme for the production of (R)-1-phenylethanol and showed

excellent E in the enantioselective hydrolysis of racemic 1-phenylethyl acetate. This observation added a new biocatalyst to the bio-catalytic toolbox, which opens new prospects to synthesize chiral intermediates and scope to broaden its biotechnological applications. Our results provide an insight into structural and functional attributes for leptospiral  $\alpha/\beta$  hydrolases from pathogenic Leptospira.

# Chapter-5

Biophysical characterization of an outer membrane Leptospiral complement Regulator-acquiring protein A (LcpA)

#### **5.1. INTRODUCTION**

The outer membrane/surface proteins of *Leptospira* play an important role in establishing successful colonization in the host. Like many other pathogens, Leptospira uses different strategies to evade the host complement system, an important arm of innate immunity. It has been observed that pathogenic Leptospira resist complement-mediated killing, whereas saprophyte strains highly susceptible serum killing (Meri to al., 2007). Pathogenic *Leptospira* escape from complement-mediated killing through recruitment of host complement regulators; (ii) acquisition of host proteases that cleave complement proteins on the bacterial surface; and (iii) secretion of proteases that inactivate complement in the Leptospira surroundings (Fraga et al. 2016). Leptospira binds soluble host complement regulators via surface proteins such as Leptospiral endostatin-like proteins A and В (LenA LenB) (Verma et al. 2006; Stevenson al. 2007), and and et Leptospira immunoglobulin-like proteins (LigA and LigB) (Castiblanco-Valencia et al. 2012). Leptospiral complement regulator-acquiring protein A (LcpA) is a 19.5 kDa outer membrane protein. Its expression is mostly associated with pathogenic Leptospira spp. It has been demonstrated that LcpA binds to soluble host complement regulators and involve in immune evasion. LcpA protein binds to the C4b binding protein (C4BP), Factor H (FH), and the complement component of the terminal pathway, C9, and hence plays a critical role in hijacking the host complement system (Breda et al. 2015).

The structural basis of the interaction of LcpA with complement regulators is largely unknown. The protein doesn't show any identity or similarity with other proteins from the data base. Moreover, the three-dimensional structural organization of LcpA is not known. Hence, the structural characterization of LcpA and its interaction with complement regulators C4BP and FH will help understand the structural basis of immune evasion.

In the present chapter, we reported the cloning, heterologous expression, and recombinant purification LcpA using the refolding protocol. The optimum pH and temperature for its structural stability were also determined. Moreover, we observed the zinc-binding ability of the LcpA protein, which may help interact with complement regulators. We also identified the common region on the three-dimensional structure of LcpA where the C4BP and FH interact.

## **5.2. MATERIALS**

All chemicals used were procured from Sigma Aldrich and Himedia (as per mentioned in Chapter 4). Ni-NTA resins and Sephadex 200 size-exclusion columns were purchased from Qiagen and GE Healthcare, respectively. All solutions used were prepared in double-distilled water.

## **5.3. METHODOLOGY**

## 5.3.1. Cloning of *lcpA* gene into expression vector

The nucleotide sequence encoding amplified from Leptospira the LcpA was interrogans (Pomona serovar) genomic DNA by PCR using the forward primer (5' GCGGATCCTCTATGATTCTTTGTGATCATTTC 3'; BamHI cutting site is underlined) and CTAAGCTTTCATTTTTCTGGAGGAAGAACGATA the reverse primer (5' 3'; *HindIII* cutting site is underlined). The **PCR** product was digested with BamHI and HindIII (NEB) and ligated into different expression vectors such as pET28a (+), pET28a-SUMO, pCold 1, and pET23a, which were also opened up with the same restriction enzymes. Insertion of the gene was confirmed by double digestion and DNA sequencing.

## 5.3.2. Heterologous Expression and Solubility

Confirmed constructs of the *LcpA* were transformed into *E. coli* BL21 (DE3) and Rosetta competent cells for protein expression. *E. coli* harboring recombinant plasmid was grown in

Luria Bertani (LB) supplemented with a required concentration of respective antibiotics such as 50mg/ml of kanamycin for pET28a and pET28a-SUMO and ampicillin for pET23a and pCold1 kept at 37°C on shaker incubator for overnight. 1% of overnight culture was used to inoculate 20ml of LB broth with ampicillin and incubated till OD at 600nm reached 0.4. Expression is induced by adding 0.5mM isopropyl β-D-1-thiogalactopyranoside (IPTG) at 37°C for 4 hours and 20°C for 16 hours. Cells were harvested by centrifugation at 8000rpm for 10 min at 4°C. The cell pellet was resuspended in 0.5ml lysis buffer consisting of 50 mM Tris–HCl, pH 8, 300 mM NaCl, 1 mg/mL lysozyme, and 1 mM PMSF. Cells were lysed by sonication with an amplitude of 35% (2 s ON/4 s OFF), and the insoluble fraction was collected by centrifugation (11,000rpm for 45 min at 4°C).

## 5.3.3. Purification of recombinant protein

## **5.3.3.1.** Cell lysis

Cell pellet (approximately 2 g wet weight) was re-suspended in 35 mL of lysis buffer A (50 mM Tris–HCl pH 8 and 300 mM NaCl) containing 1 mg/mL lysozyme and 1 mM PMSF, and the same was incubated on ice for 30 min. The cells were disrupted by sonication with an amplitude of 35% (2 s ON/4 s OFF), and the insoluble fraction (inclusion bodies) was collected by centrifugation (11,000rpm for 45 min at 4°C).

## **5.3.3.2. Denaturation**

The first step of the protein refolding protocol is a denaturation with 8M urea followed by refolding of the denatured sample. The initial stage of protein denaturation consisted of washing the inclusion bodies. The inclusion bodies were re-suspended in 20 mL of buffer A containing 1 M urea and sonicated (2sec ON/ 4 sec OFF) for 5min at 35% of amplitude, followed by centrifugation (11,000rpm for 40 min at 4°C). This process is repeated thrice. Subsequently, the pellet collected by centrifugation after the last washing step was re-

suspended in 10 mL of buffer A. The washed inclusion bodies were denatured using a magnetic stirrer by adding a freshly prepared 8 M urea solution dropwise until a transparent and homogeneous solution was obtained (approximately 60 mL of 8 M urea was added to each beaker).

## **5.3.3.3. Refolding**

The denatured protein sample was initially dialyzed at a 1:10 ratio against buffer A containing 10% v/v glycerol and 0.1 mM EDTA (refolding buffer) at 4°C for 4 h. Afterward, another dialysis step was performed at a 1:50 ratio against the same buffer at 4°C for 16 h followed by again dialysis with 1:50 ratio with fresh refolding buffer. The sample was centrifuged at 11,000rpm for 40 min at 4°C, and separate the supernatant containing soluble protein.

## 5.3.3.4. Ni-NTA Affinity Chromatography

Supernatant collected after refolding was passed through the Ni-NTA column, pre-equilibrated with buffer A. Wash buffers of 50ml consisting of buffer A with 0, 20, 50, and 150mM imidazole were allowed to pass through the column. The bound protein of interest was eluted with buffer A supplemented with 250 mM imidazole.

## **5.3.3.5.** Size-exclusion Chromatography

Eluted fractions from Ni-NTA chromatography were pooled and concentrated using 10kDa Amicon® Ultra-0.5 ultrafiltration before further purification through size-exclusion chromatography. The concentrated sample was loaded onto a Superdex 200 pg 16/600 (GE Healthcare, Sweden) column mounted on an AKTA Purifier. The column was preequilibrated with a buffer (50 mM Tris–HCl pH 8 and 300 mM NaCl). Eluents of the column were collected (1 ml per fraction) using a Frac-950 fraction collector at a constant flow rate of 0.5 ml/min. Eluents were analyzed using 12% SDS-PAGE.

#### 5.3.4. Circular Dichroism measurements

Secondary structure composition of LcpA were analyzed by circular dichroism (CD) spectra on a JASCO-J1500 CD spectrometer equipped with a Peltier temperature controller system. Far-UV CD spectra were recorded from 195 to 260 nm in 10 mM Tris-HCl (pH 4, 5, 6, 7, 7.5, 8, 9 and 10) at 25 °C in a quartz cuvette with a path length of 0.2 cm. The protein concentration used for the experiments was 10 μM. Three scans were recorded at a speed of 50 nm min<sup>-1</sup> to generate the final spectra. Thermostability of purified LcpA in buffer solution of 10 mM Tris-HCl of pH 7.5 was studied by collecting CD spectra at different temperatures ranging from 20-90 °C. Fractions that unfolded in varying temperatures were determined by considering the value of ellipticity at 222nm. Secondary structure contents were examined with the Dichroweb tool using K2D programme (Andrade et al. 1993; Whitmore and Wallace 2008).

## 5.3.5. Prediction of metal ion binding

Protein sequence was analyzed using the SMART (Simple Modular Architecture Research Tool) server to identify the domains and metal binding sites. SMART allows the identification and annotation of genetically mobile domains and the analysis of domain architectures. It also identifies the metal binding motifs (Letunic et al. 2021).

#### **5.3.6.** Intrinsic Fluorescence Spectroscopy

Fluorescence spectroscopic analysis of LcpA with different Zn<sup>2+</sup> ion concentrations was executed using Jasco Spectrofluorometer (FP-8500). The excitation and emission wavelengths were set to 280nm and 300-400nm respectively. Purified protein of 5μM in 10mM Tris-HCl buffer solution was used in the experiment. Protein with 0-5μM concentrations of ZnCl<sub>2</sub> (mole ratios of protein to ZnCl<sub>2</sub>, 1:0.2, 1:0.4 and 1:1) was incubated at room temperature for 30 minutes. After an excitation, the intrinsic fluorescence emission spectra were recorded between 300 to 400 nm at 25°C. The path length of the quartz cuvette was 0.2 cm.

## 5.3.7. Secondary structure prediction and homology modelling

PSIPRED server was used to predict the secondary structure composition. A two-step ANN algorithm based on position-specific scoring matrices generated by PSI-BLAST is used in PSIPRED (McGuffin et al. 2000). Three-dimensional structure was modelled using AlphaFold followed by energy minimization using a Swiss PDB viewer (SPDV) (Guex and Peitsch 1997; Jumper et al. 2021). Ramachandran plot and Prosa web tool were used to validate the structure (Laskowski et al. 1993; Wiederstein and Sippl 2007).

## 5.3.8. Crystallization Screening

The crystallization screening of homogeneously purified LcpA was set up using the protocol mentioned for LABH-1 crystallization in chapter 4. Briefly, a purified protein of 9mg/ml was allowed to combine with crystallization screens using the crystallization robot. Sitting drop vapour diffusion method was used to screen the crystallization conditions. The incubation temperature was  $22^{\circ}$ C and  $4^{\circ}$ C. Crystallization plates were kept under the observation using the Olympus stereo microscope until the drops dry off completely. Crystallization hits were recorded and same were tried to improve the crystal size using hanging drop method into 24 well plates. Concentrations of different components of the hits were varied individually. The drops size was 4  $\mu$ L which consist of protein to reservoir ratio 1:1 and 1:2. Moreover, seeding techniques were also used to improve the quality of crystals.

## 5.3.9. X-ray diffraction

The crystals were obtained from LcpA protein in different crystallization conditions. These crystals were tested at in-house XRD facility at CCMB, Hyderabad. Similar protocol was applied as per mentioned in X-ray diffraction and data collection of LABH-1 (described in Chapter 4).

## 5.3.10. Molecular Docking

To assess the interaction of LcpA protein with an  $\alpha$ -chain of C4BP and FH molecules, the ClusPro server (Kozakov et al. 2017) was used where the default parameters were considered for docking. ClusPro server displays top 10 the best docked complex structure depending on maximum cluster size and lowest energy score. The interactions in a docked complex were analysed using PDBsum tool (Laskowski et al. 2018) and visualized in PyMol.

## 5.3.11. Molecular Dynamic Simulation

The stability of interactions between LcpA and an alpha chain of C4BP was tested using molecular dynamic simulation in GROMACS v 2020.4 with OPLS-AA (Optimized Potential for Liquid Simulations-All Atoms) force field. The TIP4P was selected as a water model and the box type was dodecahedron box with a distance of 1.2 nm between protein and the box. The system charges were neutralized either by adding Na<sup>+</sup> ion or Cl<sup>-</sup> ions. The electrostatic interactions were treated using the Particle Mesh Ewald (PME) method, with a coulomb cutoff of 1 nm, a Fourier spacing of 0.16 nm with a fourth order interpolation. Energy minimization was performed using the conjugate gradient algorithm with convergence criteria of 1kJ mol<sup>-1</sup> nm<sup>-1</sup>. System was equilibrated with temperature (298 K) followed by pressure (1 bar). Position restrained dynamics was run for 100 ps during both temperature and pressure equilibration by applying a force constant of 1000 kJ mol<sup>-1</sup> nm<sup>-1</sup> on protein atoms. The production simulations were run for 100ns with a time step of 2fs with the atomic coordinates saved for every 2 ps. LINCS algorithm was used for Constraints. The root mean square deviations (RMSD), root mean square fluctuations (RMSF), and radius of gyration were respectively calculated using the gmx rms, gmx rmsf, and gmx gyrate commands implemented in the GROMACS. The graphs were plotted using XMGRACE.

## 5.3.12. Phylogenetic analysis

Protein sequence of LcpA from *L. interrogans* serover copenhageni and its homologous protein sequences from the different pathogenic, saprophytes and intermediate species of *Leptospira* were retrieved from uniprotkb database. The homologous proteins with highest percentage of identity were identified by performing pBLAST against the different species of *Leptospira*. The dataset consist of LcpA and its homologous proteins was employed to generate the phylogeny using the maximum likelihood method. The percentage of replicate trees in which the associated taxa clustered together in the bootstrap test (1000 replicates) are shown next to the branches, only percentages higher than 60 were considered. Initial trees for the heuristic search were obtained automatically by applying Neighbor-Join and BioNJ algorithms to a matrix of pairwise distances estimated using the JTT model, and then selecting the topology with superior log likelihood value. This analysis was performed with amino acid sequences from 20 pathogenic, intermediate and saprophyte species of *Leptospira* for LcpA. Evolutionary analyses were conducted in MEGA 11 (Tamura et al. 2021).

## 5.4. RESULTS

#### 5.4.1. LcpA overexpressed as inclusion body

The ORF of the *lcpA* gene was cloned into suitable expression vectors such as pET28a (+), pET28a SUMO, pCold1, and pET23a (+). Initially, the *lcpA* construct in pET28a (+) was overexpressed in a reasonable quantity in the BL21 (DE3) cell. Unfortunately, the protein was not found in soluble fractions even after trying all possible troubleshooting. Attempts were also made to have a soluble expression in the presence of chaperones. Chaperones containing plasmids such as pGro7 and pGKJE8 were co-expressed in BL21(DE3) cells. Still, lcpA expression was in an insoluble fraction (**Figure 5.1A**). Later, the gene was moved into the pET28-SUMO vector to get protein expression in the soluble fraction. The SUMO tag usually provides solubility to the protein. However, the expression trial of this clone in BL21 (DE3)

also did not give a soluble protein (**Figure 5.1B**). Most of the expressed protein was an inclusion body in the expression cell. Similarly, *lcpA* clones in pCold-1 and pET23a vectors were used for soluble expression, but attempts were unsuccessful (**Figure 5.1C and D respectively**). In all cases, the expression of LcpA was observed very well but did not yield a soluble protein.

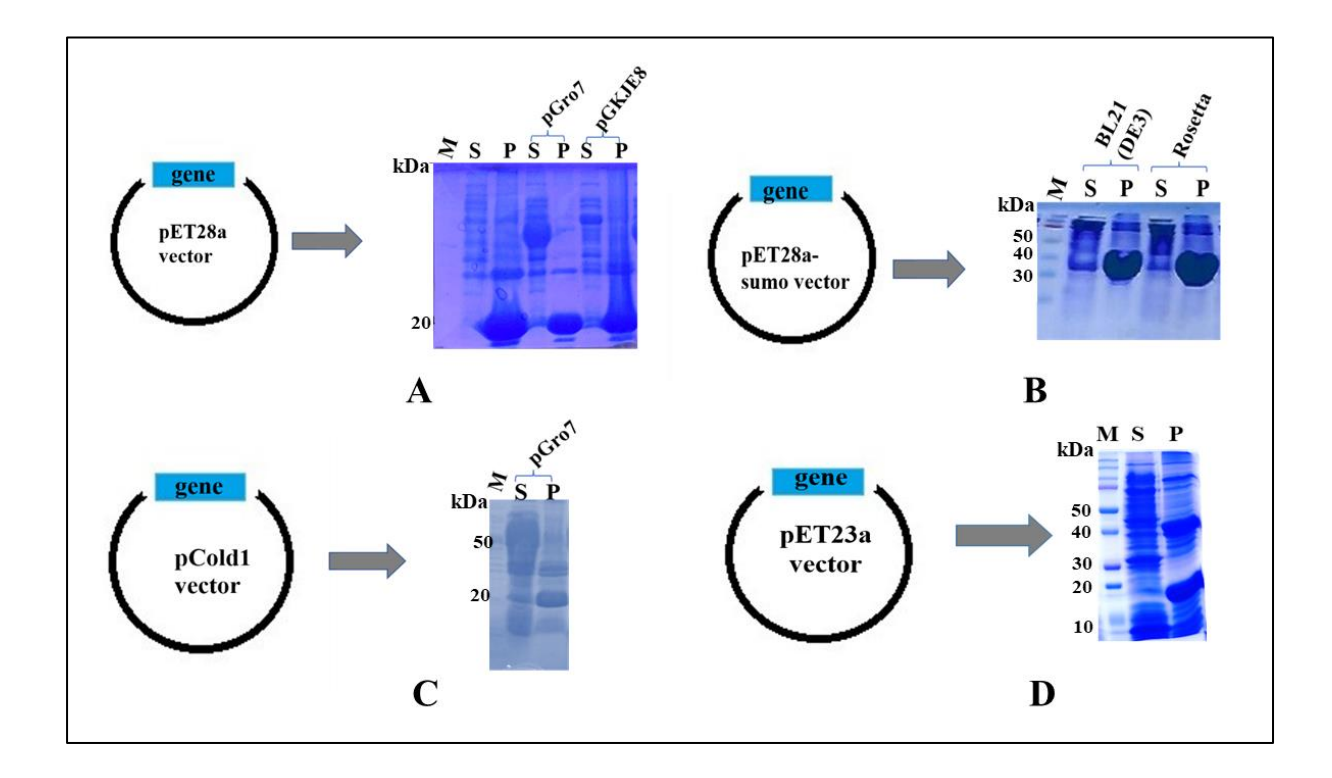
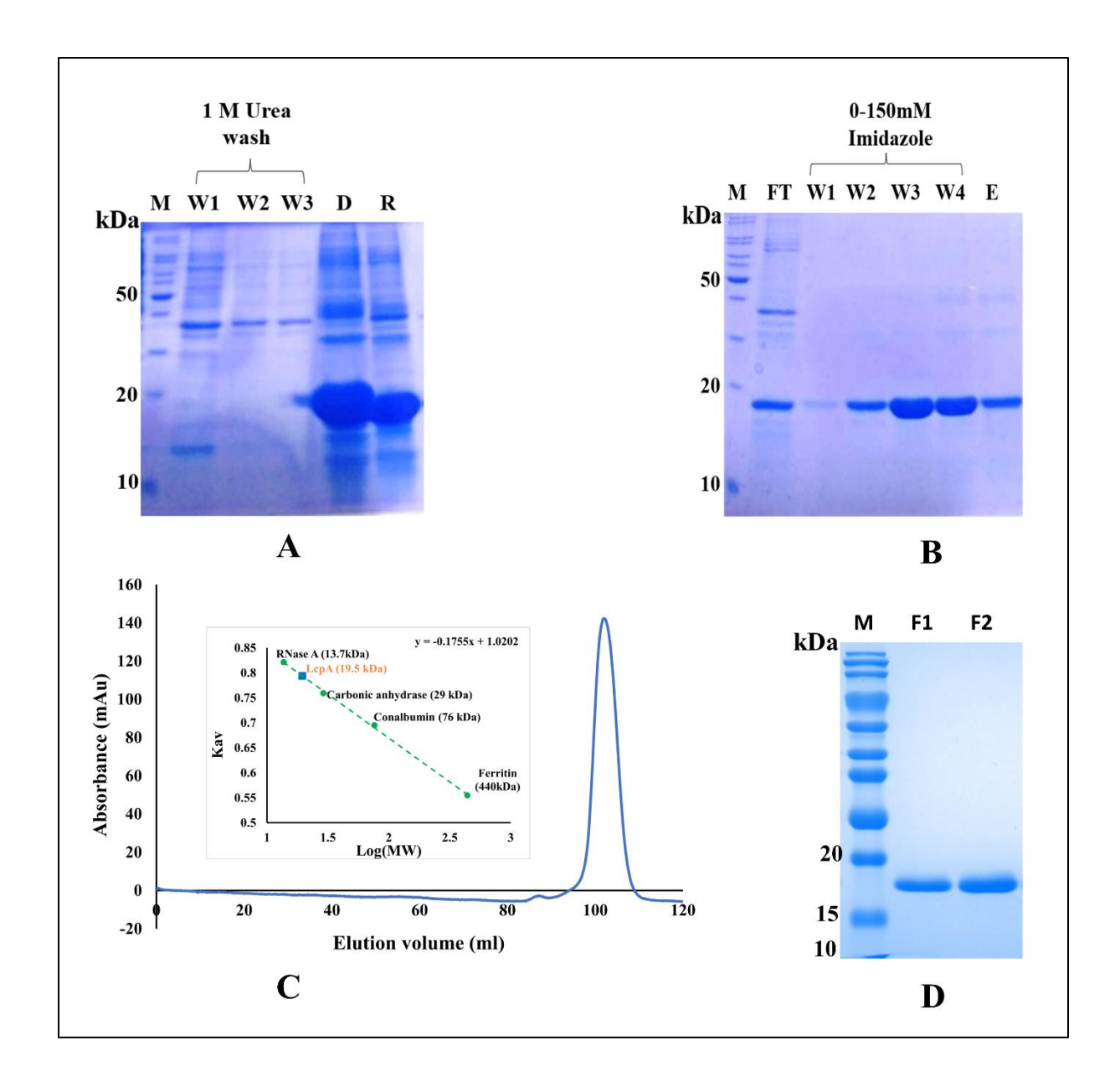


Figure 5.1. 12% SDS-PAGE showing overexpression and solubility of recombinant LcpA.

(A) Clones in pET28a expressed in BL21(DE3) and co-expressed with pGro7 and pGKJE8 chaperones (B) clones in pET28a-SUMO expression in BL21(DE3) and Rosetta cell, (C) Clones in pCold1 and co-expressed with pGro7 chaperon (D) Clones in pET23a. Pallet and supernatant are denoted as P and S, respectively.

## 5.4.2. Refolded LcpA exits as a monomer in solution

The recombinant LcpA was purified from the inclusion body using the refolded protocol. The denatured sample was allowed to refold proteins by incubating it in a refolding buffer for 16 hrs at 4°C. Fortunately, the desired protein (LcpA of around 20 kDa) was not lost in 1M urea washes, and the protein was intact in the denatured and refolded samples. However, in addition to LcpA, several non-specific proteins appeared in the refolded sample (**Figure 5.2A**). Hence, LcpA, after refolding, was further purified using Ni-NTA affinity chromatography. Elution from the Ni-NTA column yielded pure LcpA (**Figure 5.2B**). The yield of refolded purified LcpA protein was 14mg from 1 L of bacterial culture. In the size-exclusion chromatography experiment, the LcpA was eluted at the volume corresponding to a protomer mass of 19.5 kDa, suggesting the purified LcpA exists as a monomer in the solution (**Figure 5.2C and D**). Since LcpA is an outer membrane protein isolated using a refolding procedure, it is important to examine its secondary structure composition and the effect of varying pH and temperature.



**Figure 5.2. Refolding and purification of recombinant LcpA.** (**A**) Depicts the denaturation and refolding of recombinant LcpA. W, D, and R labels indicate washing sample with a washing buffer containing 1 M Urea, denatured sample in 8M urea, and refolded sample, respectively (B) 12% SDS-PAGE showing samples from Ni-NTA affinity chromatography. Flow through, washed, and eluted samples are indicated as FT, W, and E (C) Size-exclusion chromatogram of purified protein sample depicting the elution volume, (D) 12% SDS-PAGE showing fractions collected from the gel filtration chromatography.

## 5.4.3. LcpA exhibits moderate structural stability

Secondary structure composition plays a crucial role in understanding the stability of proteins and folding patterns. Bacterial outer membrane proteins often contain extended β-strands and surface-exposed loops, which connect the β-strands and help in interactions with host proteins. In our investigation, the far-UV CD spectrum of the recombinant LcpA displayed two negative peaks at 222 and 208 nm, shown in the left panel of Figure 5.3A. Secondary structure contents were determined from the data derived from CD spectroscopy using the Dichroweb analysis tool. It showed α-helical content of 18% and β-strands of 34% in the purified protein at pH 7 (Figure 5.3A). Furthermore, theoretical estimation of secondary structure contents yielded 23% and 41% α-helix and β-strands, respectively. An interaction in any biomolecule is disturbed when it is subjected to physical changes, such as temperature or pH. In proteins, variation in pH and temperature causes the globules to unfold and the helical structure to uncoil. As a result, the biological activity of proteins gets disturbed. As expected, the structure composition was changed when it shifted from neutral to acidic pH and even at an alkaline pH of 10. However, there were no significant structural changes with the pH range of 7.5 to 9 (Figure 5.3A). Moreover, thermal stability analysis using CD spectroscopy at different temperatures showed moderate stability with a Tm of 55°C (Figure 5.3B).

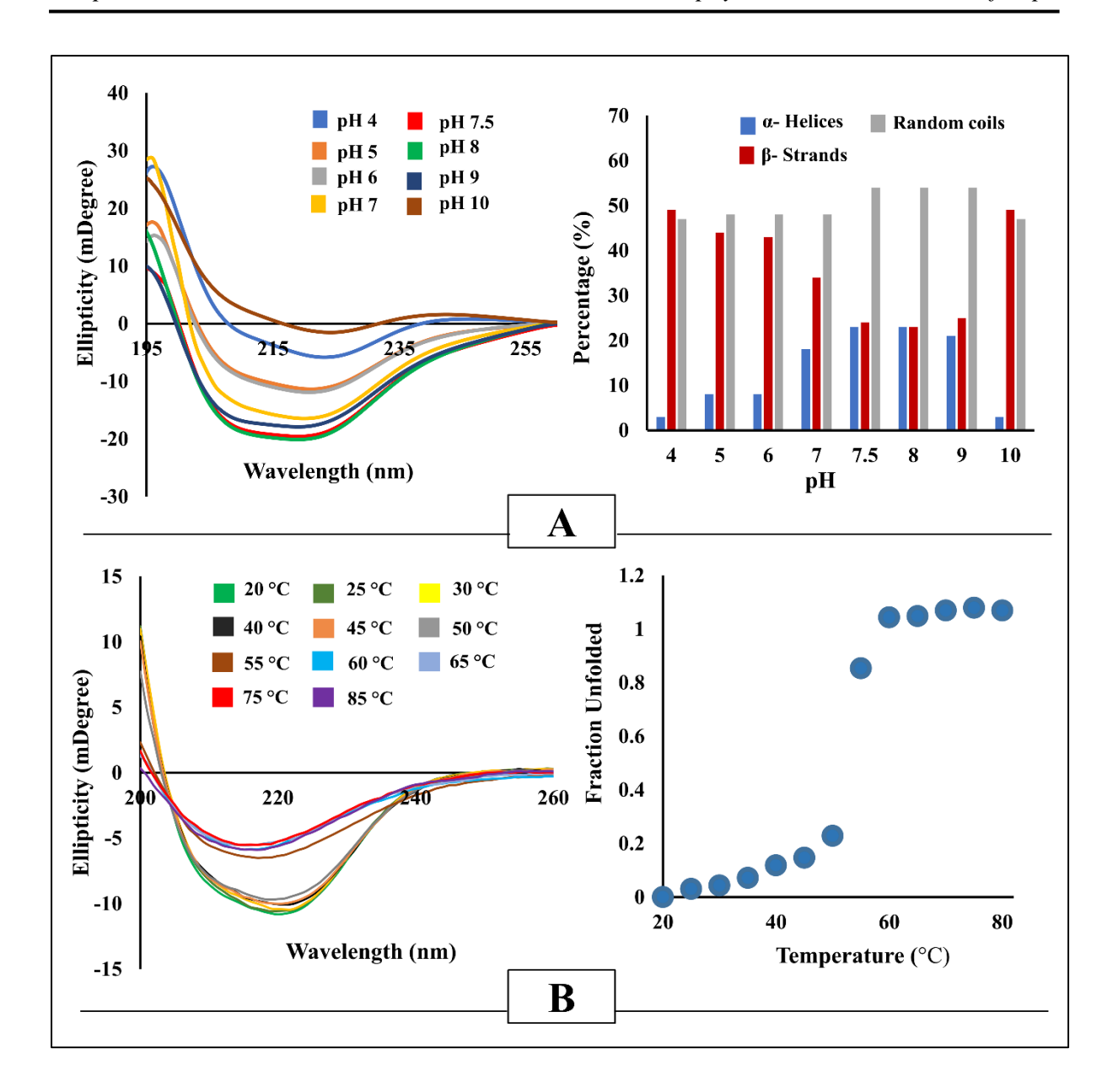


Figure 5.3. Structural stability analysis of LcpA using circular dichroism spectroscopy.

(A) Far UV CD spectra recorded from 260nm to 195nm at different pH conditions varying from pH 4 to 10 (Left panel), and the percentages of  $\alpha$ -helices,  $\beta$ -strands, and random coils determined at pH 4 to 10 (Right panel), (B) far UV CD spectra recorded at 20-85°C (left panel) and fraction unfolded calculated from the spectra of different temperature points (right panel).

# 5.4.4. LcpA has ability to bind zinc

Several pathogens sequester the essential metals with the help of outer membrane/surface proteins. Bacteria maintain metal homeostasis, particularly of the three most important metals for metabolism — zinc, iron, and manganese (Chandrangsu et al. 2017). Moreover, few reports suggest the involvement of zinc in complement evasion. The SMART bioinformatics tool suggested the Zinc finger motif at the N-terminus of the LcpA. In addition, ligand binding with the protein is also investigated with the COACH server. This server also suggested zinc binding with the LcpA. Like the SMART tool, the server also suggested Zinc binding residues mostly from the N-terminal end of the protein. C11 ( $\beta$ 1), D12 ( $\beta$ 1), N15 (loop region between  $\beta$ 1-  $\beta$ 2), C20 (loop region between  $\beta$ 1-  $\beta$ 2), and T57 (loop region between  $\alpha$ 1-  $\beta$ 4) are the residues and regions predicted to bind with the zinc. The binding of Zn2+ with the LcpA was also investigated using intrinsic fluorescence spectroscopy. A change of intrinsic fluorescence intensity and shift in emission wavelength with increasing concentration of Zn<sup>2+</sup> suggest the binding of Zn<sup>2+</sup> with the protein. The emission wavelength was observed to be decreased in increasing concentration of Zn<sup>2+</sup> ions. The results revealed an increase in fluorescence intensity and a considerable shift in wavelength with increasing Zn<sup>2+</sup> concentrations. (Figure **5.4A**). This demonstrates unequivocally that zinc binding introduces conformational changes in LcpA.

# 5.4.5. Zinc binding brings structural modifications

The  $\alpha$ -helices and  $\beta$ -strands, which differ from protein to protein and even depending on where the protein is located, constitute the secondary structure of proteins. Our CD spectroscopy findings demonstrate the modifications in the protein's secondary structure compositions in response to zinc binding. More negative ellipticity at 208 and 222nm wavelengths was observed with increased ZnCl<sub>2</sub> concentrations (Left panel of Figure 5.4B). The percentage of

 $\alpha$ -helices and  $\beta$ -strands of the protein were increased and decreased, respectively, when the protein was incubated with a molar ratio of protein and ZnCl<sub>2</sub> as 1:1 and 1:2 (Right panel of figure 5.4B). Such structural changes depict Zn<sup>2+</sup>ions influence the protein structure composition and folding.

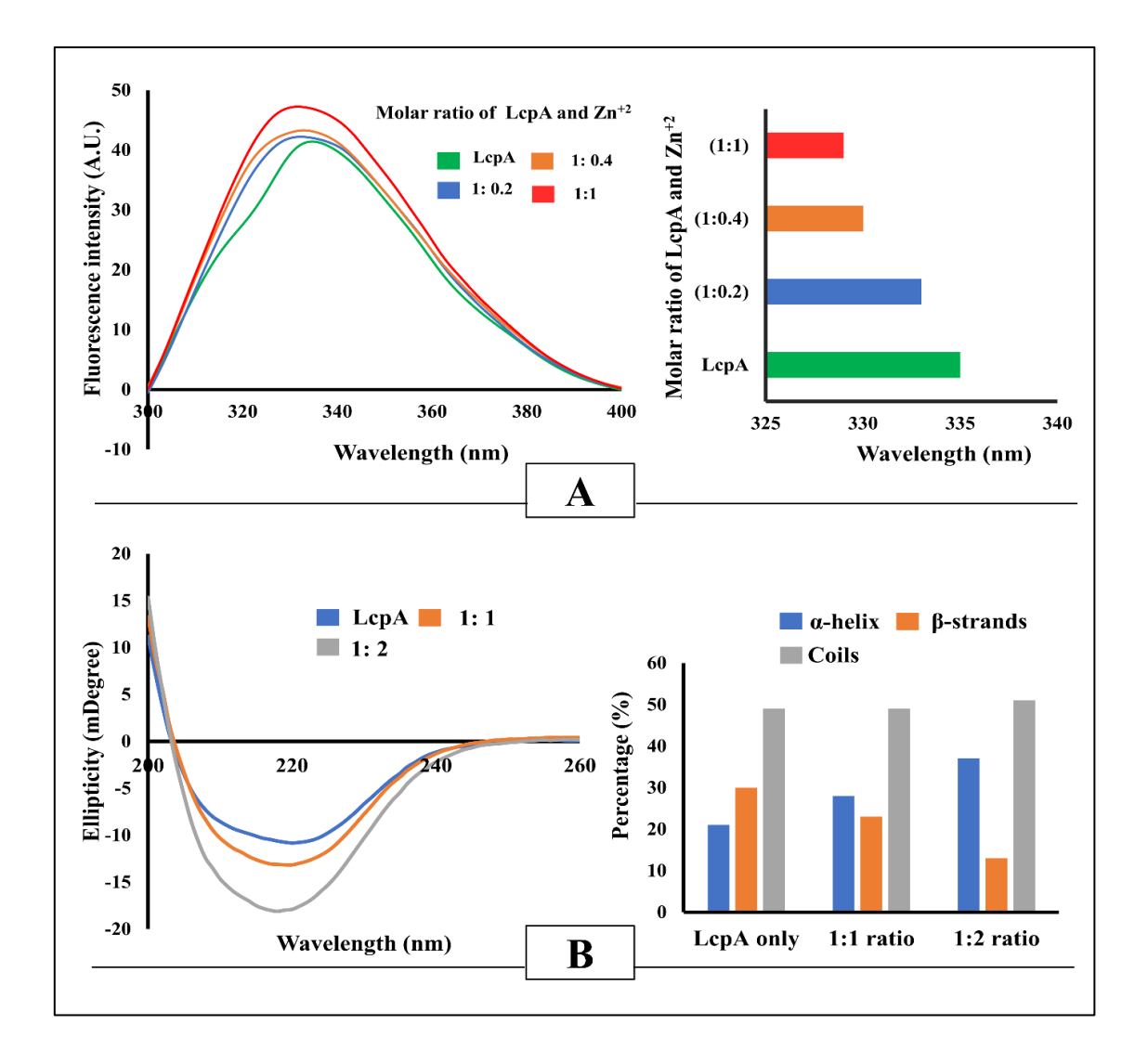


**Figure 5.4. Metal binding analysis** (**A**) Interaction study of zinc with LcpA using the intrinsic fluorescence measurement. The left panel shows the change in fluorescence spectra recorded at distinct molar ratios of LcpA and zinc, and the right panel highlights the wavelength shift at the respective ratios. (**B**) Far-UV CD spectra of LcpA were incubated with zinc chloride in 1:1 and 1:2 molar ratios (Left panel). The right panel shows the change in the percentage of secondary structure compositions upon Zinc binding.

### 5.4.6. Crystallization and Diffraction

Various commercially available crystallization screens were used to obtain crystallization hits of LcpA. Many attempts with multiple modifications were made, but unfortunately, conditions always gave heavy precipitation in the drops. A crystallization hit was observed with 6mg/ml protein in 0.1M BICINE pH 9, 2% v/v 1, 4-Dioxane, 10% w/v polyethylene glycol 20000) (**Figure 5.5 A**). Moreover, the protein of 8mg/ml in 50 mM Tris HCl pH 8, NaCl 100 mM with 25μM of ZnCl<sub>2</sub> yielded small-sized crystals with precipitation in conditions such as 0.2 M Calcium acetate hydrate 0.1 M Sodium cacodylate pH 6.5, 18% w/v PEG 8000 and 0.2M ammonium phosphate monobasic, 0.1M Tris pH 8.5, 50% v/v MPD), (**Figure 5.5 B and C**). However, these conditions were attempted to optimize in the hanging drop method. Unfortunately, no improvements were observed. The same tiny crystals were exposed to the in-house X-ray source for the diffraction. Unfortunately, no diffraction was observed, and these crystals turned out to be salt crystals.

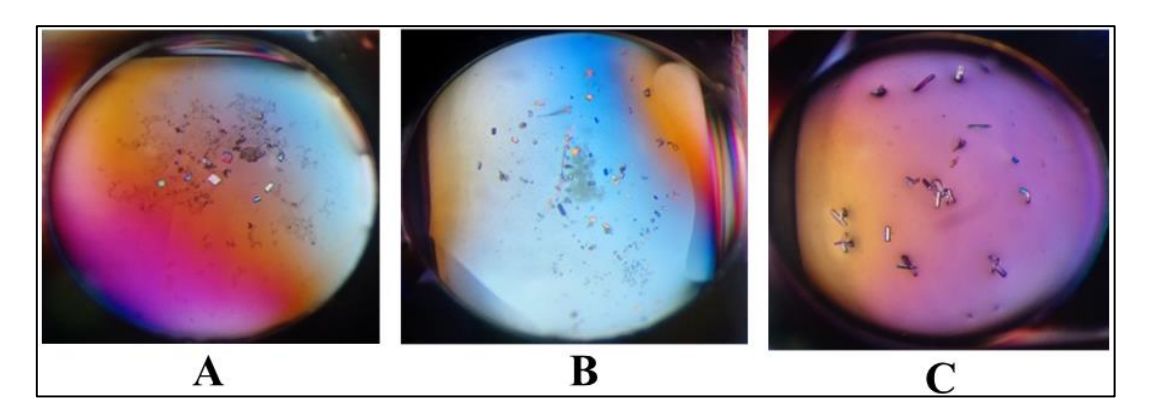


**Figure 5.5.** Crystallization conditions obtained for LcpA. Three crystallization hits were observed from the commercially available Crystal Screens. (A) Crystal screen at H12 (0.1M BICINE pH 9, 2% v/v 1, 4-Dioxane, 10% w/v polyethylene glycol 20000), (B) structure screen at B8 (0.2 M Calcium acetate hydrate 0.1 M Sodium cacodylate pH 6.5, 18% w/v PEG 8000), and (C) Structure screen at E8 (0.2M ammonium phosphate monobasic, 0.1M Tris pH 8.5, 50% v/v MPD).

### 5.4.7. 3-D Structural model of LcpA

The three-dimensional structure was modeled using the alphaFold, which showed considerable Ramachandran plot statistics. Validation by the Ramachandran plot showed approximately 100% residues in the favored and allowed regions (Figure 5.6 B). The model structure also possesses a ProSA Z-score of -5.22, which validates the quality of the model structure model (Figure 5.6 C). These statistics indicated that the modelled structure posed ideal bond lengths and bond angles. The three-dimensional structural model revealed that the LcpA contained four  $\alpha$ -helices and ten  $\beta$ -strands (**Figure 5.6 A**). Ten  $\beta$ -strands are arranged in an anti-parallel way, forming two β-sheets. Strands and sheets are connected via loops and helices. This arrangement seems similar to an Ig-like domain. Structural similarity search through the DALI server yielded a top hit of protein SYG-1, a cell adhesion molecule (CAM) with an Iglike fold (Shen and Bargmann 2003). This structure showed only 7% structural identity with the LcpA structure model. Unfortunately, no equivalent structural domain family was observed in the Pfam search. The total secondary structure content in the 3-D-structure model had 23.6% and 41.21%  $\alpha$ -helices and  $\beta$ -strands, respectively. These contents were almost similar to the secondary structure composition of 17% α-helices and 34% β-strands determined by the circular dichroism spectroscopy. The electrostatic surface charge of LcpA indicates a big patch of negative charge surface (Figure 5.7). This arises due to 20 glutamic acid residues and three aspartic acids. The negative surface might be involved in binding with positive metal ions. This patch may involve binding with host proteins. The LcpA is known to bind host complement regulators such as C4BP and factor H.

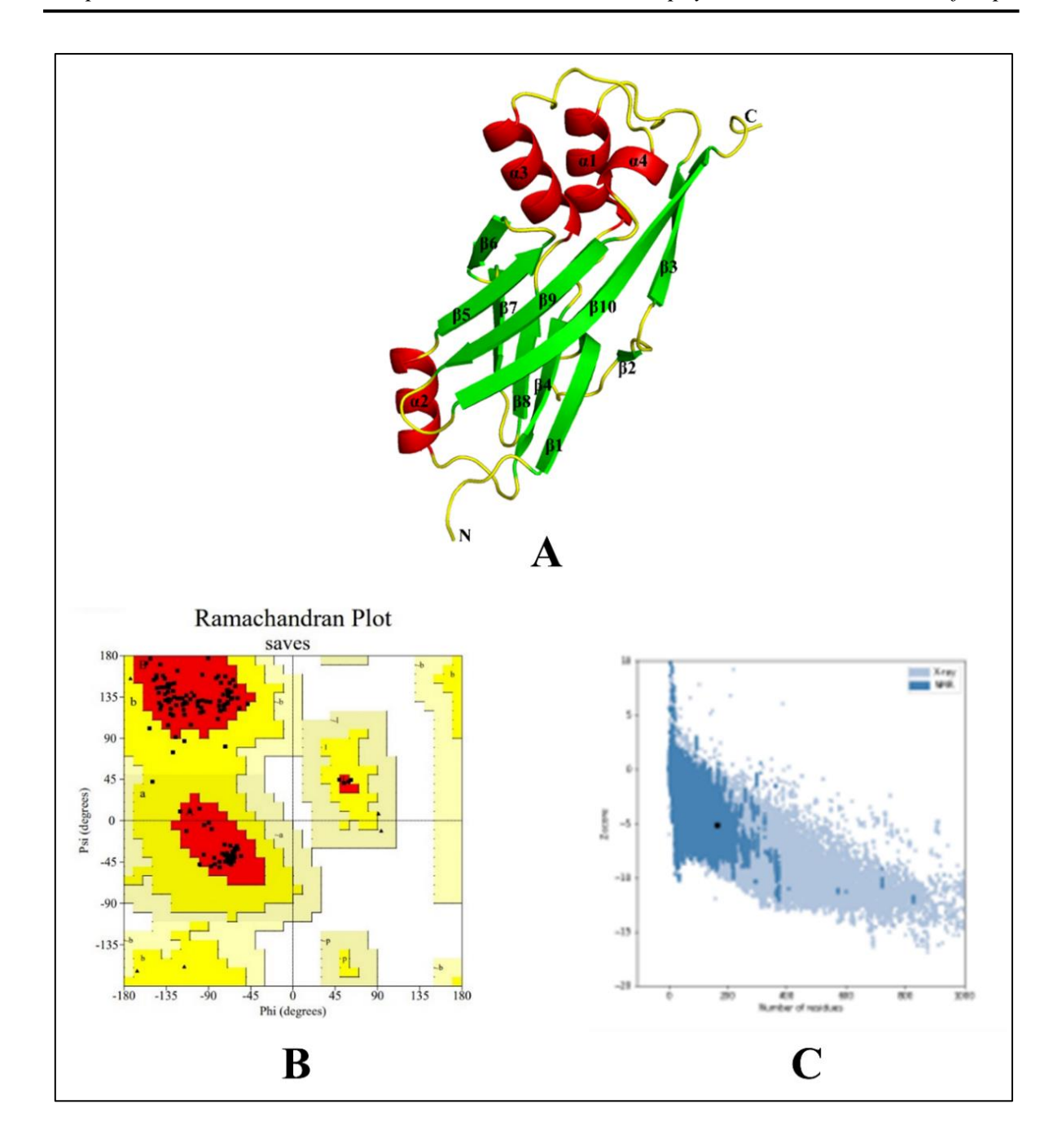
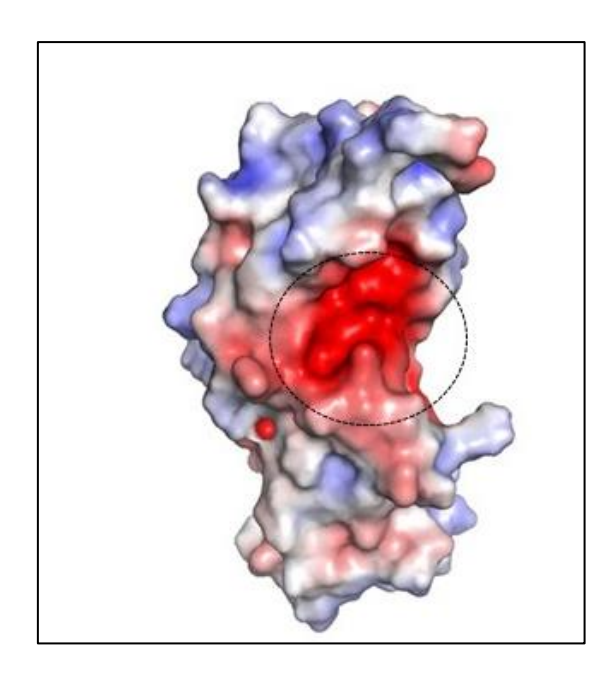


Figure 5.6. Three-dimensional structural model. (A) Shows LcpA modeled structure by Alphafold. Helices, strands, and loops are depicted in red, green, and yellow cartoons, respectively. Helices and strands are also labeled. (B) Ramachandran plot generated through Procheck for validating structural model (C) Structure model validation through Prosa tool. The black dot in the shaded area indicates the quality of the model.



**Figure 5.7: Electrostatic surface charge.** Negative surface patch is shown in circle. Red and blue surface indicate negative and positive charges distribution of LcpA surface.

# 5.4.8. C4BP and FH bind to mid to N-terminus of the LcpA

A literature study suggests the interaction of LcpA with an α-chain of C4BP (Breda et al., 2015). The α-chain of C4BP comprises eight complement control proteins (CCPs) domains. However, the interacting domain of LcpA and the atomic level of interactions are not known yet. Hence, the LcpA structural model was docked with the CCP1-8 α-chain of C4BP to understand the protein-ligand interactions. In a molecular docking study, CCP6-8 domains were found to be engaged in binding with the LcpA (**Figure 5.8A**). The N-terminal residues of the LcpA, such as H13, E33, E44, and R55, and a few central residues, such as E91, R92, E94, K114, E115, and K118, were observed to interact with CCP6 and CCP domains. These residues of the LcpA are involved in forming hydrogen bonds with R334, Y343, R331, R356, E346, R331, and E346 of the CCP6 domain and S394, S396, and E400 of the CCP7 domain. Additionally, 125 non-bonded contacts and seven salt bridges were also formed

among LcpA and CCP6-7. Many ionic interactions were observed between the two proteins. Few glutamic acids of LcpA were observed to bind with CCP6 and CCP7.

LcpA is also reported to bind with another complement regulator factor H (FH). The docking showed that LcpA binds with CCP 8, 9, 18, 19, and 20 domains of FH (**Figure 5.8B**). Interestingly, residues of LcpA, such as His13, Arg55, Arg92, Glu94, and Glu115, are involved in interaction with both C4BP as well as FH (**Figure 5.8C**). LcpA residues and the residues from its interacting partner C4BP and FH, which establish the hydrogen bonds, are mentioned in **Table 5.1**.

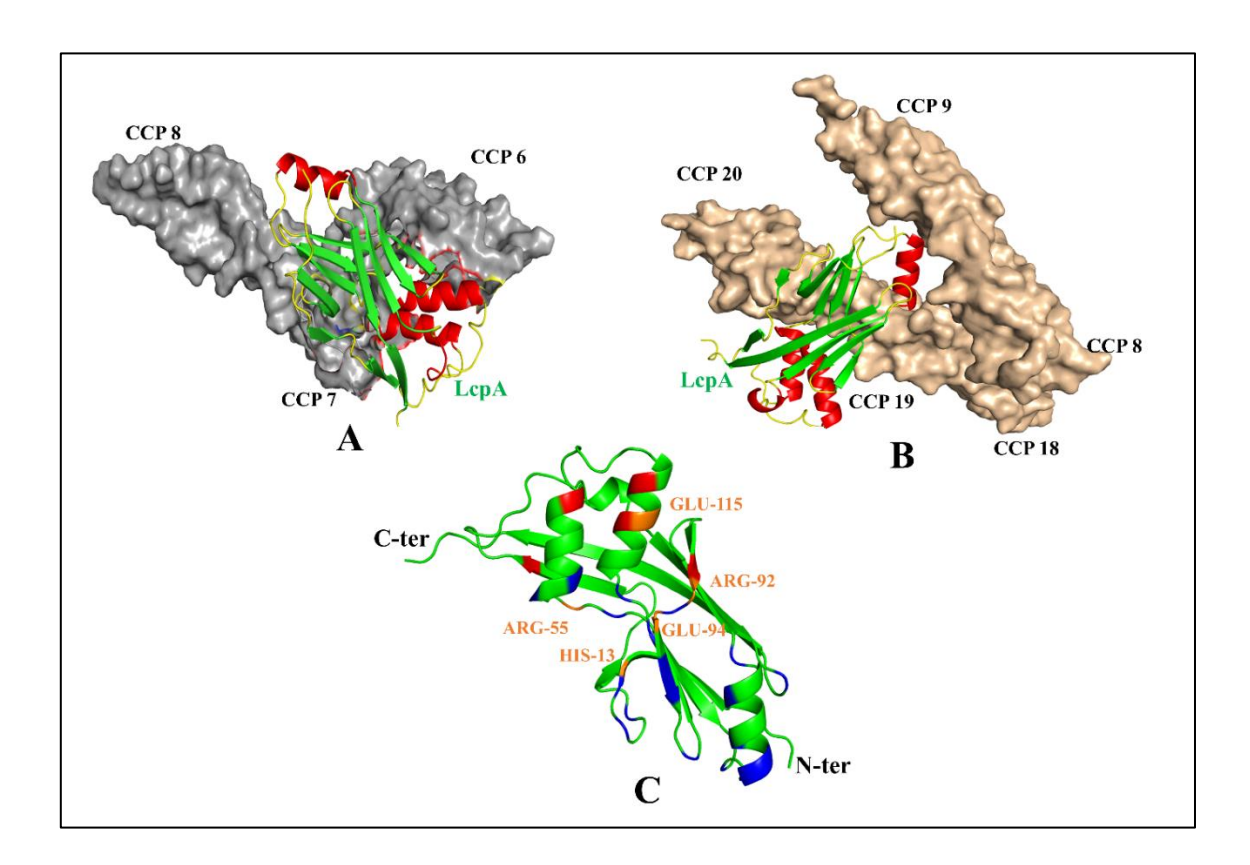


**Figure 5.8.** Complex structure model (A) Complex structural model of LcpA with CCP6-8 of C4BP. LcpA and CCP6-8 are shown in cartoon and surface representation, respectively (B). Complex structural model of LcpA with FH. LcpA and FH are represented in cartoon and surface, respectively (C) 3-D LcpA showing C4BP interacting region (Red), FH interacting region (Blue), and the common region of LcpA (orange) where both C4BP and FH interact.

Table 5.1. Amino acid residues involved in interactions

Atoms from LcpA	Atoms of C4BP (domain)	Atoms of FH (domain)
His 13	Ser 394 (7)	Lys 1188 (20)
Phe 14	-	Asn 1140 (19)
Arg 16	-	Tyr 1142 (19)
Arg 16	-	Tyr 1190 (20)
Glu 19	-	Arg 1171 (19)
Glu 33	Ser 396 (7)	-
Glu 44	Arg 334 (6)	-
Glu 44	Arg 334 (6)	-
Glu 44	Tyr 343 (6)	-
Tyr 51	-	Gln 1143 (19)
His 53	-	Gly 1194 (20)
Arg 55	Glu 400 (7)	Arg 1192 (20)
Thr 57	-	Arg 1192 (20)
Lys 67	-	Met 515 (9)
Pro 70	-	Ile 511 (8)
Pro 70	-	Val 513 (9)
Ser 71	-	Asp 510 (8)
Lys 74	-	Asp 510 (8)
Lys 77	-	Asp 1119 (19)
Tyr 80	-	Gln 1137 (19)
Glu 91	Arg 331 (6)	-
Arg 92	Arg 356 (6)	Thr 1121 (19)
Met 93	-	Gln 1137 (19)
Glu 94	Arg 356 (6)	Gln 1137 (19)
Glu 94	Arg 356 (6)	-
Glu 94	Arg 356 (6)	-
Phe 96	-	Cys 1138 (19)
Glu 97	-	Asn 1140 (19)
Glu 100	-	Met 515 (9)
Phe 106	-	Leu 1141 (19)
Tyr 108	-	Tyr 1142 (19)
Lys 114	Glu 346 (6)	-
Glu 115	Arg 331 (6)	Arg 1149 (19)
Lys 118	Glu 346 (6)	-
Ser 144		Leu 479 (8)

# **5.4.9.** Molecular Dynamic Simulation

A molecular Dynamic Simulation was performed to assess the stability and dynamic behavior of the LcpA, and LcpA-CCP6-8 docked complex for 100ns. Some key parameters such as Root

Mean Square Deviations (RMSD), RMSF, and radius of gyration of the docked complex after simulation were examined. RMSD values represent the overall stability, which means the lesser the RMSD, the higher the stability in the molecule or complex. The RMSD trajectory of LcpA depicts the system as having adequate stability throughout the simulation time, with not much change overall. For complexes, the system stabilizes at around 5ns. RMSD of the complex shows reductions at first, then progressively increases from ~55.8 ns onwards, from ~0.35 nm to ~0.72 nm at ~100 ns (**Figure 5.9A**).

The compactness of the molecule during simulation is measured in terms of radius of gyration (Rg). The Rg of apo protein (LcpA) and a complex were analysed and plotted with respect to simulation time. There is an apparent reduction in the size of the complex protein over the simulation time, reducing from ~2.7nm to ~2.6nm. It indicates the compaction in the protein complex over time, which is considered good for its stability. For apo protein, there is no change in Rg (Figure 5.9B). In addition, Root Mean Square Fluctuations (RMSF) of the residues in the complex were determined. In apo protein (1 to 165 Residues) and in CCP6-8 (166 to 343 Residues) of the complex, the terminal residues have more fluctuations (Figure 5.9C). The RMSF of residues in apo protein followed the same trend as in complexes, not exceeding the RMSF of 0.27nm (Figure 5.9D). Interestingly, we observed that the H-bond forming residues His13, Arg55, Arg92, Glu94, and Glu115 of LcpA have comparatively lower RMSF, which are involved in C4BP and FH bindings.

.

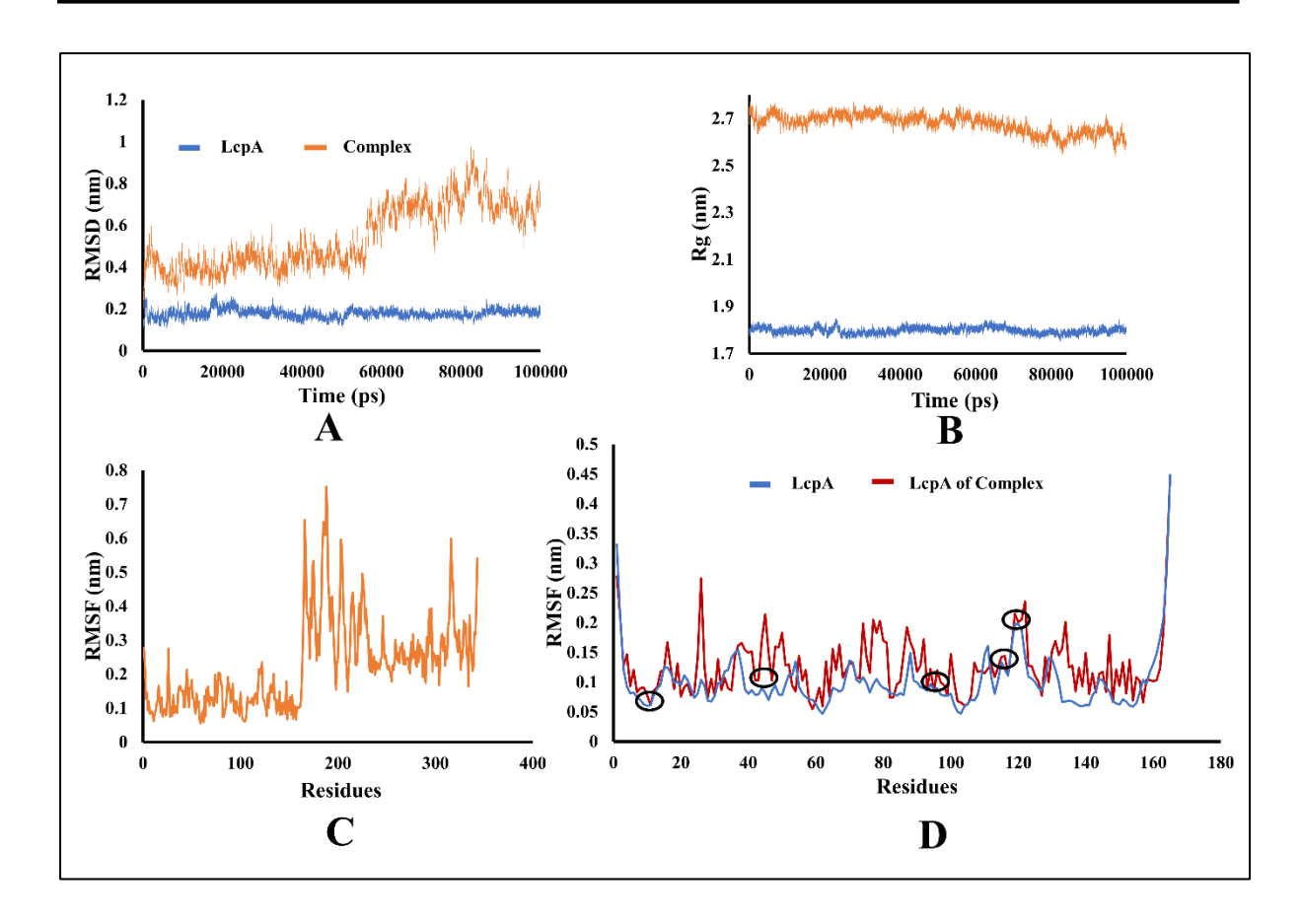


**Figure 5.9. MDS plots of LcpA and LcpA-CCP6-8 complex.** (A) C-alpha RMSD variation with respect to simulation time. (B) The radius of gyration changes with time. (C) RMSF of all atoms of LcpA-CCP6-8 complex, and (D) RMSF of LcpA and LcpA complex. Back circles denote the H-bond forming residues with comparatively lower RMSF variation.

# 5.4.10. Conservation analysis among pathogenic, saprophytic and intermediates species of *Leptospira*

Protein sequence identity of LcpA was compared against the pathogenic, saprophytic, and intermediate species of *Leptospira* in order to perform a phylogenetic study using pBLAST. Findings revealed the identity of 80-97% in pathogenic species, 52-54% in intermediate species, and 30-37% in saprophytes (**Table 5.2**). According to the phylogenetic analysis study,

LcpA protein is clustered with pathogenic species of Leptospiral with the greatest bootstrap score, indicating its highest conservation among pathogenic Leptospiral species (**Figure 5.10**).

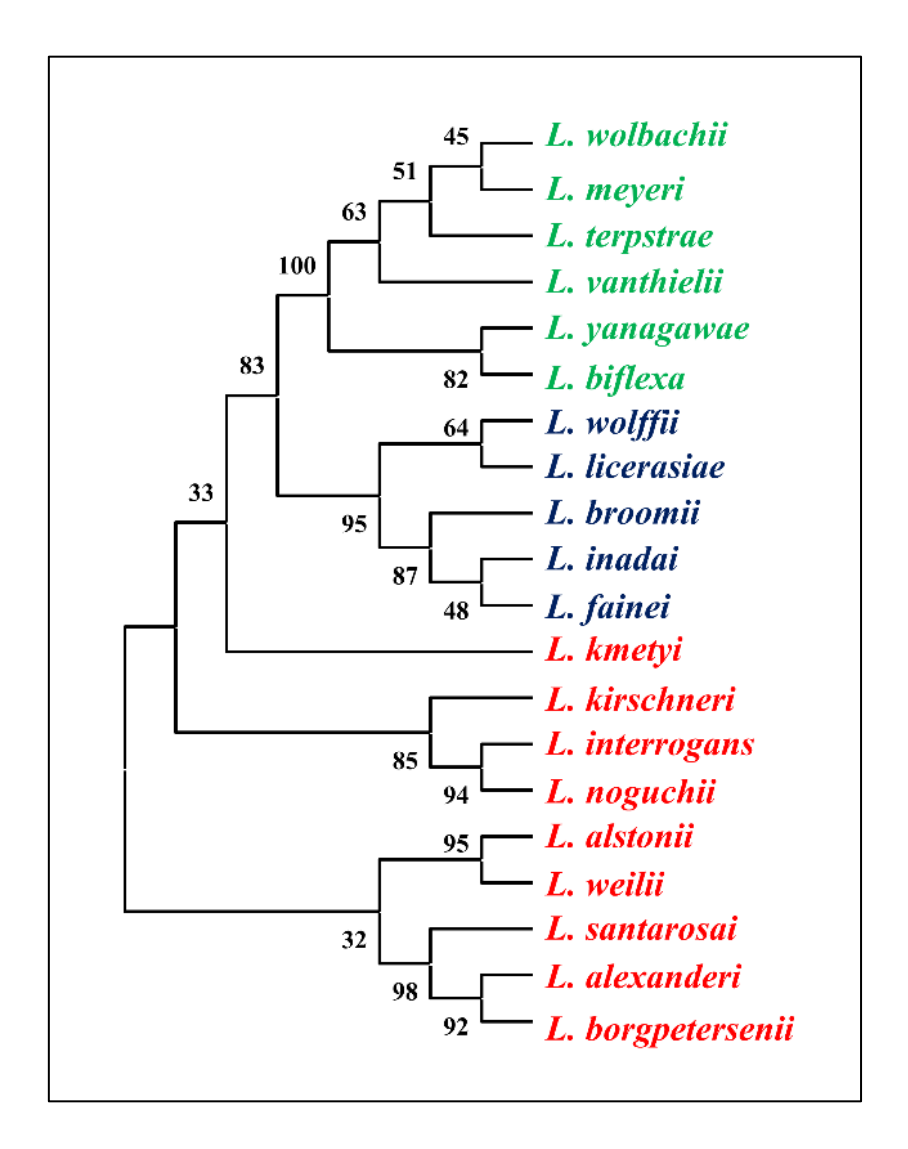


**Figure 5.10. Phylogenetic analysis of LcpA and related sequences.** Phylogenetic tree with the set of proteins identified after pBLAT against the proteome of different pathogenic, intermediates and saprophytic Leptospiral species. The bootstrap values (1000 replicates) are shown next to the branches. The pathogenic, intermediates and saprophytic species of are shown in red, blue and green, respectively.

Table 5.2. Identity of LcpA among different Leptospiral species

Sr. No.	Group	Species	Identity (%)
1 Pathogenic	Pathogenic	L. interogans	100
		L. kirschneri	96.34
		L. noguchii	97.38
		L. alstonii	78.65
		L. weilii	81.77
		L. alexanderi	81.35
		L. borgpetersenii	80.31
		L. santarosai	79.27
		L. kmetyi	79.90
2 Intermediates	Intermediates	L. fainei	54.80
		L. broomii	53.11
		L. wolffii	52.57
		L. licerasiae	51.96
		L. inadai	52.84
3 Saprophyte	Saprophyte	L. wolbachii	32.61
		L. yanagawae	34.21
		L. biflexa	36.97
		L. vanthielii	32.41
		L. terpstrae	30.67
-		L. meyeri	33.77

### **5.5. CONCLUSIONS**

The yield of refolded LcpA protein is fairly good, that is, 14mg from the pellet that was harvested out of one liter of bacterial culture. Purified refolded LcpA exists as a monomer in solution and contains 18% of  $\alpha$ -helices and 34% of  $\beta$ -strands at pH 7. However, the theoretical estimation of secondary structure contents yielded 23% and 41%  $\alpha$ -helices and  $\beta$ -strands, respectively. Besides, it possesses moderate thermostability with a Tm of 55°C and maintains its native structure in the pH range of 7.5 to 9. Our fluorescence spectroscopy and CD spectroscopy study demonstrated the interaction of zinc with LcpA, which also led to conformational changes in protein structure. Moreover, the 3-D structural model revealed that the LcpA contained four  $\alpha$ -helices and ten  $\beta$ -strands where  $\beta$ -strands are run in the anti-parallel direction, forming two  $\beta$ -sheets. The arrangement of sheets, loops, and helices is similar to an Ig-like domain. Docking of C4BP and FH with the LcpA revealed a few common interacting

residues on the LcpA. Molecular dynamic simulation of the LcpA-C4BP docked complex displayed stable complex formation. Notably, the phylogenetic study of LcpA shows its conservation among different pathogenic Leptospiral species, which helps to add significance to the study.

# Chapter-6

Discussion

Leptospirosis is the most common, worldwide emerging, zoonotic infectious disease prevalent in regions with tropical and sub-tropical climates where the environmental moisture favours the survival of pathogen *Leptospira* (Costa et al. 2015; Thibeaux et al. 2017). Annually, more than 1 million patients and 60000 deaths are recorded from the Leptospirosis (Ko et al. 2009b; Costa et al. 2015). Various outer membrane and secretory proteins from pathogenic organisms play paramount roles in establishing successful infection. Such proteins usually interact with the host's ECM and also have critical roles in sequestering or degrading the complement components and evading the host immune surveillance (Sorokin 2010; Tomlin and Piccinini 2018). Several outer membrane proteins from *Leptospira* such as Lig A/B, Len A/B, and Lsa30 are reported to interact with the host's ECM and complement regulators (Vieira1 et al. 2013; Fraga et al. 2016; Takahashi et al. 2022). Few reports identified the function of Leptospiral complement regulator-acquiring protein A (LcpA) and Elongation factor-Tu in acquiring complement regulators (Barbosa et al. 2010; Wolff et al. 2013; Moore et al. 2021). Moreover, leptospires produce many other proteins exported to the outer membrane or the secretory. Identification and functional characterization of such proteins may provide critical details of pathogenesis-associated mechanisms.

Many computational tools such as TMHMM, Cello, Target P, and Secretome are available to predict outer membrane and exported proteins from Gram-positive and Gram-negative bacteria. These tools helped to predict 144 proteins as outer membrane proteins from the proteome of *Mycobacterium tuberculosis* (Carvalho et al. 2008). Similarly, Rana et al. used these approaches to predict outer membrane proteins from *Mycobacterium avium* (Rana et al. 2014). In chapter 2, we exploited all tools to predict exported proteins from the pathogenic Leptospiral proteome. Presence of signal peptides, number of transmembrane helices, and lipo box were considered to avoid ambiguity of prediction. The study yielded 199 potent outer membrane proteins and 117 proteins secreted by classical and non-classical secretory pathways

(Figure 2.3A-B). A few proteins, such as LIC 11574 and LIC 13411, from potent outer membrane proteins list were experimentally reported as outer membranes and functionally reported as adhesins (Evangelista et al. 2014). In addition, one of the proteins, LIC 13322, has been reported experimentally as outer membrane protease, which displays a proteolytic activity against the complements C3 and C6 (Barbosa and Isaac 2020). Our prediction result is in-line with the experimental studies reported. Exported proteins from pathogenic organisms belong to different enzymatic classes and have been reported to modulate host proteins. One of the secretory proteins from Helicobacter pylori belonging to the protease class cleaves tight junction proteins from the host's epithelial cells to establish the infection (Marques et al. 2021). An extracellular protein belonging to  $\alpha/\beta$  hydrolase superfamily from *Staphylococcus* cleaves the host's complement components. This protein also lipolyzes immune-stimulating factors to assist in evading host immune systems. Moreover, one of the esterases from *Streptococcus spp*. is a crucial virulent factor (Zhu et al. 2009; Chen and Alonzo 2019). In pathogenic Leptospira, thermolysin of the metalloprotease family is the only known hydrolytic enzyme that cleaves the host's complement component molecule, C3 (Chura-Chambi et al. 2018). The prediction of the functional classification of exported proteins from pathogenic *Leptospira* suggests that these proteins may have different functional classes (**Figure 2.3 C**). Among them, proteases and  $\alpha/\beta$  hydrolase representation are comparatively higher than others, indicating these may have a role in pathogenesis. Bioinformatics analysis also predicts the virulence nature of the  $\alpha/\beta$  hydrolases from *Leptospira*. This is not surprising,  $\alpha/\beta$  hydrolases from *Mycobacterium* tuberculosis are reported as virulent factors and potentially have crucial roles in immune evasion and in establishing the infection (Johnson 2016).

The exported  $\alpha/\beta$  hydrolases comprised a conserved lipase motif "G/AXSXG" and catalytic triad Ser-Asp-His (**Figure 2.4 and 2.5**). This motif and catalytic triads are usually present in lipases and esterases (Kourist et al. 2010; Gutiérrez-Domínguez et al. 2022). The LIC\_11463

and LIC\_12988 from Leptospira were structurally similar to the known lipases of Staphylococcus species. Lipases from S. aureus have been reported to interfere with the host immune system (Chen and Alonzo 2019). Only two conserved catalytic triad residues, Ser and Asp/Glu were present in LIC\_10995 and LIC\_11103 (Figure 2.5). However, their structural folds are also similar to lipases. The absence of His residue from the catalytic triad may be substituted by either a water molecule or other residue. A similar catalytic dyad was found in ExoU of P. aeruginosa which possesses lipolytic activity (Sato et al. 2003). In addition, a lipid acyl hydrolase in Patatin also consist of the active catalytic dyad (Rydel et al. 2003). These examples support the possibility that the absence of one residue from the catalytic triad may also behave as  $\alpha/\beta$  hydrolases. The comparative sequence analysis among other *Leptospira* species reveals that all five putative  $\alpha/\beta$  hydrolases are mostly conserved among pathogenic species (Figure 2.8). Such conservation among pathogenic species of *Leptospira* predicts the probable role in Leptospiral pathogenesis. Our *in-silico* study suggests that these five proteins, similar to those found in other infections, may play a role in leptospiral pathogenesis, most likely by destroying host elements. These results call for more in-vitro investigation to comprehend such proteins in better ways.

Consequently, the cloning and protein purifications of all five putative  $\alpha/\beta$  hydrolases (LABHs) such as LIC\_11463, LIC\_11183, LIC\_11103, LIC\_10995, and LIC\_12988 were attempted where we could successfully purify two proteins, LIC\_11463 (LABH-1) and LIC\_11103 (LABH-2). These purified proteins such as LABH-1 and LABH-2 were found to be monomer in solution. However, the oligomeric state of many  $\alpha/\beta$  hydrolases either exists as dimers, tetramers, hexamers, octamers, or even 12 mers in nature (Dimitriou et al. 2017). An esterase of  $\alpha/\beta$  hydrolase superfamily, lipA3 from thermophilic bacteria *T. tengcongensis* were monomers at the pH optima of 9.5 (Rao et al. 2011). Lipase from *B. subtilis* and an esterase from thermophilic bacterium *Bacillus sp.* were reported as monomers and were fairly stable

within the pH range from 7.0 to 8.0 (Ahmad et al. 2008; Ding et al. 2015). Many oligomeric states were also reported for carboxylesterase. For example, thermostable carboxylesterase from an archaeon, *Sulfolobus shibatae*, is reported mostly as dimers and tetramers (Ejima et al. 2004). In another example, a stereoselective esterase (Est) from *Pseudomonas putida* was reported to exist as a trimer in solution (Elmi et al. 2005).

Usually, esterases and lipases display enzymatic activity over the broader range of temperature and pH. A lipase from *C. viswanathii* exhibits its maximum activity at a pH 4 (Yao et al. 2021). Here, the significant impact of pH and temperature on the LABH's hydrolytic activity is reported in chapter 4. The LABH-1 and LABH-2 displayed the optimum activity at pH 8 and pH 8.5 respectively. These experiments suggest that the LABH-1 and 2 prefer alkaline pH for its activity. Similarly, Lipases from *B. stearothermophilus* and *B. thermocatenulatus* were also reported to have highest activity in alkaline pH range (Schmidt-Dannert et al. 1996; Kim et al. 2000). Similar to the lipases, the pH optimum of esterase from *T. tengcongensis*, *B. subtilis* and *B. licheniformis* were reported in the alkaline pH range (pH 8-10) and also shown to have maximum stability in the alkaline pH (Macarie et al. 1999; Eggert et al. 2001; Rao et al. 2011). Many bacterial esterase/lipases activity is modulated by several divalent ions such as Ca<sup>2+</sup>, Zn<sup>2+</sup> etc. (Yang et al. 2009, 2010; Zarafeta et al. 2016; Xing et al. 2021). Therefore, Ca<sup>2+</sup> and Zn<sup>2+</sup> effects on hydrolytic activity of LABH-1 were examined, where, no significant change in hydrolytic activity was observed (Figure 4.4).

Besides, the temperature is also an essential parameter for catalytic activity of an enzyme. Various  $\alpha/\beta$  hydrolases exhibit different thermostability due to structural diversity and secondary structure contents. Lipases display a range of optimum temperatures. For example, an extracellular lipase from *A. niger* GZUF36 displayed maximum activity at 40 °C (Xing et al. 2021). An esterase from *T. tengcongensis*, thermophilic lipases from *Burkholderia ubonensis* and *Janibacter* spp R02 exhibit optimum temperatures of 65 and 80 °C, respectively

(Rao et al. 2011; Yang et al. 2016; Castilla et al. 2017). The activity of LABH-1 and 2 was investigated under different reaction temperatures (25-80 °C). We observed that LABH-1 displayed highest activity in the range of 50-65 °C, while LABH-2 was most active at room temperature only (**Figure 4.3 and 4.18**). It is evident that LABH-1 demonstrated more thermostability over LABH-2.

The enzyme kinetic parameters of LABHs demonstrated the preference of substrates. LABH-1 and LABH-2 prefer the substrates containing small-chain fatty acids for their activity. But, when we compare them, LABH-1 displayed significantly greater hydrolytic activity than LABH-2. Similar lipolytic activity was found in the lipases from B. thermocatenulatus and B. stearothermophilus (Schmidt-Dannert et al. 1996; Kim et al. 2000). The esterase from B. subtilis and B. licheniformis has been reported to prefer substrates with medium to short-chain fatty alkyl esters (Macarie et al. 1999; Eggert et al. 2001). In addition, the active site mutant (S151A) of LABH-1 did not display any activity suggesting the catalytic role of Ser151 in the native LABH-1. Fortunately, LABH-1 showed sequence similarity of 38% as well as structural homology with the lipase from Staphylococcus spp. One report recently revealed the inhibitory action of lipase inhibitor, or listat over the lipase from Staphylococcus aureus (SAL) with the IC50 of 2.4 µM (Kitadokoro et al. 2020). In our inhibition assay study, LABH-1 activity was sharply reduced in presence of the lipase inhibitor, or listat and IC50 was found to be ~1.8 µM, comparable to SAL. Interestingly, there is decrease in Vmax with increase in the concentration of inhibitor where the Km remained unchanged which clearly shows that inhibition is non-competitive.

Structurally,  $\alpha/\beta$  hydrolase superfamily members mostly share a common fold. The fold usually consists of eight parallel  $\beta$ -strands and six  $\alpha$ -helices grouped in a half-barrel-like structure (Dimitriou et al. 2017). The overall content of secondary structures varies among lipases, esterases, and proteases. The structural investigation of purified LABH-1 using CD

spectroscopy depicted the α-helical content of 43% and a β-strands of 16% at pH 7.5 (Figure **4.1**). Similar to LABH-1, a novel  $\alpha/\beta$ -Hydrolase (LvFSH) from *Litopenaeus vannamei* possesses 31% α-helix, and 18% β-sheets (Garcia-Orozco et al. 2019). Furthermore, LABH-1 shows moderate thermostability with melting temperature (Tm) of approximately 60 °C. When we tested the structural conformation at varying pH levels, it showed a moderate stability at pH 7 to 11 but significantly lost the native structure at pH of 5-6. To understand the threedimensional structure of the protein and to map the binding sites for substrates and inhibitors on the protein structure, we attempted to crystallize it. We could get some useful crystallization conditions where the protein was successfully crystallized, but unfortunately, the structure could not be solved due to its poor resolution data. Hence, as mentioned in chapter 2, the AlphaFold modelled LABH-1 structure was utilized to identify the binding sites for substrates and the inhibitor. The total secondary structure composition in the 3D-structure model was 44% and 12%  $\alpha$ -helices and  $\beta$ -strands, respectively. This composition was comparable to the secondary structure determined by the circular dichroism spectroscopy. Furthermore, in our docking study of LABH-1 with the substrate p-Nitrophenyl butyrate and an inhibitor orlistat, the best-docked substrate was observed to bind at the active site cavity with docking energy of −6.7 kcal mol<sup>-1</sup>. The substrate was surrounded by protein residues W69, S151, P180, L214, F273, I294, V295, and H318 (within 5Å distance). The oxygen of the sessile ester bond of the substrate was near the active site residue, Ser151, and observed to form a hydrogen bond with the Ser151 residue. The inhibitor orlistat was bound at the binding pocket LABH-1 suggested by the 3D DogSite scorer with a binding energy of -7.7 kcal mol<sup>-1</sup>. This inhibitor binding site is distinct from the catalytic site (Figure 4.12). Since the mode of orlistat inhibition was noncompetitive, it is assumed that the binding of orlistat may cause the conformational changes in the structure that may have an inhibitory effect on the LABH-1 activity.

Moreover, LABH-1 is enantioselective and has bio-catalytic applications in the generation of enantio-pure (R)-1-Phenylethanol from the lipase substrate racemic 1-phenylethyl acetate (**Figure 4.15**). (R)-1-Phenylethanol is an important chiral intermediate that finds application in Solvatochromic dye, an inhibitor of cholesterol intestinal adsorption, as an ophthalmic preservative and used in the pharmaceutical, fine chemical, and perfume industry (Suan and Sarmidi 2004). Lipase catalysed kinetic resolution using acylation and deacylation are the two well-known methods of production of (R)-1-phenylethanol. Literature analysis of the existing biocatalytic methods of enantioselective deacylation of racemic 1-phenylethyl acetate, which the current approach involves, revealed that only a few enzymes are known to catalyse such transformation. The prominent among them are Candida antarctica lipase B (CALB), Pseudomonas cepacia lipase (PCL), Candida cylindracea lipase (CCL), and Pseudomonas Sp lipase (PSL) that exhibited (R)-selectivity and produced (R)-1-phenylethanol (Laumen and Schneider 1988; Merabet-Khelassi et al. 2012; Zaidi et al. 2015; Melais et al. 2016), while Candida rugose lipase, and Porcine pancreatic lipase have shown (S)-selectivity (Jia et al. 2013; Velasco-Lozano et al. 2016). The enantioselectivity, E of LABH-1 in the kinetic resolution of racemic 1-phenylethyl acetate was >500 which is found to be similar or better than CALB, PCL and PSL. Further, LABH-1 catalyzed transformation required only 8 h compared to CALB catalyzed kinetic resolution that required 24 to 72 h depending on the reaction conditions (Merabet-Khelassi et al. 2012; Zaidi et al. 2015; Melais et al. 2016). Hence, LABH-1 was not only found to be an efficient enzyme for the production of (R)-1phenylethanol but also showed excellent E in the enantioselective hydrolysis of racemic 1phenylethyl acetate. Our findings add a new biocatalyst to the biocatalytic toolbox, which opens new prospects to synthesize chiral intermediates and scope to broaden its biotechnological applications.

In addition to the enzymatic functions, several  $\alpha/\beta$  hydrolases are also involved in modulating host immune response and, hence, responsible in immune evasion. In *Haemonchus contortus*,  $\alpha/\beta$  hydrolases protein modulates the host cytokines, mainly by enhancing IL-10 production and suppressing the production of IL-4, IFN- $\gamma$ , and TGF- $\beta$  (Lu et al. 2021). In *Streptococcus*, secreted esterase is found to be virulent factor, and  $\alpha/\beta$  hydrolases in Mycobacterium tuberculosis have various functions including the modulation in immune response and hence in immune evasion (Zhu et al. 2009; Johnson 2016). Similarly, our preliminary study on mice macrophages suggests the LABH-1 protein has the potential to modulate the host immune response by enhancing the TNF- $\alpha$  and IL-10 mRNA expressions.

Additionally, Leptospira also acquires fluid-state complement regulators such as C4BP, Factor H, FHL-1, FHR-1, etc, on its cell surface and also bind to several Extracellular matrix (ECM) components and plasma proteins, such as laminin, collagen, fibronectin, elastin, proteoglycans, fibringens, and plasmingens. Usually, pathogens regulate the complement stimulation using its outer membrane proteins which control the complement cascade activations, such as CD59like protein of B. burgdorferi, PspC protein from Streptococcus pneumoniae (Andre et al. 2017; Skare et al. 2020). So far, proteins containing the members of leptospiral endostatin-like protein family (Len A and B), Lig A, Lig B, and LcpA from Leptospira interrogans are recognized for binding with complement regulators such as C4BP, FH, vitronectin and complement component C9 (Barbosa et al. 2010; Castiblanco-Valencia et al. 2012; Breda et al. 2015). LcpA is among the most studied leptospiral proteins but lacks three-dimensional structure and the information of its binding regions with host targets such as C4BP and Factor H. As stated in chapter 5, under the heterologous expression system, LcpA was over-expressed, which led to the formation of inclusion bodies. Although several efforts were taken to get the protein into soluble fraction, every time, the protein was in the pellet of the cell lysate, where it formed the inclusion bodies. Therefore, LcpA was purified using a refolding protocol with a

good yield. The protomer size of LcpA was found to be 19.5kDa and observed to exist as a monomer in solution (**Figure 5.2**). Similarly, OmpA, a C4BP-binding outer membrane protein from *E. coli*, is monomeric. However, Factor H interacts with the outer membrane protein CspA from *B. burgdorferi* and is a dimer (**Skare et al. 2020**).

The purified LcpA contains 18% of α-helices and 34% of β-strands at neutral pH. Major outer membrane proteins (>70 proteins) from gram negative bacteria are rich in  $\beta$  strands and consist of β barrel folds which differ in size from eight to 22 β-strands (Shearer et al. 2019). The stability of outer membrane proteins is influenced by several factors, including environmental temperature and pH. LcpA showed significant structural stability between pH 7 and 9. Moreover, the thermal analysis suggested that the LcpA was moderately stable with a Tm of 55°C (Figure 5.3). The Lig protein from Leptospira is a Ca2+-binding protein; the bound Ca<sup>2+</sup> ions induce the interaction with the host fibronectin (Lin et al. 2008; Raman et al. 2010). Another report suggested that Lig protein favored Mg<sup>2+</sup> instead of Ca<sup>2+</sup> in nuclease activity study (Kumar et al. 2022a). The Sht protein from Streptococcus agalactiae acquires the zinc metal and facilitate the zinc homeostasis and also responsible for factor H binding (Moulin et al. 2019). In our study, LcpA also interacted with Zn<sup>2+</sup>, as both CD and fluorescence spectroscopy demonstrated. With increase in zinc concentration, there was higher percentage of  $\alpha$ -helices and decrease in  $\beta$ -strands in the LcpA structure (**Figure 5.4**). Moreover, when the LcpA protein sequence was analyzed for presence of zinc binding motif, interestingly, we found the Zinc finger motif at N-terminus of the protein, which support the zinc binding nature of LcpA.

As mentioned in  $5^{th}$  chapter, the crystallization of LcpA was initially performed. A few crystallization hits were found, but unfortunately, these conditions did not yield diffraction-quality crystals. Therefore, three-dimensional structure was modelled using Alphafold. The structure reveals the presence of  $\beta$ -barrel domain with four  $\alpha$ -helices and ten  $\beta$ -strands. Protein

structure with β-barrel domain and rich in β-strands is the distinctive quality of the outer membrane proteins (Shearer et al. 2019). Our analysis revealed the secondary structure composition of the modelled structure was 23.6% and 41.21% α-helices and β-strands, respectively. These contents were similar to the secondary structure compositions determined by the circular dichroism spectroscopy. Upon infection, LcpA helps *Leptospira* by binding with complement regulators C4BP and FH. The molecular docking of LcpA with complement regulators revealed stable interaction. Moreover, the complex was stabilized by several H-bonds and salt bridges (**Figure 5.6 and Table 5.1**). Our study mapped a common binding site in LcpA for C4BP and FH. The information about the binding sites will provide insight into the structural basis of interaction.

Overall, this research work emphasizes on prediction, in-silico, and biochemical characterization of potent outer membrane and secretory putative  $\alpha/\beta$  hydrolases. LABH-1 is also demonstrated to be the efficient enzyme for the production of (R)-1- phenylethanol. This finding expanded the biocatalytic arsenal by adding the novel biocatalyst which opens up the new opportunities for the production of chiral intermediates. Moreover, this study yields the comprehensive understanding of structural and functional characteristics of these hydrolases from pathogenic *leptospira*. Over and above these findings, our study also highlights the structural attributes of one of the outer membrane proteins LcpA, and its binding with host targets such as C4BP and FH. This study may provide the basis for identifying the potential therapeutic targets.

# **B**ibliography

- Abe K, Kuribayashi T, Takabe K, Nakamura S (2020) Implications of back-and-forth motion and powerful propulsion for spirochetal invasion. Sci Rep 10:1–8. https://doi.org/10.1038/s41598-020-70897-z
- Adler B, de la Pena Moctezuma A (2010) Leptospira and leptospirosis. Vet Microbiol 140:287–296. https://doi.org/10.1016/j.vetmic.2009.03.012
- Afroz S, Giddaluru J, Abbas MM, Khan N (2016) Transcriptome meta-analysis reveals a dysregulation in extra cellular matrix and cell junction associated gene signatures during Dengue virus infection. Sci Rep 6:1–12. https://doi.org/10.1038/srep33752
- Ahmad S, Kamal MZ, Sankaranarayanan R, Rao NM (2008) Thermostable Bacillus subtilis Lipases: In Vitro Evolution and Structural Insight. J Mol Biol 381:324–340. https://doi.org/10.1016/j.jmb.2008.05.063
- Amamura TA, Fraga TR, Vasconcellos SA, et al (2017) Pathogenic Leptospira secreted proteases target the membrane attack complex: A potential role for thermolysin in complement inhibition. Front Microbiol 8:1–16. https://doi.org/10.3389/fmicb.2017.00958
- Andersson A, Dahlbäck B, Hanson C, et al (1990) Genes for C4b-binding protein α- and β-chains (C4BPA and C4BPB) are located on chromosome 1, band 1q32, in humans and on chromosome 13 in rats. Somat Cell Mol Genet 16:493–500. https://doi.org/10.1007/BF01233199
- Andrade MA, Chacón P, Merelo JJ, Morán F (1993) Evaluation of secondary structure of proteins from uv circular dichroism spectra using an unsupervised learning neural network. Protein Eng Des Sel 6:383–390. https://doi.org/10.1093/protein/6.4.383
- Andre GO, Converso TR, Politano WR, et al (2017) Role of Streptococcus Pneumoniae

- proteins in evasion of complement-mediated immunity. Front Microbiol 8:1–20. https://doi.org/10.3389/fmicb.2017.00224
- Barbosa AS, Abreu PAE, Neves FO, et al (2006) A newly identified leptospiral adhesin mediates attachment to laminin. Infect Immun 74:6356–6364. https://doi.org/10.1128/IAI.00460-06
- Barbosa AS, Abreu PAE, Vasconcellos SA, et al (2009) Immune evasion of Leptospira species by acquisition of human complement regulator C4BP. Infect Immun 77:1137–1143. https://doi.org/10.1128/IAI.01310-08
- Barbosa AS, Isaac L (2020) Strategies used by Leptospira spirochetes to evade the host complement system. FEBS Lett 594:2633–2644. https://doi.org/10.1002/1873-3468.13768
- Barbosa AS, Monaris D, Silva LB, et al (2010) Functional characterization of LcpA, a surface-exposed protein of Leptospira spp. that binds the human complement regulator C4BP.

  Infect Immun 78:3207–3216. https://doi.org/10.1128/IAI.00279-10
- Bendtsen JD, Kiemer L, Fausbøll A, Brunak S (2005) Non-classical protein secretion in bacteria. BMC Microbiol 5:1–13. https://doi.org/10.1186/1471-2180-5-58
- Bharti AR (2003) Leptospirosis: a zoonotic disease of global importance. Lancet Infect Dis 3:757–71. https://doi.org/10.1016/s1473-3099(03)00830-2
- Bjorn P. Johansson, Oonagh Shannon LB (2008) IdeS: A Bacterial Proteolytic Enzyme with Therapeutic Potential. PLoS One 3:e1692. https://doi.org/10.1371/Citation
- Blom AM, Villoutreix BO, Dahlbäck B (2003) Mutations in α-Chain of C4BP that Selectively Affect Its Factor I Cofactor Function. J Biol Chem 278:43437–43442. https://doi.org/10.1074/jbc.M306620200

- Blom AM, Villoutreix BO, Dahlbäck B (2004) Functions of human complement inhibitor C4b-binding protein in relation to its structure. Arch Immunol Ther Exp (Warsz) 52:83–95
- Bonhomme D, Santecchia I, Vernel-Pauillac F, et al (2020) Leptospiral LPS escapes mouse TLR4 internalization and TRIF-associated antimicrobial responses through O antigen and associated lipoproteins. PLoS Pathog 16:1–26. https://doi.org/10.1371/JOURNAL.PPAT.1008639
- Breda LCD, Hsieh CL, Castiblanco Valencia MM, et al (2015) Fine Mapping of the Interaction between C4b-Binding Protein and Outer Membrane Proteins LigA and LigB of Pathogenic Leptospira interrogans. PLoS Negl Trop Dis 9:1–18. https://doi.org/10.1371/journal.pntd.0004192
- Budihal SV, Perwez K (2014) Leptospirosis diagnosis: Competancy of various laboratory tests.

  J Clin Diagnostic Res 8:199–202. https://doi.org/10.7860/JCDR/2014/6593.3950
- Carvalho P, Stanley AM, Rapoport TA (2008) Identification of outer membrane proteins of Mycobacterium tuberculosis. Bone 23:1–7. https://doi.org/10.1016/j.tube.2008.02.004.Identification
- Casanovas-Massana (2018) crossm Quantification of Leptospira interrogans Survival in Soil and. Appl Environmental Microbiol 84:1–11
- Castiblanco-Valencia MM, Fraga TR, Pagotto AH, et al (2016) Plasmin cleaves fibrinogen and the human complement proteins C3b and C5 in the presence of Leptospira interrogans proteins: A new role of LigA and LigB in invasion and complement immune evasion.

  Immunobiology 221:679–689. https://doi.org/10.1016/j.imbio.2016.01.001
- Castiblanco-Valencia MM, Fraga TR, Silva LB Da, et al (2012) Leptospiral immunoglobulinlike proteins interact with human complement regulators factor H, FHL-1, FHR-1, and

- C4BP. J Infect Dis 205:995–1004. https://doi.org/10.1093/infdis/jir875
- Castilla A, Panizza P, Rodríguez D, et al (2017) A novel thermophilic and halophilic esterase from Janibacter sp. R02, the first member of a new lipase family (Family XVII). Enzyme Microb Technol 98:86–95. https://doi.org/10.1016/j.enzmictec.2016.12.010
- Chakraborty A, Ghosh S, Chowdhary G, et al (2012) DBETH: A database of bacterial exotoxins for human. Nucleic Acids Res 40:615–620. https://doi.org/10.1093/nar/gkr942
- Chen L, Yang J, Yu J, et al (2005) VFDB: A reference database for bacterial virulence factors.

  Nucleic Acids Res 33:325–328. https://doi.org/10.1093/nar/gki008
- Chen X, Alonzo F (2019) Bacterial lipolysis of immune-activating ligands promotes evasion of innate defenses. Proc Natl Acad Sci U S A 116:3764–3773. https://doi.org/10.1073/pnas.1817248116
- Chiriboga J, Barragan V, Arroyo G, et al (2015) Chiriboga 2015. 21:2141–2147
- Choy HA (2012) Multiple activities of ligb potentiate virulence of Leptospira interrogans:

  Inhibition of alternative and classical pathways of complement. PLoS One 7:.

  https://doi.org/10.1371/journal.pone.0041566
- Choy HA, Kelley MM, Chen TL, et al (2007) Physiological osmotic induction of Leptospira interrogans adhesion: LigA and LigB bind extracellular matrix proteins and fibrinogen.

  Infect Immun 75:2441–2450. https://doi.org/10.1128/IAI.01635-06
- Chung M-C, Popova TG, Millis BA, et al (2006) Secreted Neutral Metalloproteases of Bacillus anthracis as Candidate Pathogenic Factors. J Biol Chem 281:31408–31418. https://doi.org/10.1016/s0021-9258(19)84053-x
- Chura-Chambi RM, Fraga TR, da Silva LB, et al (2018) Leptospira interrogans thermolysin refolded at high pressure and alkaline pH displays proteolytic activity against complement

- C3. Biotechnol Reports 19:e00266. https://doi.org/10.1016/j.btre.2018.e00266
- Cleary PP, Prahbu U, Dale JB, et al (1992) Streptococcal C5a peptidase is a highly specific endopeptidase. Infect Immun 60:5219–5223. https://doi.org/10.1128/iai.60.12.5219-5223.1992
- Costa F, Hagan JE, Calcagno J, et al (2015) Global Morbidity and Mortality of Leptospirosis:

  A Systematic Review. PLoS Negl Trop Dis 9:0–1.

  https://doi.org/10.1371/journal.pntd.0003898
- Cserhalmi M, Papp A, Brandus B, et al (2019) Regulation of regulators: Role of the complement factor H-related proteins. Semin Immunol 45:. https://doi.org/10.1016/j.smim.2019.101341
- da Silva LB, Miragaia LDS, Dantas Breda LC, et al (2015) Pathogenic Leptospira species acquire factor H and vitronectin via the surface protein LcpA. Infect Immun 83:888–897. https://doi.org/10.1128/IAI.02844-14
- de Oliveira NR, Santos FDS, dos Santos VAC, et al (2023) Challenges and Strategies for Developing Recombinant Vaccines against Leptospirosis: Role of Expression Platforms and Adjuvants in Achieving Protective Efficacy. Pathogens 12:. https://doi.org/10.3390/pathogens12060787
- Dimitriou PS, Denesyuk A, Takahashi S, et al (2017) Alpha/beta-hydrolases: A unique structural motif coordinates catalytic acid residue in 40 protein fold families. Proteins Struct Funct Bioinforma 85:1845–1855. https://doi.org/10.1002/prot.25338
- Ding J, Wang C, Xie Z, et al (2015) Properties of a newly identified esterase from bacillus sp. K91 and its novel function in diisobutyl phthalate degradation. PLoS One 10:1–17. https://doi.org/10.1371/journal.pone.0119216

- Dirar BG (2021) Leptospirosis in Animal and its Public Health Implications: A Review Leptospirosis in Animal and its Public Health Implications: A Review. 34:845–853. https://doi.org/10.5829/idosi.wasj.2016.34.6.103113
- Dunay S, Bass J, Stremick J (2016) Leptospirosis: a Global Health Burden in Review. Emerg

  Med Open Access 6:. https://doi.org/10.4172/2165-7548.1000336
- Eberhardt J, Santos-Martins D, Tillack AF, Forli S (2021) AutoDock Vina 1.2.0: New Docking Methods, Expanded Force Field, and Python Bindings. J Chem Inf Model 61:3891–3898. https://doi.org/10.1021/acs.jcim.1c00203
- Eggert T, Van Pouderoyen G, Dijkstra BW, Jaeger KE (2001) Lipolytic enzymes LipA and LipB from Bacillus subtilis differ in regulation of gene expression, biochemical properties, and three-dimensional structure. FEBS Lett 502:89–92. https://doi.org/10.1016/S0014-5793(01)02665-5
- Eggert T, Van Pouderoyen G, Pencreac'h G, et al (2002) Biochemical properties and three-dimensional structures of two extracellular lipolytic enzymes from Bacillus subtilis.

  Colloids Surfaces B Biointerfaces 26:37–46. https://doi.org/10.1016/S0927-7765(02)00033-4
- Ejima K, Liu J, Oshima Y, et al (2004) Molecular cloning and characterization of a thermostable carboxylesterase from an archaeon, Sulfolobus shibatae DSM5389: Non-linear kinetic behavior of a hormone-sensitive lipase family enzyme. J Biosci Bioeng 98:445–451. https://doi.org/10.1016/S1389-1723(05)00310-5
- Elisa ALVAREZ-MACARIE VA-M& JB (1999) Characterization of a Thermostable Esterase

  Activity from the Moderate Thermophile Bacillus licheniformis. Biosci Biotechnol

  Biochem 63:1865–1870. https://doi.org/https://doi.org/10.1271/bbb.63.1865

- Elmi F, Lee HT, Huang JY, et al (2005) Stereoselective esterase from Pseudomonas putida IFO12996 reveals  $\alpha/\beta$  hydrolase folds for D- $\beta$ -acetylthioisobutyric acid synthesis. J Bacteriol 187:8470–8476. https://doi.org/10.1128/JB.187.24.8470-8476.2005
- Emanuelsson O, Brunak S, von Heijne G, Nielsen H (2007) Locating proteins in the cell using TargetP, SignalP and related tools. Nat Protoc 2:953–971. https://doi.org/10.1038/nprot.2007.131
- Emanuelsson O, Nielsen H, Brunak S, Von Heijne G (2000) Predicting subcellular localization of proteins based on their N-terminal amino acid sequence. J Mol Biol 300:1005–1016. https://doi.org/10.1006/jmbi.2000.3903
- Evangelista K V., Coburn J (2010) Leptospira as an emerging pathogen: A review of its biology, pathogenesis and host immune responses. Future Microbiol 5:1413–1425. https://doi.org/10.2217/fmb.10.102
- Evangelista K V., Hahn B, Wunder EA, et al (2014) Identification of Cell-Binding Adhesins of Leptospira interrogans. PLoS Negl Trop Dis 8:. https://doi.org/10.1371/journal.pntd.0003215
- Evangelista K V., Lourdault K, Matsunaga J, Haake DA (2017) Immunoprotective properties of recombinant LigA and LigB in a hamster model of acute leptospirosis. PLoS One 12:1–21. https://doi.org/10.1371/journal.pone.0180004
- Faisal SM, Varma VP, Subathra M, et al (2016) Leptospira surface adhesin (Lsa21) induces

  Toll like receptor 2 and 4 mediated inflammatory responses in macrophages. Sci Rep 6:1–

  14. https://doi.org/10.1038/srep39530
- Faisal SM, Yan WW, Chen CS, et al (2008) Evaluation of protective immunity of Leptospira immunoglobulin like protein A (LigA) DNA vaccine against challenge in hamsters.

- Vaccine 26:277–287. https://doi.org/10.1016/j.vaccine.2007.10.029
- Figueira CP, Croda J, Choy HA, et al (2011) Heterologous expression of pathogen-specific genes ligA and ligB in the saprophyte Leptospira biflexa confers enhanced adhesion to cultured cells and fibronectin. BMC Microbiol 11:. https://doi.org/10.1186/1471-2180-11-129
- Fraga TR, Courrol DDS, Castiblanco-Valencia MM, et al (2014) Immune evasion by pathogenic Leptospira strains: The secretion of proteases that directly cleave complement proteins. J Infect Dis 209:876–886. https://doi.org/10.1093/infdis/jit569
- Fraga TR, Isaac L, Barbosa AS (2016) Complement evasion by pathogenic Leptospira. Front Immunol 7:1–7. https://doi.org/10.3389/fimmu.2016.00623
- Garba Bashiru & Abdul Rani Bahaman (2018) Advances & challenges in leptospiral vaccine development. Indian J Med Res 15–22. https://doi.org/10.4103/ijmr.IJMR\_1022\_16
- Garcia-Nieto RM, Rico-Mata R, Arias-Negrete S, Avila EE (2008) Degradation of human secretory IgA1 and IgA2 by Entamoeba histolytica surface-associated proteolytic activity. Parasitol Int 57:417–423. https://doi.org/10.1016/j.parint.2008.04.013
- Garcia-Orozco KD, Cinco-Moroyoqui F, Angulo-Sanchez LT, et al (2019) Biochemical characterization of a novel α/β-hydrolase/FSH from the white shrimp Litopenaeus vannamei. Biomolecules 9:674. https://doi.org/10.3390/biom9110674
- Garg A, Gupta D (2008) VirulentPred: A SVM based prediction method for virulent proteins in bacterial pathogens. BMC Bioinformatics 9:1–12. https://doi.org/10.1186/1471-2105-9-62
- Goarant C (2016) Leptospirosis: risk factors and management challenges in developing countries. Res Rep Trop Med Volume 7:49–62. https://doi.org/10.2147/rrtm.s102543

- Guedes IB, Souza GO de, Castro JF de P, et al (2022) Improvement of the enrichment used in the EMJH medium (Ellinghausen–McCullough–Johnson–Harris) for the cultivation of Leptospira spp. Rev Argent Microbiol 54:95–99. https://doi.org/10.1016/j.ram.2021.03.002
- Guerrier G, D'Ortenzio E (2013) The Jarisch-Herxheimer Reaction in Leptospirosis: A Systematic Review. PLoS One 8:. https://doi.org/10.1371/journal.pone.0059266
- Guex N, Peitsch MC (1997) SWISS-MODEL and the Swiss-PdbViewer: An environment for comparative protein modeling. Electrophoresis 18:2714–2723. https://doi.org/10.1002/elps.1150181505
- Gutiérrez-Domínguez DE, Chí-Manzanero B, Rodríguez-Argüello MM, et al (2022)

  Identification of a Novel Lipase with AHSMG Pentapeptide in Hypocreales and

  Glomerellales Filamentous Fungi. Int J Mol Sci 23:.

  https://doi.org/10.3390/ijms23169367
- Haake DA (2015) Leptospirosis in humans
- Haake DA, Matsunaga J (2021) Leptospiral Immunoglobulin-Like Domain Proteins: Roles in Virulence and Immunity. Front Immunol 11:1–21. https://doi.org/10.3389/fimmu.2020.579907
- Hawkins T, Luban S, Kihara D (2006) Enhanced automated function prediction using distantly related sequences and contextual association by PFP. Protein Sci 15:1550–1556. https://doi.org/10.1110/ps.062153506
- Heck LW, Alarcon PG, Kulhavy RM, et al (1990) Degradation of IgA proteins by Pseudomonas aeruginosa elastase. J Immunol 144:2253–2257. https://doi.org/10.4049/jimmunol.144.6.2253

- Hofmeyer T, Schmelz S, Degiacomi MT, et al (2013) Arranged sevenfold: Structural insights into the C-terminal oligomerization domain of human C4b-binding protein. J Mol Biol 425:1302–1317. https://doi.org/10.1016/j.jmb.2012.12.017
- Hoke DE, Egan S, Cullen PA, Adler B (2008) LipL32 is an extracellular matrix-interacting protein of Leptospira spp. and Pseudoalteromonas tunicata. Infect Immun 76:2063–2069. https://doi.org/10.1128/IAI.01643-07
- Holm L (2022) Dali server: structural unification of protein families. Nucleic Acids Res 50:W210–W215. https://doi.org/10.1093/nar/gkac387
- Holmquist M (2005) Alpha Beta-Hydrolase Fold Enzymes Structures, Functions and Mechanisms. Curr Protein Pept Sci 1:209–235. https://doi.org/10.2174/1389203003381405
- Hornsby RL, Alt DP, Nally JE (2020) Isolation and propagation of leptospires at 37 °C directly from the mammalian host. Sci Rep 10:9620. https://doi.org/10.1038/s41598-020-66526-4
- Hotelier T, Renault L, Cousin X, et al (2004) ESTHER, the database of the α/β-hydrolase fold superfamily of proteins. Nucleic Acids Res 32:145–147. https://doi.org/10.1093/nar/gkh141
- Izurieta R, Galwankar S, Clem A (2008) Leptospirosis: The "mysterious" mimic. J Emerg

  Trauma Shock 1(1):21–33. https://doi.org/10.4103/0974-2700.40573
- Jan AT (2017) Outer Membrane Vesicles (OMVs) of gram-negative bacteria: A perspective update. Front Microbiol 8:1–11. https://doi.org/10.3389/fmicb.2017.01053
- Javed S, Azeem F, Hussain S, et al (2018) Bacterial lipases: A review on purification and characterization. Prog Biophys Mol Biol 132:23–34.

- https://doi.org/10.1016/j.pbiomolbio.2017.07.014
- Jeong H, Barbe V, Lee CH, et al (2009) Genome Sequences of Escherichia coli B strains REL606 and BL21(DE3). J Mol Biol 394:644–652. https://doi.org/10.1016/j.jmb.2009.09.052
- Jia R, Hu Y, Liu L, et al (2013) Enhancing catalytic performance of porcine pancreatic lipase by covalent modification using functional ionic liquids. ACS Catal 3:1976–1983. https://doi.org/10.1021/cs400404f
- Johnson G (2016) The α/β Hydrolase Fold Proteins of Mycobacterium tuberculosis, with Reference to their Contribution to Virulence. Curr Protein Pept Sci 18:190–210. https://doi.org/10.2174/1389203717666160729093515
- Jon T. Skare BLG (2020) Complement Evasion by Lyme Disease Spirochetes. Trends Microbiol 889–899. https://doi.org/10.1016/j.tim.2020.05.004.
- Jones DT, Taylor WR, Thornton JM (1992) The rapid generation of mutation data matrices from protein sequences. Bioinformatics 8:275–282. https://doi.org/10.1093/bioinformatics/8.3.275
- Jumper J, Evans R, Pritzel A, et al (2021) Highly accurate protein structure prediction with AlphaFold. Nature 596:583–589. https://doi.org/10.1038/s41586-021-03819-2
- Juncker AS, Willenbrock H, von Heijne G, et al (2003) Prediction of lipoprotein signal peptides in Gram-negative bacteria. Protein Sci 12:1652–1662. https://doi.org/10.1110/ps.0303703
- Kanjanavas P, Khuchareontaworn S, Khawsak P, et al (2010) Purification and characterization of organic solvent and detergent tolerant lipase from thermotolerant Bacillus sp. RN2. Int J Mol Sci 11:3783–3792. https://doi.org/10.3390/ijms11103783
- Karpagam KB, Ganesh B (2020) Leptospirosis: a neglected tropical zoonotic infection of

- public health importance—an updated review. Eur J Clin Microbiol Infect Dis 39:835—846. https://doi.org/10.1007/s10096-019-03797-4
- Kitadokoro K, Tanaka M, Hikima T, et al (2020) Crystal structure of pathogenic Staphylococcus aureus lipase complex with the anti-obesity drug orlistat. Sci Rep 10:3–7. https://doi.org/10.1038/s41598-020-62427-8
- Ko AI, Goarant C, Picardeau M (2009a) Leptospira: The dawn of the molecular genetics era for an emerging zoonotic pathogen. Nat Rev Microbiol 7:736–747. https://doi.org/10.1038/nrmicro2208
- Ko AI, Goarant C, Picardeau M (2009b) Leptospira: The dawn of the molecular genetics era for an emerging zoonotic pathogen. Nat Rev Microbiol 7:736–747. https://doi.org/10.1038/nrmicro2208
- Koebnik R, Locher KP, Van Gelder P (2000) Structure and function of bacterial outer membrane proteins: Barrels in a nutshell. Mol Microbiol 37:239–253. https://doi.org/10.1046/j.1365-2958.2000.01983.x
- Kopp A, Hebecker M, Svobodová E, Józsi M (2012) Factor H: A complement regulator in health and disease, and a mediator of cellular interactions. Biomolecules 2:46–75. https://doi.org/10.3390/biom2010046
- Kourist R, Jochens H, Bartsch S, et al (2010) The α/β-hydrolase fold 3DM database (ABHDB) as a tool for protein engineering. ChemBioChem 11:1635–1643. https://doi.org/10.1002/cbic.201000213
- Kozakov D, Hall DR, Xia B, et al (2017) The ClusPro web server for protein-protein docking.

  Nat Protoc 12:255–278. https://doi.org/10.1038/nprot.2016.169
- Kumar P, Chang YF, Akif M (2022a) Characterization of novel nuclease and protease activities

- among Leptospiral immunoglobulin-like proteins. Arch Biochem Biophys 727:109349. https://doi.org/10.1016/j.abb.2022.109349
- Kumar P, Chang YF, Akif M (2022b) Characterization of novel nuclease and protease activities among Leptospiral immunoglobulin-like proteins. Arch Biochem Biophys 727:109349. https://doi.org/10.1016/j.abb.2022.109349
- Kumar P, Chang YF, Akif M (2022c) Characterization of novel nuclease and protease activities among Leptospiral immunoglobulin-like proteins. Arch Biochem Biophys 727:109349. https://doi.org/10.1016/j.abb.2022.109349
- Kumar P, Lata S, Shankar UN, Akif M (2021) Immunoinformatics-Based Designing of a Multi-Epitope Chimeric Vaccine From Multi-Domain Outer Surface Antigens of Leptospira. Front Immunol 12:1–14. https://doi.org/10.3389/fimmu.2021.735373
- Kumari A, Gupta R (2015) Functional Characterisation of Novel Enantioselective Lipase TALipA from Trichosporon asahii MSR54: Sequence Comparison Revealed New Signature Sequence AXSXG Among Yeast Lipases. Appl Biochem Biotechnol 175:360–371. https://doi.org/10.1007/s12010-014-1268-5
- Kyriakidis I, Samara P, Papa A (2011) Serum TNF-α, sTNFR1, IL-6, IL-8 and IL-10 levels in Weil's syndrome. Cytokine 54:117–120. https://doi.org/10.1016/j.cyto.2011.01.014
- Laarman AJ, Ruyken M, Malone CL, et al (2011) Staphylococcus aureus Metalloprotease

  Aureolysin Cleaves Complement C3 To Mediate Immune Evasion . J Immunol 186:6445–6453. https://doi.org/10.4049/jimmunol.1002948
- Laskowski RA, Jabłońska J, Pravda L, et al (2018) PDBsum: Structural summaries of PDB entries. Protein Sci 27:129–134. https://doi.org/10.1002/pro.3289
- Laskowski RA, MacArthur MW, Moss DS, Thornton JM (1993) PROCHECK: a program to

- check the stereochemical quality of protein structures. J Appl Crystallogr 26:283–291. https://doi.org/10.1107/s0021889892009944
- Laumen K, Schneider MP (1988) A Highly Selective Ester Hydrolase from. J Chem Soc Chem Commun 598–600. https://doi.org/DOI https://doi.org/10.1039/C39880000598
- Lee SH, Kim S, Park SC, Kim MJ (2002) Cytotoxic activities of Leptospira interrogans hemolysin SphH as a pore-forming protein on mammalian cells. Infect Immun 70:315–322. https://doi.org/10.1128/IAI.70.1.315-322.2002
- Lehmann JS, Matthias MA, Vinetz JM, Fouts DE (2014) Leptospiral pathogenomics. Pathogens 3:280–308. https://doi.org/10.3390/pathogens3020280
- Letunic I, Khedkar S, Bork P (2021) SMART: Recent updates, new developments and status in 2020. Nucleic Acids Res 49:D458–D460. https://doi.org/10.1093/nar/gkaa937
- Li S, Ojcius DM, Liao S, et al (2010) Replication or death: Distinct fates of pathogenic Leptospira strain Lai within macrophages of human or mouse origin. Innate Immun 16:80–92. https://doi.org/10.1177/1753425909105580
- Lin YP, Raman R, Sharma Y, Chang YF (2008) Calcium binds to leptospiral immunoglobulin-like protein, LigB, and modulates fibronectin binding. J Biol Chem 283:25140–25149. https://doi.org/10.1074/jbc.M801350200
- Lu M, Tian X, Zhang Y, et al (2021) Protection studies of an excretory–secretory protein HcABHD against Haemonchus contortus infection. Vet Res 52:1–16. https://doi.org/10.1186/s13567-020-00871-0
- M. Kim CT (2004) Outer membrane protein A and OprF Versatile roles in Gram- negative bacterial infections. Brain Lang 88:1–20. https://doi.org/10.1111/j.1742-4658.2012.08482.x.Outer

- Maia MAC, Bettin EB, Barbosa LN, et al (2022) Challenges for the development of a universal vaccine against leptospirosis revealed by the evaluation of 22 vaccine candidates. Front Cell Infect Microbiol 12:1–18. https://doi.org/10.3389/fcimb.2022.940966
- Marques MS, Costa AC, Osório H, et al (2021) Helicobacter pylori PqqE is a new virulence factor that cleaves junctional adhesion molecule A and disrupts gastric epithelial integrity.

  Gut Microbes 13:1–21. https://doi.org/10.1080/19490976.2021.1921928
- Matsunaga J, Sanchez Y, Xu X, Haake DA (2005) Osmolarity, a key environmental signal controlling expression of leptospiral proteins LigA and LigB and the extracellular release of LigA. Infect Immun 73:70–78. https://doi.org/10.1128/IAI.73.1.70-78.2005
- Matsunaga J, Schlax PJ, Haake DA (2013) Role for cis-Acting RNA sequences in the temperature-dependent expression of the multiadhesive lig proteins in Leptospira interrogans. J Bacteriol 195:5092–5101. https://doi.org/10.1128/JB.00663-13
- MB T, AF T, ALTO N (2021) The leptospiral LipL21 and LipL41 proteins exhibit a broad spectrum of interactions with host cell components. Virulence 12:2798–2813. https://doi.org/10.1080/21505594.2021.1993427
- Mcarthur DB (2019) Since January 2020 Elsevier has created a COVID-19 resource centre with free information in English and Mandarin on the novel coronavirus COVID-19. The COVID-19 resource centre is hosted on Elsevier Connect, the company's public news and information. Nurs Clin N Am 54:297–311
- McGuffin LJ, Bryson K, Jones DT (2000) The PSIPRED protein structure prediction server.

  Bioinformatics 16:404–405. https://doi.org/10.1093/bioinformatics/16.4.404
- Meganathan Y, Vishwakarma A, Ramya M (2022) Biofilm formation and social interaction of Leptospira in natural and artificial environments. Res Microbiol 173:.

- https://doi.org/10.1016/j.resmic.2022.103981
- Mei GY, Yan XX, Turak A, et al (2010) AidH, an alpha/beta-hydrolase fold family member from an ochrobactrum sp. strain, Is a novel N-acylhomoserine lactonase. Appl Environ Microbiol 76:4933–4942. https://doi.org/10.1128/AEM.00477-10
- Melais N, Aribi-Zouioueche L, Riant O (2016) Effet de la structure du groupe partant sur l'énantiosélectivité des lipases lors de la résolution cinétique du 1-phényl éthanol. Comptes Rendus Chim 19:971–977. https://doi.org/10.1016/j.crci.2016.05.002
- Melican K, Sandoval RM, Kader A, et al (2011) Uropathogenic escherichia coli P and type 1 fimbriae act in synergy in a living host to facilitate renal colonization leading to nephron obstruction. PLoS Pathog 7:2–13. https://doi.org/10.1371/journal.ppat.1001298
- Merabet-Khelassi M, Houiene Z, Aribi-Zouioueche L, Riant O (2012) Green methodology for enzymatic hydrolysis of acetates in non-aqueous media via carbonate salts. Tetrahedron Asymmetry 23:828–833. https://doi.org/10.1016/j.tetasy.2012.06.001
- Meri T, Murgia R, Stefanel P, et al (2005) Regulation of complement activation at the C3-level by serum resistant leptospires. Microb Pathog 39:139–147. https://doi.org/10.1016/j.micpath.2005.07.003
- Michal Potempa\*,†, Jan Potempa†,‡, Marcin Okroj\*, Katarzyna Popadiak\*,† SE, Ky-Anh Nguyen¶, Kristian Riesbeck∫ and AMB (2008) Binding of complement inhibitor C4b-binding protein contributes to serum resistance of Porphyromonas gingivalis. J Immunol 181:5537–5544. https://doi.org/https://doi.org/10.4049/jimmunol.181.8.5537
- Mikulski M, Boisier P, Lacassin F, et al (2015) Severity markers in severe leptospirosis: a cohort study. Eur J Clin Microbiol Infect Dis 34:687–695. https://doi.org/10.1007/s10096-014-2275-8

- Mishra M, Ressler A, Schlesinger LS, Wozniak DJ (2015) Identification of OprF as a complement component C3 binding acceptor molecule on the surface of Pseudomonas aeruginosa. Infect Immun 83:3006–3014. https://doi.org/10.1128/IAI.00081-15
- Miyoshi S (2013) Extracellular proteolytic enzymes produced by human pathogenic vibrio species. Front Microbiol 4:1–8. https://doi.org/10.3389/fmicb.2013.00339
- Mohammed H, Nozha C, Hakim K, Abdelaziz F (2011) LEPTOSPIRA: Morphology, Classification and Pathogenesis. J Bacteriol Parasitol 02:6–9. https://doi.org/10.4172/2155-9597.1000120
- Moore SR, Menon SS, Cortes C, Ferreira VP (2021) Hijacking Factor H for Complement Immune Evasion. Front Immunol 12:1–23. https://doi.org/10.3389/fimmu.2021.602277
- Moulin P, Rong V, Ribeiro Silva A, et al (2019) Defining the role of the Streptococcus agalactiae Sht-family proteins in zinc acquisition and complement evasion. J Bacteriol 201:1–16. https://doi.org/10.1128/JB.00757-18
- Myung-Hee KIM, Hyung-Kwoun KIM, Jung-Kee LEE, Sun-Yang PARK T-KO (2000)

  Thermostable Lipase of Bacillus stearothermophilus: High-level Production, Purification, and Calcium-dependent Thermostability. Biosci Biotechnol Biochem 64:280–286. https://doi.org/https://doi.org/10.1271/bbb.64.280
- Nahori M-A, Fournié-Amazouz E, Que-Gewirth NS, et al (2005) Differential TLR Recognition of Leptospiral Lipid A and Lipopolysaccharide in Murine and Human Cells. J Immunol 175:6022–6031. https://doi.org/10.4049/jimmunol.175.9.6022
- Nardini M, Dijkstra BW (1999) α/β hydrolase fold enzymes: The family keeps growing. Curr Opin Struct Biol 9:732–737. https://doi.org/10.1016/S0959-440X(99)00037-8
- Nguyen L, Chimunda T (2023) Neuro-leptospirosis A batty diagnostic enigma. IDCases

- 32:e01731. https://doi.org/10.1016/j.idcr.2023.e01731
- Nielsen H, Engelbrecht J (1997) Identification of prokaryotic and eukaryotic signal peptides and prediction of their cleavage sites Artificial neural networks have been used for many biological. Protein Eng 10:1–6. https://doi.org/10.1142/S0129065797000537
- Norma J. Greenfield (2009) Using circular dichroism collected as a funcion of temperature to determine the thermodynamics of protein unfolding and binding interactions. Nat Protoc 1:2527–2535. https://doi.org/10.1038/nprot.2006.204.Using
- Palaniappan RUM, Ramanujam S, Chang YF (2007) Leptospirosis: Pathogenesis, immunity, and diagnosis. Curr Opin Infect Dis 20:284–292. https://doi.org/10.1097/QCO.0b013e32814a5729
- Park BS, Lee JO (2013) Recognition of lipopolysaccharide pattern by TLR4 complexes. Exp Mol Med 45:. https://doi.org/10.1038/emm.2013.97
- Perz V, Baumschlager A, Bleymaier K, et al (2016) Hydrolysis of Synthetic Polyesters by Clostridium botulinum Esterases. Biotechnol Bioeng 113:1024–34. https://doi.org/10.1002/bit.25874
- Pete Chandrangsu1, Christopher Rensing2,3,4 and JDH (2017) Metal Homeostasis and Resistance in Bacteria. Nat Rev Microbiol 15:338–350. https://doi.org/doi:10.1038/nrmicro.2017.15.
- Picardeau M (2017) Virulence of the zoonotic agent of leptospirosis: Still terra incognita? Nat Rev Microbiol 15:297–307. https://doi.org/10.1038/nrmicro.2017.5
- Pietrocola G, Nobile G, Rindi S, Speziale P (2017) Staphylococcus aureus manipulates innate immunity through own and host-expressed proteases. Front Cell Infect Microbiol 7:1–15. https://doi.org/10.3389/fcimb.2017.00166

- Punta M, Coggill PC, Eberhardt RY, et al (2012) The Pfam protein families database. Nucleic Acids Res 40:290–301. https://doi.org/10.1093/nar/gkr1065
- Putz EJ, Nally JE (2020) Investigating the Immunological and Biological Equilibrium of Reservoir Hosts and Pathogenic Leptospira: Balancing the Solution to an Acute Problem? Front Microbiol 11:. https://doi.org/10.3389/fmicb.2020.02005
- Raja V, Natarajaseenivasan K (2015) Pathogenic, diagnostic and vaccine potential of leptospiral outer membrane proteins (OMPs). Crit Rev Microbiol 41:1–17. https://doi.org/10.3109/1040841X.2013.787387
- Raman R, Rajanikanth V, Palaniappan RUM, et al (2010) Big domains are novel Ca2+-binding modules: Evidences from big domains of Leptospira immunoglobulin-like (Lig) proteins. PLoS One 5:. https://doi.org/10.1371/journal.pone.0014377
- Rana A, Rub A, Akhter Y (2014) Proteome-scale identification of outer membrane proteins in Mycobacterium avium subspecies paratuberculosis using a structure based combined hierarchical approach. Mol Biosyst 10:2329–2337. https://doi.org/10.1039/c4mb00234b
- Rao L, Xue Y, Zhou C, et al (2011) A thermostable esterase from Thermoanaerobacter tengcongensis opening up a new family of bacterial lipolytic enzymes. Biochim Biophys
   Acta Proteins Proteomics 1814:1695–1702.
   https://doi.org/10.1016/j.bbapap.2011.08.013
- Reis EAG, Hagan JE, Ribeiro GS, et al (2013) Cytokine Response Signatures in Disease Progression and Development of Severe Clinical Outcomes for Leptospirosis. PLoS Negl Trop Dis 7:1–7. https://doi.org/10.1371/journal.pntd.0002457
- Ripoche J, Day AJ, Harris TJR, Sim RB (1988) The complete amino acid sequence of human complement factor H. Biochem J 249:593–602. https://doi.org/10.1042/bj2490593

- Rizvi M, Azam M, Sultan A, et al (2014) Original Article Role of IL-8 , IL-10 and TNF-  $\alpha$  level in pathogenesis of leptospiral acute hepatitis syndrome. Ann Pathol Lab Med 1:A10–A17
- Robert X, Gouet P (2014) Deciphering key features in protein structures with the new ENDscript server. Nucleic Acids Res 42:320–324. https://doi.org/10.1093/nar/gku316
- Rodriguez De Cordoba S, Esparza-Gordillo J, Goicoechea De Jorge E, et al (2004) The human complement factor H: Functional roles, genetic variations and disease associations. Mol Immunol 41:355–367. https://doi.org/10.1016/j.molimm.2004.02.005
- Rydel TJ, Williams JM, Krieger E, et al (2003) The crystal structure, mutagenesis, and activity studies reveal that patatin is a lipid acyl hydrolase with a Ser-Asp catalytic dyad. Biochemistry 42:6696–6708. https://doi.org/10.1021/bi027156r
- Saha S, Raghava GPS (2006) AlgPred: Prediction of allergenic proteins and mapping of IgE epitopes. Nucleic Acids Res 34:202–209. https://doi.org/10.1093/nar/gkl343
- Saha S, Raghava GPS (2007) BTXpred: Prediction of bacterial toxins. In Silico Biol 7:405–412
- Sambasiva RR (2003) Leptospirosis in India and the Rest of the World. Brazilian J Infect Dis 178–193. https://doi.org/10.1590/s1413-86702003000300003.
- Samrot A V., Sean TC, Bhavya KS, et al (2021) Leptospiral infection, pathogenesis and its diagnosis—a review. Pathogens 10:1–30. https://doi.org/10.3390/pathogens10020145
- Santos JC, Handa S, Fernandes LGV, et al (2023) Structural and biochemical characterization of Leptospira interrogans Lsa45 reveals a penicillin-binding protein with esterase activity.

  Process Biochem 125:141–153. https://doi.org/10.1016/j.procbio.2022.12.010
- Sato H, Frank DW, Hillard CJ, et al (2003) The mechanism of action of the Pseudomonas

- aeruginosa-encoded type III cytotoxin, ExoU. EMBO J 22:2959–2969. https://doi.org/10.1093/emboj/cdg290
- Schmidt-Dannert C, Rúa ML, Atomi H, Schmid RD (1996) Thermoalkalophilic lipase of Bacillus thermocatenulatus. I. Molecular cloning, nucleotide sequence, purification and some properties. Biochim Biophys Acta Lipids Lipid Metab 1301:105–114. https://doi.org/10.1016/0005-2760(96)00027-6
- Sethi S, Sharma N, Kakkar N, et al (2010) Increasing trends of leptospirosis in Northern India:

  A clinico-epidemiological study. PLoS Negl Trop Dis 4:1–7.

  https://doi.org/10.1371/journal.pntd.0000579
- Sharma S, Bhatnagar R, Gaur D (2020) Complement Evasion Strategies of Human Pathogenic Bacteria. Indian J Microbiol 60:283–296. https://doi.org/10.1007/s12088-020-00872-9
- Shearer J, Jefferies D, Khalid S (2019) Outer Membrane Proteins OmpA, FhuA, OmpF, EstA, BtuB, and OmpX Have Unique Lipopolysaccharide Fingerprints. J Chem Theory Comput 15:2608–2619. https://doi.org/10.1021/acs.jctc.8b01059
- Shen K, Bargmann CI (2003) The immunoglobulin superfamily protein SYG-1 determines the location of specific synapses in C. elegans. Cell 112:619–630. https://doi.org/10.1016/S0092-8674(03)00113-2
- Shin W-H, Lee GR, Heo L, et al (2014) Prediction of Protein Structure and Interaction by GALAXY Protein Modeling Programs. Bio Des 2:01–11
- Sievers F, Wilm A, Dineen D, et al (2011) Fast, scalable generation of high-quality protein multiple sequence alignments using Clustal Omega. Mol Syst Biol 7:. https://doi.org/10.1038/msb.2011.75
- Sorokin L (2010) The impact of the extracellular matrix on inflammation. Nat Rev Immunol

- 10:712–723. https://doi.org/10.1038/nri2852
- Steffen Moller, Michael D. R. Croning RA (2001) Evaluation ofmethods for the prediction of membrane spanning regions. Bioinformatics 17:646–653. https://doi.org/https://doi.org/10.1093/bioinformatics/18.1.218
- Stevenson B, Choy HA, Pinne M, et al (2007) Leptospira interrogans endostatin-like outer membrane proteins bind host fibronectin, laminin and regulators of complement. PLoS One 2:. https://doi.org/10.1371/journal.pone.0001188
- Suan CL, Sarmidi MR (2004) Immobilised lipase-catalysed resolution of (R,S)-1-phenylethanol in recirculated packed bed reactor. J Mol Catal B Enzym 28:111–119. https://doi.org/10.1016/j.molcatb.2004.02.004
- Suminda GGD, Bhandari S, Won Y, et al (2022) High-throughput sequencing technologies in the detection of livestock pathogens, diagnosis, and zoonotic surveillance. Comput Struct Biotechnol J 20:5378–5392. https://doi.org/10.1016/j.csbj.2022.09.028
- Syed M. Faisal, Sean P. McDonough and Y-FC (2012) Leptospira: Invasion, Pathogenesis and Persistence. Pathog Spirochetes Strateg Evas Host Immun Persistence 1–265. https://doi.org/10.1007/978-1-4614-5404-5
- Takahashi MB, Teixeira AF, Nascimento ALTO (2022) Host Cell Binding Mediated by Leptospira interrogans Adhesins. Int J Mol Sci 23:. https://doi.org/10.3390/ijms232415550
- Tamura K, Stecher G, Kumar S (2021) MEGA11: Molecular Evolutionary Genetics Analysis

  Version 11. Mol Biol Evol 38:3022–3027. https://doi.org/10.1093/molbev/msab120
- Tanaka M, Kamitani S, Kitadokoro K (2018) Staphylococcus aureus lipase: Purification, kinetic characterization, crystallization and crystallographic study. Acta Crystallogr Sect

- F Struct Biol Commun 74:567–570. https://doi.org/10.1107/S2053230X18010506
- Taylor RG, Walker DC, McInnes RR (1993) E.coli host strains. Nucleic Acids Res 21:1677–1678
- Thibeaux R, Geroult S, Benezech C, et al (2017) Seeking the environmental source of Leptospirosis reveals durable bacterial viability in river soils. PLoS Negl Trop Dis 11:1–14. https://doi.org/10.1371/journal.pntd.0005414
- Thomas DD, Higbie LM (1990) In vitro association of leptospires with host cells. Infect Immun 58:581–585. https://doi.org/10.1128/iai.58.3.581-585.1990
- Tiesinga JJW, Pouderoyen G Van, Nardini M, et al (2007) Structural Basis of Phospholipase

  Activity of Staphylococcus hyicus lipase. 8530:447–456.

  https://doi.org/10.1016/j.jmb.2007.05.041
- Tokmakov AA, Kurotani A, Sato KI (2021) Protein pI and Intracellular Localization. Front Mol Biosci 8:1–6. https://doi.org/10.3389/fmolb.2021.775736
- Toma C, Okura N, Takayama C, Suzuki T (2011) Characteristic features of intracellular pathogenic Leptospira in infected murine macrophages. Cell Microbiol 13:1783–1792. https://doi.org/10.1111/j.1462-5822.2011.01660.x
- Tomlin H, Piccinini AM (2018) A complex interplay between the extracellular matrix and the innate immune response to microbial pathogens. Immunology 155:186–201. https://doi.org/10.1111/imm.12972
- Torgerson PR, Hagan JE, Costa F, et al (2015) Global Burden of Leptospirosis: Estimated in Terms of Disability Adjusted Life Years. PLoS Negl Trop Dis 9:1–14. https://doi.org/10.1371/journal.pntd.0004122
- Trott O, Olson AJ (2009) AutoDock Vina: Improving the speed and accuracy of docking with

- a new scoring function, efficient optimization, and multithreading. J Comput Chem 31:NA-NA. https://doi.org/10.1002/jcc.21334
- Varghese PM, Murugaiah V, Beirag N, et al (2021) C4b Binding Protein Acts as an Innate Immune Effector Against Influenza A Virus. Front Immunol 11:1–14. https://doi.org/10.3389/fimmu.2020.585361
- Velasco-Lozano S, López-Gallego F, Rocha-Martin J, et al (2016) Improving enantioselectivity of lipase from Candida rugosa by carrier-bound and carrier-free immobilization. J Mol Catal B Enzym 130:32–39. https://doi.org/10.1016/j.molcatb.2016.04.006
- Verma A, Hellwage J, Artiushin S, et al (2006) LfhA, a novel factor H-binding protein of Leptospira interrogans. Infect Immun 74:2659–2666. https://doi.org/10.1128/IAI.74.5.2659-2666.2006
- Vieira ML, Fernandes LG, Domingos RF, et al (2014) Leptospiral extracellular matrix adhesins as mediators of pathogen-host interactions. FEMS Microbiol Lett 352:129–139. https://doi.org/10.1111/1574-6968.12349
- Vieira ML, Teixeira AF, Pidde G, et al (2018) Leptospira interrogans outer membrane protein lipl21 is a potent inhibitor of neutrophil myeloperoxidase. Virulence 9:414–425. https://doi.org/10.1080/21505594.2017.1407484
- Vieira1 ML, , Luis G. Fernandes1, 2, Renan F. Domingos1, 2, Rosane Oliveira1 2, Gabriela H.
  Siqueira1, 2, Natalie M. Souza1, 2, Aline R.F. Teixeira1, 2 MVA, & Ana L.T.O.
  Nascimento1 2 (2013) Leptospiral extracellular matrix adhesins as mediators of pathogen–host interactions. 129–139
- Volkamer A, Kuhn D, Rippmann F, Rarey M (2012) Dogsitescorer: A web server for automatic

- binding site prediction, analysis and druggability assessment. Bioinformatics 28:2074–2075. https://doi.org/10.1093/bioinformatics/bts310
- Volz MS, Moos V, Allers K, et al (2015) Specific CD4 T-cell reactivity and cytokine release in different clinical presentations of leptospirosis. Clin Vaccine Immunol 22:1276–1284. https://doi.org/10.1128/CVI.00397-15
- Wang H, Wu Y, Ojcius DM, et al (2012) Leptospiral hemolysins induce proinflammatory cytokines through toll-like receptor 2-and 4-mediated JNK and NF-κB signaling pathways. PLoS One 7:. https://doi.org/10.1371/journal.pone.0042266
- Whitmore L, Wallace BA (2008) Protein secondary structure analyses from circular dichroism spectroscopy: Methods and reference databases. Biopolymers 89:392–400. https://doi.org/10.1002/bip.20853
- Wiederstein M, Sippl MJ (2007) ProSA-web: Interactive web service for the recognition of errors in three-dimensional structures of proteins. Nucleic Acids Res 35:407–410. https://doi.org/10.1093/nar/gkm290
- Witchell TD, Eshghi A, Nally JE, et al (2014) Post-translational Modification of LipL32 during

  Leptospira interrogans Infection. PLoS Negl Trop Dis 8:.

  https://doi.org/10.1371/journal.pntd.0003280
- Wolff DG, Castiblanco-Valencia MM, Abe CM, et al (2013) Interaction of Leptospira elongation factor Tu with plasminogen and complement factor H: A metabolic leptospiral protein with moonlighting activities. PLoS One 8:1–10. https://doi.org/10.1371/journal.pone.0081818
- Xing S, Zhu R, Cheng K, et al (2021) Gene Expression, Biochemical Characterization of a sn-1, 3 Extracellular Lipase From Aspergillus niger GZUF36 and Its Model-Structure

- Analysis. Front Microbiol 12:1–16. https://doi.org/10.3389/fmicb.2021.633489
- Yan W, Faisal SM, McDonough SP, et al (2009) Immunogenicity and protective efficacy of recombinant Leptospira immunoglobulin-like protein B (rLigB) in a hamster challenge model. Microbes Infect 11:230–237. https://doi.org/10.1016/j.micinf.2008.11.008
- Yang J, Sun J, Yan Y (2010) lip2, a novel lipase gene cloned from Aspergillus niger exhibits enzymatic characteristics distinct from its previously identified family member. Biotechnol Lett 32:951–956. https://doi.org/10.1007/s10529-010-0238-4
- Yang J, Zhang B, Yan Y (2009) Cloning and expression of pseudomonas fluorescens 26-2 lipase gene in pichia pastoris and characterizing for transesterification. Appl Biochem Biotechnol 159:355–365. https://doi.org/10.1007/s12010-008-8419-5
- Yang W, He Y, Xu L, et al (2016) A new extracellular thermo-solvent-stable lipase from Burkholderia ubonensis SL-4: Identification, characterization and application for biodiesel production. J Mol Catal B Enzym 126:76–89. https://doi.org/10.1016/j.molcatb.2016.02.005
- Yao W, Liu K, Liu H, et al (2021) A Valuable Product of Microbial Cell Factories: Microbial Lipase. Front Microbiol 12:1–16. https://doi.org/10.3389/fmicb.2021.743377
- Yu C-S, Lin C-J, Hwang J-K (2004) Predicting subcellular localization of proteins for Gramnegative bacteria by support vector machines based on n -peptide compositions . Protein Sci 13:1402–1406. https://doi.org/10.1110/ps.03479604
- Zaïdi A, Merabet-Khelassi M, Aribi-Zouioueche L (2015) CAL-B-Catalyzed Enantioselective Deacetylation of Some Benzylic Acetate Derivatives Via Alcoholysis in Non-aqueous Media. Catal Letters 145:1054–1061. https://doi.org/10.1007/s10562-014-1470-7
- Zarafeta D, Moschidi D, Ladoukakis E, et al (2016) Metagenomic mining for thermostable

esterolytic enzymes uncovers a new family of bacterial esterases. Sci Rep 6:1–16. https://doi.org/10.1038/srep38886

Zhu H, Liu M, Sumby P, Lei B (2009) The secreted esterase of group A Streptococcus is important for invasive skin infection and dissemination in mice. Infect Immun 77:5225–5232. https://doi.org/10.1128/IAI.00636-09



**Appendix Table 1.**List of Uniport IDs potent outer membrane and secretory proteins

S. No.	Potent OM proteins	Potent secretory proteins (classical pathway)	Potent secretory proteins (Non classical pathway)
1	Q72SP8	Q72Q25	Q72T34
2	Q72P44	Q72R35	Q72MV3
3	Q72NZ7	Q72U34	Q72U35
4	Q72SC6	Q72N52	Q72RA2
5	Q72NF0	Q72VS2	Q72NE0
6	Q72UW3	Q72Q84	Q72P75
7	Q72N40	Q72U36	Q72VQ6
8	Q72N36	Q72N53	Q72LT3
9	Q72QW7	Q72V06	Q72M37
10	Q72T11	Q72P45	Q72TJ2
11	Q72SL3	Q72TZ4	Q72TM0
12	Q72TF3	Q72V40	Q72R13
13	Q72UF4	Q72VD0	Q72PI4
14	Q72SV8	Q72W52	Q72P32
15	Q72PV3	Q72U33	Q72P74
16	Q72MB8	Q72M98	Q75FB8
17	Q72SC1	Q72RS6	Q72SG0
18	Q72LW4	Q72Q54	Q72QR2
19	Q75G15	Q72W18	Q72QK1
20	Q72RQ0	Q72VC9	Q72LZ3
21	Q72U49	Q72Q00	Q72T33
22	Q72U40	Q72TZ9	Q72UI3
23	Q75G30	Q72RY5	Q72SX6
24	Q75FH5	Q75FJ7	Q72UD4
25	Q72PJ4	Q72UE9	Q72NA6
26	Q72TA9	Q72TM2	Q72P00
27	Q72RC3	Q72LX6	Q72RV1
28	Q72P99	Q72TW2	Q72W70
29	Q72S78	Q72UY3	Q72QY9
30	Q72SF4	Q72R17	Q72TI1
31	Q72MH2	Q72NW3	Q72P94
32	Q72TA0	Q72TD3	Q72RV2
33	Q72P24	Q72Q60	Q72LX5
34	Q72SX3	Q72UL8	
35	Q75FI7	Q72TC3	

36	Q72MW3	Q72TZ6	
37	Q72RW5	Q72TE8	
38	Q72NU8	Q72SJ4	
39	Q72T42	Q72TW6	
40	Q75FM7	Q72MU1	
41	Q72TK9	Q75FN0	
42	Q72U85	Q72WC8	
43	Q72S50	Q72RP8	
44	Q72TJ3	Q72N72	
45	Q72S63	Q72N74	
46	Q72PN2	Q72UA1	
47	Q75FN8	Q72SZ5	
48	Q72RX6	Q72QA3	
49	Q72NY5	Q72TT9	
50	Q72PU3	Q72QW2	
51	Q72SE7	Q72QA4	
52	Q72S13	Q72S98	
53	Q72MW9	Q72UG2	
54	Q72PV8	Q72VC4	
55	Q72ME1	Q72UZ3	
56	Q72TG3	Q72PF3	
57	Q72VQ7	G1UB65	
58	Q72UC0	Q72SB7	
59	Q72Q15	Q72VI1	
60	Q75G03	Q72MF6	
61	Q72VH9	Q72VD2	
62	Q72P31	Q72QL4	
63	Q72W36	Q72SW8	
64	Q72VI3	Q72Q26	
65	Q75FM5	Q72M70	
66	Q72TD5	Q72MY9	
67	Q72TD4	Q72TP4	
68	Q72M28	Q72TQ4	
69	Q72VH1	Q72U83	
70	Q72SZ4	Q72NE3	
71	Q72ND6	Q72VD1	
72	Q72U07	Q72T12	
73	Q72PY0	Q72M84	
74	Q72RT0	Q72QY3	
75	Q72PH2	Q72PX8	
76	Q72V07	Q72PX7	

77	Q72N60	Q72PK7	
78	Q72M95	Q72M92	
79	Q72W35	Q72N50	
80	Q72P27	Q72MX9	
81	Q72LZ6	Q72VC8	
82	Q72TR5	Q72PF2	
83	Q72SP3	Q72Q92	
84	Q72SN4	Q72V01	
85	Q75FZ0	Q12 V 01	
86	Q72LV8		
87	Q72R97		
88	Q72VG8		
89	Q72NB4		
90	Q72QX6		
91	Q72RT7		
92	Q72P35		
93	Q72P20		
94	Q75G21		
95	Q72VF0		
96	Q72RK6		
97	Q72LS3		
98	Q72Q55		
99	Q72UL5		
100	Q72M30		
101	Q72SK2		
102	Q72SE8		
103	Q72LS4		
104	Q75FC3		
105	Q72TB0		
106	Q72TB8		
107	Q72VJ5		
108	Q72P08		
109	Q72SV4		
110	Q72VD9		
111	Q72N85		
112	Q72QZ3 Q72TJ5		
113	_ `		
114	Q72MV0		
116	Q72Q59 Q72WA3		
117	Q72WA3		
117	Q72MY4		
119	Q72R45		
120	Q72SK8		
121	Q72TQ3		
122	Q72QQ7		
144	\\\\\\\\\\\\\\\\\\\\\\\\\\\\\\\\\\\\\\		

123			
124	123	O72PA0	
125		`	
126		`	
127			
128		`	
129		`	
130   Q72UX0		`	
131   Q72S33			
132		•	
133         Q72QX0           134         Q72M25           135         Q72NU9           136         Q72VT9           137         Q72NI0           138         Q72US9           139         Q75FU4           140         Q72VN8           141         Q72NP1           142         Q75FY9           143         Q72PH1           144         Q72MF8           145         Q72PY4           146         Q72LY2           147         Q72SB6           148         Q72PW3           149         Q72M85           151         Q72SI3           152         Q75FU9           153         Q72S95           154         Q72RM7           155         Q72LS2           156         Q72PU4           157         Q72UFO           158         Q72RF2           159         Q72R06           160         Q72SR3           161         Q72Q11           162         Q72TA2           163         Q72RK7           165         Q72QU8		`	
134         Q72M25           135         Q72NU9           136         Q72VT9           137         Q72NJO           138         Q72US9           139         Q75FU4           140         Q72VN8           141         Q72NPI           142         Q75FY9           143         Q72PHI           144         Q72MF8           145         Q72PY4           146         Q72LY2           147         Q72SB6           148         Q72PW3           149         Q72MX3           150         Q72M85           151         Q72SI3           152         Q75FU9           153         Q72SP5           154         Q72RM7           155         Q72LS2           156         Q72PU4           157         Q72UF0           158         Q72RF2           159         Q72R06           160         Q72SR3           161         Q72Q11           162         Q72TA2           163         Q72RX7           165         Q72UW8           166         Q72QL3 </td <td></td> <td>_</td> <td></td>		_	
135         Q72NU9           136         Q72VT9           137         Q72NI0           138         Q72US9           139         Q75FU4           140         Q72VN8           141         Q72NP1           142         Q75FY9           143         Q72PH1           144         Q72MF8           145         Q72PY4           146         Q72LY2           147         Q72SB6           148         Q72PW3           149         Q72MX3           150         Q72M85           151         Q72SI3           152         Q75FU9           153         Q72SP5           154         Q72RM7           155         Q72LS2           156         Q72PU4           157         Q72UF0           158         Q72RF2           159         Q72R06           160         Q72SR3           161         Q72Q11           162         Q72TA2           163         Q72RX7           164         Q72QL3           167         Q72QP2		` `	
136         Q72VT9           137         Q72NJ0           138         Q72US9           139         Q75FU4           140         Q72VN8           141         Q72NP1           142         Q75FY9           143         Q72PH1           144         Q72MF8           145         Q72PY4           146         Q72LY2           147         Q72SB6           148         Q72PW3           149         Q72MX3           150         Q72M85           151         Q72SI3           152         Q75FU9           153         Q72S95           154         Q72RM7           155         Q72LS2           156         Q72PU4           157         Q72UF0           158         Q72RF2           159         Q72R06           160         Q72SR3           161         Q72Q11           162         Q72TA2           163         Q72RK7           165         Q72U8           166         Q72QL3           167         Q72QP2		`	
137         Q72NJ0           138         Q72US9           139         Q75FU4           140         Q72VN8           141         Q72NP1           142         Q75FY9           143         Q72PH1           144         Q72MF8           145         Q72PY4           146         Q72LY2           147         Q72SB6           148         Q72PW3           149         Q72MX3           150         Q72M85           151         Q72SI3           152         Q75FU9           153         Q72S95           154         Q72RM7           155         Q72LS2           156         Q72PU4           157         Q72UF0           158         Q72RF2           159         Q72R06           160         Q72SR3           161         Q72Q11           162         Q72TA2           163         Q72RK7           165         Q72U8           166         Q72QP2		`	
138       Q72US9         139       Q75FU4         140       Q72VN8         141       Q72NP1         142       Q75FY9         143       Q72PH1         144       Q72MF8         145       Q72PY4         146       Q72LY2         147       Q72SB6         148       Q72PW3         149       Q72MX3         150       Q72M85         151       Q72SI3         152       Q75FU9         153       Q72S95         154       Q72RM7         155       Q72LS2         156       Q72PU4         157       Q72UF0         158       Q72F2         159       Q72R06         160       Q72SR3         161       Q72Q11         162       Q72TA2         163       Q72R33         164       Q72RK7         165       Q72UW8         166       Q72QP2		`	
139       Q75FU4         140       Q72VN8         141       Q72NP1         142       Q75FY9         143       Q72PH1         144       Q72MF8         145       Q72PY4         146       Q72LY2         147       Q72SB6         148       Q72PW3         149       Q72MX3         150       Q72M85         151       Q72SI3         152       Q75FU9         153       Q72SP5         154       Q72RM7         155       Q72LS2         156       Q72PU4         157       Q72UF0         158       Q72RF2         159       Q72R06         160       Q72SR3         161       Q72Q11         162       Q72TA2         163       Q72R33         164       Q72W8         165       Q72UW8         166       Q72QP2		`	
140       Q72VN8         141       Q72NP1         142       Q75FY9         143       Q72PH1         144       Q72MF8         145       Q72PY4         146       Q72LY2         147       Q72SB6         148       Q72PW3         149       Q72MX3         150       Q72M85         151       Q72SI3         152       Q75FU9         153       Q72S95         154       Q72RM7         155       Q72LS2         156       Q72PU4         157       Q72UFO         158       Q72RF2         159       Q72R06         160       Q72SR3         161       Q72Q11         162       Q72TA2         163       Q72RK7         165       Q72UW8         166       Q72QL3         167       Q72QP2		`	
141       Q72NP1         142       Q75FY9         143       Q72PH1         144       Q72MF8         145       Q72PY4         146       Q72LY2         147       Q72SB6         148       Q72PW3         149       Q72MX3         150       Q72M85         151       Q72SI3         152       Q75FU9         153       Q72S95         154       Q72RM7         155       Q72LS2         156       Q72PU4         157       Q72UFO         158       Q72FF2         159       Q72R06         160       Q72SR3         161       Q72QI1         162       Q72TA2         163       Q72R33         164       Q72RK7         165       Q72UW8         166       Q72QL3         167       Q72QP2		`	
142       Q75FY9         143       Q72PH1         144       Q72MF8         145       Q72PY4         146       Q72LY2         147       Q72SB6         148       Q72PW3         150       Q72M85         151       Q72SI3         152       Q75FU9         153       Q72SP5         154       Q72RM7         155       Q72LS2         156       Q72PU4         157       Q72UF0         158       Q72RF2         159       Q72R06         160       Q72SR3         161       Q72Q11         162       Q72TA2         163       Q72R33         164       Q72K7         165       Q72UW8         166       Q72QL3         167       Q72QP2		`	
143       Q72PH1         144       Q72MF8         145       Q72PY4         146       Q72LY2         147       Q72SB6         148       Q72PW3         150       Q72M85         151       Q72SI3         152       Q75FU9         153       Q72S95         154       Q72RM7         155       Q72LS2         156       Q72PU4         157       Q72UF0         158       Q72RF2         159       Q72R06         160       Q72SR3         161       Q72Q11         162       Q72TA2         163       Q72R33         164       Q72RK7         165       Q72UW8         166       Q72QL3         167       Q72QP2		`	
144       Q72MF8         145       Q72PY4         146       Q72LY2         147       Q72SB6         148       Q72PW3         150       Q72M85         151       Q72SI3         152       Q75FU9         153       Q72S95         154       Q72RM7         155       Q72LS2         156       Q72PU4         157       Q72UF0         158       Q72RF2         159       Q72R06         160       Q72SR3         161       Q72Q11         162       Q72TA2         163       Q72R33         164       Q72K7         165       Q72UW8         166       Q72QL3         167       Q72QP2		,	
145       Q72PY4         146       Q72LY2         147       Q72SB6         148       Q72PW3         149       Q72MX3         150       Q72M85         151       Q72SI3         152       Q75FU9         153       Q72S95         154       Q72RM7         155       Q72LS2         156       Q72PU4         157       Q72UF0         158       Q72RF2         159       Q72R06         160       Q72SR3         161       Q72Q11         162       Q72TA2         163       Q72R33         164       Q72RK7         165       Q72UW8         166       Q72QL3         167       Q72QP2		`	
146       Q72LY2         147       Q72SB6         148       Q72PW3         149       Q72MX3         150       Q72M85         151       Q72SI3         152       Q75FU9         153       Q72S95         154       Q72RM7         155       Q72LS2         156       Q72PU4         157       Q72UF0         158       Q72RF2         159       Q72R06         160       Q72SR3         161       Q72Q11         162       Q72TA2         163       Q72R33         164       Q72RK7         165       Q72UW8         166       Q72QL3         167       Q72QP2	-	`	
147       Q72SB6         148       Q72PW3         149       Q72MX3         150       Q72M85         151       Q72SI3         152       Q75FU9         153       Q72S95         154       Q72RM7         155       Q72LS2         156       Q72PU4         157       Q72UF0         158       Q72RF2         159       Q72R06         160       Q72SR3         161       Q72Q11         162       Q72TA2         163       Q72R33         164       Q72RK7         165       Q72UW8         166       Q72QL3         167       Q72QP2	-	`	
148       Q72PW3         149       Q72MX3         150       Q72M85         151       Q72SI3         152       Q75FU9         153       Q72S95         154       Q72RM7         155       Q72LS2         156       Q72PU4         157       Q72UF0         158       Q72RF2         159       Q72R06         160       Q72SR3         161       Q72Q11         162       Q72TA2         163       Q72R33         164       Q72RK7         165       Q72UW8         166       Q72QL3         167       Q72QP2		`	
150     Q72M85       151     Q72S13       152     Q75FU9       153     Q72S95       154     Q72RM7       155     Q72LS2       156     Q72PU4       157     Q72UF0       158     Q72RF2       159     Q72R06       160     Q72SR3       161     Q72Q11       162     Q72TA2       163     Q72R33       164     Q72RK7       165     Q72UW8       166     Q72QL3       167     Q72QP2	148	`	
151 Q72SI3 152 Q75FU9 153 Q72S95 154 Q72RM7 155 Q72LS2 156 Q72PU4 157 Q72UF0 158 Q72RF2 159 Q72R06 160 Q72SR3 161 Q72Q11 162 Q72TA2 163 Q72R3 164 Q72RK7 165 Q72UW8 166 Q72QL3 167 Q72QP2	149	Q72MX3	
152       Q75FU9         153       Q72S95         154       Q72RM7         155       Q72LS2         156       Q72PU4         157       Q72UF0         158       Q72RF2         159       Q72R06         160       Q72SR3         161       Q72Q11         162       Q72TA2         163       Q72R33         164       Q72RK7         165       Q72UW8         166       Q72QL3         167       Q72QP2	150	Q72M85	
153       Q72S95         154       Q72RM7         155       Q72LS2         156       Q72PU4         157       Q72UF0         158       Q72RF2         159       Q72R06         160       Q72SR3         161       Q72Q11         162       Q72TA2         163       Q72R33         164       Q72RK7         165       Q72UW8         166       Q72QL3         167       Q72QP2	151	Q72SI3	
153       Q72S95         154       Q72RM7         155       Q72LS2         156       Q72PU4         157       Q72UF0         158       Q72RF2         159       Q72R06         160       Q72SR3         161       Q72Q11         162       Q72TA2         163       Q72R33         164       Q72RK7         165       Q72UW8         166       Q72QL3         167       Q72QP2	152	Q75FU9	
155       Q72LS2         156       Q72PU4         157       Q72UF0         158       Q72RF2         159       Q72R06         160       Q72SR3         161       Q72Q11         162       Q72TA2         163       Q72R33         164       Q72RK7         165       Q72UW8         166       Q72QL3         167       Q72QP2	153	Q72S95	
156       Q72PU4         157       Q72UF0         158       Q72RF2         159       Q72R06         160       Q72SR3         161       Q72Q11         162       Q72TA2         163       Q72R33         164       Q72RK7         165       Q72UW8         166       Q72QL3         167       Q72QP2	154	Q72RM7	
157       Q72UF0         158       Q72RF2         159       Q72R06         160       Q72SR3         161       Q72Q11         162       Q72TA2         163       Q72R33         164       Q72RK7         165       Q72UW8         166       Q72QL3         167       Q72QP2	155	Q72LS2	
158       Q72RF2         159       Q72R06         160       Q72SR3         161       Q72Q11         162       Q72TA2         163       Q72R33         164       Q72RK7         165       Q72UW8         166       Q72QL3         167       Q72QP2	156	Q72PU4	
159       Q72R06         160       Q72SR3         161       Q72Q11         162       Q72TA2         163       Q72R33         164       Q72RK7         165       Q72UW8         166       Q72QL3         167       Q72QP2	157	Q72UF0	
160     Q72SR3       161     Q72Q11       162     Q72TA2       163     Q72R33       164     Q72RK7       165     Q72UW8       166     Q72QL3       167     Q72QP2	158	Q72RF2	
161       Q72Q11         162       Q72TA2         163       Q72R33         164       Q72RK7         165       Q72UW8         166       Q72QL3         167       Q72QP2	159	Q72R06	
162       Q72TA2         163       Q72R33         164       Q72RK7         165       Q72UW8         166       Q72QL3         167       Q72QP2	160	Q72SR3	
163       Q72R33         164       Q72RK7         165       Q72UW8         166       Q72QL3         167       Q72QP2	161	Q72Q11	
164       Q72RK7         165       Q72UW8         166       Q72QL3         167       Q72QP2	162	Q72TA2	
165     Q72UW8       166     Q72QL3       167     Q72QP2	163	Q72R33	
166 Q72QL3 167 Q72QP2	164	Q72RK7	
167 Q72QP2	165	Q72UW8	
	166	Q72QL3	
168 Q72TP9	167	Q72QP2	
	168	Q72TP9	

169	Q72V11	
170	Q72S17	
171	Q72SI6	
172	Q72MP9	
173	Q72Q28	
174	Q72T00	
175	Q75FJ2	
176	Q72UE6	
177	Q72QP6	
178	Q72VF1	
179	Q72S91	
180	Q72W16	
181	Q75FS1	
182	Q72VH2	
183	Q72VL1	
184	Q72QX5	
185	Q72TW4	
186	Q72Q87	
187	Q72W87	
188	Q72TW8	
189	Q72NR9	
190	Q72QQ3	
191	Q72RR2	
192	Q72MI0	
193	Q75FN6	
194	Q75FY8	
195	Q72UE8	
196	Q72TL5	
197	Q72VA3	
198	Q72M45	
199	Q72MW4	

### **Publications**



Contents lists available at ScienceDirect

#### International Journal of Biological Macromolecules

journal homepage: www.elsevier.com/locate/ijbiomac





### Biochemical characterization, substrate and stereoselectivity of an outer surface putative $\alpha/\beta$ hydrolase from the pathogenic *Leptospira*

Umate Nachiket Shankar<sup>a</sup>, Mohit<sup>b</sup>, Santosh Kumar Padhi<sup>b</sup>, Mohd Akif<sup>a,\*</sup>

- a Laboratory of Structural Biology, Department of Biochemistry, School of Life Sciences, University of Hyderabad, Hyderabad, Telangana, India
- b Biocatalysis and Enzyme Engineering Laboratory, Department of Biochemistry, School of Life Sciences, University of Hyderabad, Hyderabad, Telangana, India

#### ARTICLE INFO

#### Keywords: Leptospiral $\alpha/\beta$ hydrolase (LABH) Esterase Lipases Biochemical characterization Substrate and stereoselectivity

#### ABSTRACT

The genome of pathogenic *leptospira* encodes a plethora of outer surface and secretory proteins. The outer surface or secreted  $\alpha/\beta$  hydrolases in a few pathogenic organisms are crucial virulent factors. They hydrolyze host immune factors and pathogen's immune-activating ligands, which help pathogens to evade the host's innate immunity. In this study, we report biochemical characterizations, substrate and stereoselectivity of one of the leptospiral outer surface putative  $\alpha/\beta$  hydrolases, IQB77\_09235 (LABH). Purified LABH displayed better kinetic parameters towards small water-soluble esters such as *p*-nitrophenyl acetate and *p*-nitrophenyl butyrate. The LABH exhibited moderate thermostability and displayed a pH optimum of 8.5. Remarkably, a phylogenetic study suggested that LABH does not cluster with other characterized bacterial esterases or lipases. Protein structural modeling revealed that some structural features are closely associated with *Staphylococcus hycus* lipase (SAH), a triacylglycerol hydrolase. The hydrolytic activity of the protein was found to be inhibited by a lipase inhibitor, orlistat. Biocatalytic application of the protein in the kinetic resolution of racemic 1-phenylethyl acetate reveals excellent enantioselectivity (E > 500) in the production of (R)-1-phenylethanol, a valuable chiral synthon in several industries. To our knowledge, this is the first detailed characterization of outer surface  $\alpha/\beta$  hydrolases from leptospiral spp.

#### 1. Introduction

Leptospirosis is a neglected tropical zoonosis caused by many pathogenic *leptospiral* species [1]. Approximately 1 million cases of severe leptospirosis have been reported, with nearly 60,000 deaths per year globally [2]. Leptospirosis imposes a great challenge for diagnosis and treatment due to having similar symptoms to other diseases such as malaria, influenza, hepatitis, yellow fever, etc. [3,4]. Moreover, the emergence of many antigenic diverse serovars among pathogenic *leptospira* poses difficulties for an effective vaccine design [4]. New therapeutics and effective vaccines are essentially warranted, which creates a tactical demand for a better understanding of the virulence and pathogenesis of pathogenic *Leptospira*.

The genome of pathogenic *leptospira* encodes a plethora of proteins targeted on the outer surface and as secretory proteins. The functional role of many of these proteins is not yet investigated in details. Surface

proteins such as Leptospiral Immunoglobulin-like protein (Lig), Leptospira surface antigens (Lsa), Leptospiral complement acquiring protein A (LcpA), and a few leptospiral lipoproteins (LipL) are well characterized as their roles in virulence and pathogenesis [5–8]. Lig is a well-known vaccine candidate whose antigenic region is well-described [9]. Many of these surface proteins bind to the host extracellular matrix components laminin and fibronectin and facilitate the infection [10,11]. Few are reported to play a crucial role in evading the host complement system [5]. A recent report suggests that Ig-domains of Lig proteins possess a novel nuclease activity, which may be required to cleave host NET [12]. However, the role of many other surface and secretory proteins needs to be investigated.

Our proteome mining identified many outer membranes and secretory proteins with probable hydrolyzing functions (data communicated). The protein with an  $\alpha/\beta$  hydrolase domain that possesses hydrolyzing function is classified into the  $\alpha/\beta$  hydrolase superfamily.

Abbreviations: Ni-NTA, Ni-Nitrilotriacetic acid; Kb, Kilobase; IPTG, Isopropyl-D-thiogalactopyranoside; PMSF, Phenylmethylsulfonyl fluoride; Da, Dalton; PDB, Protein Data Bank; ORF, Open reading frame; CD, Circular dichroism; RMSD, Root mean square deviation; HPLC, High performance liquid chromatography; ee, Enantiomeric excess.

E-mail address: akif@uohyd.ac.in (M. Akif).

<sup>\*</sup> Corresponding author.





# Immunoinformatics-Based Designing of a Multi-Epitope Chimeric Vaccine From Multi-Domain Outer Surface Antigens of *Leptospira*

Pankaj Kumar<sup>†</sup>, Surabhi Lata<sup>†</sup>, Umate Nachiket Shankar and Mohd. Akif<sup>\*</sup>

Laboratory of Structural Biology, Department of Biochemistry, School of Life Sciences, University of Hyderabad, Hyderabad, India

#### OPEN ACCESS

#### Edited by:

Jochen Mattner, University of Erlangen—Nuremberg, Germanv

#### Reviewed by:

Abdelrahman Hamza Abdelmoneim, Al-Neelain University, Sudan Alok Jain, Birla Institute of Technology—Mesra, India

#### \*Correspondence:

Mohd. Akif akif@uohyd.ac.in

<sup>†</sup>These authors have contributed equally to this work

#### Specialty section:

This article was submitted to Vaccines and Molecular Therapeutics, a section of the journal Frontiers in Immunology

> Received: 02 July 2021 Accepted: 08 November 2021 Published: 30 November 2021

#### Citation:

Kumar P, Lata S, Shankar UN and Akif M (2021) Immunoinformatics-Based Designing of a Multi-Epitope Chimeric Vaccine From Multi-Domain Outer Surface Antigens of Leptospira. Front. Immunol. 12:735373. doi: 10.3389/fimmu.2021.735373 Accurate information on antigenic epitopes within a multi-domain antigen would provide insights into vaccine design and immunotherapy. The multi-domain outer surface Leptospira immunoglobulin-like (Lig) proteins LigA and LigB, consisting of 12-13 homologous bacterial Ig (Big)-like domains, are potential antigens of Leptospira interrogans. Currently, no effective vaccine is available against pathogenic Leptospira. Both the humoral immunity and cell-mediated immunity of the host play critical roles in defending against Leptospira infection. Here, we used immunoinformatics approaches to evaluate antigenic B-cell lymphocyte (BCL) and cytotoxic T-lymphocyte (CTL) epitopes from Lig proteins. Based on certain crucial parameters, potential epitopes that can stimulate both types of adaptive immune responses were selected to design a chimeric vaccine construct. Additionally, an adjuvant, the mycobacterial heparin-binding hemagglutinin adhesin (HBHA), was incorporated into the final multi-epitope vaccine construct with a suitable linker. The final construct was further scored for its antigenicity, allergenicity, and physicochemical parameters. A three-dimensional (3D) modeled construct of the vaccine was implied to interact with Toll-like receptor 4 (TLR4) using molecular docking. The stability of the vaccine construct with TLR4 was predicted with molecular dynamics simulation. Our results demonstrate the application of immunoinformatics and structure biology strategies to develop an epitope-specific chimeric vaccine from multi-domain proteins. The current findings will be useful for future experimental validation to ratify the immunogenicity of the chimera.

Keywords: Leptospira interrogans, antigenic epitope, outer surface antigen, vaccine, Leptospira immunoglobulinlike protein, subunit vaccine, immunoinformatics

#### INTRODUCTION

Leptospirosis is categorized as an emerging and neglected tropical zoonotic disease worldwide. It is considered a public health problem globally, with an estimated 1 million leptospirosis cases reported each year, causing deaths of around 60,000 (1–3). The infection usually shows symptoms such as headache, chills, illness, and muscle aches, and a more severe form of disease is associated with

1



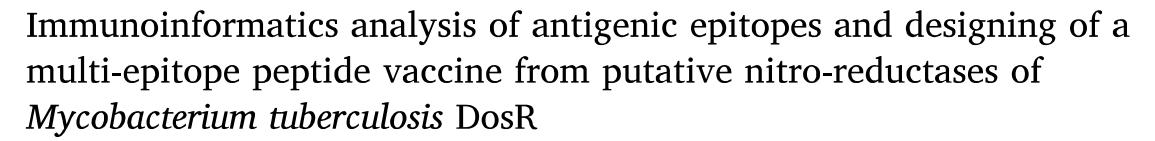
Contents lists available at ScienceDirect

#### Infection, Genetics and Evolution

journal homepage: www.elsevier.com/locate/meegid



Research paper





Mohd. Shiraz, Surabhi Lata, Pankaj Kumar, Umate Nachiket Shankar, Mohd. Akif\*

Department of Biochemistry, School of Life Sciences, University of Hyderabad, Hyderabad 500046, India

#### ARTICLE INFO

Keywords:
Mycobacterium tuberculosis
Nitro-reductases
Antigenic T-cell epitopes
Peptide vaccine
Dormancy
DosR

#### ABSTRACT

Mycobacterium tuberculosis (Mtb) resides in alveolar macrophages as a non-dividing and dormant state causing latent tuberculosis. Currently, no vaccine is available against the latent tuberculosis. Latent Mtb expresses ~48 genes under the control of DosR regulon. Among these, putative nitroreductases have significantly high expression levels, help Mtb to cope up with nitrogen stresses and possess antigenic properties. In the current study, immunoinformatics methodologies are applied to predict promiscuous antigenic T-cell epitopes from putative nitro-reductases of the DosR regulon. The promiscuous antigenic T-cell epitopes prediction was performed on the basis of their potential to induce an immune response and forming a stable interaction with the HLA alleles. The highest antigenic promiscuous epitopes were assembled for designing an in-silico vaccine construct. A TLR-2 agonist Phenol-soluble modulin alpha 4 was exploited as an adjuvant. Molecular docking and Molecular Dynamics Simulations were used to predict the stability of vaccine construct with the immune receptor. The predicted promiscuous epitopes may be helpful in the construction of a subunit vaccine against latent tuberculosis, which can also be administered along with the BCG to increase its efficacy. Experimental validation is a prerequisite for the in-silico designed vaccine construct against TB infection.

#### 1. Introduction

Mycobacterium tuberculosis (Mtb) is a multifaceted pathogen causing Tuberculosis (TB), which remains one of the prominent reasons for mortality worldwide. According to the WHO global TB 2020 report, millions of people are currently infected with Mtb. Among that less than 10% of the total infected individuals are affected with active TB; and while more than 90% of individuals are afflicted with latent tuberculosis where Mtb resides inside infected macrophages for a longer period of time in an inactive metabolic state and non-transmissible form but reversible state, known as "dormancy". The population of latent tuberculosis infection (LTBI) individuals indeed responsible for a major obstruction to TB control strategies. Although antibiotic treatment offers standard care for active TB, its effectiveness against latent TB is doubtful. The current protective Bacillus-Calmette-Guerin (BCG) TB vaccine - a live-attenuated Mycobacterium bovis vaccine (Eddine and Kaufmann, 2005)- is known to protect against dreadful forms of TB in young children (Corbett et al., 2003). However, it does not show efficient and consistent protection in adults against pulmonary TB and also it doesn't protect from reactivation of the latent TB infection. Hence, significant efforts for the development of new vaccines/therapies that can prevent latent Mtb infection are desperately needed. Dormancy in Mtb is characterized as a state of low pH, nutrient deprivation, hypoxia, and nitric oxide, which triggers an upregulation of a set of ~48 genes (~1.2% of the Mtb genome), known as Dormancy Survival Regulon or DosR (Voskuil et al., 2003). Functions of most DosR regulon gene products are unknown, but many of them are found to be immunodominant that elicit a strong T-cell response. It has been reported that DosR regulon triggers a T-cell response and IFN-y inducing capability. Rv1733c, Rv2029c, Rv2627c, and Rv2628 were found to elicit a strong immune response as compared to CFP-10, a well-recognized antigen for Mtb infection (Leyten et al., 2006). Rv1813c, Rv2628, Rv2029c, and Rv2659c were also reported as latency antigens with a good humoral immune response and produce a higher number of CD4<sup>+</sup> cells (Liang et al., 2019). Therapeutic effects of these antigens were studied in the endogenous resurgence mouse TB model. In fact, in the same study, Rv2626c and Rv2032 latency antigens were reported to induce a significant effect on CD4<sup>+</sup> and CD8<sup>+</sup> cells (Liang et al., 2019). These two

E-mail address: akif@uohyd.ac.in (Mohd. Akif).

<sup>\*</sup> Corresponding author.

# Anti-Plagiarism report

Proteome analysis, biochemical and structural characterization of outer membrane and secretory proteins from pathogenic Leptospira

by Umate Nachiket Shankar

Librarian

Indira Gandhi Memorial Library
UNIVERSITY OF HYDERABAD
Central University P.O.
HYDERABAD-500 046

**Submission date:** 29-Feb-2024 10:22AM (UTC+0530)

Submission ID: 2307638170

**File name:** Umate\_Nachiket\_Shankar.pdf (6.73M)

Word count: 32620 Character count: 179983 Proteome analysis, biochemical and structural characterization of outer membrane and secretory proteins from pathogenic Leptospira

from	n pathoge	nic Leptospira		<i>3</i> 1	
ORIGINA	LITY REPORT				
32 SIMILAR	2% RITY INDEX	11% INTERNET SOURCES	30% PUBLICATIONS	<b>7</b> % STUDENT P	'APERS
PRIMARY	SOURCES				
1	Kumar P characte stereose α/β hydr Leptospi	lachiket Shanka adhi, Mohd Aki rization, substra lectivity of an o olase from the ra", Internation olecules, 2022	f. "Biochemical ate and uter surface p pathogenic	l utative	21%
2	Submitte Hyderab Student Paper	ed to University ad	of Hyderabad	ı	2%
3	prr.hec.g	•			1 %
4	WWW.MC	•			<1%
5		a. Santos, Lilian Aline Crucello et	· · · · · · · · · · · · · · · · · · ·		<1%

Clelton A. Santos, Lilian L. Beloti, Marcelo A.S. Toledo, Aline Crucello et al. "A novel protein refolding protocol for the solubilization and purification of recombinant peptidoglycan-

associated lipoprotein from Xylella fastidiosa overexpressed in Escherichia coli", Protein Expression and Purification, 2012

Publication

"Spirochete Biology: The Post Genomic Era", Springer Science and Business Media LLC, 2018

<1%

**Publication** 

Submitted to University of Huddersfield
Student Paper

<1%

Gunasekaran Dhandapani, Thoduvayil Sikha, Aarti Rana, Rahul Brahma, Yusuf Akhter, Madathiparambil Gopalakrishnan Madanan. " Comparative proteome analysis reveals pathogen specific outer membrane proteins of ", Proteins: Structure, Function, and Bioinformatics, 2018

<1%

Publication

Pankaj Kumar, Yung-Fu Chang, Mohd. Akif.
"Characterization of novel nuclease and protease activities among Leptospiral immunoglobulin-like proteins", Archives of Biochemistry and Biophysics, 2022

Publication

<1%

Kavyashree Manjunath, Kanagaraj Sekar.
"Molecular Dynamics Perspective on the
Protein Thermal Stability: A Case Study Using

<1%

## SAICAR Synthetase", Journal of Chemical Information and Modeling, 2013

Publication

11	ngc.cdfd.org.in Internet Source	<1%
12	www.ncbi.nlm.nih.gov Internet Source	<1%
13	teses.usp.br Internet Source	<1%
14	oro.open.ac.uk Internet Source	<1%
15	Angela Silva Barbosa, Lourdes Isaac. " Strategies used by spirochetes to evade the host complement system ", FEBS Letters, 2020 Publication	<1%
16	Current Topics in Microbiology and Immunology, 2015. Publication	<1%
17	blut-appointment.com Internet Source	<1%
18	www.science.gov Internet Source	<1%
19	Amit Katiyar. "Identification of miRNAs in sorghum by using bioinformatics approach", Plant Signaling & Behavior, 02/01/2012	<1%

20	www.researchgate.net Internet Source	<1%
21	Rana, Aarti, Abdur Rub, and Yusuf Akhter. "Proteome-scale identification of outer membrane proteins in Mycobacterium avium subspecies paratuberculosis using a structure based combined hierarchical approach", Molecular BioSystems, 2014. Publication	<1%
22	Submitted to Rutgers University, New Brunswick Student Paper	<1%
23	link.springer.com Internet Source	<1%
24	docplayer.com.br Internet Source	<1%
25	www.biorxiv.org Internet Source	<1%
26	Ghanem, A "Trends in lipase-catalyzed asymmetric access to enantiomerically pure/enriched compounds", Tetrahedron, 20070219 Publication	<1%
27	Umate Nachiket Shankar, Mohit, Santosh Kumar Padhi, Mohd Akif. "Biochemical	<1%

characterization, substrate and stereoselectivity of an outer surface putative α/β hydrolase from the pathogenic Leptospira", International Journal of Biological Macromolecules, 2023

**Publication** 

**Publication** 

Nadeesha R. Ileperuma, Sean D. G. Marshall, Christopher J. Squire, Heather M. Baker et al. "High-Resolution Crystal Structure of Plant Carboxylesterase AeCXE1, from, and Its Complex with a High-Affinity Inhibitor Paraoxon", Biochemistry, 2007

<1%

Submitted to Universiti Malaysia Sabah

<1%

Pankaj Kumar, Pallavi Vyas, Syed M. Faisal, Yung-Fu Chang, Mohd Akif. "Crystal structure of a variable region segment of Leptospira host-interacting outer surface protein, LigA, reveals the orientation of Ig-like domains", International Journal of Biological Macromolecules, 2023

<1%

Publication

Marcell Cserhalmi, Alexandra Papp, Bianca Brandus, Barbara Uzonyi, Mihály Józsi. "Regulation of regulators: Role of the complement factor H-related proteins", Seminars in Immunology, 2019

<1%

32	Submitted to University of Reading Student Paper	<1%
33	acikbilim.yok.gov.tr Internet Source	<1%
34	www.frontiersin.org Internet Source	<1%
35	Submitted to Queen Mary and Westfield College Student Paper	<1%
36	repositorium.sdum.uminho.pt Internet Source	<1%
37	Submitted to Mahidol University Student Paper	<1%
38	patents.google.com Internet Source	<1%
39	Submitted to Universiti Tunku Abdul Rahman Student Paper	<1%
40	roderic.uv.es Internet Source	<1%
41	Leandro Carvalho Dantas Breda, Silvio Arruda Vasconcellos, Dewton de Moraes Vasconcelos, Lourdes Isaac. "Binding of human complement C1 sterase inhibitor to Leptospira spp.", Immunobiology, 2018	<1%

42	Navid Nezafat, Zeinab Karimi, Mahboobeh Eslami, Milad Mohkam, Sanam Zandian, Younes Ghasemi. "Designing an efficient multi-epitope peptide vaccine against Vibrio cholerae via combined immunoinformatics and protein interaction based approaches", Computational Biology and Chemistry, 2016 Publication	<1%
43	www.jmbfs.org Internet Source	<1%
44	Edoardo Saccenti. "The war of tools: how can NMR spectroscopists detect errors in their structures?", Journal of Biomolecular NMR, 04/2008 Publication	<1%
45	academic.oup.com Internet Source	<1%
46	code.bioconductor.org Internet Source	<1%
47	www.dbt.univr.it Internet Source	<1%
48	Clelton A. Santos, Anete P. Souza. " Solubilization, Folding, and Purification of a Recombinant Peptidoglycan-Associated Lipoprotein (PAL) Expressed in ", Current Protocols in Protein Science, 2018	<1%

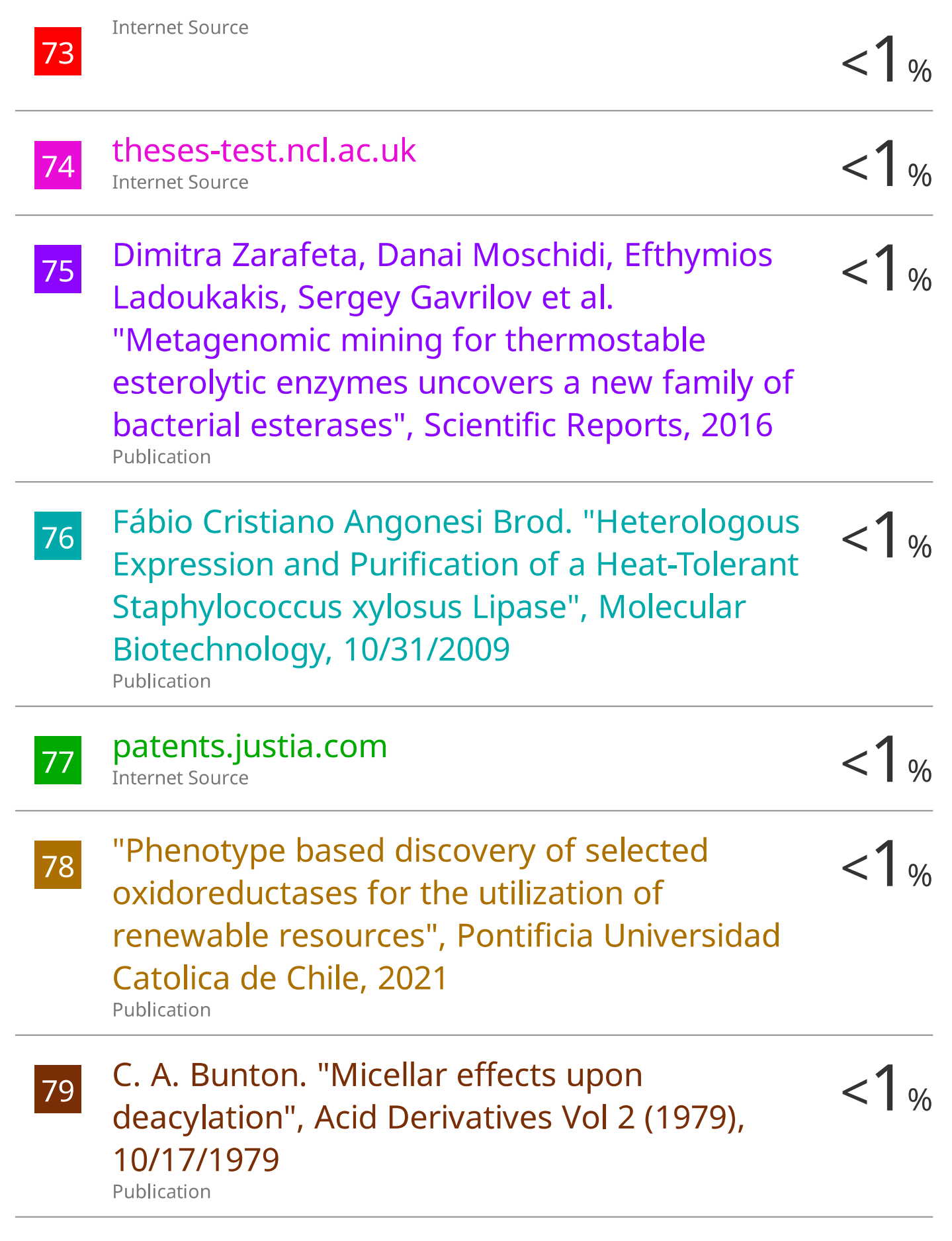
49	Zélia Silva, Maria-Manuel Sampaio, Anke Henne, Alex Böhm, Ruben Gutzat, Winfried Boos, Milton S. da Costa, Helena Santos. " The High-Affinity Maltose/Trehalose ABC Transporter in the Extremely Thermophilic Bacterium HB27 Also Recognizes Sucrose and Palatinose ", Journal of Bacteriology, 2005 Publication	<1%
50	jscholarship.library.jhu.edu Internet Source	<1%
51	journals.plos.org Internet Source	<1%
52	Submitted to Coventry University Student Paper	<1%
53	Stella W. L. Milferstaedt, Marie Joest, Sebastian N. W. Hoernstein, Lennard L. Bohlender et al. " Differential GTP-dependent polymerization of recombinant Physcomitrella FtsZ proteins ", Cold Spring Harbor Laboratory, 2024 Publication	<1%
54	tjlab.ustc.edu.cn Internet Source	<1%
55	Liszewski, M, and John Atkinson. "Regulatory Proteins of Complement", The Human	<1%

### Complement System in Health and Disease, 1998.

Publication

56	Submitted to RMIT University Student Paper	<1%
57	noexperiencenecessarybook.com Internet Source	<1%
58	www.ajol.info Internet Source	<1%
59	www.wjgnet.com Internet Source	<1%
60	yanglab.qd.sdu.edu.cn Internet Source	<1%
61	M. CHENIK, S. LAKHAL, N. BEN KHALEF, L. ZRIBI, H. LOUZIR, K. DELLAGI. "Approaches for the identification of potential excreted/secreted proteins of parasites ", Parasitology, 2006 Publication	<1%
62	Submitted to University of Sheffield Student Paper	<1%
63	core.ac.uk Internet Source	<1%
64	doras.dcu.ie Internet Source	<1%

65	getd.libs.uga.edu Internet Source	<1%
66	www.en.pms.ifi.lmu.de Internet Source	<1%
67	Jao, S.C "Hydrolysis of organophosphate triesters by Escherichia coli aminopeptidase P", Journal of Molecular Catalysis. B, Enzymatic, 20040102 Publication	<1%
68	Saswat Hota, Md Saddam Hussain, Manish Kumar. "ErpY-like Lipoprotein of Outsmarts Host Complement Regulation by Acquiring Complement Regulators, Activating Alternative Pathways, and Intervening in the Membrane Attack Complex ", ACS Infectious Diseases, 2022 Publication	<1%
69	Submitted to University of Bath Student Paper	<1%
70	Submitted to University of East London Student Paper	<1%
71	docplayer.net Internet Source	<1%
72	hdl.handle.net Internet Source	<1%



Submitted to National University of Singapore

Publication

Tatiana Rodrigues Fraga, Eneas Carvalho, Lourdes Isaac, Angela Silva Barbosa. "Leptospira and leptospirosis", Elsevier BV, 2024 <1%

Publication

Submitted to University of Hong Kong
Student Paper

<1%

assets.researchsquare.com
Internet Source

<1%



<1 % <1 %

#### theses.hal.science Internet Source

Exclude quotes On Exclude bibliography On Exclude matches

< 14 words



#### University of Hyderabad Hyderabad- 500 046, India

#### PLAGIARISM FREE CERTIFICATE

This is to certify that the similarity index of this thesis as checked by the Library of the University of Hyderabad is 32%. Out of this, 23% similarity has been found from the candidate's (Umate Nachiket Shankar) own publications which form the adequate part of the thesis. The details the of student's publication are as follows:

#### Paper

Shankar, UN. Mohit, Padhi, SK and Akif, M. (2023) Biochemical characterization, substrate and stereoselectivity of an outer surface putative  $\alpha/\beta$  hydrolase from the pathogenic Leptospira. International Journal of Biological Macromolecules 229, 803–813

% Similarity

23% (Source No.1, 2 & 27)

About 9% similarity was identified from external sources in the present thesis which is in accordance with the regulations of the University. All the publications related to this thesis have been appended at the end of the thesis. Hence the present thesis may be considered to be plagiarism free.

Dr. Mohd. Akif

Supervisord. Akif, Ph.D. / मुहम्मद आकिफ, पीएवडी
Associate Professor / एसोसिएट प्रोफेसर
Department of Biochemistry / जैव रसायन विभाग
School of Life Sciences / जीव विज्ञान विद्यालय
University of Hyderabad / हैदराबाद विश्वविद्यालय
Prof. CR Rao Road / प्रो आर राव रोड
Gachibowli / गायीबावली, Hyderabad / हैदराबाद-46.

Date of Registration: 06/08/2016 Date of Expiry : 08/07/2024

#### UNIVERSITY OF HYDERABAD SCHOOL OF LIFE SCIENCES DEPARTMENT OF BIOCHEMISTRY

#### PROFORMA FOR SUBMISSION OF THESIS/DISSERTATION

: Umate Nachiket Shankar 4. Name of the Candidate

2. Roll No. : 16 LBPHOG

3. Year of Registration : 2016

Proteome analysis, biochemical and structural characterization of the outermembrane and secretary proteins from pathogenic Leptospira. Dr. Mohd. Akif, University of Hyderabad. 4. Topic

5. Supervisor(s) and affiliations

Whether extension/re-registration granted: Yes, order ID: UH/AR/A |2024/527 6. (Specify below) Re-registration Date: 09/01/2024

7. Date of submission : 04/03/2024

Last class attended on (M.Phil/Pre-Ph.D): 24 105 2023 8.

Whether tuition fee for the current period Paid: Receipt No. & Dt: 9.

10.

Whether thesis submission fee paid: Receipt No & Dt: Yes, 29/01/2024

Transaction No. - 240129191418227

Transaction No. - 240129191418227 : Receipt No & Dt: Yes, No dues cleared 11. Whether hostel dues cleared through E. governance.

Whether a summary of the dissertation enclosed: Yes 12.

Superviser (sp. D.) नुसम्पद्ध निर्माण प्रीएव Signature Professor / एसोसिप्य स्मिन्यर Department of Biochemistry / जैव रसायन विसाग School of Life Sciences / जीव विज्ञान विद्यालय University of Hyderabad / हैदराबाद विश्वविद्यालय
Signature लेकिसिटवd / प्रो आर राव रोड Deani, of the School

Forwarded on

Sv. Naen versity of Hyderabad भीवविज्ञान सम्बद्धः । ६ समाद विश्वविद्यालय

idik प्रश्वानकात्वन (University of Hyderab हैवरविद् (Hyderabad-500046, INDIA

संकाय अध्यक्ष / Dean जीव विज्ञान संकाय / School of Life Sciences हैदराबाद विश्वविद्यालय / University of Hyderabad हैदराबाद / Hyderabad-500 046.

Dear ] ses | 400 Dear | ses /445